Molecular analysis of Smc5/6-dependent sumoylation and ubiquitination

Eva Irene Ibars Estiarte

Universitat de Lleida

TESI DOCTORAL

Molecular analysis of Smc5/6-dependent sumoylation and ubiquitination

Eva Irene Ibars Estiarte

Memòria presentada per optar al grau de Doctor per la Universitat de Lleida
Programa de Doctorat en Salut

Director/a

Jordi Torres Rosell
Gemma Bellí Martínez

Tutor/a

Neus Colomina Gabarrella

2021

El camí de la punxa conclou sempre en la rosa.

Vicent Andrés Estellés

Als meus pares,

A la meva germana,

A l'Albert.

AGRAÏMENTS

Mirant amb perspectiva tots aquests anys de formació científica, d'esforç i de dedicació constants, m'adono que sense l'orientació, el suport, l'exemple, i l'afecte de moltes persones amb les que m'he creuat al llarg d'aquest camí, i d'altres que hi han estat des de sempre, jo no hagués arribat fins aquí. A totes elles, vull dedicar-los aquest treball i donar-los les gràcies per haver-me acompanyat en aquesta etapa.

En primer lloc, vull agrair al meu director de tesi per donar-me l'oportunitat de treballar en aquest projecte i poder créixer científicament. Gràcies Jordi per tot el que m'has ensenyat durant aquests anys i per saber guiar aquesta tesi amb experiència i rigor. Gràcies a tu també Gemma, la meva co-directora, pel teu optimisme i per confiar tant en mi. El teu esforç i dedicació incansables han sigut claus per aconseguir aquests resultats. Gràcies a la meva tutora, Neus C, per la teva energia positiva, els consells i l'ajuda incondicional que brindes a tothom.

Vull agrair també a la resta de membres de cicle cel·lular amb els qui he compartit aquesta trajectòria. Especialment a l'Eloi, per donar-me l'oportunitat d'incorporar-me en aquest grup mentre feia el màster i per despertar-me interès per la recerca. Gràcies pels consells i el suport que ens dones, i sobretot per fer més lleugeres les llargues hores al despatx amb el teu punt d'humor. Gràcies a tota la gent de CYC amb qui he coincidit durant el transcurs d'aquesta tesi, Neus P, Paco, Celia, Sonia, Mariel, he après molt de vosaltres. I sobretot a vosaltres, Sònia, Tània, Marc, Marta G, Turi, Roger, Neus, Marta Rafel, per la pinya que hem fet i per alegrar-me sempre els dies. Aquesta tesi també és una mica vostra.

A tu, Sònia, quina sort coincidir! Amb el temps hem anat teixint una amistat que va més enllà de les poiates. Gràcies per tots els moments, per la teva empatia, pels cafès, les confessions, les trucades i les rialles compartides. Has estat un pilar molt important per mi durant aquests quatre anys, i sé que ho seguiràs sent. T'estimo molt!

Tània, vas ser la meva guia des de l'inici quan vaig aterrar en aquest laboratori i no en podia haver tingut una de millor. Gràcies per la paciència, pels consells, per fer-me sentir a gust des del primer dia i per tot el que em vas ensenyar, vam formar un bon equip!

Gràcies Marc, per ser-hi sempre i solucionar moltes de les meves liades. Has estat un suport incondicional durant tots aquests anys i m'has ajudat moltíssim. Puc dir que sens dubte has après que compartir és viure! Hem intentat arreglar el món, ens hem picat molt i hem rigut encara més. T'he de confessar que ho trobaré a faltar.

Marta, vam entrar el mateix dia al laboratori i ens vam entendre des del primer moment. Durant aquests anys hem compartit èxits i fracassos, tardes de riures descontrolats, trossets de les nostres vides, i ens hem fet sempre costat. Gràcies per fer-ho tot tan fàcil, em sento molt feliç d'haver compartit aquest llarg recorregut juntes.

Turi, no saps com trobo a faltar el ritme caribenyo i els post-its sorpresa. Gràcies pel teu suport moral i per les receptes pels bons i pels mals moments que sempre ens treien un somriure. Per deixar-me envair-te la poiata cada dos per tres i per les llargues converses que m'arreglaven les tardes. Només per tot això ja ha valgut la pena.

Roger, vas entrar com de puntetes al laboratori i ha sigut genial descobrir-te. Qui ens ho havia de dir, que amb el temps crearíem aquest vincle que ens faria explicar-nos la vida com si ens coneguéssim de sempre. Gràcies per regalar-me tants moments de riures, de converses absurdes i algun que altre ensurt. Sé que trobaràs a faltar el meu circ ambulant!

Neus, tu vas aparèixer més tard al laboratori però tinc la sensació que hi has estat des de sempre. Gràcies per ser tan transparent i per ensenyar-me que mai res no és tan important. Encara que no t'ho sembli he après moltíssim de tu, i estic segura que aconseguiràs el que et proposis perquè t'ho mereixes.

Marta Rafel, per mi sempre seràs de CYC. Gràcies per la teva autenticitat, per alegrar-me tants matins i per preocupar-te sempre pels altres. Trobaré molt a faltar les converses i compartir entre rialles totes aquelles aventures que només et passen a tu... Gràcies per tots aquests moments!

Gràcies també a totes les companyes de l'IRB amb qui he tingut la sort de coincidir durant aquests anys i amb les que hem compartit aniversaris, dinars, converses, rialles, carnavals i jocs de taula. Gràcies Isidre, Pau, Maria, Maite, Alba, Coral, Cris, Laura, Aurora, Núria, Alícia, Àuria, per tots els moments que ajudaven a amenitzar el dia a dia, dins i fora dels laboratoris.

D'altra banda, vull donar les gràcies al Dr. David Reverter per acollir-me durant uns dies al seu laboratori i donar-me l'oportunitat d'aprendre noves tècniques i protocols. Gràcies també a tot el grup d'Estructura de Proteïnes del IBB, especialment a la Jara i a la Nathalia, per dedicar-me el vostre temps i per fer-me sentir tan a gust.

I, com no podia ser d'altra manera, a les meves amigues, la família que s'escull. Portem tota una vida juntes, compartint de ben a prop cada moment vital dels nostres camins. I jo, en aquest, no podia haver tingut millors companyes de viatge: onze dones increïbles, inspiradores, valentes, i rebels. Sou les llunes que més brillen, gràcies per ser el meu far en tants moments. Em sento molt afortunada de tenir-vos, us estimo molt.

Gràcies també als marmotes i a totes amb les que compartim els vespres de divendres a la segona oficina, les escapades i els plans d'estiu improvisats. Quin plaer desconnectar de les rutines així!

Però, sens dubte, tot el que sóc i el que he aconseguit ho dec a la meva família. Als meus padrins, els que hi són i els que ja no. D'ells he après la tenacitat, la rebel·lia, l'esforç i l'amor incondicional. Als tiets i cosins, gràcies pel vostre interès i suport. Al Lennon i al Kuro, que també són la meva família i m'alegren els dies com ningú.

A la meva germana, la millor persona que conec, GRÀCIES. Per no tenir mai un no per a mi, i ajudar-me en cada cosa que faig, en cada projecte que emprenc, en cada idea que tinc i, perquè no dir-ho, en cada paper que he d'omplir... Ets el meu àngel de la guarda, i saps que aquesta tesi

te la dec molt a tu. Gràcies a tu també Jacob, per la teva energia positiva i per fer-la tan feliç. I a tu, petita Bruc, que acabes d'arribar i de remoure-ho tot. Gràcies per aparèixer a les nostres vides i fer-nos adonar d'allò que és important de veritat. Tu encara no ho entens, però una rialla teva ho cura tot. La padrineta t'estima molt!

I, per descomptat, als meus pares. M'heu ensenyat a pensar amb esperit crític i a lluitar pel que crec. M'heu educat sense tabús i amb llibertats. M'heu recolzat en cada decisió, i us heu deixat la pell perquè aconseguís els meus propòsits, per difícil que fos, i perquè arribés allà on jo volgués. M'heu donat arrels i m'heu dibuixat ales. Gràcies per creure sempre en mi més que jo mateixa. Us estimo molt.

I per últim a tu, Albert, el meu company de vida i d'aventures. Has suat al meu costat cada pàgina d'aquesta tesi, i saps millor que ningú que aquest ha estat un camí llarg i costerut. Però tenir-te al costat ho fa tot més fàcil. Gràcies per la teva paciència infinita, pel teu suport incondicional i per treure sempre el millor de mi. Junts som imparables.

ABSTRACT

Eukaryotic cells devote large efforts to maintain the integrity of their genome. The Structural Maintenance of Chromosomes (SMC) complexes, which include cohesin, condensin and Smc5/6, coordinate multiple chromosomal activities that safeguard our genome. Particularly, the Smc5/6 complex plays crucial roles in DNA repair by homologous recombination, replication fork stability and sister chromatid resolution, and it is the most unknown member of the SMC family. Unlike cohesin and condensin, it contains two RING-type domains: one in the Nse1 subunit, with potential ubiquitin ligase activity, and the other in the Nse2 subunit, which has been shown to mediate the transfer of SUMO to substrate proteins.

Nse2 binds to the Smc5 coiled-coil through its essential N-terminal domain, whereas its C-terminal half, coding for the SUMO ligase domain, is dispensable for cell survival. Despite this, Nse2-dependent sumoylation of SMC complexes and other chromosomal targets has been reported to control several biological pathways directly involved in genome integrity. However, the processes that regulate its E3 ligase activity remain poorly understood. In this study, we describe a novel mechanism by which the interaction between a positively-charged patch in the coiled-coil of Smc5 and DNA stimulates the Nse2 SUMO E3 ligase activity. In addition, we have performed a detailed functional analysis of the different structural features present in the C-terminal domain of Nse2 in yeast. This characterization reveals that the last C-terminal alpha-helix, which has been related to a rare genetic disorder, has an important structural function and directly affects Nse2 stability. In addition, we have identified two regions that enhance sumoylation *in vitro*. To our surprise, our results also show that mutations in conserved residues coordinating the zinc ion do not impair Smc5-sumoylation *in vivo.*

The other RING-type subunit of the Smc5/6 complex, Nse1, has also been described to promote DNA repair functions and to maintain genome stability. However, no targets for its ubiquitin-E3 ligase activity have been identified until now. Here, we use label-free quantitative proteomics to compare the ubiquitinome of wild type and *nse1* RING mutant cells. Particularly, the largest subunit of the RNA POL I, Rpa190, is less ubiquitinated in *nse1* mutant cells. Rpa190 is modified during active transcription, and non-ubiquitinable *rpa190-KR* cells are sensitive to transcriptional elongation inhibitors and are resistant to BMH-21-mediated proteasomal degradation.

Overall, these results provide novel information on the regulation and targets of the Smc5/6-dependent SUMO and ubiquitin ligase activities, which are a critical part of the mechanisms used by the Smc5/6 complex to preserve the integrity of the genome.

RESUM

Les cèl·lules eucariotes dediquen grans esforços per mantenir la integritat del seu genoma. Els complexos SMC (Structural Maintenance of Chromosomes), que inclouen la cohesina, la condensina i el complex Smc5/6, coordinen múltiples activitats cromosòmiques que protegeixen el nostre genoma. Particularment, el complex Smc5/6 té un paper clau en la reparació de l'ADN per recombinació homòloga, l'estabilització de les forquilles de replicació i la resolució de les cromàtides germanes, i és el membre més desconegut de la família SMC. A diferència de la cohesina i la condensina, conté dos dominis de tipus RING: un en la subunitat Nse1, amb potencial activitat ubiqüitina lligasa, i l'altre en la subunitat Nse2, que regula la transferència de SUMO a les proteïnes substrat.

Nse2 s'uneix al coiled-coil de Smc5 a través del seu domini essencial N-terminal, mentre que la seva meitat C-terminal, que codifica per el domini SUMO lligasa, és prescindible per a la supervivència cel·lular. Malgrat això, la sumoilació de diferents subunitats dels SMC i d'altres dianes cromosòmiques depenent de Nse2 controla diverses vies biològiques directament implicades en el manteniment de la integritat genòmica. Tot i això, els processos que regulen la seva activitat SUMO E3 lligasa segueixen sent poc coneguts. En aquest estudi, es descriu un nou mecanisme mitjançant el qual la interacció entre un sensor carregat positivament en el braç de Smc5 i l'ADN estimula l'activitat SUMO E3 lligasa de Nse2. A més a més, hem realitzat un detallat anàlisi funcional de les diferents característiques estructurals presents al domini C-terminal de Nse2 en llevat. Aquesta caracterització revela que l'hèlix alfa C-terminal, que s'ha associat amb un desordre genètic rar, té una funció estructural important i afecta directament a l'estabilitat de Nse2. D'altra banda, hem identificat dues regions que incrementen la sumoilació *in vitro.* Sorprenentment, els nostres resultats també mostren que mutacions puntuals en residus conservats que coordinen l'àtom de zinc no afecten a la sumoilació *in vivo* de Smc5.

L'altra subunitat del complex Smc5/6 amb un domini RING, Nse1, s'ha descrit que promou funcions de reparació de l'ADN i que manté l'estabilitat del genoma. Tot i això, fins al moment, no s'han descrit dianes per la seva activitat E3 lligasa. Aquí, fem servir proteòmica quantitativa sense marcatge per tal de comparar l'ubiquitinoma de cèl·lules wild type o mutants en el RING de Nse1. Particularment, la subunitat més gran de l'ARN POL I, Rpa190, està menys ubiquitinada en les cèl·lules *nse1* mutants. Rpa190 es modifica durant la transcripció activa, i els mutants no-ubiquitinables *rpa190-KR* són sensibles a inhibidors de l'elongació transcripcional i són resistents a la degradació proteasomal regulada per BMH-21.

En conjunt, aquests resultats proporcionen noves dades sobre la regulació i les dianes de les activitats SUMO i ubiquitina lligasa dependents de Smc5/6, que són una part crucial dels mecanismes usats pel complex Smc5/6 per tal de preservar la integritat del genoma.

RESUMEN

Las células eucariotas dedican grades esfuerzos para mantener la integridad de su genoma. Los complejos SMC (Structural Maintenance of Chromosomes) que incluyen la cohesina, la condensina y el complejo Smc5/6, coordinan múltiples actividades cromosómicas que protegen nuestro genoma. Particularmente, el complejo Smc5/6 tiene un papel crucial en la reparación del ADN por recombinación homóloga, la estabilización de las horquillas de replicación y la resolución de cromátidas hermanas, y es el miembro más desconocido de la familia SMC. A diferencia de la cohesina o la condensina, tiene dos dominios de tipo RING: uno en la subunidad Nse1, con potencial actividad ubiquitina ligasa, y el otro en la subunidad Nse2, del que se ha descrito que regula la transferencia de SUMO a las proteínas sustrato.

Nse2 se une al coiled-coil de Smc5 a través de su dominio esencial N-terminal, mientras que su mitad C-terminal, que codifica por el dominio SUMO ligasa, es prescindible para la supervivencia celular. Aun así, la sumoilación de diferentes subunidades SMC y otras dianas cromosómicas dependiente de Nse2 controla varias vías biológicas directamente implicadas en el mantenimiento de la integridad genómica. Sin embargo, los procesos que regulan su actividad E3 ligasa siguen siendo poco conocidos. En este estudio, describimos un nuevo mecanismo mediante el cual la interacción entre un sensor cargado positivamente en el brazo de Smc5 y el ADN estimula la actividad SUMO E3 ligasa de Nse2. Además, hemos realizado un detallado análisis funcional de las diferentes características estructurales presentes en el dominio C-terminal de Nse2 en levadura. Esta caracterización revela que la hélice alfa C-terminal, que se ha asociado con un desorden genético raro, tiene una importante función estructural y afecta directamente la estabilidad de Nse2. Además, hemos identificado dos regiones que incrementan la sumoilación *in vitro*. Sorprendentemente, nuestros resultados también muestran que las mutaciones puntuales en residuos conservados que coordinan el átomo de zinc no afectan a la sumoilación *in vivo* de Smc5.

La otra subunidad del complejo Smc5/6 con un dominio RING, Nse1, se ha descrito que promueve funciones de reparación del ADN y que mantiene la estabilidad del genoma. Sin embargo, hasta la fecha, no se han descrito dianas para su actividad ubiquitina-E3 ligasa. Aquí, usamos proteómica cuantitativa sin marcaje para comparar el ubiquitinoma de células wild type y mutantes en el RING de Nse1. Particularmente, la subunidad mayor de la ARN POL I, Rpa190, está menos ubiquitinada en el células *nse1* mutantes. Rpa190 se modifica durante la transcripción activa, y los mutantes no-ubiquitinables *rpa190-KR* son sensibles a inhibidores de elongación transcripcional y son resistentes a la degradación proteasomal mediada por BMH-21.

En conjunto, estos resultados proporcionan nuevos datos en la regulación y las dianas de las actividades SUMO y ubiquitina ligasa dependientes de Smc5/6, que son una parte crucial de los mecanismos usados por el complejo Smc5/6 para preservar la integridad del genoma.

TABLE OF CONTENTS

TABLE OF CONTENTS

ABBREVIATIONS

ABBREVIATIONS

Ala- Alanine

ALT- Alternative lengthening of telomeres

Amp- Ampicillin

APC/C- Anaphase-promoting complex/cyclosome

ARS- Autonomously replicating sequence

ATP- Adenosine triphosphate

Bp- Base pair

BS- Bloom syndrome

CAR- Cohesin associated region

CCD- Catalytic cysteine domain

Cdc48- Cell division control protein 48

CF- Core Factor

CIA- Cytosolic Iron-sulfur cluster assembly

CP- Chromatin pellet

CPT-Camptothecin

CRL- Cullin-RING ligases

CTD- C-terminal domain

Cys- Cysteine

DDB1- Damage-specific DNA binding protein 1

dhJ- double holliday junctions

DMSO- Dimethyl sulfoxide

DNA- Deoxyribonucleic acid

DSB- Double strand break

dsDNA- double-stranded DNA

DUBs- Deubiquitinating enzymes

E. coli- *Escherichia coli*

E1- Equation 1

E2- Equation2

E3- Equation 3

EID- E1A-like inhibitor of differentiation

ERCs- Extra-chromosomal rDNA circles

ETS- External transcribed spacer

FA- Formic acid

G1 phase- Gap1 phase

G2 phase- Gap2 phase

Glu- Glutamic acid

GTF- General transcription factor

GTP- Guanosine triphosphate

GST- Glutathione *S*-transferase

HBV- Hepatitis B Virus

HECT- Homologous to the E6AP carboxyl terminus

HR- Homologus recombination

HU- Hydroxyurea

IGS- Intergenic spacer

IR- Ionizing radiation

KDa- Kilodalton

LB- Luria-Bertani

Leu- Leucine

LOH- Loss of heterozygosity

M phase- Mitosis phase

MAGE- Melanoma associated antigen

MeCN- Acetronitrile

MJD- Machado-Josephin disease

MMS- Methyl methanesulfonate

mRNA- Messenger RNA

NHEJ- Non-homologus end joining

NH-RING- *Nse1-Homolog* RING

Ni-NTA- Nickel nitrilotriacetic acid

Nm- Nanometers

Nrd1-Nab3 - Nuclear pre-mRNA Down-regulation 1- Nuclear polyAdenylated RNA-Binding 3

Nse- Non Smc Element

Nsmce2- Non-Structural Maintenance Of Chromosomes Element 2

NTS-Non-transcribed spacer

OD- Optical density

ORI- Origin of replication

OTU- Ovarian Tumor-related proteases

PAF- Polymerase II-Associated Factor

PCNA- Proliferative Cell Nuclear Antigen

PCR- Polymerase Chain Reaction

PHL-Phleomycin

PIAS- Protein inhibitor of activated signal transducer and activator of transcription

PIC-Preinitiation complex

PML-Promyelocytic leukemia

Pol I- Polymerase I

Polyub- polyubiquitination

PRR- Postreplication repair

rARS- rDNA autonomously replicating sequence

RBR- RING-between-RING

rDNA-ribosomal DNA

RFB- Replication fork barrier

RING- Really interesting new gene

RNA- Ribonucleic acid

RPA190- RNA Polymerase A190

rpm- rotations per minute

rRNA- ribosomal RNA

RT- Room temperature

S phase- Synthesis phase

S. cerevisiae- *Saccharomyces cerevisiae*

S. pombe- *Schizosaccharomyces pombe*

SC- Synthetic Complete

Scc1- Sister Chromathid Cohesion 1

Scc3- Sister Chromathid Cohesion 3

SDC-Sodium Deoxicholate

SENP- Sentrin/SUMO-specific proteases

Ser- Serine

SIM- SUMO Interacting Motif

SMC- Structural Maintenance of Chromosomes

SN- Supernatant

snoRNAs- small nucleolar RNAs

SPE- Solid phase extraction

STR- Sgs1-Top3-Rmi1

STUbls- SUMO-targeted ubiquitin ligases

SUMO- Small Ubiquitin like modifier

TBP- TATA-box binding protein

TCEP- Tris(2-carboxyethyl)phosphine

TFA- Trifluoroacetic acid

Top2- Topoisomerase II

TOP2A- Topoisomerase II alpha

tRNA- transfer RNA

Ts- Thermosensitive

TSS- Transcription start site

UAF- Upstream Activating Factor

UBA- Ubiqutin-activating enzyme E1

Ub-Ubiquitin/ubiquitinated

UBL- Ubiquitin-like

UCH- Carboxyl-terminal hydrolases

UFD- Ubiquitin-Fold Domain

ULP-Ubiquitin-like protein-specific proteases

USP- Ubiquitin-specific processing proteases

UTP- Uridine triphosphate

UV-Ultraviolet light

WCE- Whole cell extract

WB- Western Blot

WT-Wild type

YP- Yeast extract peptone

YPD- Yeast extract peptone dextrose

INTRODUCTION

1. INTRODUCTION

The maintenance of the genomic integrity and the correct transfer of the genetic material to the progeny are a constant concern for any living organism. Dealing with the vulnerability of the genome to DNA damage, and coordinating DNA repair with cell division are crucial to avoid genome instability and ensure its survival.

Remarkably, many cell signalling and DNA repair pathways are regulated by dynamic and reversible post-translational modifications, like phosphorylation, acetylation, sumoylation or ubiquitination. These modifications result in a wide variety of biological effects, such as the control of protein localization or degradation, the activation of DNA repair mechanisms, or the regulation of protein-protein interactions.

1.1 Ubiquitin and Ubiquitin-Like proteins (UbLs)

Ubiquitin (Ub) is a small 76-residue regulatory protein present in all eukaryotic organisms, and one of the most evolutionarily conserved genes (Goldstein et al., 1975). In cells, ubiquitin can be found either free or conjugated to other substrates through the ubiquitin conjugation system. It can be transiently attached to a huge amount of proteins; and although most Ub pathways involve the degradation of the modified proteins by the proteasome, in functional terms, ubiquitination is a versatile biologic tool that modulates protein functions and regulates several cellular processes.

In a similar manner, Ubiquitin-Like proteins (UbLs), a gene family of proteins that share structural and functional similarities with ubiquitin, modify protein substrates and control several physiological processes. They constitute two different groups: Type1-Ub like proteins (which include SUMO or NEDD8), that carry a C-terminal diglycine motif required for conjugation; and Type2 Ub-Like domain proteins, which are not directly cleaved to substrates and lack the C-terminal diglycine motif (Walters et al., 2004).

1.1.1 The Ubiquitin pathway

Protein ubiquitination is a post-translational modification catalysed by E1, E2 and E3 enzymes that consists in the covalent linkage between ubiquitin and the target protein. The attachment of a single Ub molecule to the substrate is called monoubiquitination, whereas the repetition of this first conjugating process leads to the subsequent assembly of polyubiquitin chains (Pickart & Eddins, 2004). In a biochemical point of view, the first Ub molecule binds to an amino group through its C-terminal carboxyl-diglycine motif. When polyubiquitination occurs, another Ub molecule binds through its C-terminal domain to one of the seven lysine residues on the free N-

terminus of the first Ub. K-48 polyubiquitin chains trigger proteins to be degraded by the proteasome. Interestingly, the participation of deubiquitinating enzymes before protein destruction allows the release and recycle of ubiquitin molecules (Piper & Stringer, 2011), maintaining a dynamic and equilibrated system between free and conjugated ubiquitin. In contrast, K63-kinked chains are not used for proteolysis but they are frequently linked to DNA repair functions or changes in intracellular localization. Branched chains with different types of linkages can also be formed, often leading to the proteasomal degradation signalling.

In the Ub-conjugation system, the formation of an isopeptide bond between ubiquitin and the target protein is an ATP-dependent multi-step process that requires the sequential action of 3 different enzymes. First, an E1-activating enzyme hydrolyses ATP and forms a thioester bond between an internal E1 cysteine and the C-terminus of the ubiquitin protein (Haas & Rose, 1982). Then, activated ubiquitin is transferred to an E2 conjugating enzyme by a trans-thiol esterification reaction. Finally, an E3 ligase catalyses the last step of the reaction by juxtaposing a lysine residue of the substrate protein and the E2-Ub thioester (Buetow et al., 2018)(Figure 1).

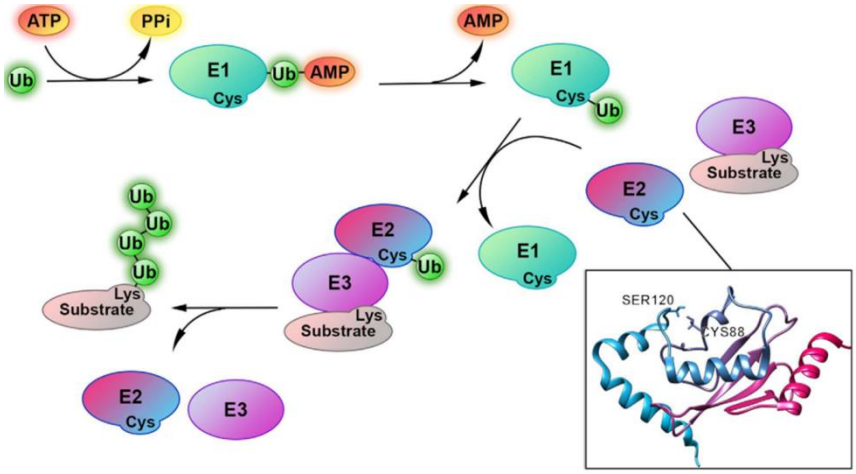

Figure 1. Ubiquitination pathway. Ubiquitination starts with the ubiquitin (green sphere) activation by an E1 enzyme in an ATP-dependent manner. Subsequently, Ub is transferred to a conserved cysteine in the E2 conjugating enzyme. Finally, the E2 catalyses the Ub transfer to the substrate lysine, forming together an isopeptide bond with the E3 ligase enzyme. Figure from (Valimberti et al., 2015).

1.1.1.1 E1 activating enzymes

E1 activating enzymes initiate the Ub-conjugation pathway and are the only components that require ATP for their activity. E1s contain three different domains: an adenylation domain that binds ATP and ubiquitin, a Catalytic Cysteine domain (CCD) that binds activated ubiquitin, and a carboxyl-terminal Ubiquitin-Fold Domain (UFD) which binds to specific E2 conjugating enzymes (Schulman, 2010).

Ubiquitin-activation itself is a three-step process that starts with the Ub-adenylation at its C-terminal glycine and the subsequent formation of an Ub-AMP intermediate. This reaction is followed by the conversion of this intermediate to a thioester bond and the final activation and adenylation of a second Ub-molecule (Haas & Rose, 1982). *Saccharomyces cerevisiae* cells have a single E1 enzyme for ubiquitin, encoded by the UBA1 gene (ubiquitin-activating enzyme E1 1), which is essential for viability (Mcgrath et al., 1991). UBA1 codes for a 114 kDa protein with two active sites that allow the recruitment of two ubiquitin molecules at the same time. One of them is bound to the adenylation domain in E1, while the second one is covalently bound to the active cysteine just before being transferred to the E2 (Schäfer et al., 2014). In contrast, two ubiquitin E1s have been identified to date in human cells, UBA1 and UBA6; which are poorly related and have distinct catalytic mechanisms (Schulman, 2010).

1.1.1.2 E2 conjugating enzymes

E2 conjugating enzymes have multiple roles apart from transferring ubiquitin or UBL molecules from E1s to E3s enzymes. In fact, it has been described that E2s also determine whether the final modified substrate becomes mono or polyubiquitinated (Windheim et al., 2008). They are characterized by the presence of a highly conserved Ubiquitin-Conjugation domain (UBC) that adopts a specific α/β-folding. It contains the E2 active site and the E3-binding site. Additionally, some E2s have N and C-terminal extensions that modulate the E2-specific functionality (M. Wenzel, K. Stoll, 2011), and few of them form part of larger multi-domain proteins.

From a biochemical point of view, once ubiquitin has been activated by an E1, it is transferred to the catalytic active Cysteine (Cys88) present in the UBC domain, generating a thioester bond. Then, the E2 catalyses the formation of an isopeptide bond between the C-terminus of Ub and a lysine residue in the substrate, in a reaction that requires the participation of an E3 ligase. E2 conjugating enzymes are critical players in the ubiquitin conjugation pathway, as they regulate the formation and the topology of poly-ubiquitin chains (Wijk & Timmers, 2010) and the processivity of these reactions (Stewart et al., 2016).

In yeast, eleven E2 ubiquitin-conjugating enzymes have been identified, including Ubc2/Rad6 and Ubc13 which are involved in DNA repair; or Cdc34, which is essential for viability and participates in the cell cycle regulation (Finley et al., 2012). Whereas the human genome encodes for more than 40 E2s, and all of them interact with a single E1 enzyme and with multiple E3s (Valimberti et al., 2015).

1.1.1.3 E3 ligase enzymes

E3 ligases are a large family of enzymes that catalyse the final step of the ubiquitin cascade. They can be classified in three different types depending on the structure of its E2-Ub binding domain

and the mechanisms of the ubiquitin transfer to the substrate (Buetow et al., 2018). The most abundant ones are the RING (Really Interesting New Gene) E3 ligases. They are characterised by the presence of a RING domain that contains conserved cysteine and histidine residues. These residues coordinate two zinc atoms that maintain the folding of the RING domain. Alternatively, the U-box structure contains a similar catalytic domain without the zinc-binding sites. Both RING and U-box domains recruit and activate E2 conjugating enzymes by forming an E2-E3 complex (Morreale & Walden, 2016). RING E3 ligases act as scaffold proteins by promoting the direct transfer of E2-Ub to the target protein (Deshaies & Joazeiro, 2009), and some of them can form multi-subunit complexes like Cullin-RING ligases (CRL) or the anaphase-promoting complex/cyclosome (APC/C) (Zheng & Shabek, 2017). In addition, STUbLs or ULS are a novel class of E3 ligases (SUMO-targeted ubiquitin ligases) containing both SIM (SUMO Interacting Motif) and RING domains. In budding yeast the STUbL complex is composed by Slx5 and Slx8 subunits, and they recognize sumoylated proteins and facilitate its ubiquitination for proteasomal degradation (Sriramachandran & Dohmen, 2014).

The second group of E3s are the HECT (homologous to the E6AP carboxyl terminus) ligases. HECT ligases contain an N-terminal specific protein binding region, which interacts with the ubiquitin charged E2, and an active C-terminal HECT domain responsible of the catalytic transfer of ubiquitin to the substrate. In contrast to RING E3s, HECT ligases form an Ub-HECT thioester intermediate through its catalytic cysteine (Zheng & Shabek, 2017), previous to the final ubiquitin transfer from the E3 to the target protein. The ligase activity of HECT E3s is tightly coordinated by the association to other regulatory proteins through its N-terminal motif, and an E2 efficient interaction.

Finally, the last group of E3 ligases are the RING-between-RING (RBR) enzymes. They contain two RING domains separated by a between-RING region (RING1-bR-RING2). Like HECT ligases, RBR ligases first recruit ubiquitin to its catalytic cysteine, forming a thioester intermediate and then transfer ubiquitin to the final acceptor (Morreale & Walden, 2016). Concretely, RING1 recruits E2-Ub and transfers ubiquitin to the active cysteine in the RING2.

Yeast cells encode tens of E3s and human cells have over 600 E3 ligases. This process needs to be tightly coordinated. Ubiquitination starts with controls on the E3-substrate interaction specificity. In this regard, several screenings have permitted to identify conserved interacting sequences in substrates targeted by specific E3 ligases (Iconomou & Saunders, 2016).

1.1.1.4 Deubiquitinating enzymes

Other important regulators of the ubiquitin system are the deubiquitinating enzymes (DUBs). DUBs are a large group of proteases that reverse ubiquitination by cleavage of ubiquitin from target substrates. Eukaryotic cells contain different families of ubiquitin specific DUBs: the Ubiquitin Carboxyl-terminal hydrolases (UCH), which hydrolyse thioester and amide bonds at the

carboxyl terminus of ubiquitin molecules (Wilkinson, 1998); the Ubiquitin-specific processing proteases (USP/UBP in yeast), which constitute the largest family of DUBs and have a highly conserved structure (Baker et al., 1992); the Ovarian Tumor-related proteases (OTU); the Ataxin-3 related to the Machado-Josephin disease (MJD); and the JAB1/MPN/Mov34 metalloenzyme (JAMM/MPN+) proteases.

In addition to their active catalytic core, DUBS contain ubiquitin-binding regions and other protein-protein interaction domains that control their functions. In fact, DUB catalytic activity or localization can be regulated by post-translational modifications such as ubiquitination, sumoylation or phosphorylation (Reyes et al., 2009).

Among their biochemical activities, DUBs are involved in the processing of Ub-precursors and in the release and recycling of polyubiquitin chains before being degraded by the proteasome (Clague et al., 2012). Remarkably, it has been reported that there is a specific regulation of deubiquitination, and that DUBs have a certain substrate-specificity (Amerik & Hochstrasser, 2004); indicating that ubiquitin conjugation and deubiquitination pathways must be tightly regulated.

1.1.2 Cellular functions

Protein post-translational modification by conjugation to ubiquitin often leads to proteasomal degradation of the targeted protein. However, ubiquitination is involved in many other cellular processes determined by the specific types of linkages with the substrate, and the topology of ubiquitin chains (Akutsu et al., 2016). In this regard, substrates can be ubiquitinated at a single or multiple lysines (mono- and multi-monoubiquitination), or forming ubiquitin chains (polyubiquitination), that can bifurcate when an Ub molecule is ubiquitinated at two or more sites forming branched chains (Figure 2).

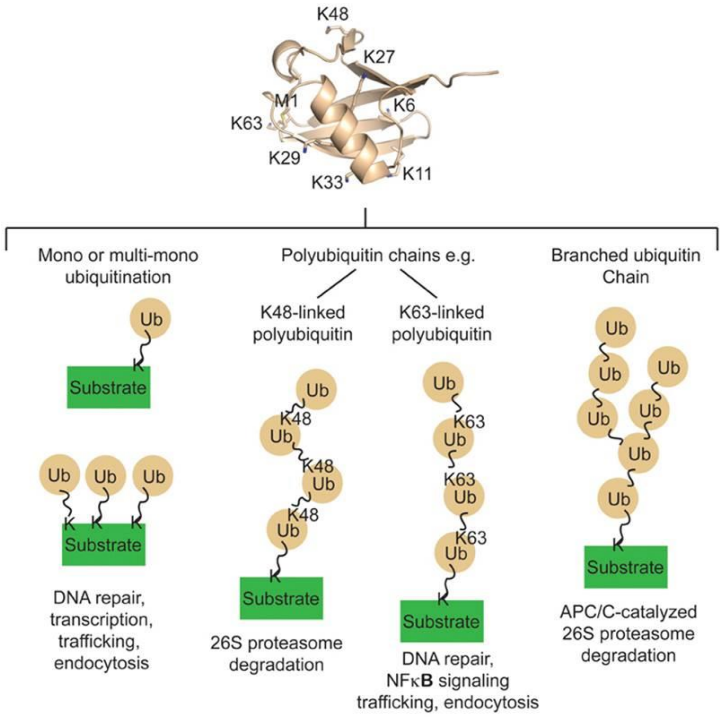

Figure 2. Substrate ubiquitination outcomes. Monoubiquitination and multi-monoubiquitination pathways are linked to DNA repair, transcription, and intracellular trafficking mechanisms. Polyubiquitin chains, can be formed linked to the K48, leading to the proteasomal degradation of the substrate; or to the K63, resulting in the activation of DNA repair, cellular trafficking or endocytosis pathways. The formation of branched ub-chains is involved in the APC/C proteasomal degradation. Figure from (Buetow et al., 2018).

In the last decades, many non-proteolytic cellular roles have been attributed to ubiquitin modifications, starting with the involvement of K63 multi-monoubiquitin chains in DNA repair (Spence et al., 1995); the implication of BRCAI-BARD ubiquitination in its tumor suppressor functions (W. Wu et al., 2008); the role of K29 linkages in the inhibition and regulation of the Wnt/β-catenin developmental pathway (Tauriello & Maurice, 2010); or the involvement of phosphorylated ubiquitin chains by PINKI in the development of Parkinson's disease (Herhaus & Dikic, 2015). In fact, ubiquitin modifications are involved in several biological processes in human cells, most of them crucial for cell viability. For this reason, they must be tightly controlled. Hence, deregulated ubiquitination can lead to several neurodegenerative pathologies such as Alzheimer, Huntington or Parkinson's diseases, and it is the responsible of a wide range of human cancers and other pathological syndromes.

In yeast cells, one of the most important roles of ubiquitin conjugation is the regulation of DNA repair and DNA-damage tolerance mechanisms. PCNA monoubiquitination rescues stalled replication forks by promoting translesion synthesis mechanisms, whereas PCNA polyubiquitination protects cells from mutagenesis by signalling an error-free lesion bypass (W. Zhang et al., 2011). Moreover, ubiquitin modifications are important in the regulation of transcription and heterochromatic silencing in buddying yeast. Therefore, K123

monoubiquitination of the histone H2B in *S. cerevisiae* cells regulates nucleosome reassembly and restores chromatin structure during Pol II transcriptional elongation (Fleming et al., 2008). During ribosomes biogenesis, ubiquitination also becomes an important regulatory modification. Hence, ubiquitination of the 40S ribosome induces the degradation of stalled ribosomes (Matsuo et al., 2017). In addition, several pre-rRNA processing factors are ubiquitinated, indicating an important role for the ubiquitin-proteasome system in ribosomal synthesis. Thus, disruption of this pathway results in multiple defects, such as an accumulation of 90S pre-ribosomes, altered Pol I gene transcription levels or a defective 90S processing and maturation (Stavreva et al., 2006). Apart from that, ubiquitin has another interesting link with ribosomes. In yeast and mammalian cells ubiquitin is encoded by four genes, UBI1, UBI2, UBI3 and UBI4. Particularly, the UBI4 gene codes for a polyubiquitin precursor formed by five ubiquitin copies in tandem, and its expression is restricted to cellular stress situations. In contrast, UBI1-UBI3 genes code for a fusion protein consisting on a single N-terminal ubiquitin fused to ribosomal proteins (Ozkaynak et al., 1987). Therefore, it has been recently suggested that ubiquitin might contribute to the efficient folding and expression of the fused ribosomal proteins (Martín-Villanueva et al., 2019).

In addition, the correct regulation of the cell cycle is also signalled by ubiquitination pathways. For instance, the 26S-mediated proteasomal degradation of several APC/C targets during mitosis mediates metaphase to anaphase transition (Ostapenko et al., 2012). Furthermore, ubiquitin modifications of transmembrane proteins trigger endocytosis and intracellular trafficking (d'Azzo et al., 2005), and can regulate protein localization.

1.2 The Sumoylation pathway

SUMOs (Small Ubiquitin-like Modifiers) are members of the evolutionarily conserved ubiquitin-like family of proteins required for viability in most eukaryotic organisms. SUMO-1, was identified as a 101 amino acid protein with homology with ubiquitin in mammalian cells (Mahajan et al., 1997). Since then, SUMO has been found covalently attached to several proteins, modifying its multiple targets and regulating various cellular processes such as DNA elongation and transcription, DNA repair or sister chromatid resolution.

Yeasts express a single SUMO paralog, named Smt3 in *S. cerevisiae*, whereas four SUMO isoforms have been found in mammalian cells: SUMO-1, SUMO-2, SUMO-3 and SUMO-4. The three-dimensional crystal of SUMO-1 reveals that although having a low sequence identity with ubiquitin, both show a similar fold (Jürgen Dohmen, 2004).

Similarly to the ubiquitin conjugation system, sumoylation involves the formation of an isopeptide bond between the C-terminal carboxyl of the SUMO protein and a lysine residue in the substrate. This pathway is catalysed by an E1 activating enzyme, an E2 conjugating enzyme and a SUMO E3 ligase; forming a cascade of enzymatic reactions.

1.2.1 SUMO conjugation

Prior to the Sumoylation pathway, SUMO proteins are translated as immature precursors. ULP in yeast or SENP in mammalian cells (ubiquitin-like protease/sentrin-specific protease) are members of a family of thiol peptidases that process SUMO precursors and also act as deconjugating enzymes (Mukhopadhyay & Dasso, 2007). Sumoylation starts with the activation of the SUMO C-terminus by a specific E1 enzyme in an ATP-dependent manner. The SUMO activating enzyme E1, composed by the two subunits AOS1/SAE1 and UBA2/SAE2, catalyses a three-step activation of SUMO. First, the E1 catalyses the adenylation of the SUMO catalytic cysteine in an ATP·Mg^{2+}-dependent manner (Lois & Lima, 2005). Next, a high-energy thioester bond is formed between UBA2 and the C-terminus of SUMO by ATP hydrolysis. Once activated, SUMO is finally transferred to the catalytic cysteine in the E2 conjugating enzyme 9 (UBC9), forming a thioester intermediate. Then, UBC9 catalyses the transfer of SUMO to the target protein in an E3 ligase-dependent manner. However, differently to the ubiquitin conjugating pathway, sumoylation can also occur in the absence of an E3 (Figure 3). When required, E3 ligases recruit E2-thioester intermediates and the substrate protein, stimulating the SUMO transfer from the E2 to the target, by the recognition of consensus motifs containing a lysine acceptor residue (Gareau & Lima, 2010), and thus, contributing to a substrate specificity.

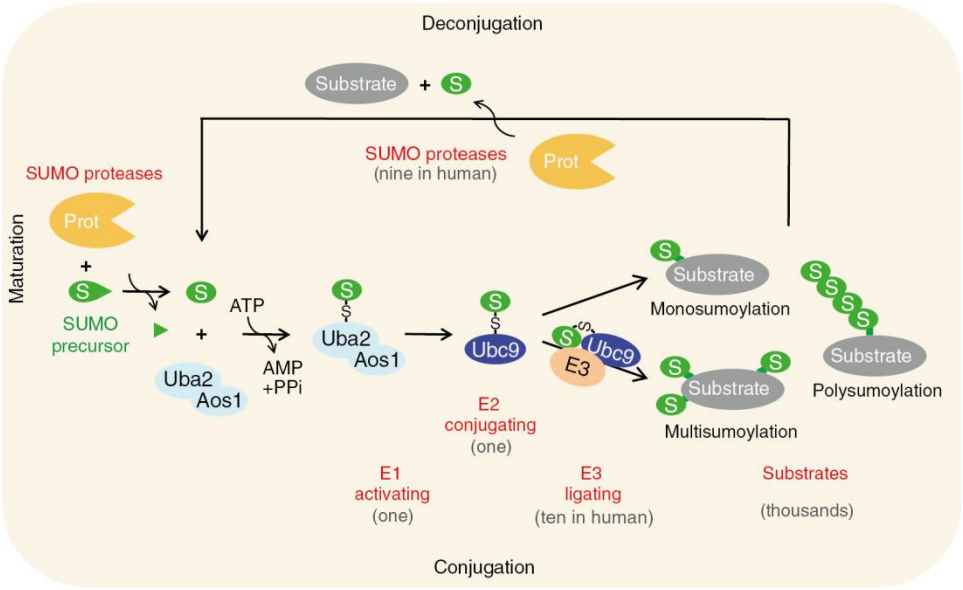

Figure 3. SUMO conjugation and deconjugation cycle. Sumoylation starts with the maturation of the SUMO precursor by specific SUMO proteases. Mature SUMO molecules are activated by an E1 enzyme (Aos1/Uba2) in an ATP-dependent reaction. Then, the SUMO molecule is transferred to an E2 conjugating enzyme (Ubc9), resulting in a thioester bond formation. Finally, SUMO is transferred by the help of an E3 ligase to the substrate. Target proteins can be mono-, multi-, or poly-sumoylated. Figure from (Pichler et al., 2017).

There are different types of E3 ligases, but most of them are members of the Siz/PIAS (protein inhibitor of STAT) family, which includes Siz1, Siz2, Zip3 and Mms21 in yeast. They contain an SP-RING domain and act in a similar way as Ub-RING E3s, stimulating and enhancing SUMO conjugation although not being essentials for sumoylation (Schmidt & Müller, 2002). In mammalian cells, other E3 ligases have been identified such as the RanBp/Nup358 or CBX proteins, which do not contain an SP-RING and mediate SUMO ligation in a distinct mechanism from the PIAS family (O Kerscher, 2016).

1.2.2 SUMO deconjugation

As it happens with ubiquitin, SUMO conjugation is a reversible process. Therefore, SUMO conjugates can be cleaved by the SUMO-specific proteases ULPs/SENPs, and removed from the target proteins. In higher eukaryotes there are six SENPs (sentrin/SUMO-specific proteases) often classified in three different groups depending on its cellular location. Nonetheless, other SUMO proteases called DeSI-1, DeSI-2 and USPL1 have been recently identified in addition to SENPS in mammals. They are also cysteine proteases but with a minor relevance and very specific targeting (Shin et al., 2012).

Yeast cells, in contrast, have only two SUMO proteases: Ulp1 and Ulp2 (ubiquitin-like protein-specific proteases). Interestingly, Ulp1 plays a dual role during sumoylation, as it matures Smt3 for SUMO conjugation by cleaving off the C-terminal sequence and exposing the diGly motif used by the E1, and mediates the de-sumoylation of nuclear and cytosolic proteins (Yeh, 2009). Whereas Ulp2 has a single isopeptidase activity and is required for the removal of SUMO chains from nuclear proteins (Bylebyl et al., 2003).

The structure of SUMO proteases is composed by a C-terminal catalytic domain required for the removal of the SUMO moiety from the substrates, and a poorly conserved N-terminal region that regulates their intracellular location, what determines the specificity of SUMO proteases for its substrates (S. Li & Hochstrasser, 2002). Moreover, they harbour putative SIM motifs that enhance protease binding to sumoylated substrates (Hickey et al., 2012).

SUMO proteases are involved in many cellular processes and have diverse functions. Consequently, their activity has to be tightly regulated. Ulp1, for instance, is an essential protein required for the efficient transition from G2 to the M phase of the cell cycle (S.-J. Li & Hochstrasser, 1999). Furthermore, the catalytic function of SENP proteases has also been linked to DNA repair through NHEJ (non-homologous end joining) and HR (homologus recombination) (Garvin et al., 2017).

1.2.3 Targets and effects of SUMO modification

Unlike ubiquitin, SUMO conjugation is not required for proteasomal destruction. However, cellular effects of SUMO modification are very versatile and depend on the nature of the target protein. Hence, sumoylation functions have been linked to DNA repair, protein interaction, the regulation of protein localization, the assembly of protein complexes by the interaction of SUMO and SIM domains (Oliver Kerscher, 2007), or to direct changes in the activities of modified substrates (Gareau & Lima, 2010). In fact, SUMO acts synergistically on several proteins, and it has been proposed to target and modify a protein group rather than singular proteins (Psakhye & Jentsch, 2012).

SUMO conjugates appear to be enriched at nuclear structures, modifying proteins with important roles in the regulation of chromatin structure and the maintenance of genome integrity (Zhao, 2018). Moreover, since early findings involved SUMO with the RanGAP1 nuclear translocation, sumoylation has been also shown to play an important role in nucleoplasmatic trafficking (Stade et al., 2002). In addition, studies in the tumor suppressor PML (Promyelocytic leukemia) demonstrated that PML sumoylation is necessary for the recruitment of other protein partners and in the PML-Nuclear Body formation, implicated in the genome maintenance and senescence induction (Ivanschitz et al., 2013).

Furthermore, sumoylation plays also an important role in transcriptional control. In most cases, sumoylation of different transcription factors and histones is associated with a transcriptional repression, thereby modulating gene expression (Rosonina et al., 2017).

Other nuclear consequences of SUMO conjugation are important during mitosis. Indeed, sumoylation of centromeric proteins, like the Topoisomerase II (Top2), activate a mitotic checkpoint important for the proper mitotic progression and for achieving a correct chromosome segregation (Yoshida & Azuma, 2016). In addition, sumoylation of PCNA at DNA damaged sites has been found to prevent DSB formation and to promote an error-free DNA damage replication process (Gali et al., 2012), thus, revealing an important function for sumoylation in providing genome stability and DNA repair.

1.3 SMC complexes

The Structural Maintenance of Chromosomes (SMC) complexes, which include cohesin, condensin and the Smc5/6 complex in eukaryotic cells, participate in multiple chromosomal activities controlling sister chromatid cohesion, chromosome condensation and DNA segregation and repair (Jeppsson, Kanno, et al., 2014).

The structure of SMC proteins is evolutionary conserved. They consist of a central hinge domain flanked by two coiled coil motifs and two nucleotide binding domains: an N-terminal walker A and

a C-terminal walker B (Hirano, 2002) (Figure 4A). An electron microscopy study described that the two coiled coils are orientated in a self-folded antiparallel arrangement (Melby et al., 1998) which joins the N and C-terminal globular domains forming an ATP binding site. SMC complexes dimerize through their hinge domain. Then, other non SMC proteins bind to the heterodimer to regulate its activity. One of them, a subunit member of the kleisin family, connects the two ATPase heads forming a ring-shaped structure that will be eventually loaded onto DNA. In SMC complexes, their catalytic domain suffers conformational changes in an ATP-dependent manner: ATP binding induces ATPase heads engagement in SMC complexes, and ATP hydrolysis leads to its dissociation (Hirano, 2002).

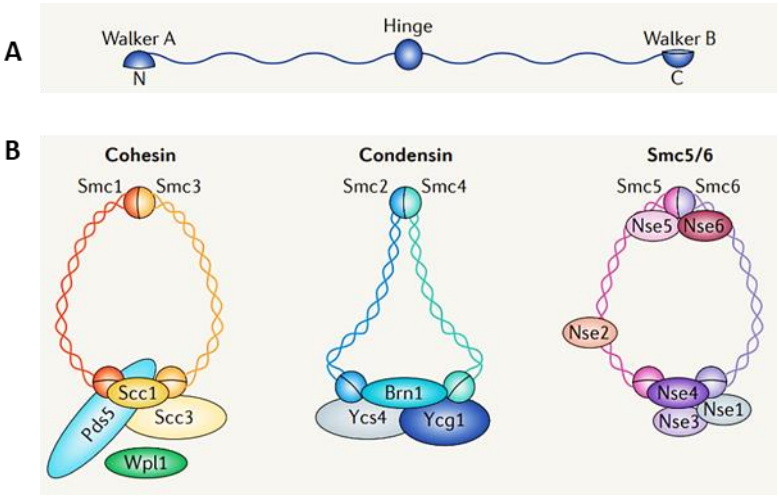

Figure 4. The SMC family of proteins. (A) Schematic representation of the different domains present in Smc proteins: an N-terminal Walker A, a central hinge region and the C-terminus Walker B domain. **(B)** Composition and molecular structure of the different SMC complexes associated with its Nse proteins: cohesin, condensin and the Smc5/6 complex**.** Figures from (Jeppsson, Kanno, et al., 2014)

The SMC family of proteins is present in all domains of life and they are essential for growth. Bacterial cells present only a single SMC protein which forms homodimers, whereas eukaryotes have six different SMC proteins, forming heterodimers at the core of the cohesin, condensin and Smc5/6 complex (Hirano, 2005) (Figure 4B).

1.3.1 Cohesin

Cohesin is a multi-protein complex composed by four subunits: Smc1, Smc3, and two non-smc proteins: the Scc1/Rad21 α-kleisin subunit and Scc3. These four subunits can topologically engage chromatin and control chromosome organization.

The main role of the cohesin complex is to regulate sister chromatid cohesion during cell division until anaphase, when chromatids segregate to opposite poles of the mitotic spindle (Losada et al.,

1998). However, it has been reported that cohesin also participates in many other chromosomal activities such as DNA damage repair (Litwin et al., 2018) or in the regulation of gene expression (Dorsett & Merkenschlager, 2013).

Association of Smc1 and Smc3 with Scc1 subunit forms a tripartite ring that entraps DNA. During G1, the chromosomal loading of the cohesin ring requires ATP hydrolysis mediated by the Scc2-Scc4 loader complex (NIPBL-MAU2 in mammals) (Arumugam et al., 2003). In the replication phase, cohesion between both sister chromatids needs to be established. For that, the cohesin acetyltransferase Eco1, acetylates two DNA sensing lysines (K112 and K113) of the Smc3 ATPase head, which results in the establishment of sister chromatid cohesion (Ben-shahar et al., 2008). Along the cell cycle, cohesin can associate with Wpl1/Wap1 and Pds5 partners to enable its dissociation from the DNA (Figure 5). Moreover, apart from acetylation, other modifications have been proposed to regulate cohesin activity, such as phosphorylation or sumoylation. In *S. cerevisiae* for example, the core components of the cohesin complex Smc1-Smc3 and its associated factors Scc1, Scc3 and Pds5 are sumoylated during the S phase, independently on Smc3 acetylation. Thus, cohesin Sumoylation is also needed in budding yeast for sister chromatid cohesion establishment (Almedawar et al., 2012).

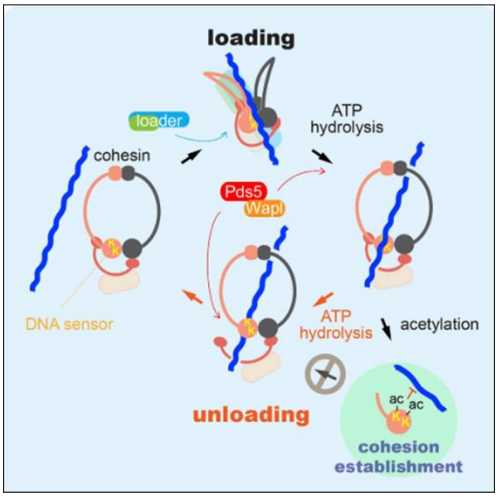

Figure 5. Model for cohesin loading and unloading onto DNA. DNA-sensing lysines in Smc3 trigger ATP hydrolysis to open the SMC head interface, facilitating cohesin loading onto chromatin. Whereas Wapl disengages the kleisin subunit after ATP binding, thus permitting DNA exit. Figure from (Murayama & Uhlmann, 2015).

Interestingly, recent studies have demonstrated that the ATPase heads can adopt two different states *in vivo*: a canonical one in which the heads remain engaged (E heads), or a juxtaposed one, in which the heads are rotated in the presence of ATP (J heads) (Figure 6). These two states occur throughout the cell cycle and create different compartments that entrap DNA. However, acetylation of Smc3 during S phase is more frequent in the J-head conformation, indicating that sister DNA entrapment in the kleisin space may be a chromatid cohesion feature throughout the genome (Chapard et al., 2019).

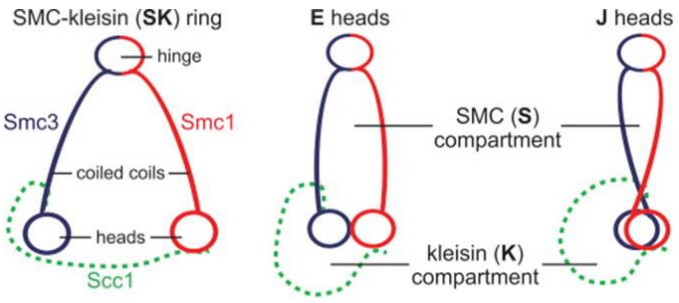

Figure 6. Schematic representation of the cohesin compartments. Figure from (Chapard et al., 2019)

1.3.2 Condensin

Condensin was first characterized in *S. cerevisiae* as a nuclear SMC complex essential for cell growth and chromosome segregation. SMC2, which forms the core of the condensin complex together with SMC4, was defined as a new gene functionally related with SMC1 but with non-redundant roles in the maintenance of genome stability (Strunnikov et al., 1995). Thus, its biological function in compacting DNA in condensed chromosomes during mitosis and meiosis defined condensin as a new subgroup of SMC proteins.

The condensin complex is formed by the Smc2-Smc4 coiled-coil ATPases and three regulatory proteins named Ycs4, Ycg1 and Brn1 in budding yeast. The kleisin subunit Brn1 binds to the end of the ATPase domains and recruits Ycs4 and Ycg1 to the condensin ring. These accessory proteins coordinate the activity of the complex.

In vertebrates, two different condensin isoforms have been identified, called condensin I and condensin II. Yeast cells, in contrast, only have one condensin complex, which is similar to condensin I in mammals (Hirano, 2012). Condensin I and II have distinct roles in organizing mitotic chromosomes. Specifically, condensin II compacts chromosomes axially during early prophase, and when missing, chromatids loss rigidity and become bent and twisted. In contrast, condensin I is conserved from yeast to humans; it associates with chromosomes in prometaphase and plays a predominant role in chromosome assembly (Green et al., 2012). Therefore, its loss destabilizes condensation of chromatin loops.

1.3.3 SMC5/6 Complex

First discovered in fission yeast, the Smc5/6 is the latest SMC complex described and the most unknown. It contains eight subunits: Smc5 and Smc6, which constitute the core of the complex, and six non-smc subunits (Nse proteins), from Nse1 to Nse6. Smc5/6, as the other SMC complexes, plays an important role in maintaining the integrity of the genome. Specifically, the Smc5/6 complex is involved in chromosome replication, segregation and repair mechanisms (Figure 7).

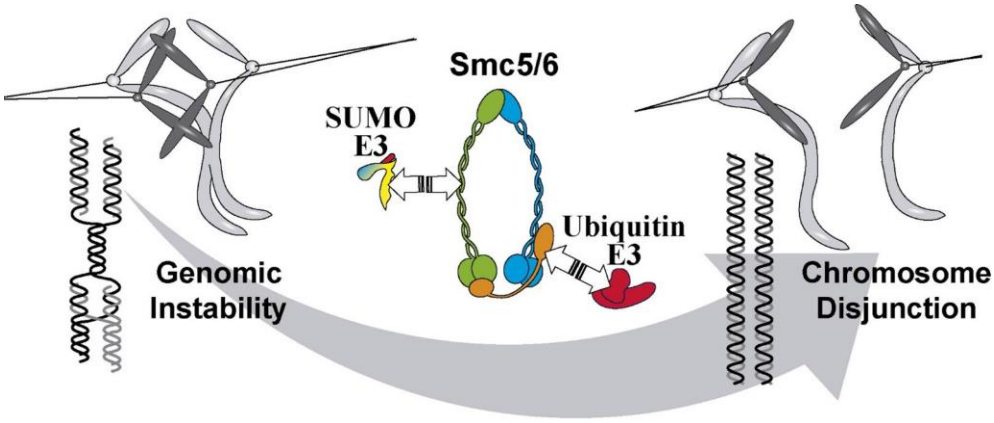

Figure 7. Overall view of the Smc5/6 complex and its role in the maintenance of the genome integrity.

Smc6 was first identified in *Schizosaccharomyces pombe* as Rad18, an essential gene necessary for DNA damage repair (Lehmann et al., 1995). Later, Smc5 (Spr18 in fission yeast) was described as the partner of Smc6 (Fousteri & Lehmann, 2000), forming together a high molecular-weight complex (Sergeant et al., 2005). The Smc5-Smc6 heterodimer has ATPase activity and binds to chromosomal DNA *in vivo* through different binding domains in order to perform its functions (Roy et al., 2015).

Nse4 is the Kleisin subunit of the complex and binds to the neck region in Smc6, and to the ATPase domain in Smc5. Nse4 also interacts with Nse1 and Nse3 to form a stable subcomplex that mediates the chromatin association of the entire holocomplex. Nse3 is a member of the MAGE (melanoma-associated antigen) family of proteins, which is highly conserved; whereas Nse4 belongs to the EID (E1A-like inhibitor of differentiation) family (Hudson et al., 2011). The third component of the Nse1-Nse3-Nse4 subcomplex, Nse1, is a RING finger protein that has ubiquitin E3 ligase activity. The Nse1-Nse3 pair binds to DNA through highly conserved positive residues that confer a DNA binding surface in Nse3 (Zabrady et al., 2016). The interaction with DNA regulates the loading of the complex on chromatin.

The Nse5 and Nse6 dimer associates with the ATPase heads of Smc5 and Smc6 in *S. pombe*, and to the coiled coil near ATPase in humans. Both subunits are required for viability in budding yeast but not in fission yeast. In higher eukaryotes Nse5 and Nse6 homologues (Slf1 and Slf2) promote Smc5/6 recruitment to DNA damaged sites (Räschle et al., 2015).

Finally, the Nse2/Mms21 subunit binds to the Smc5 coiled coil domain. Its C-terminus codes for an SP-RING (Siz/PIAS RING) domain with SUMO (small ubiquitin-like modifier) ligase activity (Andrews et al., 2005) (Zhao & Blobel, 2005) (Potts & Yu, 2005). Although Nse2 is essential for viability, deletion of its SP-RING motif is not lethal (Zhao & Blobel, 2005). However, mutations in the SUMO ligase domain confer sensitivity to DNA damaging agents such as hydroxyurea (HU), methyl methanesulfonate (MMS), ultraviolet light (UV) or ionizing radiation (IR) (Andrews et al., 2005) (Zhao & Blobel, 2005) (Potts & Yu, 2005); thus, indicating an important role for the sumoylation activity of Nse2 in the DNA damage response.

1.3.3.1 E3 ligases in the SMC5/6 complex

As mentioned, the Smc5/6 complex contains two RING-type E3 enzymes: the Nse1 ubiquitin ligase and the Nse2 SUMO ligase. The main role of the RING domain is to mediate protein-protein interactions. In the context of ubiquitin-like modifiers, the RING domain mediates the transfer of ubiquitin or SUMO molecules from the E2 conjugating enzyme to the substrate protein.

For Nse2/Mms21, the E3 catalytic activity is an SP-RING in its C-terminal domain with a SUMO ligase activity observed both *in vivo* and *in vitro,* first described in *S. cerevisiae* (Zhao & Blobel, 2005), in *S. pombe* (Andrews et al., 2005), and in human cells (Potts & Yu, 2005). Whereas Nse1 contains a C-terminal RING-like motif that confers ubiquitin E3 ligase activity *in vitro,* and the recruitment of Smc5/6 to DNA lesions (Pebernard, Perry, et al., 2008). Both genes are essential, they are conserved from yeast to humans, and the loss of function of its E3 catalytic activity sensitizes cells to DNA damage (McDonald et al., 2003).

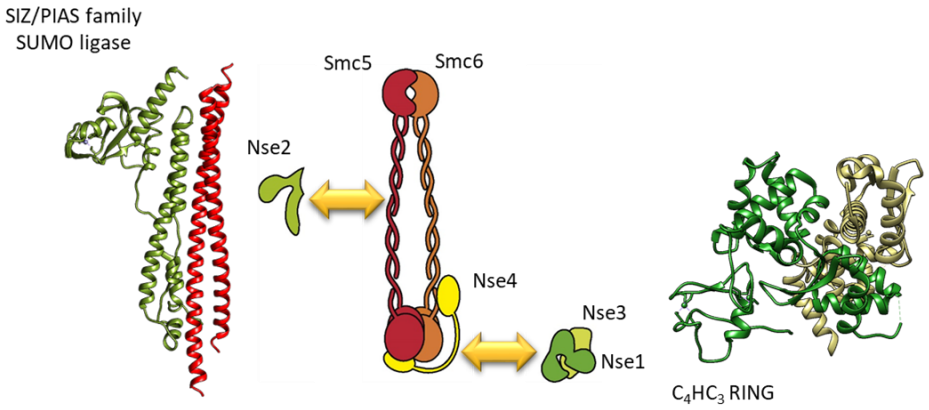

Figure 8. Schematic representation of the Smc5/6 complex and its two RING-type subunits. Smc5 (in red) together with Smc6 (in orange) form the core of the complex. Nse2 and Nse1 E3 ligases are shown in green. Nse3 (in yellow) functions as a cofactor of the Nse1 ubiquitin ligase. The kleisin subunit Nse4 is indicated in yellow.

1.3.3.1.1 NSE1 ubiquitin ligase

The Nse1 ubiquitin ligase was first identified as a novel non-smc protein in the *S. cerevisiae* Smc5/6 complex (Fujioka, 2002) containing a RING-like finger motif; what presumably suggested that it could have catalytic activity. RINGs are cysteine or histidine rich domains that coordinate two zinc-atoms in a cross-brace conformation (Borden, 2000). Particularly, the RING finger domain of Nse1 is different from other variants, and forms a new subclass, called NH-RING, that is evolutionarily conserved across different Nse1 homologues (Pebernard, Perry, et al., 2008). It is composed by a central β-sheet, an α-helix and two zinc-binding sites. Interestingly, NH-RINGs contain the C_4HC_3 RING consensus, closely related to the PHD motif (plant homology domain) and different from the conventional C_3HC_4 consensus found in other RING domains.

Although mutants in the RING domain are viable, it has been demonstrated that this domain promotes DNA repair functions in the Smc5/6 complex (Pebernard, Perry, et al., 2008). Thus, *nse1* thermosensitive mutations compromise genomic stability in *S. cerevisiae* yeast cells. Specifically, the *nse1-101* mutant containing three amino acid changes (G175E, S207T and G332D) arrests in the G2/M phase of the cell cycle at the restrictive temperature, displays UV and MMS sensitivity at permissive temperatures and is defective in postreplication repair (PRR) in UV-irradiated DNA (Santa Maria et al., 2007). *nse1-C274A* mutant cells, carrying a mutation in the RING domain that presumably unfolds its structure, show an aberrant morphology and have severe growth defects at 30ºC and also under DNA damaging conditions (Santa Maria et al., 2007).

Other isolated mutations have been studied for Nse1 such as the substitution of H306 and C309 zinc coordinating residues to alanines. Both residues are located in the C-terminal RING domain and are highly conserved in evolution. *nse1-H306A,C309A* double mutant cells are sensitive to genotoxic stress and defective in the interaction with Nse3 and other subunits of the Smc5/6 complex (Wani et al., 2018).

In human cells, it has been described that Nse1 ubiquitinates its MAGE-G1 *in vitro* and that its E3 ligase activity is enhanced by Nse3 (Doyle et al., 2010) (Kozakova et al., 2015). Other studies also describe a role for the human Nse1 in targeting the cytosolic iron-sulfur assembly (CIA) component MMS19 for its ubiquitination and degradation (Weon et al., 2018). Remarkably, in this case, Nse1 associates with a different MAGE, MAGE-F1. MAGE-F1 does not interact with Smc5 or Smc6, and it forms an alternative complex together with Nse1; which diversifies Nse1 E3 ligase activities outside the Smc5/6 complex.

Hence, it seems that the E3 ligase activity of Nse1 displays an important role in maintaining the integrity of the genome. However, no more targets for Nse1 have been described until now, and its ubiquitin ligase activity in yeast has been never characterized (Pebernard, Perry, et al., 2008).

1.3.3.1.2 NSE2/MMS21 SUMO ligase

Nse2, initially named Mms21, was first characterized in a study performed in 1977 in which MMS-sensitive mutants of *S. cerevisiae* were isolated (Prakash & Prakash, 1977). Many years later, Nse2 was described as a SUMO E3 ligase (Andrews et al., 2005) (Zhao & Blobel, 2005) (Potts & Yu, 2005), being the RING domain essential for its E3 ligase activity *in vitro.* Various sumoylation targets of Nse2 have been described until now (recently reviewed in (Solé-Soler & Torres-Rosell, 2020)). For example, Smc5 appears to be sumoylated both *in vivo and in vitro* by Mms21. Interestingly, Smc5/6 dependent sumoylation also regulates the cohesin complex (Almedawar et al., 2012) (N. Wu et al., 2012). Moreover, Nse2 sumoylates STR (Sgs1-Top3-Rmi1) components to regulate its recombination activity (Bermúdez & Aragón, 2017), which is involved in the dissolution of double Holliday junctions (dHJ) permitting a correct mitotic segregation (Bonner et al., 2016).

The structure of Nse2 in complex with its binding site in Smc5 shows that it uses its N-terminal domain for docking onto the coiled coil domain of Smc5 (Figure 9A). When this interaction is perturbed, cells have growth defects and are sensitive to DNA damage (Duan et al., 2009) (Bermúdez-López et al., 2015). In contrast, the C-terminal part of the protein, which contains the SUMO ligase domain, is not essential for viability. Despite this, the SUMO ligase activity of Nse2 has a role in the chromosome recombination and sister chromatid resolution (Bermúdez-López et al., 2015).

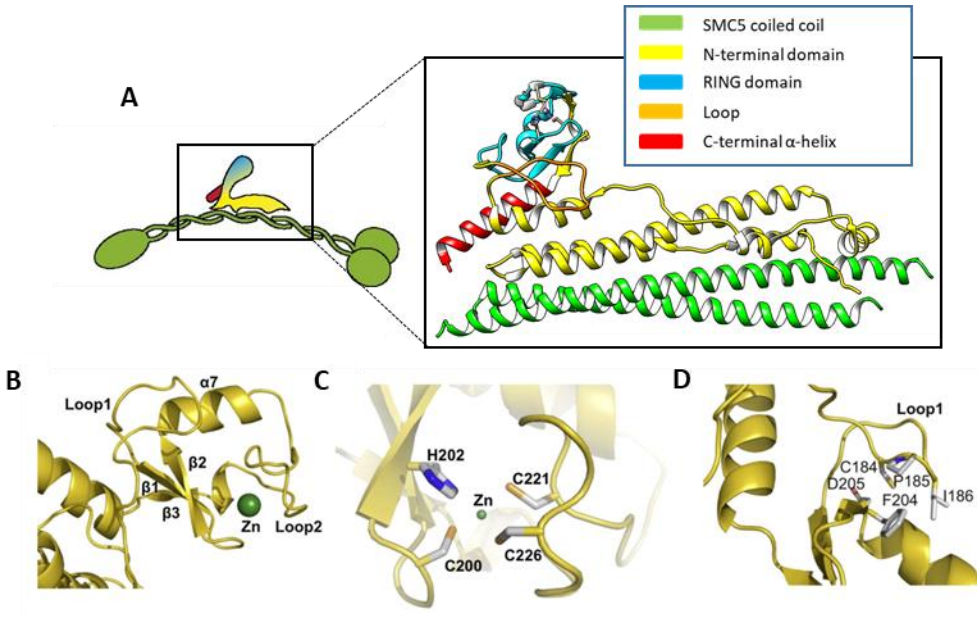

Figure 9. Nse2 structure. (A) Schematic representation of the Nse2 binding to the ARM domain of Smc5 (in green). The N-terminal (in yellow), C-terminal (in red), loop (in orange) and RING domain (in blue) of Nse2 are indicated. **(B)** Structure of the SP-RING of Nse2, containing two loops, three beta sheets, a short helix and a zinc atom in green. **(C)** View of the central zinc ion coordinated by the histidine H202 and the cysteines C200, C221 and C226. **(D)** View of the coordination of the loop 1 by the indicated residues. B, C and D figures from (Duan et al., 2009).

From a structural point of view, the SP-RING is composed of two loops (loop1 and loop2), one of them coordinating a zinc atom and the other stabilized by five conserved residues; one short helix (α7) and three β sheets (β1-3) (Duan et al., 2009) (see Figure 9B).

In human cells, *NSMCE2* (the homologous human gene for NSE2) plays a key role in the maintenance of the genome. Among other functions, Nsmce2 prevents mitotic DNA damage from replication stress (Pond et al., 2018) and participates in resolving TOP2A-mediated DSB-repair intermediates produced during replication (Verver et al., 2016). Consequently, mutations in the *NSMCE2* gene or its related pathways may result in severe abnormalities and human diseases.

The Bloom syndrome (BS) is one of the pathologies potentially linked to *NSMCE2*, and is characterized by a growth deficiency, progeria, immune failure, insulin resistance, and a major cancer incidence. It is caused by the loss of function of the bloom helicase BLM (the SGS1 homolog in human cells) (Cunniff et al., 2017). BLM is sumoylated in an *NSMCE2*-dependent manner. SUMO modification regulates BLM functions in homologous recombination (HR) and in repair of damaged replication forks (Ouyang et al., 2009). Two studies have recently shown that auto-sumoylated Smc5/6 complexes recruit STR subunits (Bermúdez-López et al., 2016), and that Nse2-dependent sumoylation of Sgs1 and Top3 activates the STR recombinogenic function (Bermúdez & Aragón, 2017) (Pond et al., 2018) (Bonner et al., 2016).

Nonetheless, it has been described that *NSMCE2* SUMO ligase activity is not essential for mice development. In contrast, *NSMCE2*-deficiency in adult mice results in an accelerated aging, a decreased lifespan and an increased tumor incidence, which are pathological hallmarks of the BS (Jacome et al., 2015). Despite this, Jacome and co-workers demonstrated that *NSMCE2* activity was independent of BLM in these cells.

Besides, the characterization of two unrelated female patients with shared pathologies (growth impairment, insulin resistance and gonadal failure) has allowed the identification of mutations in *NSMCE2* related with their clinical features, and the description of a novel syndrome of primordial dwarfism. Both patients carried two different frameshift mutations in *NSMCE2*: one of them, p.Ser116Leufs*18, is located a few residues before the RING domain and results in the truncation of the C-terminal part of the gene; whereas the p.Ala234Glufs*4 mutation maintains an intact RING domain and carries a deletion of the last 14 amino acid of the protein, disrupting the C-terminal α-helix (Payne et al., 2014). Apparently, these mutations result in lower levels of *NSMCE2* and auto-sumoylation deficiencies for the p.Ser116Leufs*18 mutants *in vitro.*

Moreover, the *in vivo NSMCE2/MMS21* deficiency in zebrafish causes a dwarf phenotype that can be rescued by a wild type (WT) *NSMCE2* mRNA but not with the SUMO-deficient mRNA variant identified in the patients (Payne et al., 2014). Together, these results link the loss of function of *NSMCE2* with primordial dwarfism, possibly due to the impaired ability of the *NSMCE2*-deficient cells to deal with replicative stress and associated DNA damage, as proposed Payne *et al.*

1.3.3.2 SMC5/6 functions

Smc5/6 wide variety of chromosomal activities place the complex at the center of the regulation of genomic stability. In this regard, Smc5/6 plethora of genomic functions encompass DNA repair, replication fork stability, telomere maintenance and chromosome segregation. However, novel publications have attributed other roles to the Smc5/6 complex beyond its classical implication in DNA repair. Notably, as reviewed in (Aragón, 2018), Smc5/6 has been recently associated with the inhibition of viral genome transcription and with human diseases.

1.3.3.2.1 SMC5/6 functions in DNA damage repair

Initially, Rad18 (Smc6 in *S. cerevisiae*) functions in *S. pombe* were linked to DNA damage repair. Thus, Lehmann *et al.* described Rad18 as a conserved gene involved in DNA replication and required for excision repair (Lehmann et al., 1995). In addition, many authors have demonstrated that mutations in all subunits of the complex exhibit DNA damage sensitivity and defects in DNA repair; such as *smc5-6* or *smc6-9* conditional mutants (Torres-Rosell et al., 2005), *nse1-101* and *nse1-C274A* point mutations (Santa Maria et al., 2007), *mms21-1* (Prakash & Prakash, 1977) or *nse4-ts* (Hu et al., 2005) thermosensitive mutants. Interestingly, epistasis analysis with RAD51 and RAD52 genes, involved in homologous pairing during recombination, indicated a role for the Smc5/6 complex in DNA repair by homologus recombination (HR) (Lehmann et al., 1995) (McDonald et al., 2003). In addition, many studies have shown that Smc5/6 complexes are enriched in double strand breaks (DSBs), and its inactivation leads to reduced sister-chromatid recombination (De Piccoli et al., 2006). In fact, both cohesin and the Smc5/6 complex are recruited to DSBs (Lindroos et al., 2006). Cohesin facilitates repair by holding sister chromatids together, whereas the Smc5/6 complex assists the HR-mediated repair of DNA lesions (Lindroos et al., 2006) (Figure 10A). Remarkably, in addition to its direct role in promoting sister chromatid recombination at DSBs, Smc5/6 complex Nse2-dependent sumoylation of cohesin is needed for sister chromatid resolution in response to DNA damage (McAleenan et al., 2012) (N. Wu et al., 2012). Cohesin becomes sumoylated mainly at its Scc1 α-kleisin subunit by Nse2 upon exposure to DNA damage, which is a prerequisite for DNA cohesion at DSB-proximal regions (McAleenan et al., 2012) (Figure 10A). However, such modification does not only occur during DNA damage events, but also under unperturbed conditions. Hence, Nse2-dependent SUMO modification of cohesin is also required for the entrapment of sister chromatids at undamaged cells (Almedawar et al., 2012).

Remarkably, the Smc5/6 complex is also able to activate mechanisms to tolerate lesions produced by different DNA damaging agents, such as DNA fragmentations produced by the alkylating agent methyl-methanesulfonate (MMS). In fact, the Smc5/6 complex responds to a wide variety of genotoxic agents, such as hydroxyurea (HU), ultraviolet light (UV) or camptothecin (CPT) (A. Kegel & Sjögren, 2010). Particularly, MMS treatment blocks nucleotide incorporation, inhibiting replication elongation and threatening the integrity of the genome (Groth et al., 2010).

Interestingly, after exposure to MMS, yeast cells respond to this stressful stimulus by enhancing Smc5/6 sumoylation, suggesting that this modification participates in the MMS-induced DNA repair (Andrews et al., 2005). In this regard, it has also been reported that Nse2-dependent sumoylation is required to counteract aberrant recombination structures at MMS-stalled replication forks (Branzei et al., 2006). The subnuclear localization of the Smc5/6 complex changes upon genotoxic stresses, and Nse2-dependent sumoylation of Nse4 promotes its MMS-induced subtelomeric accumulation (Pebernard, Schaffer, et al., 2008). In addition, we have recently shown that Smc5 is specifically sumoylated in response to MMS under damaged replication forks conditions. Thus, in order to prevent the use of more mutagenic pathways, Smc5-sumoylation relieves Mph1 inactivation promoting fork regression at damaged sites (Zapatka et al., 2019). Overall, published data show that the Smc5/6 complex uses different mechanisms at damaged replication forks to bypass lesions and preserve genomic stability.

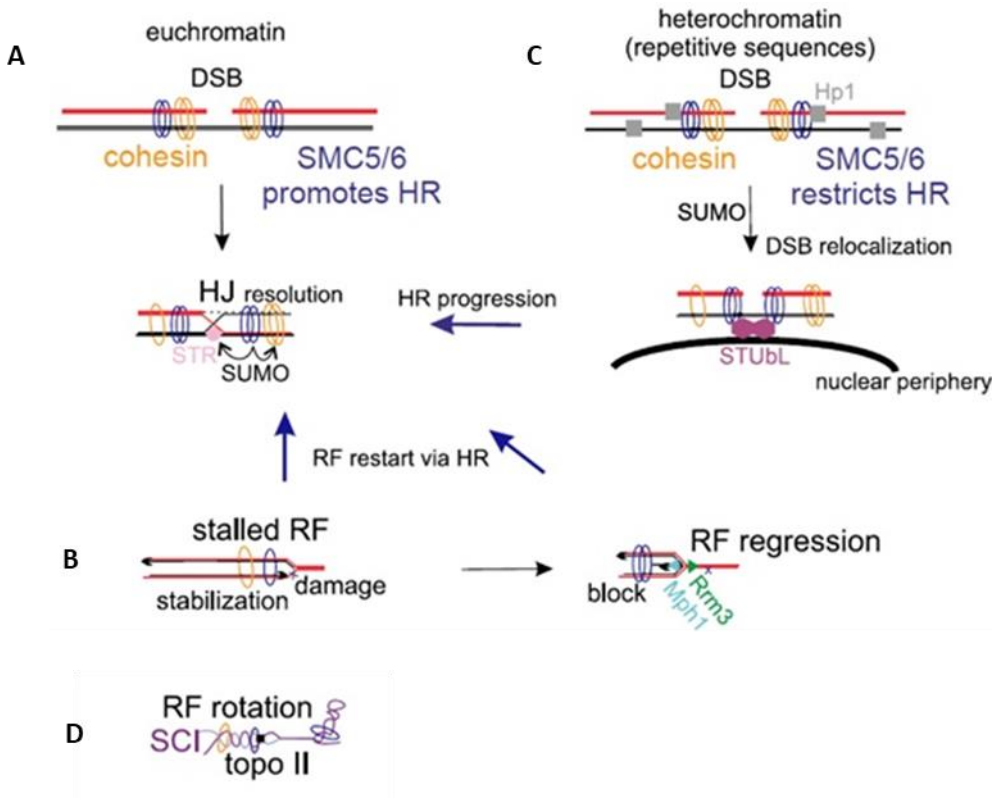

Figure 10. Roles for the Smc5/6 complex in the maintenance of genomic stability. (A) SMC5/6 (blue ring) promotes HR repair at DSB by different mechanisms. First, Smc5/6-dependent cohesin (yellow ring) sumoylation upon DNA damage maintains cohesion at chromatin lesions. Then, Smc5/6 sumoylates the STR complex (pink circle), that promotes dHJ resolution. **(B)** At a stalled replication fork, Smc5/6 promotes it restart via HR (blue arrows). Smc5/6 stabilizes replication forks and inhibits Mph1-mediated fork regression. Rrm3 permits replication at rDNA pausing sites**. (C)** SMC5/6 binds to Hp1 (grey square) and blocks HR. Nse2-dependent sumoylation promotes the transient relocalization of the DSB to the nuclear periphery, where Smc5/6 interacts with the STUbL complex (violet hexagons); that promotes HR progression (blue arrow). **(D)** SMC5/6 promotes fork rotation to relax superhelical tensions by stabilizing SCIs during replication. Figure from (Palecek, 2019).

1.3.3.2.2 SMC5/6 functions in DNA replication and chromosome segregation

Several studies have reported that Smc5/6 functions are important for assisting the DNA replication machinery and for the removal of toxic replication structures. This is evidenced by the hypersensitivity of *smc5/6* mutants to MMS or HU, drugs that block replication forks; and by the accumulation of recombination intermediates in cells with compromised *smc5/6* functions.

In response to DNA damage or replication stress, cells may accumulate stalled forks and X-shaped DNA structures, collectively referred to as sister chromatid junctions (SCJs) (Liberi et al., 2005). During mitosis, the two sister chromatids resulting from DNA replication are pulled to opposite poles of the mitotic spindle. To this end, cells have to previously remove any physical interactions between their sister chromatids. The removal of SCJs requires the orchestrated action of several nucleases and helicases, including the Bloom helicase BLM/Sgs1. Interestingly, loss of Smc5/6 function or its SUMO ligase activity lead to segregation defects and an accumulation of SCJs (Bermudez-Lopez et al., 2010), indicating an important role for the Smc5/6 complex in the resolution of these intermediates. Smc5/6 mediates the sumoylation of the Sgs1-Top3-Rmi1 (STR) complex, which dissolves X-shaped DNA structures during S phase (Figures 10B, A) (Bonner et al., 2016) (Bermúdez-López et al., 2016). In addition, Smc5/6 inhibits the fork regression activity of Mph1, the buddying yeast homolog of the human Fanconi anemia protein M (FANCM), further suppressing the accumulation of X-shaped DNA intermediates (Y. H. Chen et al., 2009). Hence Smc5/6 counteracts recombination using at least two different mechanisms, one involving the SUMO-mediated regulation of the STR complex and the other one the direct inhibition of the Mph1 motor protein (X. P. Peng et al., 2018).

Remarkably, further studies have revealed that the replication process is specially challenged at the highly transcribed rDNA locus. As previously published, Smc5/6 is enriched at the rDNA repetitive regions, and has an important role in preventing accumulation of Holliday junctions and ongoing replication forks, thus ensuring rDNA segregation (Torres-Rosell et al., 2005). Indeed, buddying yeast *smc5/6* mutants exhibit rDNA nondisjunction phenotypes as a consequence of mitotic entry with unfinished replication (Torres-Rosell, De Piccoli, et al., 2007). Thus, when Smc5/6 complex functions are compromised, cells fail to overcome the DNA replication obstacles present in each repetitive region. Moreover, the Smc5/6 complex is also involved in the recombinational repair of DSB in rDNA repeats. The Smc5/6 complex promotes the transient relocalization of the lesion to an extranucleolar compartment before its association with the recombination machinery (Torres-Rosell, Sunjevaric, et al., 2007). Outside heterochromatin, Smc5/6 interacts with the SUMO-targeted ubiquitin-ligase (STUbL/RENi) complex that in turn, promotes HR progression (Figure 10C).

Overall, although the detailed mechanisms used by the Smc5/6 complex during DNA replication and segregation remain to be deciphered; they might be probably related with the regulation of superhelical tensions at replication forks. In this regard, it has been suggested that the Smc5/6 complex chromosomal association promotes fork rotation in sister chromatids to relax topological

tensions by stabilizing sister chromatid intertwines (SCIs) during replication (Figure 10D) (Andreas Kegel et al., 2011).

1.3.3.2.3 Novel roles of Smc5/6

Although the Smc5/6 complex is the most unknown member of the SMC family, its potential role in the maintenance of the genomic integrity has aroused a general interest in many researchers. Therefore, recent data about possible new functions of the complex that have not been previously described are providing new information to the field. These novel roles include the transcription inhibition of viral genomes and its relation to human pathologies.

Interestingly, recent publications indicate a potential function for the Smc5/6 complex in the transcription inhibition of the Hepatitis B Virus (HBV) (Murphy et al., 2016) (Decorsière et al., 2016). The HBV regulatory protein HBX promotes the expression of the viral genome in an HBV human infection by enhancing transcription in extrachromosomal DNA templates. For that, HBX binds to DNA binding protein 1 (DDB1), which assembles a larger E3 ubiquitin ligase complex that targets Smc5/6 for degradation (Murphy et al., 2016). Indeed, the Smc5/6 complex has been reported to repress viral transcription and HBV gene expression in human cells in a still undefined process (Murphy et al., 2016) (Decorsière et al., 2016).

Finally, it has been recently shown that alterations in the Smc5/6 complex in human cells lead to severe genetic abnormalities, such as the previously explained *NSMCE2*–associated primordial dwarfism syndrome. Moreover, recent studies have demonstrated that destabilization of the Smc5/6 complex is associated with a chromosome breakage syndrome that leads to a severe lung disease (van der Crabben et al., 2016). In addition, very recent published results suggest a link between Smc5/6 functions with the Fanconi Anemia pathway (FA) in the maintenance of the genome integrity (Rossi et al., 2020). Overall, these data also suggest an important role for the Smc5/6 complex in mammalian cells, as its deregulation has been associated to a broad spectrum of human pathologies.

1.4 DNA transcription

In molecular biology, DNA transcription is the primary step in gene expression. In general terms, transcription is the process by which our cells copy their genetic information from a DNA template sequence and synthesize a complementary RNA copy or transcript. Eukaryotic transcription, in contrast to the prokaryotic process, relies on three different enzymes synthesizing different RNA precursors. Accordingly, RNA Polymerase I (Pol I) transcribes ribosomal RNA, the main catalytic component of ribosomes; RNA polymerase II (Pol II) transcribes the DNA into protein-encoding mRNA precursors; and RNA Polymerase III (Pol III) is specialized in transcribing tRNAs, the 5S rRNA and other short non-coding RNAs. Although the transcription process and machinery have several

similarities between the three polymerases, Pol II transcription has a major complexity (Figure 11).

Thus, DNA transcription is a vital step in gene expression and must be tightly regulated. It is carried out in three subsequential stages: initiation, elongation and termination. Initiation starts at the 5' end Transcription Start Site (TSS) situated in the core promoter sequence of the gene, where a large set of general transcription factors (GTFs) are recruited, and the preinitiation complex (PIC) is assembled (Haberle & Stark, 2018). The PIC is formed by the association of Pol II and the TFIID, TFIIA, TFIIB, TFIIF, TFIIE, and TFIIH transcription factors, that act together positioning Pol II at the gene TSS in order to open the DNA bubble and initiate RNA synthesis. One of the GTFs forming the preinitiation complex, TFIID, contains a TATA-box binding protein (TBP) and other factors associated to TBP. During the PIC assembly, TBP binds to the TATA box, a repetitive consensus sequence found in the core promoter, that enables transcription initiation (Nogales et al., 2017). After that, TFIIF interacts with TFIIB and recruits RNA Pol II to the PIC (H. T. Chen & Hahn, 2004). Finally, TFIIE and TFIIH regulate Pol II activity and are required for the DNA opening of the promoter. The TFIIH factor contains three subunits with catalytic activity: XPB and XPD helicases, and CDK7 kinase. The XPB ATPase activity is involved in the core promoter opening by rotating downstream DNA (T. K. Kim et al., 2000) and forming a transcription bubble. The initial unpaired region is maintained opened by TFIIH until the formation of the first RNA nucleotides. Then, the C-terminal Pol II phosphorylation depending on the CDK7 facilitates the transition of Pol II to the elongation phase.

Studies comparing the initiation machinery between Pol I, II and III demonstrated that it is highly conserved (Vannini & Cramer, 2012). In fact, the three polymerases share a core conserved initiation complex constituted by the polymerase, the TBP-protein and the transcription factors TFIIB, TFIIE, and different related protein subunits in the case of Pol I and III instead of the Pol II-TFIIF. However, different peripheral factors are used in Pol I and III for the recognition and regulation of the promoter at the initiation phase.

At an early elongation stage, the short RNA transcripts synthesized are very unstable and the Polymerase has to deal with a high abortive rate of templates. During transcription initiation, Pol II remains at the promoter until the reach of 10-15 phosphodiester bonds, when a productive RNA synthesis starts. Thus, involving the Pol II release from the promoter and resulting in the promoter clearance (Holstege et al., 1997). At initial steps of transcriptional elongation, Serin5 in the C-terminal domain (CTD) of Pol II, becomes phosphorylated by TFIIH at promoter regions. This modification leads to the recruitment of other processing factors (Komarnitsky et al., 2000) such as the mRNA capping enzyme required for the 5'-end processing, the Nrd1-Nab3 complex and the PAF (Polymerase II-Associated Factor) complex. These factors protect the nascent RNA from degradation and permit the dissociation of initiation-specific factors (Svejstrup et al., 1997).

During elongation, Pol II catalyzes the synthesis of new RNA along the DNA template in a 5' to 3' direction in a channel-filling process. Interestingly, as elongation proceeds, Ser2 phosphorylation at the CTD of Pol II predominates over the Ser5 modification. Thereby, permitting the attachment

of elongation factors, mRNA 3' end processing and termination factors (Phatnani & Greenleaf, 2006).

One of the major differences in transcriptional elongation between the three eukaryotic polymerases is the time spent in this process, being the Pol III the most different, as it catalyzes the synthesis of shorter nucleotide transcripts.

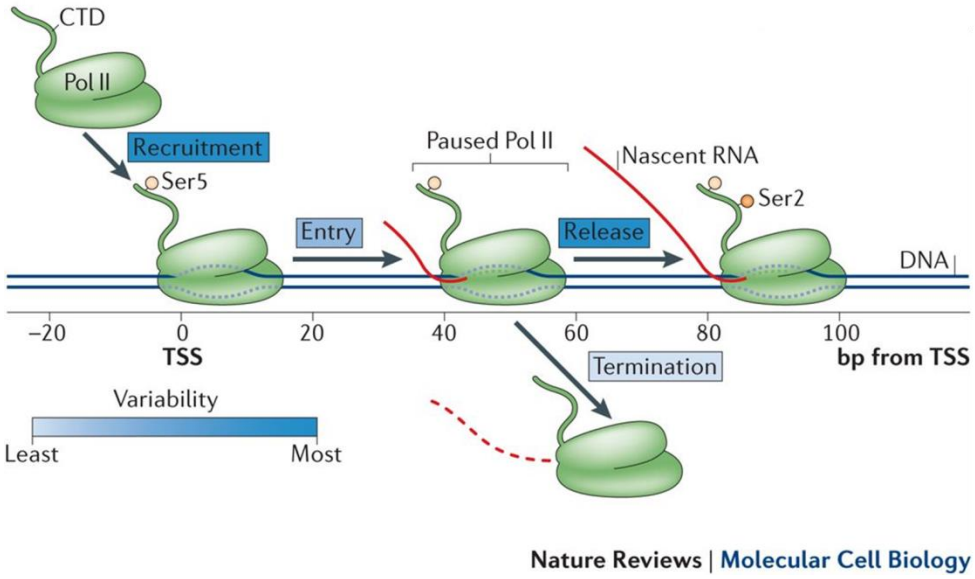

Figure 11. Eukaryotic Pol II transcription. Graphic representation of the Pol II transcriptional process, which is initiated with the recruitment of the polymerase to the promoter and followed by the transcription imitation and entry to the pause site. As elongation proceeds, Pol II releases from the promoter and Serin2 phosphorylation increases. At the termination step Pol II is finally dissociated from the DNA. Blue labels defining the steps indicate the variability rate of each process. Figure from (Jonkers & Lis, 2015)

In *S. cerevisiae*, for protein-coding genes, the termination mechanism is triggered by the recruitment of the Pcf11 subunit by Phospho-Ser2, which interacts with the CTD in complex with a CPF-CF subunit, Clp1. Then, the newly synthetized RNA is cleaved by the CPF endonuclease Ysh1 (CPSF-73 in humans) at its 3' end and it becomes polyadenylated. Next, the conserved exonuclease Rat1 (XRN2 in humans) acts in a 5'-3' direction and mediates Pol II dissociation from the DNA in a process commonly known as "torpedo" termination (Luo & Bentley, 2004).

Nonetheless, the termination process differs between the three eukaryotic polymerases. For instance, Pol I recruits the Reb1p DNA-binding factor which promotes termination at 93 bp downstream of the end of the 25S mature rRNA (Reeder et al., 1999) in the majority of cases. Alternatively, the 10% of Pol I molecules stop at a second fail-safe terminator at 250 bp. In contrast to Pol I and Pol II, in which termination occurs at a short nucleotide sequence, transcription termination by the eukaryotic Pol III is autonomous, and requires the interaction of other subunits to its catalytic center that regulate the termination process (Aneeshkumar G. Arimbasseri, Keshab Rijal, 2013).

1.4.1 Ribosomal DNA

The ribosomal DNA (rDNA) is a genetic sequence that codes for ribosomal RNA (rRNA), a type of non-coding RNA that is an integral (and catalytic) part of the ribosome. The rDNA is composed by tandem repeated arrays of the rDNA gene separated by non-transcribed spacers (NTS). Each repeat or transcription unit contains an external transcribed spacer (ETS), the 25S large and the 18S small subunits, and the 5.8S gene, which will be processed into a mature pre-rRNA molecules. Between the rDNA subunits there are two internal transcribed spacers (ITS): ITS1 located between 18S and 5.8S genes, and ITS2 situated between 5.8S and 25S regions. In addition, most eukaryotes contain another rDNA gene, coding for the 5S rRNA subunit (Long & Dawid, 1980). Polymerase I (Pol I) transcribes the 18S, 25S and 5.8S (47S genes in humans or 35S in yeast) that are processed into mature mRNAs, with the exeption of the 5S rRNA that is transcribed by Pol III.

The rDNA transcription by Pol I takes place in the nucleolus, a region in the nucleus of a cell composed by several proteins, DNA and RNA molecules where ribosomes are assembled and that has a role in the organization and stability of the genome (Kobayashi, 2008). Human cells have around 300 copies of 47S rDNA repeats distributed on the short arms of the chromosomes 13, 14, 15, 21 and 22. Whereas in yeast, there are approximately 150-200 35S rDNA tandem repeats located in a single cluster at the right arm of chromosome XII (Petes, 1979) (Figure 12). Nonetheless, eukaryotic cells have a general conserved rDNA structural organization.

Particularly in yeast, between the two transcribed 5S and 35S there are several non-transcribed subunits within the two intergenic spacers which contain regulatory elements for rDNA transcription. Thus, *S. cerevisiae* ITS1 contains a replication fork barrier (RFB) site where Fob1 docks (see Figure 12). The recognition of RBF sequence and binding by Fob1 has a role in replication inhibition in the opposite direction of the 35S transcription, preventing the collision between the transcription and replication machineries (Kobayashi, 2003). ITS1 also contains a non-coding bidirectional Pol II promoter, E-pro, whose transcription stimulates cohesin dissociation and is required for rDNA amplification. In addition, the ITS2 domain, contains an rDNA autonomously replicating sequence (rARS) that is used as an origin of replication, and a cohesin associated region (CAR) (Salim & Gerton, 2019). In human cells, most of these regulatory elements are conserved, and also contain an origin of replication (ORI) within the intergenic spacers (Little et al., 1993), and an RNA Pol I transcription terminator complex called Sal-box that acts as the RFB, arresting replication forks bidirectionally (Akamatsu & Kobayashi, 2015).

The number of copies of the rDNA array is highly variable and it suffers dynamic changes within a population of cells. However, cells have different mechanisms to regulate the size of the rDNA locus, trying to maintain a stable number of copies. In *S. cerevsiae*, Fob1 is the responsible of the rDNA copy number fluctuation. In fact, the Fob1-dependent replication fork block leads to the formation of DSB and an increase in chromosomal instability. Subsequently, HR repair of DSB results in the expansion or contraction of the rDNA repeats (Kobayashi et al., 1998). In the last decades, several *S. cerevisiae* genetic screenings have permited to identify genes involved in the

regulation of the rDNA copy number variability such as the Sir2 histone deacetylase that stabilizes repetitive DNA by silencing transcription by RNA pol II at ITS1. Therefore, cellular stress or DNA-damage induced situations result in an aberrant recombination, an increase in the extra-chromosomal rDNA circles (ERCs) formation, and a rDNA instability-driven senescence (Kobayashi, 2008).

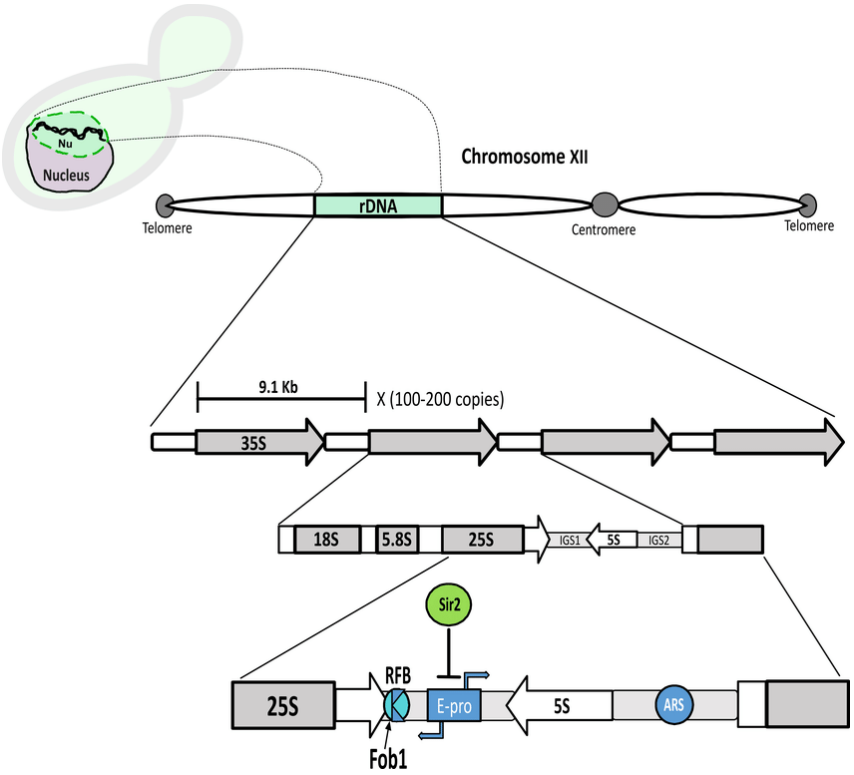

Figure 12. Schematic structure of the yeast rDNA array. Figure from (Matos-Perdomo & Machín, 2019).

1.4.2 RNA Polymerase I and ribosomes biogenesis

Transcription of the 18S, 5.8S and 25S RNAs by RNA Pol I (hereafter referred to as Pol I) is the first step for ribosomes biogenesis and represents 60% of the total transcriptional activity in eukaryotic cells (Moss & Stefanovsky, 2002). From a structural point of view, yeast Pol I is a 590 kDa complex composed by 14 subunits. Particularly, the two larger subunits A190 and A135 (according to their molecular weight) constitute the core of Pol I. The other five catalytic core subunits (Rpb5, Rpb6, Rpb8, Rpb10, and Rpb12) are shared among the three polymerases and are essential for their structural integrity and enzymatic activity (see Table 1 and Figure 13) (Lanzendörfer et al., 1997). The AC40-AC19 subcomplex that is identical in Pol III and homologus to Rpb3-Rpb11 Pol II subunits, is also found in the central core of Pol I, which is completed by the A12.2 subunit, required for RNA cleavage (Kuhn et al., 2007). Outside the core, the A14/A43 subcomplex which is the counterpart of Rpb4-Rpb7 heterodimer in Pol II and C17-C25 in Pol III (Peyroche et al., 2002),

interacts with the Pol I core and to the Rrn3 factor to promote transcription initiation. Finally, the subcomplex formed by A49-A34.5 subunits has homology with the C37-C53 subcomplex in Pol III and is not present in Pol II, although it has similar features with the TFIIF and TFIIE factors and enhances transcriptional elongation (Wild & Cramer, 2012).

Polymerase part	Pol I subunit	MW (kDa)	Corresponding Pol II subunit	Subunit type	Corresponding Pol III subunit	Subunit type
Core	**A190**	186.4	Rpb1	Homolog	C160	Homolog
Core	**A135**	135.7	Rpb2	Homolog	C128	Homolog
Core	**AC40**	37.7	Rpb3	Homolog	AC40	Common
Core	**AC19**	16.2	Rpb11	Homolog	AC19	Common
Core	**A12.2**	13.7	Rpb9	Homolog	C11	Homolog
Core	**Rpb5**	25.1	Rpb5	Common	Rpb5	Common
Core	**Rpb6**	17.9	Rpb6	Common	Rpb6	Common
Core	**Rpb8**	16.5	Rpb8	Common	Rpb8	Common
Core	**Rpb10**	8.3	Rpb10	Common	Rpb10	Common
Core	**Rpb12**	7.7	Rpb12	Common	Rpb12	Common
Subcomplex A14/43	**A14**	14.6	Rpb4	Counterpart	C17	Counterpart
Subcomplex A14/43	**A43**	36.2	Rpb7	Counterpart	C25	Counterpart
Subcomplex A49/34.5	**A49**	46.7	RAP74	Specific	C37	Counterpart
Subcomplex A49/34.5	**A34.5**	26.9	RAP30	Specific	C53	Counterpart
Total	-	589.6	-	-	-	

Table 1. Polymerase I subunits and their homology with Pol II and Pol III. Table adapted from (Kuhn et al., 2007) and (Wild & Cramer, 2012).

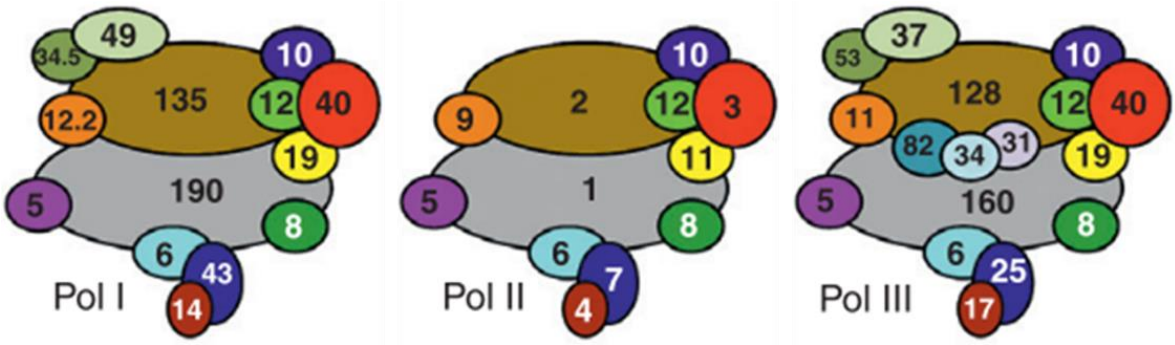

Figure 13. Schematic comparison between the different RNA polymerases subunits. Counterpart or homologus subunits shared with two or the three polymerases are illustrated with the same color. Figure adapted from (Wild & Cramer, 2012).

This eukaryotic multisubunit complex is highly conserved in evolution and the composition of Pol I enzyme also shows conservation with Pol II and Pol III (Table 1, Figure 13). Apart from Pol I, the full transcription machinery requires other associated factors and co-activators that cooperate to ensure rDNA transcription. Hence, yeast Pol I synthesizes rRNA by working in a coordinated manner with a specific set of transcription factors: Upstream Activating Factor (UAF), TATA-binding protein (TBP), Core Factor (CF), and Rrn3, which form the pre-initiation complex (PIC) (Keener et al., 1998). The CF (SL1 human ortholog) is composed by the Rrn6, Rrn7 and Rrn11 polypeptides, and it interacts with Rrn3, UAF and TBP and mediates a basal level of transcription. When it is free, Pol I adopts a dimeric structure, whereas its binding with Rrn3 stabilitzes its monomeric form (Milkereit et al., 1997). Pol I-Rrn3 binding functions as a bridge between the polymerase and the transcription factors and promotes the recruitment of Pol I to the rDNA promoter at the core factor (Peyroche et al., 2000). Furthermore, the Rrn7 subunit plays an analogous role to TFIIB and participates in the formation of the preinitiation complex. When UAF (composed by Rrn5, Rrn9, Rrn10 and histones H3 and H4) together with TBP, stabilize the CF association with the promoter, Pol I initiation rates increase. At a later elongation phase, the Rpa49-Rpa43 subcomplex from an adjacent polymerase promotes the release of the Rrn3 initiation factor from the transcribing Pol I (Albert et al., 2011), which might be recycled for a posterior Pol I-Rrn3 complex formation (Figure 14). Notably, the quantity of Pol I-Rrn3 complexes available represents a rate limiting step for Pol I transcription initiation, but the regulation of this association remains to be detailed. Indeed, several signaling pathways regulate Pol I initiation *in vivo.* One of them, the target of rapamycin complex 1 (TORC1), controls ribosomes biogenesis in response to nutrient availability (Loewith et al., 2002). Thus, TORC1 inhibition by rapamycin results in a reduction of Pol I-Rrn3 complexes and in a transcriptional repression (Laferté et al., 2006). In addition, it has been recently described that the Ccr4-Not complex, also found in the Pol II system, acts downstream of TORC1 nutrient signalling pathway and regulates Pol I initation and elongation activities (Laribee et al., 2015).

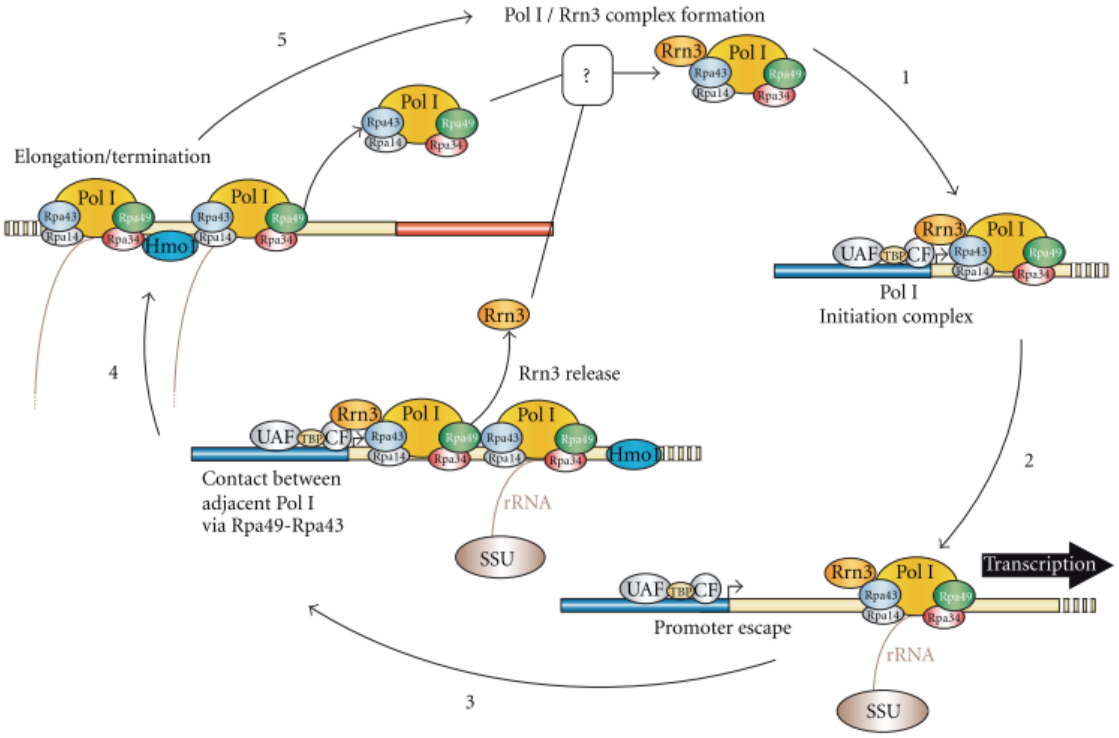

Figure 14. Pol I transcription cycle in *S. cerevisiae.* (1) Pol I-Rrn3 complex recruitment to an rDNA promoter and formation of the preinitiation complex. (2) The cotranscriptional SSU processome recruitment is coupled with the promoter escape and rRNA synthesis. (3) The Rpa49-Rpa43 subcomplex from an adjacent polymerase promotes Rrn3 release from the transcribing Pol I. (4) rRNA maturation and processing occurs cotranscriptionally. (5) Pol I is recycled by reassociation with Rrn3 for the next transcription cycle in a still undefinded process. Figure from (Albert et al., 2012).

However, it has to be remarked that not only Pol I initiation but also an elongation rate regulation is needed for optimal ribosome synthesis (Schneider et al., 2007). In this regard, although the mechanisms that control transcriptional elongation are not fully described, several Pol I elongation regulatory factors (many of them shared with Pol II) have been well characterized. First, for a processive elongation, the DNA clamp, the structure by wich polymerases bind to the DNA, must be closed. Spt5, a conserved elongation factor, has been reported to close the DNA clamp and to interact with other Pol I subunits that regulate Pol I functions, such as Paf1, Spt4 or Spt6 (Albert et al., 2012). Particularly, the Paf1 complex associates with the rDNA and stimulates Pol I elongation (Y. Zhang et al., 2009). Another regulatory element for Pol I elongation is the FACT (facilitates chromatin transcription) complex, which is composed by Spt16 and Pob3 subunits and also interacts with Spt5 in yeast. Pol I elongation needs an open chromatin structure without nucleosome barriers in the transcribing rRNA genes (Merkl et al., 2020). In mammalian cells, FACT has been proposed to be a general modulator of chromatin structure for transcription, as it desestabilizes the histone octamer and promotes the transient displacement of H2A-H2B dimers from nucleosomes; thus facilitating transcriptional elongation (Birch et al., 2009). In addition, different studies have revealed other components involved in the removal of transcription obstacles or in chromatin remodeling. In this regard, Rpa34.5/49 and Rpa12.2 subunits have been described to facilitate Pol I passage through nucleosomes (Merkl et al., 2020); and the high

mobility group (HMG) protein, Hmo1, which assists in transcribing rDNA, is needed for the creation of a specialized chromatin state devoid of histones that facilitates Pol I transcriptional elongation (Merz et al., 2008).

Finally, at the termination stage, the transcription complex is dissasembled and Pol I is reclycled for the next transcription cycle (Figure 14). Similar to the Pol II-employed torpedo mechanism, Pol I transciption termination has been proposed to start with the rRNA cleavage by the endonuclease Rnt1 and the following progressive dissociation of the Pol I-DNA association by the Rat1 exonuclease and the Sen1 helicase (Zomerdijk, 2013).

As ribosomes biogenesis occurs co-transcriptionally, transcription of rRNA genes by RNA Pol I becomes the first rate-limiting step for their synthesis. Accordingly, several upstream factors act as master regulators of protein synthesis and have positive effects in Pol I transcription.

The synthesis of the 35S rRNA (yeast)/47S (human) by Pol I is the precursor of ribosomes biogenesis and the mature 18S, 5.8S and 25S (yeast)/28S (human) rRNAs. The 5S pre-RNA transcribed by Pol III in the opposite direction is incorporated later in the nascent pre-ribosome. Several *trans*-acting factors and ribosomal proteins assemble with the 35S pre-rRNA to form a macromolecular pre-ribosomal complex named 90S or the small subunit (SSU) processome (Grandi et al., 2002). As elongation proceeds, the 35S nascent transcript is processed and modified co-transcriptionally by small nucleolar ribonucleoproteins (snoRNPs) (David Tollervey & Kos, 2010) through methylation and pseudouridylation reactions that stabilise the pre-ribosomes structure and modulate their functions. Subsequently, 35S processing consists on the removal of the external (5’ ETS and 3’ ETS) and internal transcribed spacers (ITS1 and ITS2) from the rRNA transcript through complex endonucleolytic and exonucleolytic reactions (Henras et al., 2015). Thus, resulting in the division of the 18S, 5.8S and 25S pre-rRNA precursors and separation of the maturation pathways of the pre-40 and pre-60 particles (Thomson et al., 2013) (Figure 15). Maturation of the large subunit (60S), that contains the 5S, 5.8 and 25/28S rRNAs and 46 ribosomal proteins (r-proteins), starts at the nucleolus and undergoes a final assembly at the cytoplasm (Nissan et al., 2002). Pre-60S particles associate with several nucleolar factors forming a multiprotein complex. As maturation proceeds, some of these proteins are removed or substituted by other transient and export factors, and finishes with few constituents for the final cytoplasmic maturation. Pre-40S particles (composed by the 18S rRNA and 33 r-proteins) in contrast, are rapidly exported to the cytoplasm for a complete maturation. During this process, several checkpoint and quality control mechanisms become activated in order to avoid later defects in protein quality.

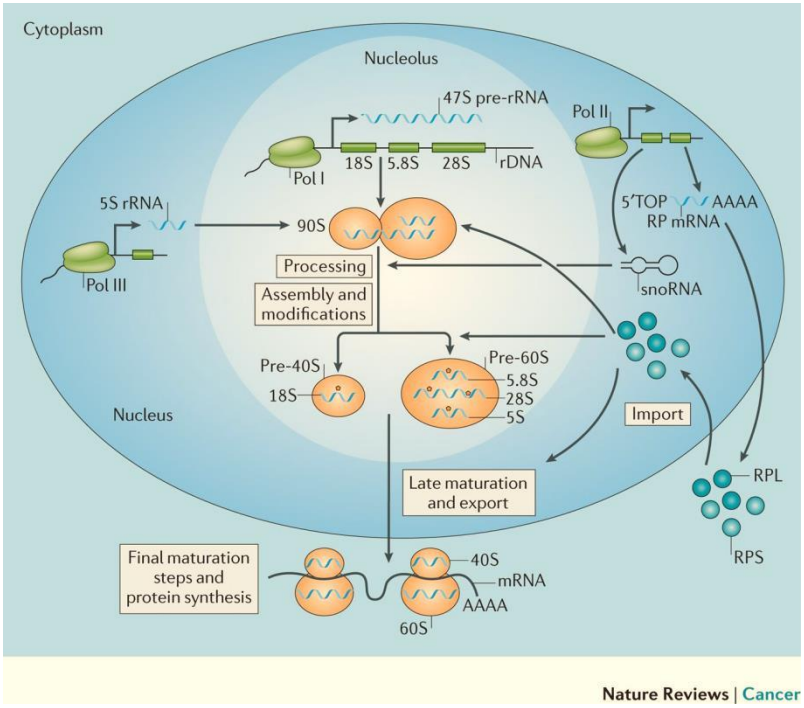

Figure 15. Schematic representation of mammalian ribosome biogenesis. In the nucleolus, pol I transcribes the 47S pre-rRNA, which is then assembled in the 90S processome. The 90S processome will be finally processed and modified (thanks to snoRNAs) into the 40S and 60S ribosomal subunits, which suffer a final cytoplasmic maturation after their nuclear export. rRNA modifications are represented in the figure as orange pentagons. Pol II and Pol III participate also in the ribosomal biogenesis process. In humans, 5S rRNA is transcribed by Pol III in the nucleoplasm, and Pol II transcribe protein coding mRNAs, and synthesize snoRNAs, RPL (large subunit ribosomal proteins) and RPS (small subunit ribosomal proteins). Figure from (Pelletier et al., 2017)

1.4.2.1 *RPA190*

RPA190 is the gene encoding for the A190 largest subunit of the yeast RNA Pol I (RPA194 in human cells), and shows sequence homology with the β' subunit of the bacterial polymerase, the C220 (Rpb1) subunit in Pol II and the Rpc160 subunit in Pol III. In yeast, it encodes for a 186 kilodalton polypeptide chain, it has a conserved zinc-binding motif at its N-terminal domain and forms the DNA binding cleft together with the Rpa135 subunit. Both contribute to the Pol I catalytic activity and form its active centre.

Structurally, it contains a jaw domain with an internal acidic loop, also referred to as the DNA-mimicking loop expander, inside the DNA-binding cleft. The crystal structure of the polymerase shows that the positive patch in this loop interacts with the unfolded region of the bridge helix in Rpa190, and promotes stabilization of the Rpa12 subunit (Fernández-Tornero et al., 2013). In turn, Rpa12 is required for cleavage of RNA Pol I (Kuhn et al., 2007) and has been implicated in promoting transcriptional termination (Prescott et al., 2004). Additionally, this Rpa190 internal loop has a regulatory function, as it avoids elongation by blocking the nucleic acid binding site when the enzyme is inactive (Fernández-Tornero et al., 2013). When compared, the structural positioning of Rpa190 and Rpa135 core subunits confer to Pol I the widest cleft of the three

polymerases and a closed clamp conformation that gives a high processivity to transcribe long rRNA precursors (Fernández-Tornero et al., 2013).

Rpa190 is essential for viability. As such, conditional thermosensitive mutations lead to decreased rRNA synthesis (Wittekind et al., 1988) (Wittekind et al., 1990). Nonetheless, since the cellular concentration of Pol I is regulated by the growth rate and responds to several environmental signals, most mutant alleles at *rpa190, rpa49, rpa12* or *rpa135* subunits impair optimal growth of the cell (Darrière et al., 2019).

Moreover, defects in the human Rpa194 are also linked to neurological pathologies. Indeed, mutations in the *POL1AR* gene encoding for Rpa194 have been recently associated with a leukodystrophy syndrome (Kara et al., 2017). Furthermore, *POL1AR* pathogenic variants are found in congenital acrofacial disorders provoked by the defective ribosomes biogenesis (Weaver et al., 2015).

Despite its essential role in ribosomes biogenesis, regulation of the largest subunit of the RNA Pol I remains poorly understood. However, recent studies revealed that ubiquitination and de-ubiquitination pathways control the stability of Rpa190. In this regard, Richardson and colleagues published that a conserved nucleolar Ubp10 ubiquitin protease mediated Rpa190 de-ubiquitination to achieve optimal levels of ribosomes and cell growth (Richardson et al., 2013). Ubp10 protease also promotes, together with Ubp8, removal of monoubiquitin molecules from histone H2B at silent chromatin (Gardner et al., 2005). Thus, H2B deubiquitination by Ubp10 is involved in telomere and gene-silencing (Emre et al., 2005), and has been recently linked to the coordination of nucleosome assembly during replication and transcription (Nune et al., 2019) .

However, deletion of *UBP10* in yeast cells leads to a dramatic slow growth phenotype that is not only due to the loss of gene silencing (Gardner et al., 2005). In fact, *ubp10Δ* cells have a reduction in 35S pre-rRNA synthesis, decreasing the overall ribosome levels as a result of Rpa190 ubiquitination dysregulation. In the absence of *UBP10* (USP36 human functional analog), Rpa190 levels drastically decrease, and the protein is degraded. Hence, ubiquitinated Rpa190 could be involved in the regulation of a concrete step during rDNA transcription or may be mediating rRNA resolution mechanisms at Pol I arrested sites (Gardner et al., 2005). However, the specific function of the Rpa190 ubiquitin action and stabilization by Ubp10 remains unknown.

In contrast, ubiquitination of the largest subunit of the RNA Pol II (Rpb1) that has sequence homology with Rpa190, is better described. Indeed, recent studies revealed that ubiquitinated Rpb1 has a dual role: it signals RNA Pol II degradation to ensure cell viability during DNA damage, indicating that ubiquitinated RNA Pol II regulates the DNA damage response; and plays a role during transcript elongation *in vivo* as it becomes ubiquitinated in response to transcriptional arrest (Somesh et al., 2007). As it happens with Rpa190, Rpb1 deubiquitination by Upb3 controls its stability. Thus, Upb3 has been proposed to prevent proteolysis of arrested RNA Pol II (Kvint et al., 2008).

1.4.2.2 RNA Pol I Inhibitors

As an up-regulation of rRNA pre-ribosomal synthesis is a hallmark of several human cancers (Montanaro et al., 2008), Pol I inhibition has been a widely studied strategy for cancer therapy. Indeed, several molecules have been recently described to inhibit RNA Pol I transcriptional elongation. Some of them, however, are not specific for RNA Pol I and have been used for decades, such as 6-azauracil (6AU); a pyrimidine biosynthetic inhibitor that sensitizes cells with defective Pol II elongation factors in yeast (Hubert et al., 1983) (Hampsey, 1997). 6AU specifically depletes the intracellular GTP and UTP pools, which when combined with mutations in the transcriptional elongation machinery can result in cell growth arrest.

In contrast, CX-5461 is a specific inhibitor of the RNA Pol I rRNA synthesis, and shows no effect on Pol II. Due to its capacity to reduce ribosomal biogenesis in malignant cells, it has been proposed as a potential therapeutic strategy to target multiple myeloma (Hans C. et al., 2017). Also a new role for ellipticine in specifically targeting RNA Pol I has been recently described as a potent anticancer treatment. Ellepticine compunds are able to selectively impair the Pol I preintiation complex and consequently, alter ribosome biogenesis (Andrews et al., 2013).

Moreover, extensive screenings have allowed the identification of a chemical library of synthetic small molecules involved in the activation of the p53 tumor suppressor pathway (Peltonen et al., 2010). Four of them (BMH-9, BMH-21, BMH-22, BMH-23) do not activate a DNA damage response and specifically inhibit Pol I. BMH-9, BMH-22 and BMH-23 cause a decrease in the human RPA194 catalytic subunit in a proteasome-dependent manner resulting in nucleolar stress (Peltonen et al., 2015). The other molecule, BMH-21, is a DNA intercalator that binds to rich GC-sequences, blocks rRNA precursor synthesis and alters the nucleolar structure (Peltonen et al., 2014). In fact, BMH-21 is a specific inhibitor of the largest subunit of the RNA Pol I, RPA190/ RPA194, and causes the disassembly of the full polymerase from the rDNA (Peltonen et al., 2014). Degradation of Rpa194 in BMH-21 treated cells occurs in a ubiquitin-proteasome dependent manner. Thus, BMH-21 is supposed to increase polyubiquitination of Rpa194, and both overexpression of the USP36 DUB, or the addition of MG132 proteasome inhibitor rescue Rpa194 from being degraded (Peltonen et al., 2014). Due to its very recent discovery, BMH-21 mechanism of action is not fully deciphered. Nevertheless, a novel publication has provided more details about the conserved effects of this drug in human and yeast cells. Interestingly, BMH-21 requires the preinitation complex for Rpa190/Rpa194 degradation, as it only impairs transcribing complexes. Of note, Rpa135 is also needed for Rpa190 stability and BMH-21 dependent Rpa190 degradation, and it becomes partially relocated to the cytoplasm after the BMH-21 treatment. Overall, these new data suggest that BMH-21 acts by directly inhibiting the transcriptional elongation activity of Pol I, resulting in a decrease of full-length rRNA transcripts (Wei et al., 2018). Comparatively, Rpb1 ubiquitination mediates its proteasomal degradation in response to a transcriptional arrest (Somesh et al., 2007).

OBJECTIVES

2. OBJECTIVES

Nse2 binds to the central part of the Smc5 ARM (Duan et al., 2009), and this interaction has been described to be crucial for the sumoylation and chromosome disjunction functions of the Smc5/6 complex (Bermúdez-López et al., 2015). However, despite the relevance of the Nse2-SUMO ligase activity on genomic stability, how its E3 ligase activity is controlled remains unknown. In addition, the role of different regions in the C-terminal domain has not been analyzed. Critically, the removal of last alpha-helix domain, without alteration of the RING domain, results in a primordial dwarfism-associated syndrome in humans (Payne et al., 2014). The other RING-type subunit of the Smc5/6 complex, Nse1, has also been described to promote DNA repair functions and to maintain genome integrity (Pebernard, Perry, et al., 2008). However, and differently to Nse2, no targets for Nse1 and its ubiquitin-E3 ligase activity have been identified until now.

In this thesis we aimed to get a better understanding of the two RING domain subunits in the Smc5/6 complex. To this end, we set out to:

- Characterize how DNA regulates the SUMO ligase activity of Nse2.
- Characterize the role of different sub-structures in the Nse2 C-terminal part: an internal loop connecting the N- and C-terminal domains, the RING domain, the C-terminal alpha-helix, and a C-terminal Sumo Interacting Motif (SIM).
- Use a proteomic screen to identify Nse1 ubiquitination targets.
- Study the ubiquitin-dependent regulation of one of the targets identified in the screen, the largest subunit in the RNA Polymerase I complex.

MATERIALS AND METHODS

3. MATERIALS AND METHODS

3.1 Yeast methods

3.1.1 Yeast Strains

Strain	Genotipe	Reference
YTR27	*MATa his3Δ200 leu2Δ0 met15Δ0 trpΔ63 ura3Δ0 SMC5-9MYC TRP*	Lab collection
YTR30	*MATa his3Δ200 leu2Δ0 met15Δ0 trpΔ63 ura3Δ0 GAL-3HA-SMC6:HIS3MX6*	Lab collection
YTR248	*MATa ade2-1 trp1Δ2 can1-100 leu2-3,112 his3-11,15 ura3-52*	Lab collection
W303	*MATalpha ade2-1 trp1Δ2 can1-100 leu2-3,112 his3-11,15 ura3-52 rad5-535*	Euroscarf
YTR314	*MATa his3-Δ200 leu2-3, 112 lys2-801 trp1-1 (am) ura3-52 Pol30-K164R*	M. Foinani
Y407	*Mat a his3Δ1 leu2Δ0 met15Δ0 ura3Δ0 mms2::kanMX4*	EUROSCARF
Y423	*MATa his3Δ1 leu2Δ0 met15Δ0 ura3Δ0*	E. Herrero
Y478	*Mata his3Δ1 leu2Δ0 met15Δ0 ura3Δ0 siz1::kanMX4*	EUROSCARF
YRP727	*MATa his3-Δ1 leu2-3,112 trp1Δ ura3-52 nse1::hisG pCEN-LEU2-nse1-101 (G175E, S207T, and G332D)*	Prakash lab
YRP787	*MATa his3-Δ1 leu2-3,112 trp1Δ ura3-52 nse1::hisG pCEN-LEU2-nse1(C274A)*	Prakash lab
YMB794	*MATa his3Δ1 leu2Δ0 met15Δ0 ura3Δ0 6HF-smt3:kanMX6 SMC5-9myc:HIS3MX6*	Lab collection
YTR907	*MATa ade2-1 trp1Δ2 can1-100 leu2-3,112 his3-11,15 ura3-52 6HF-SMT3:KanMX4*	Lab collection
YSM2228	*HKY579-10A MATa ade2-1 can1-100 his3-11,15 leu2-3,112 trp1-1 ura3-1 RAD5+ Smc1-6HA:HIS3MX6*	Lab collection
YMB2272	*MATa his3Δ1 leu2Δ0 met15Δ0 ura3Δ0 + Sgs1-6HA::natNT2*	Lab collection

YMB2315	*MATa his3Δ1 leu2Δ0 met15Δ0 ura3Δ0 6HF-smt3:kanMX6 SMC5-9myc (HIS) + Mms21-6HA::natNT2*	Lab collection
YTR2422	*MATa his3Δ1 leu2Δ0 met15Δ0 ura3Δ0 6HF-smt3:kanMX6 mms21Δc::hphMX4 SMC5-9myc:HIS3MX6*	Lab collection
YIR2620	*MATa his3Δ1 leu2Δ0 met15Δ0 ura3Δ0 6HF-smt3:kanMX6*	Lab collection
YSB2699	*MATa his3Δ1 leu2Δ0 met15Δ0 ura3Δ0 6HF-smt3:kanMX6 rpa135-6HA::natNT2*	Lab collection
YSB2701	*MATa his3Δ1 leu2Δ0 met15Δ0 ura3Δ0 6HF-smt3:kanMX6 rpa190-6HA::natNT2*	Lab collection
YSB2705	*MATa his3Δ1 leu2Δ0 met15Δ0 ura3Δ0 6HF-smt3:kanMX6 mms21Δc::hphMX4 rpa135-6HA::natNT2*	Lab collection
YSB2707	*MATa his3Δ1 leu2Δ0 met15Δ0 ura3Δ0 6HF-smt3:kanMX6 mms21Δc::hphMX4 rpa190-6HA::natNT2*	Lab collection
YTR2751	*MATa his3Δ1 leu2Δ0 met15Δ0 ura3Δ0 6HF-smt3:kanMX6 SMC5-9myc:HIS3MX6 mms21Δ29C-6HA:natNT2*	This study
YNC2839	*MATa his3Δ1 leu2Δ0 met15Δ0 ura3Δ0 + RPA190-6HA::natNT2*	Lab collection
YIR3070	*MATa his3Δ1 leu2Δ0 met15Δ0 ura3Δ0 6HF-smt3:kanMX6 mms21C-H:HIS3MX6*	Lab collection
YTB3215	*MATa his3Δ1 leu2Δ0 met15Δ0 ura3Δ0 6HF-smt3:kanMX6 SMC5-9myc:HIS3MX6; mms21 ΔSIM::natNT2*	This study
YTB3216	*MATa his3Δ1 leu2Δ0 met15Δ0 ura3Δ0 6HF-smt3:kanMX6 SMC5-9myc:HIS3MX6 MMS21(DEL 160-176)-6HA:natNT2*	This study
YGC3410	*HKY579-10A MATa ade2-1 can1-100 his3-11,15 leu2-3,112 trp1-1 ura3-1 RAD5+ Mms21-6HA::hph*	Lab collection
YGC3428	*HKY579-10A MATa ade2-1 can1-100 his3-11,15 leu2-3,112 trp1-1 ura3-1 RAD5+ SMC6-6HA::HIS3*	Lab collection
Y3607	*MATa his3-Δ1 leu2-3,112 trp1Δ ura3-52*	Prakash lab
YEI3828	*MATa his3Δ1 leu2Δ0 met15Δ0 ura3Δ0 RPA190-6HA::NAT Gal-3ha-SMC6:HIS3 YEplac195*	This study
YEI3829	*MATa his3Δ1 leu2Δ0 met15Δ0 ura3Δ0 RPA190-6HA::NAT Gal-3ha-SMC6:HIS3 YEplac195-CUP1-His7-Ubi*	This study

YTR3864	*MATa his3Δ200 leu2Δ0 met15Δ0 trpΔ63 ura3Δ0 GAL-3HA-SMC5:kanMX6 bar1::URAca 6HF-smt3:hphNT1 Nse4-6HA:natNT2 ADH1p-SMC5:9Myc*	This study
YTR3865	*MATa his3Δ200 leu2Δ0 met15Δ0 trpΔ63 ura3Δ0 GAL-3HA-SMC5:kanMX6bar1::URAca 6HF-smt3:hphNT1 Nse4-6HA:natNT2 ADH1p-SMC5(K337,K344,K354,K355E)-9Myc*	This study
YTR3867	*MATa his3Δ200 leu2Δ0 met15Δ0 trpΔ63 ura3Δ0 GAL-3HA-SMC5:kanMX6 bar1::URAca 6HF-smt3:hphNT1 Nse4-6HA:natNT2 ADH1p-SMC5(K337,K344,K354,K355,K743,K745,K764E):9Myc*	This study
YTR3869	*MATa his3Δ200 leu2Δ0 met15Δ0 trpΔ63 ura3Δ0 GAL-3HA-SMC5:kanMX6 bar1::URAca 6HF-smt3:hphNT1 Nse4-6HA:natNT2 ADH1p-SMC5(K743,K745,K764E)-9Myc*	This study
YTR3871	*MATa his3Δ200 leu2Δ0 met15Δ0 trpΔ63 ura3Δ0 GAL-3HA-SMC5:kanMX6 bar1::URAca 6HF-smt3:hphNT1 Nse4-6HA:natNT2 ADH1p-SMC5(K743,5 R):9Myc*	This study
YFD3914	*MATa his3Δ1 leu2Δ0 met15Δ0 ura3Δ0 RPA190-6HA::natNT2 YEplac195-CUP1-HIS7-Ubi*	This study
YFD 3916	*MATa his3Δ1 leu2Δ0 met15Δ0 ura3Δ0 RPA190-6HA::natNT2 YEplac195*	This study
YEI3959	*MATa his3Δ1 leu2Δ0 met15Δ0 ura3Δ0 RPA190-6HA::natNT2 mms21ΔC::hphNT1*	This study
YEI3968	*Mata leu2-3,112 ura3-1 his3-11 trp1-1 ade2-1 can1-100 fob1::hphMX4 (rDNA copy number 25) Rpa190-6HA:kanMX6 YEplac195-CUP1-HIS7-Ubi*	This study
YEI3969	*Mata leu2-3,112 ura3-1 his3-11 trp1-1 ade2-1 can1-100 fob1::hphMX4 (rDNA copy number 190) Rpa190-6HA:KanMX6 YEplac195-CUP1-HIS7-Ubi*	This study
YEI3980	*MATa his3Δ1 leu2Δ0 met15Δ0 ura3Δ0 + RPA190-6HA::natNT2 mms21ΔC::hphNT1 YEplac195-CUP1-HIS7-Ubi*	This study
YEI4055	*MATa his3-Δ1 leu2-3,112 trp1Δ ura3-52 nse1::hisG pCEN-LEU2-nse1-101 (G175E, S207T, and G332D) pYM14 (Rpa190-6HA) YEplac195-CUP1-HIS7-Ubi*	This study
YNC4059	*MATa his3Δ1 leu2Δ0 met15Δ0 ura3Δ0 6HF-smt3:kanMX6 SMC5 (K337, 344, 355, 357, 743, 745, 764 E)-6HA::HphNT1*	This study
YNC4063	*MATa his3Δ1 leu2Δ0 met15Δ0 ura3Δ0 6HF-smt3:kanMX6 SMC5 (K 743, 745 R)-6HA::HphNT1*	This study
YNC4065	*MATa his3Δ1 leu2Δ0 met15Δ0 ura3Δ0 6HF-smt3:kanMX6 SMC5 (K 743, 745, 764 E)-6HA::HphNT1*	This study
YNC4067	*MATa his3Δ1 leu2Δ0 met15Δ0 ura3Δ0 6HF-smt3:kanMX6 SMC5 (K 743, 745 E)-6HA::HphNT1*	This study
YNC4071	*MATa his3Δ1 leu2Δ0 met15Δ0 ura3Δ0 6HF-smt3:kanMX6 SMC5 (K337, 344 E)-6HA::HphNT1*	This study

Y4148	*MATa cdc48-2::KanMX6 his3Δ1 leu2Δ0 ura3Δ0 met15Δ0*	Boone Library
Y4157	*MATa cdc48-3::KanMX6 his3Δ1 leu2Δ0 ura3Δ0 met15Δ0*	Boone Library
Y4183	*MATa cdc48-4601::KanMX6 his3Δ1 leu2Δ0 ura3Δ0 met15Δ0*	Boone Library
Y4193	*mms21-1::KanR MATa, his3D1 leu2D0 ura3D0 met15D0*	Boone Library
Y4220	*MATa cdc48-1::KanMX6 his3Δ1 leu2Δ0 ura3Δ0 met15Δ0*	Boone Library
YEI4238	*MATa his3Δ1 leu2Δ0 met15Δ0 ura3Δ0 6HF-smt3:kanMX6 SMC5 (K337, 344, 355, 357 E)-6HA::Hph*	This study
YTR4251	*MATa his3Δ1 leu2Δ0 met15Δ0 ura3Δ0 6HF-smt3:kanMX6 smc5-6HA:natNT2*	This study
YEI4255	*MATa his3Δ1 leu2Δ0 met15Δ0 ura3Δ0 6HF-smt3:kanMX6 smc5(7KR)-6HA:natNT2*	This study
YTR4263	*HKY579-10A MATa ade2-1 can1-100 his3-11,15 leu2-3,112 trp1-1 ura3-1 RAD5+ Mms21-6HA::hph YCplac22-[CEN-TRP1]-ADH1p-SMC5:9Myc (Amp)*	This study
YTR4264	*HKY579-10A MATa ade2-1 can1-100 his3-11,15 leu2-3,112 trp1-1 ura3-1 RAD5+ Mms21-6HA::hph YCplac22-[CEN-TRP1]-ADH1p-SMC5(K337,K344,K354,K355,K743,K745,K764E):9Myc (Amp)*	This study
YTR4265	*HKY579-10A MATa ade2-1 can1-100 his3-11,15 leu2-3,112 trp1-1 ura3-1 RAD5+ SMC6-6HA::HIS3 YCplac22-[CEN-TRP1]-ADH1p-SMC5:9Myc (Amp)*	This study
YTR4266	*HKY579-10A MATa ade2-1 can1-100 his3-11,15 leu2-3,112 trp1-1 ura3-1 RAD5+ SMC6-6HA::HIS3 YCplac22-[CEN-TRP1]-ADH1p-SMC5(K337,K344,K354,K355,K743,K745,K764E):9Myc (Amp)*	This study
YEI4298	*HKY579-10A MATa ade2-1 can1-100 his3-11,15 leu2-3,112 trp1-1 ura3-1 RAD5+ SMC6-6HA::HIS3 YCplac22-[CEN-TRP1]-ADH1p-SMC5(K743,K745,K764E)-9Myc (Amp)*	This study
YEI4305	*HKY579-10A MATa ade2-1 can1-100 his3-11,15 leu2-3,112 trp1-1 ura3-1 RAD5+ Mms21-6HA::hph YCplac22-[CEN-TRP1]-ADH1p-SMC5(K743,K745,K764E)-9Myc (Amp)*	
YNC4307	*MATalpha can1Δ::MFA1pr-HIS3 lyp1Δ ura3Δ0leu2Δ0 his3Δ1 met15Δ0 Smc5-6HA:NAT 6HF-smt3:hph SGS1-9MYC::HIS3*	This study
YNC4309	*MATa his3D1 leu2D0 met15D0 ura3D0 6HF-smt3:kanMX6 SMC5 (K 743, 745 R)-6HA::Hph SGS1-9MYC::HIS3*	This study
YNC4311	*MATa his3D1 leu2D0 met15D0 ura3D0 6HF-smt3:kanMX6 SMC5 (K 743, 745, 764 E)-6HA::Hph SGS1-9MYC::HIS3*	This study

YTR4544	*MATa his3Δ1 leu2Δ0 met15Δ0 ura3Δ0 6HF-smt3:kanMX6 SMC5-9myc:HIS3MX6. nse2Δ24C-6HA:natNT2*	This study
YTR4546	*MATa his3Δ1 leu2Δ0 met15Δ0 ura3Δ0 6HF-smt3:kanMX6. nse2-CH-6HA:natNT2*	This study
YEI4604	*MATalpha ade2-1 can1-100 his3-11,15 leu2-3,112 trp1-1 ura3-1 RAD5+ /ade2-1 trp1D2 can1-100 leu2-3,112 his3-11,15 ura3-52 Rpa190::hphMX4 pRS314-RPA190- K408R K410R (CEN-TRP1) YEplac195*	This study
YEI4607	*MATa ade2-1 can1-100 his3-11,15 leu2-3,112 trp1-1 ura3-1 RAD5+ /ade2-1 trp1D2 can1-100 leu2-3,112 his3-11,15 ura3-52 Rpa190::hphMX4 pRS314-RPA190- K408R K410R (CEN-TRP1) YEplac195*	This study
YCC4621	*MATalpha: ade2-1 can1-100 his3-11,15 leu2-3,112 trp1-1 ura3-1 RAD5+ ura3-52 nse1(H306A, C309A)-1MYC-7HIS::KanMX6*	Lab collection
YEI4624	*MATa ade2-1 can1-100 his3-11,15 leu2-3,112 trp1-1 ura3-1 RAD5+ /ade2-1 trp1Δ2 can1-100 leu2-3,112 his3-11,15 ura3-52 Rpa190::hphMX4 pRS314-RPA190-K408R K410R-6HA:natNT2 (CEN-TRP1)*	This study
YEI4639	*MATa ade2-1 can1-100 his3-11,15 leu2-3,112 trp1-1 ura3-1 RAD5+ /ade2-1 trp1Δ2 can1-100 leu2-3,112 his3-11,15 ura3-52 Rpa190::hphMX4 pRS314-RPA190-6HA:natNT2 (CEN-TRP1)*	This study
YCC4640	*MATa: ade2-1 can1-100 his3-11,15 leu2-3,112 trp1-1 ura3-1 RAD5-535 ura3-52 NSE1-1MYC-7His::KanMX6*	Lab collection
YEI4646	*MATa ade2-1 can1-100 his3-11,15 leu2-3,112 trp1-1 ura3-1 RAD5+ /ade2-1 trp1Δ2 can1-100 leu2-3,112 his3-11,15 ura3-52 Rpa190::hphMX4 pRS314-RPA190-6HA:natNT2 (CEN-TRP1) YEplac195*	This study
YEI4647	*MATa ade2-1 can1-100 his3-11,15 leu2-3,112 trp1-1 ura3-1 RAD5+ /ade2-1 trp1Δ2 can1-100 leu2-3,112 his3-11,15 ura3-52 Rpa190::hphMX4 pRS314-RPA190-6HA:natNT2 (CEN-TRP1) YEplac195-CUP1-HIS7-Ubi*	This study
YEI4648	*MATa ade2-1 can1-100 his3-11,15 leu2-3,112 trp1-1 ura3-1 RAD5+ /ade2-1 trp1Δ2 can1-100 leu2-3,112 his3-11,15 ura3-52 Rpa190::hphMX4 pRS314-RPA190-K408R K410R-6HA:natNT2 (CEN-TRP1) YEplac195*	This study
YEI4649	*MATa ade2-1 can1-100 his3-11,15 leu2-3,112 trp1-1 ura3-1 RAD5+ /ade2-1 trp1Δ2 can1-100 leu2-3,112 his3-11,15 ura3-52 Rpa190::hphMX4 pRS314-RPA190-K408R K410R-6HA:natNT2 (CEN-TRP1) YEplac195-CUP1-HIS7-Ubi*	This study
YEI4664	*MATalpha can1Δ::MFA1pr-HIS3 lyp1Δ ura3Δ0leu2Δ0 his3Δ1 met15Δ0 RPA190-6HA:natNT2*	This study
YCC4678	*MATa: ade2-1 can1-100 his3-11,15 leu2-3,112 trp1-1 ura3-1 RAD5-535 ura3-52 NSE1-1MYC-7His::KanMX6 RPA190-6HA::natNT2*	Lab collection
YCC4680	*MATa: ade2-1 can1-100 his3-11,15 leu2-3,112 trp1-1 ura3-1 RAD5+ ura3-52 RPA190-6HA::natNT2*	Lab collection
YEI4684	*MATalpha can1Δ::MFA1pr-HIS3 lyp1Δ ura3Δ0leu2Δ0 his3Δ1 met15Δ0 RPA190-6HA:natNT2 YEplac195*	This study
YEI4726	*cdc48-1::KanR MATa, his3D1 leu2D0 ura3D0 met15D0 +URA3*	This study

YEI4730	*cdc48-2::KanR MATa, his3D1 leu2D0 ura3D0 met15D0 +URA3*	This study
YEI4732	*cdc48-3::KanR MATa, his3D1 leu2D0 ura3D0 met15D0 +URA3*	This study
YEI4736	*MATa nse5-ts3::KanMX6 his3Δ1 leu2Δ0 ura3Δ0 met15Δ0 +URA3*	This study
YEI4737	*MATa nse4-ts3::KanMX6 his3Δ1 leu2Δ0 ura3Δ0 met15Δ0 +URA3*	This study
YEI4740	*MATa mms21-1::KanMX6 his3Δ1 leu2Δ0 ura3Δ0 met15Δ0 +URA3*	This study
YEI4741	*MATa nse1-16::KanMX6 his3Δ1 leu2Δ0 ura3Δ0 met15Δ0 +URA3*	This study
YEI4743	*MATa cdc48-2::KanMX6 his3Δ1 leu2Δ0 ura3Δ0 met15Δ0 RPA190-6HA:natNT2*	This study
YEI4744	*MATa cdc48-3::KanMX6 his3Δ1 leu2Δ0 ura3Δ0 met15Δ0 RPA190-6HA:natNT2*	This study
YEI4745	*MATa cdc48-4601::KanMX6 his3Δ1 leu2Δ0 ura3Δ0 met15Δ0 RPA190-6HA:natNT2*	This study
YEI4746	*MATa cdc48-1::KanMX6 his3Δ1 leu2Δ0 ura3Δ0 met15Δ0 RPA190-6HA:natNT2*	This study
YEI4753	*MATa his3-Δ1 leu2-3,112 trp1Δ ura3-52 nse1::hisG pCEN-LEU2-nse1(C274A) RPA190-6HA:natNT2*	This study
YEI4762	*MATa his3Δ1 leu2Δ0 met15Δ0 ura3Δ0 + RPA190-6HA::NAT YEplac195*	This study
YEI4763	*MATa his3Δ1 leu2Δ0 met15Δ0 ura3Δ0 RPA190-6HA:natNT2 YEplac195-CUP1-HIS7-Ubi*	This study
YEI4765	*MATa cdc48-2::KanMX6 his3Δ1 leu2Δ0 ura3Δ0 met15Δ0 RPA190-6HA:natNT2 YEplac195-CUP1-HIS7-Ubi*	This study
YEI4767	*MATa cdc48-4601::KanMX6 his3Δ1 leu2Δ0 ura3Δ0 met15Δ0 RPA190-6HA:natNT2 YEplac195-CUP1-HIS7-Ubi*	This study
YEI4769	*MATa cdc48-1::KanMX6 his3Δ1 leu2Δ0 ura3Δ0 met15Δ0 RPA190-6HA:natNT2 YEplac195-CUP1-HIS7-Ubi*	This study
Y4770	*MATa ade2-1 can1-100 his3-11 leu2-3,112 trp1-1 ura3-1 RAD5 bar1::LEU2 ubp10::hphMX4*	Avelino Bueno

YEI4771	*MATa ade2-1 can1-100 his3-11 leu2-3,112 trp1-1 ura3-1 RAD5 bar1::LEU2 kanMX6:GAL1,10:GST-UBP10*	Avelino Bueno
YEI4780	*MATa his3-Δ1 leu2-3,112 trp1Δ ura3-52 nse1::hisG pCEN-LEU2-nse1(C274A) RPA190-6HA:natNT2 YEplac195*	This study
YEI4782	*MATa his3-Δ1 leu2-3,112 trp1Δ ura3-52 nse1::hisG pCEN-LEU2-nse1(C274A) RPA190-6HA:natNT2 YEplac195-CUP1-HIS7-Ubi*	This study
YEI4815	*MATa ade2-1 can1-100 his3-11,15 leu2-3,112 trp1-1 ura3-1 RAD5+ /ade2-1 trp1Δ2 can1-100 leu2-3,112 his3-11,15 ura3-52 Rpa190::hphMX4 pRS314-RPA190-6HA:natNT2 (CEN-TRP1) kanMX6:GAL1,10:GST-UBP10 YEplac195-CUP1-HIS7-Ubi*	This Study
YEI4820	*MATa: ade2-1 can1-100 his3-11,15 leu2-3,112 trp1-1 ura3-1 RAD5+ ura3-52 nse1(H306A, C309A)-1MYC-7HIS::KanMX6 RPA190-6HA::natNT2 YEplac195-CUP1-HIS7-Ubi*	This study
YEI4826	*W303 MATa ade2-1 can1-100 his3-11 leu2-3,112 trp1-1 ura3-1 RAD5 bar1::LEU2 ubp10::hphMX4 RPA190-6HA:natNT2*	This study
YEI4838	*W303 MATa ade2-1 can1-100 his3-11 leu2-3,112 trp1-1 ura3-1 RAD5 bar1::LEU2 ubp10::hphMX4 pRS314-RPA190-K408R K410R-6HA:natNT2 (CEN-TRP1) YEplac195-CUP1-HIS7-Ubi*	This study
YEI4852	*MATa his3Δ1 leu2Δ0 met15Δ0 ura3Δ0 RPA190-K408R K410R-6HA:natNT2 YEplac195*	This study
YGB4908	*MATa his3Δ1 leu2Δ0 met15Δ0 ura3Δ0 6HF-smt3:kanMX6 SMC5-9myc:HIS3MX6 nse2-Δ16:6HA::HphNT1*	This study
YGB4910	*MATa his3Δ1 leu2Δ0 met15Δ0 ura3Δ0 6HF-smt3:kanMX6 SMC5-9myc:HIS3MX6 nse2-ΔSIM:6HA::HphNT1*	This study
YGB4911	*MATa his3Δ1 leu2Δ0 met15Δ0 ura3Δ0 6HF-smt3:kanMX6 SMC5-9myc:HIS3MX6 nse2-ΔRING:6HA::HphNT1*	This study
YGB4913	*MATa his3Δ1 leu2Δ0 met15Δ0 ura3Δ0 6HF-smt3:kanMX6 SMC5-9myc:HIS3MX6 nse2-P194A,L195-6HA::natNT2*	This study
YGB4914	*MATa his3Δ1 leu2Δ0 met15Δ0 ura3Δ0 6HF-smt3:kanMX6 SMC5-9myc:HIS3MX6 nse2-C221-6HA::natNT2*	This study
YGB4915	*MATa his3Δ1 leu2Δ0 met15Δ0 ura3Δ0 6HF-smt3:kanMX6 SMC5-9myc:HIS3MX6 nse2-P222-6HA::natNT2*	This study
YGB4917	*MATa his3Δ1 leu2Δ0 met15Δ0 ura3Δ0 6HF-smt3:kanMX6 SMC5-9myc:HIS3MX6 nse2-C185,P186:6HA::HphNT1*	This study
YEI4921	*MATa his3Δ1 leu2Δ0 met15Δ0 ura3Δ0 6HF-smt3:kanMX6 mms21-CH::HIS3 Smc5-9myc:hphNT1*	This study

YEI4938	*MATa his3Δ1 leu2Δ0 met15Δ0 ura3Δ0 6HF-smt3:kanMX6 SMC5-9myc:HIS3MX6. NSE2-Δ16-STOP-6HA:: hph Smc1-6HA:natNT2*	This study
YEI4939	*MATa his3Δ1 leu2Δ0 met15Δ0 ura3Δ0 6HF-smt3:kanMX6 SMC5-9myc:HIS3MX6. NSE2-ΔSIM-STOP-:6HA::hph Smc1-6HA::natNT2*	This study
YEI4948	*MATa his3Δ1 leu2Δ0 met15Δ0 ura3Δ06HF-smt3:kanMX6 SMC5-9myc: HIS3MX6 Mms21-6HA:natNT2 Smc1-6HA::hph*	This study
YEI5022	*MATalpha can1Δ::MFA1pr-HIS3MX6 lyp1Δ ura3Δ0leu2Δ0 his3Δ1 met15Δ0 RPA190-K408R K410R-6HA:natNT2*	This study
YEI5023	*MATa/MATalpha ade2-1 can1-100 his3-11,15 leu2-3,112 trp1-1 ura3-1 RAD5+ /ade2-1 trp1D2 can1-100 leu2-3,112 his3-11,15 ura3-52 Rpa190::hphMX4 RPA190-K408R K410R-6HA:natNT2*	This study
YTR5093	*MATa ade2-1 his3-11,15 trp1-1 leu2-3,112 can1-100 URA3::pADH-HisUbi-tADH::ura3-1*	This study
YTR5094	*MATa: ade2-1 can1-100 his3-11,15 leu2-3,112 trp1-1 RAD5+ ura3-52 nse1(H306A, C309A)-1MYC-7HIS::KanMX6 URA3::pADH-HisUbi-tADH::ura3-1*	This study
YTR5097	*MATa: ade2-1 can1-100 his3-11,15 trp1-1 RAD5+ ura3-1 NSE1-1MYC-7His::KanMX6 LEU2::pADH-HisUbi-tADH::leu2-3,112*	This study
YTR5103	*MATa ade2-1 his3-11,15 trp1-1 leu2-3,112 can1-100 NOP1-3HA:hphNT1*	This study
YMR5104	*MATa ade2-1 his3-11,15 trp1-1 leu2-3,112 can1-100 URA3::pADH-HisUbi-tADH::ura3-1 pCDC48-6FLAG:LEU2,ARS-CEN*	This study
YMR5105	*MATa: ade2-1 can1-100 his3-11,15 leu2-3,112 trp1-1 RAD5+ ura3-52 nse1(H306A, C309A)-1MYC-7HIS::KanMX6 URA3::pADH-HisUbi-tADH::ura3-1 pCDC48-6FLAG:LEU2,ARS-CEN*	This study
YMR5112	*MATa ade2-1 his3-11,15 trp1-1 leu2-3,112 can1-100 URA3::pADH-HisUbi-tADH::ura3-1 NOP1-3HA:hphNT*	This study
YMR5113	*MATa: ade2-1 can1-100 his3-11,15 leu2-3,112 trp1-1 RAD5+ ura3-52 nse1(H306A, C309A)-1MYC-7HIS::KanMX6 URA3::pADH-HisUbi-tADH::ura3-1 NOP1-3HA:hphNT1*	This study
YGB5214	*MATa his3Δ1 leu2Δ0 met15Δ0 ura3Δ0 6HF-smt3:kanMX6 MMS21promoter-MMS21-3HA (Leu2, Amp) 177G-P Smc5-9MYC:HIS*	This study
YGB5215	*MATa his3Δ1 leu2Δ0 met15Δ0 ura3Δ0 6HF-smt3:kanMX6 MMS21(170EDD-RRR)-6HA:natNT2 Smc5-9MYC:HIS*	This study

Table 2. List of strains used in this project.

3.1.2 Culture Media

Yeast cells were grown on Synthetic Complete (SC) or on rich media (YPD) and in liquid or solid conditions. The carbon source (glucose or galactose) used in all of them was 2%. Specifically, the YP (yeast extract peptone) media contains 1% of yeast extract and 2% of peptone. Whereas the SC minimum media is composed by a 0.67% of yeast nitrogen base and 0.2% of drop-out (an amino acid combination) that needs to be completed with leucine (0.06 mg/ml), histidine (0.02 mg/ml), uracil (0.02 mg/ml) and tryptophan (0.04 mg/ml). For the auxotrophy yeast selection one of these amino acids was not added to the culture.

Yeast strains expressing antibiotic resistances were selected by adding their specific antibiotic marker to YPD media. In this study, geneticin, hygromicin B and nourseothricin were used at: 200 µg/ml, 300 µg/ml and 100 µg/ml, respectively. For the solid plates, 2% of agar powder was added to the media.

3.1.3 Growth conditions

Yeast cells were generally grown at 30ºC, except where stated. Thermosensitive mutants were grown at 25ºC. Liquid cultures were inoculated from fresh plates, grown overnight at a 150 rpm shaker in different volume flasks (depending on the number of final ODs needed), and posteriorly diluted. The optical density of the cultures was measured with the spectrophotometer at a 600 nm wavelength (1 OD_{600} corresponds to $3x10^7$ cells/ml). And exponentially cultures were collected in 50 ml tubes and centrifuged at 4.000 rpm for 2 minutes. Yeast cells in agar plates were grown for approximately 3 days at the 25ºC, 30ºC or 37ºC incubators.

3.1.4 Competent cells preparation

For preparing yeast competent cells, 50 ml of exponentially growing cultures (at OD_{600} ~1) were centrifuged in a conic tube at 4.000 rpm for 2 minutes. Supernatant was discarded and the pellet of cells was resuspended in distilled water and transferred to a 1.5 ml tube. After a second 14.000 rpm centrifugation and eliminating the supernatant, cells were resuspended with 900 µl of SORB buffer (100 mM LiOAc, 1 mM EDTA/NaOH pH 8, 10 mM Tris-HCl pH 8, 1 M sorbitol), and centrifuged during 3 minutes at 2.400 rpm. After discarding the supernatant, the pellet of cells was again resuspended in 360 µl of SORB buffer and 40 µl of salmon's sperm single stranded carrier DNA (ssDNA). Competent cells were finally aliquoted in 50 µl volumes and frozen at -80ºC for a long-term storage. This protocol was adapted from the one previously described by Knop *et al.,* at 1999 (Knop et al., 1999).

3.1.5 Yeast cells transformation

In order to transform yeast cells, 50 µl (for a PCR product) or 10 µl (for a plasmid) of competent cells were thawed on ice. For the transformation of a PCR product up to 10 µl of DNA were added to the mixture. For plasmid transformation, 1-2 µl of DNA were used. Then, cells containing the DNA were resuspended with 300 µl of buffer PEG for transformation (100 mM LiOAc, 10 mM Tris-HCl, 1 mM EDTA, 40% PEG-3350 (polyethylene glycol)), and incubated at room temperature (RT) during 30 minutes. After that, 40 µl of dimethyl sulfoxide (DMSO) was added (or approximately the 10% of the total volume), and cells were a heat shocked at 42ºC for 15 minutes in a thermoblock.
Finally, cells were centrifuged at 2.400 rpm for 3 minutes, resuspended with a few microliter of liquid media and directly plated in SC media for auxotrophy selection. For antibiotic selection, the pellet was resuspended in 1 ml of YPD media and incubated at RT for at least 3 hours to allow expression of the antibiotic resistance before plating in selection plates.

3.1.6 Yeast growth test analysis

For growth test analysis, 3 µl of wild type or mutant cells were spotted in 10-fold serial dilutions from an OD_{600}~0.5 exponential culture on solid media plates. Plates were posteriorly incubated at the adequate temperature during 2-3 days and photographed with the Chemiluminiscent Imager (Bio-Rad).

For methyl methanesulfonate (MMS) growing test analysis, MMS was added from 0.001 to 0.02% final concentrations in the YPD agar media before solidification. BMH-21 (Sigma) was added to the YPD agar at a 15 µM concentration, whereas for liquid cultures, BMH-21 was added at a 50 µM concentration for 90 minutes (Wei et al., 2018). 6-azauracil was added in SC-Ura plates at a 100 µg/ml concentration (Tansey, 2006). Camptothecin (CPT), a Topoisomerase I inhibitor, was added to YPD agar plates at 10 µg/ml.

3.1.7 Mating, sporulation and tetrad dissection

In order to generate haploid *(RPA190::hphMX4 pRS314-(CEN-TRP1)-RPA190)* wild type and (*RPA190::hphMX4 pRS314-(CEN-TRP1)-rpa190-K408,410R)* mutant strains or (*rpa190-K408,410R:natNT2 smc5-6:KanMX6)* and (*rpa190-K408,410R:natNT2 nse1-16:KanMX6)* double mutant strains, *S. cerevisiae* Mata and Matα haploid cells were mixed in a patch at a YPD plate and incubated at 25ºC for 5 hours. Afterwards, the formation of zygotes was checked at the microscope and cultured in a YPD plate. 24 hours later, the bigger colonies (probably corresponding to diploid cells) were plated on YPD plates containing the two antibiotic markers for diploid selection, and later streaked on YPD plates for 2 days to obtain single colonies. Then,

diploids were placed in liquid or solid sporulation media (2% agar, 1% potassium acetate, 0.1% yeast extract, 0.05% glucose, supplemented with uracil, histidine and leucine) during a minimum of 7 days at 25ºC. The formation of the spores was checked under the microscope.

For tetrad dissection, about 200 µl of the media containing spores was spun down. Spores were resuspended once in sterile water and thereafter, incubated 15 minutes at 30ºC with β-glucuronidase. Later, 1 ml of water was added carefully in order to stop the digestion without disrupting the tetrads, and the tube was placed on ice. Next, spores were centrifuged at 800 rpm for 10 minutes, and 15 µl of tetrads were dropped onto a YPD agar plate that was tilted so that the drop could be distributed evenly along a previously drawn vertical line.

Tetrads were dissected at the micromanipulator with a microneedle, and the four ascospores were isolated to obtain four haploid cells (two Mata and two Matα) (see Figure 16). After dissection, spores were grown at 25ºC for 2 days until the formation of separated colonies from each individual isolated cell. Then, double mutant haploids were selected by antibiotic resistances.

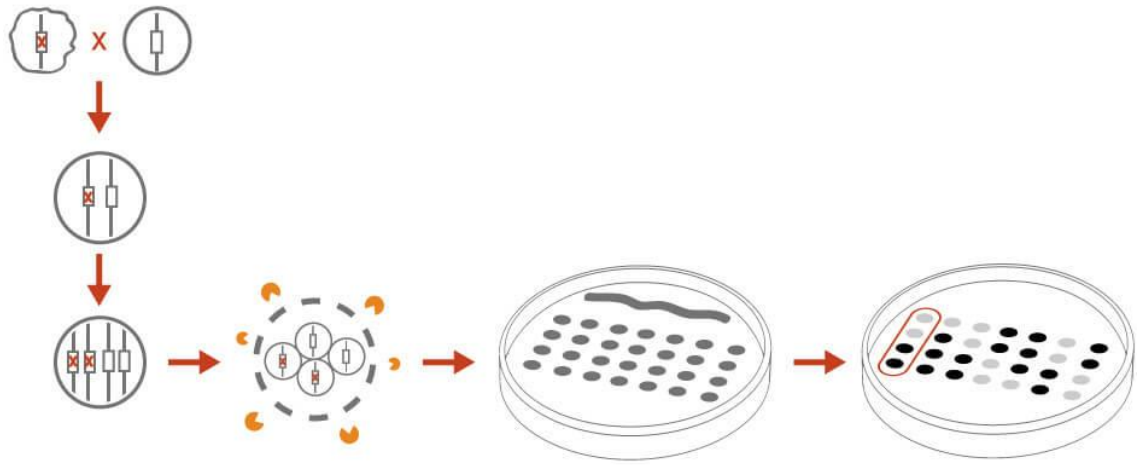

Figure 16. Representation of tetrad dissection from diploid Mata, Matα sporulated cells. Figure from SINGER Instruments.

3.1.8 Genomic DNA extraction with lithium acetate/SDS

For PCR-based applications we used the quick *S. cerevisiae* genomic DNA extraction protocol described by Lõoke and collaborators (Lõoke et al., 2011).

One colony from a fresh plate or a 1 ml overnight culture was centrifuged, resuspended with 100 µl of 200 mM lithium acetate 1% SDS solution, and incubated for 5 minutes at 70ºC. Then, we added 300 µl of 96-100% ethanol, mixed by vortexing, and spun down the DNA by centrifugation at 15.000 g for 3 minutes. After that, the pellet was washed with 70% ethanol and centrifuged again. After removing the ethanol, the pellet was finally resuspended in 100 µl of water or TE and centrifuged at 15.000 g for 15 seconds.

3.1.9 Yeast plasmid extraction

This protocol was used to recover plasmids (for example *pRS314-(CEN-TRP1)-RPA190-6HA:natNT2*, and *pRS314-(CEN-TRP1)-rpa190-K408,410R-6HA:natNT2*) from yeast cells. A 10 ml overnight culture was collected by centrifugation at maximum speed. Then, the pellet was resuspended in 250 µl of Resuspension buffer from the Thermo Scientific GeneJET plasmid miniprep kit, and 100 µl of glass beads were added to the cell suspension. Cells were broken with a mini-beadbeater cell disrupter (BioSpec Products) during 45 seconds at power 4.5. After that, the bottom of the tube was pierced with a needle and set up onto another 1.5 ml tube. The cell extract was recovered by spinning at 2.400 rpm and the upper tube containing glass beads was discarded. Then, we carried on with the plasmid miniprep protocol following the manufacturer instructions. The DNA was eluted with 25 µl of Elution buffer placed at the centre of the column, let stand for 1 minute and centrifuged for 1 minute.

5 µl of the eluted DNA were transformed into DH5α *E. coli* cells and the colonies were confirmed by PCR, digestion and sequencing.

3.1.10 Gene tagging

Gene tagging was performed following the protocol described by Janke *et al.,* (Janke et al., 2004), using a PCR-based method for recombinational integration. A set of cassette plasmids carrying a selectable marker and an epitope tag were amplified by PCR using the adequate primers to direct the insertion of the cassette to the desired locus by homologus recombination. Then, the PCR product was transformed into the yeast strain of interest and colonies were selected by the marker and later checked by Western Blot analysis.

3.2 DNA methods

3.2.1 Polymerase Chain reaction (PCR)

For the PCR reactions we used the Gene Amp PCR System 2700 (Applied BioSystems) thermocycler. The PCR mixture was generally done with 100 ng/µl of the DNA template, 2 mM of dNTPS, 300 nM of each primer, 1X buffer with $MgCl_2$, 2.6 U/reaction of the polymerase and nuclease free water up to 50 µl. The PCR parameters varied for each reaction and enzyme, but generally implied an initial denaturation step of about 2-3 minutes at 94ºC, followed by a shorter denaturation (15-30 seconds), annealing (15-30 seconds at the temperature fixed by the melting temperature of the primers used), and an elongation phase (1minute/Kb) at 72ºC for DNA products shorter up to 3 kb, or at 68ºC when amplifying products larger than 3kb length. These cycles were repeated several times (in the case of the Expand high-fidelity reaction, denaturation,

annealing and elongation steps were first repeated 10 times, followed by 20 more cycles with increasing elongation times per cycle). Amplification finished with a last 8-10 minutes elongation step. Then, the PCR product was purified (QIAquick PCR purification kit, Qiagen) or directly transformed into *S. cerevisiae* yeast competent cells.

3.2.2 DNA restriction analysis

Most of the mutant strains created by SDM were checked by restriction enzymes. For example, *rpa190-K408,410R* mutants carried a PstI restriction site that was used to detect positive colonies before sequencing them. The digestion mixture for a 20 µl reaction was done with 2 µl of the specific 10x buffer, 1 µg of DNA, 1 µl of the enzyme and the required volume of nuclease-free water. Reactions were incubated either 2 hours or overnight at the indicated temperature for each enzyme (usually at 37ºC); before being loaded onto an agarose gel and doing an electrophoresis to separate the DNA fragments.

3.2.3 DNA gel electrophoresis

For the detection and separation by size of DNA molecules we used DNA gel electrophoresis. First, we prepared the gel by melting 0.8 to 2% (depending on the DNA size) of D1 low-EEO agarose with 1X TAE buffer (40 mM Tris-HCl, 20 mM acetic acid, 1 mM EDTA, pH 8). Once the agarose was polymerized, DNA was loaded onto the gel with a Ficoll-Loading Buffer (FLB; containing 15% of ficoll-400, 0.1 M EDTA pH 8, 0.1% SDS and 0.05% bromophenol blue) and next to a 1 kb DNA ladder (Sigma). Agarose gels ran at 100 V constant voltage submerged in 1X TAE Running buffer, and were later stained in 0.5 µg/ml of ethidium bromide. Finally, DNA was detected and photographed with the Alpha DigiDoc UV transilluminator.

3.2.4 DNA fragment purification

In order to extract and purify a DNA fragment from an agarose gel, the DNA was mixed with SYBR Green Fluorescent stain before loading. After the electrophoresis, the desired DNA fragment was visualized with a transilluminator, cut from the agarose gel with a scalpel, and kept in a 1.5 ml tube. Next, the DNA fragment was extracted from the agarose and purified using the QIAquick Gel extraction Kit (Qiagen), following the manufacturer's instructions.

3.2.5 DH5α competent cell transformation

For bacterial transforming we used commercial DH5α competent cells (Invitrogen) due to its high efficiency. First, we took 50 µl aliquots from -80ºC and leaved them a few minutes on ice. Then, we added 5 µl of DNA and kept them on ice for 30 minutes. Subsequently we heat shocked competent cells at 42ºC for 20 seconds. Immediately after, cells were cooled down on ice for 2 minutes. One millilitre of LB (Luria Bertani) media was added to the tube and incubated at 37ºC for one hour to allow expression of the antibiotic resistance. Finally, cells were centrifuged at 6.000 rpm for 5 minutes, about 950 µl of media was removed, and the approximately remaining 50-100 µl were plated on LB agar plates containing 50 µg/ml of ampicillin.

3.2.6 Miniprep plasmid extraction

For miniprep plasmid extraction we used the Thermo Scientific GeneJET plasmid miniprep kit (K0503), and followed the manufacturer instructions. Cells were resuspended from a fresh LB+ Ampicillin plate where streaked isolated colonies had grown overnight at 37ºC. After lysing and neutralising cells, binding the DNA to the column and washing it, purified plasmids were eluted in 50 µl or in 30 µl volumes when higher DNA concentrations were required.

3.2.7 Recombination cloning in MC1061 competent cells

MC1061 transformation was used for recombinational cloning of inserts, as they carry a functional *recA+* gene that permits bacterial homologous recombination. Two DNAs (insert and vector), containing at least 30-40 bp of homology at each end, were prepared by PCR.

To prepare MC1061 competent cells, a 100 ml culture of MC1061 cells was grown at 37ºC until it reached an OD_{600}~0.5. The culture was centrifuged at 4.000 rpm for 5 minutes at 4ºC, the supernatant was discarded and the pellet was resuspended with 10 ml of a $CaCl_2$ solution (60 mM $CaCl_2$, 10 mM HEPES pH 7) and incubated for 2 hours on ice. Afterwards, cells were centrifuged (5 minutes, 4.000 rpm, 4ºC), and finally resuspended in 2 ml of $CaCl_2$ solution containing 15% of glycerol. 300 µl aliquots were stored at -80ºC.

For transformation, we added 3-5 µl of each PCR product to a 100 µl aliquot of MC1061 competent cells, mixed and incubated 30 minutes on ice. Then, we heat shocked cells for 2 minutes at 42ºC and cooled them down on ice for 2 minutes. Next, we added 1 ml of LB liquid media to the tube and incubated cells 1 hour at 37ºC for phenotypic expression. Later, we centrifuged cells at 4.000 rpm for 5 minutes, discarded most of the supernatant, and plated the remaining 50-100 µl on LB agar plates containing ampicillin.

3.2.8 Site-directed mutagenesis

For the construction of the *rpa190-K408,410R* and *smc5-KE* mutant plasmids , we used the PCR-SDM (site directed mutagenesis) protocol. This method was modified form the original protocol described by Weiner and colleagues, (Weiner et al., 1994). For site-directed mutation of *nse2*, we used recombination in MC1061 cells.

Primers were designed to introduce the desired mutations and in some cases, a specific restriction site to check positive colonies. The PCR reaction was done with the iProof high-fidelity polymerase from BioRad, using a yeast *RPA190* expression vector (*pRS314-(CEN-TRP1)-RPA190*) as a DNA template. The PCR-SDM product was then purified with the QIAquick PCR purification kit from Qiagen, and eluted to a final volume of 30 µl. Next, the purified DNA was phosphorylated with T4 polynucleotide kinase (Takara). The reaction was supplemented with 3 µl of the 10X Reaction Buffer (500 mM Tris-HCl pH 8.0, 100 mM $MgCl_2$ and 50 mM DTT) and with 3 µl of 10 mM ATP, added to 24 µl of the PCR product. The mixture was incubated at 37ºC for 1 hour, followed by an additional 15 minutes incubation at 75ºC to inactivate the enzyme. Later, DNA was circularized with the Rapid DNA ligation kit (Roche) for 1 hour at RT. The DNA was cleaned up (QiAquick PCR purification) to remove the buffer and the ligase. After that, part of the DNA was digested 1 hour at 37ºC with DpnI at 10 U/µl (Roche), an enzyme that specifically cleaves the methylated template DNA used in the PCR. Finally, 5 µl of the DpnI digestion were used to transform DH5α competent cells. To evaluate the efficiency of the procedure, we used a control in which the polymerase in the first PCR step was intentionally omitted.

Alternatively, a second strategy for site-directed mutagenesis was used. This strategy is similar to the recombinational cloning described above, and takes advantage of the recombination competency of MC1061 cells. To this end, 40-nucleotide forward and reverse primers are designed on the residue/s to be mutated/deleted. Both primers contain unique 3' sequences, and overlapping 5' sequences containing the desired mutation. Following PCR on a plasmid template with the Expand High Fidelity kit (Sigma), the linear products contained identical 25 to 30 bp-long sequences at each end. The DNA was purified (Qiagen) and treated with DpnI to digest the non-mutated template DNA. Finally, it was transformed in MC1061 cells, which used the identical sequences at each end to repair and circularize the DNA by recombination.

3.2.9 Plasmids used in this study

Plasmid	Description	Reference
pTR1094	*YCplac22-[CEN-TRP1]-ADH1p-SMC5:9Myc (Amp)*	Lab collection
pTR1618	*YCplac22-[CEN-TRP1]-ADH1p-SMC5(K743,5 R):9Myc (Amp)*	This study
p1785	*pRS313 (CEN-HIS3, Amp)*	Lab collection
p1787	*pRS315 (CEN-LEU2, Amp)*	Lab collection
pTR2395	*pRS315-MMS21promoter-MMS21-3HA (CEN-LEU2, Amp)*	Lab collection
p2772	*YEplac195 (URA3, Amp)*	Rodrigo Bermejo
p2773	*YEplac195-CUP1-HIS7-Ubi (URA3, Amp)*	Rodrigo Bermejo
p3618	*YCplac22-[CEN-TRP1]-ADH1p-SMC5(K337,K344,K354,K355E)-9Myc (Amp)*	David Reverter
p3707	*YCplac22-[CEN-TRP1]-ADH1p-SMC5(K337,K344,K354,K355,K743,K745,K764E):9Myc (Amp)*	David Reverter
p3710	*YCplac22-[CEN-TRP1]-ADH1p-SMC5(K743,K745,K764E)-9Myc (Amp)*	David Reverter
pEI4032	*pRS314-RPA190 (CEN-TRP1, Amp)*	Herbert Tschochner
p4056	*ADHpr-SMC5 (K743, 745 E)-9Myc (CEN-TRP1, Amp)*	David Reverter
p4058	*ADHpr-SMC5 (K337, 344 E)-9Myc (CEN-TRP1, Amp)*	David Reverter
pEI4446	*pRS314-RPA190 (CEN-TRP1, Amp) Rpa190 K408R K410R*	This sudy
pEI4637	*pRS314-RPA190-K408R K410R-6HA:natNT2 (CEN-LEU2, Amp)*	This sudy
pGB4774	Derived from pTR2395, *NSE2-P194A,L195A (CEN-LEU2, Amp)*	This study
pGB4775	Derived from pTR2395, *NSE2-C221A,C226A (CEN-LEU2, Amp)*	This study
pGB4776	Derived from pTR2395, *NSE2-P222A (CEN-LEU2, Amp)*	This study
p4831	*YIplac128-pADH-HisUbi-tADH (LEU2, Amp)*	Boris Pfander

p4833	*YIplac211-pADH-HisUbi-tADH (URA3, Amp)*	Boris Pfander
pEI4919	*pRS313 (CEN-HIS3)+ RPA190-K408R K410R-6HA:natNT2 (Amp)*	This sudy
pEI4920	*pRS315 (CEN-LEU2) + RPA190-K408R K410R-6HA:natNT2 (Amp)*	This sudy
pEI4956	*pET15b-HA-MMS21 wt (6His-HA-MMS21) Cys226* re-created by ExSite in DH5 alpha *MMS21 170EDD-RRR (Amp)*	This study
pEI4957	*pRS315-MMS21promoter-MMS21-3HA 170EDD-RRR (CEN-LEU2, Amp)*	This study
pEI4958	*pET15b-HA-MMS21 wt (6His-HA-MMS21) Cys226 re-created by ExSite in DH5 alpha MMS21 G177-P (Amp)*	This study
pEI4960	*pRS315-MMS21promoter-MMS21-3HA G177-P (CEN-LEU2, Amp)*	This study
pTR5024	*pRS314-(CEN-TRP1)-RPA190-6HA:natNT2 (Amp)*	This sudy
pEI5078	*pRS314-(CEN-TRP1)-RPA190-K408R K410R-6HA:natNT2* cloned into pBlueScript *(Amp)*	This study
pEI5079	*pRS314-(CEN-TRP1)-RPA190-K408R K410R-6HA:natNT2* cloned into pBlueScript *(Amp)*	This study
p5080	*pCDC48-6FLAG, LEU2, ARS-CEN (Amp)*	Martí Aldea
pGB5131	Derived from pTR2395, *NSE2-ΔRING* (Deletion from C184 to I243, linker added between C184-I243) *(CEN-LEU2, Amp)*	This study
pGB5132	Derived from pTR2395, *NSE2-C184A,P185A (CEN-LEU2, Amp)*	This study

Table 3. List of plasmids used in this project.

3.2.10 Generation of *SMC5* mutants

We developed different *SMC5* expression plasmids containing *KE* or *KR* mutations. By the use of the SDM protocol we introduced into the *Arm-SMC5* expression vector the following amino acid changes: *smc5-K743,745E; smc5-K743,745R; smc5-K743,745,764E (smc5-3KE); smc5-K743,734E; smc5-K337,344E; smc5-K337,K344,K354,K355E (smc5-4KE); smc5-K337,K344,K354,K355,K743,K745,K764E (smc5-7KE).* For integration into the yeast genome, we first amplified the mutated *SMC5* allele by PCR. In parallel, we amplified a gene tagging cassette (Janke et al., 2004), which contains 40 bp tails homologous to the 3' end of the *SMC5* open reading frame and to the *SMC5* 3' untranslated region. Next, we combined both PCRs to generate a product containing the *SMC5* mutant alleles, followed by a tag and a selection marker. This final

product was the transformed into yeast cells. Positive colonies were checked by their Western Blot HA signal and finally sequenced.

3.2.11 Generation of *NSE2* mutants

NSE2 mutants carrying deletions on its C-terminal domain such as *nse2Δ16, nse2ΔC*, *nse2Δ29C*, *nse2Δ24C* and *nse2ΔSIM* were constructed by direct integration in a yeast strain using a 3' cassette that deleted the corresponding fragment for each mutation and fused the truncated C-terminal domain to a tag and a marker, as described by Janke and collaborators (Janke et al., 2004). The gene shortening produced by these C-terminal truncations was analyzed by Western Blot. To maintain a tag-free C-terminus in Nse2, we also designed primers for some of these mutations containing the specific C-terminal deletion followed by a STOP codon that prevented translation of the tag. In these mutants, Nse2 could not be detected by Western Blot.

In contrast, mutants carrying the point mutations *nse2-P194,L195A; nse2-C221A; nse2-P222A; nse2-C184,P185A*; *nse2-170EDD-RRR; nse2-G177-P;* and the *nse2ΔRING;* or the *nse2Δ16I* carrying an internal deletion of 16 amino acids (160-176), were created by SDM, using a wild type *NSE2* gene cloned into a yeast expression vector as PCR template. The resultant plasmid was sequenced, and the mutant sequence was amplified by PCR. Then, the PCR product carrying the corresponding mutations was fused to a cassette carrying the 6HA tag epitope and an antibiotic resistance marker (as described above for *SMC5* mutants). Most of them were also fused to a PCR product carrying a STOP codon before the HA tag. The final PCR product was integrated by homologus recombination in yeast and colonies where checked by Western Blot, genomic PCR and enzyme restriction (whenever possible), and finally sequenced.

3.2.12 Generation of *RPA190* mutants

In order to obtain the *pRS314-(CEN-TRP1)-rpa190-K408,410R* plasmid, we did a site-directed mutagenesis. We designed pair of primers containing the two point mutations and a PstI restriction site. As previously described, we did the PCR using the yeast expression vector *pRS314-(CEN-TRP1)-RPA190* as a template. Colonies were checked by PstI digestion and sequencing. The mutant and the wild type plasmids were then transformed into a diploid yeast strain with a deletion in one of the endogenous copies of *RPA190*. By sporulation and tetrad dissection we isolated haploid yeast colonies carrying the *rpa190-K408,410R* plasmid and a deleted chromosomal *RPA190* copy. After that, we tagged Rpa190 wild type/*KR* with a 6HA:natNT2 tag and isolated the tagged vectors from their yeast strains, to obtain the *pRS314-(CEN-TRP1)-RPA190-6HA:natNT2*, and *pRS314-(CEN-TRP1)-rpa190-K408,410R*-6HA:natNT2 plasmids. To integrate the double *KR* mutation into yeast, we used the mutant vectors as PCR templates. Finally, we transformed yeast cells with the PCR product, checked for the absence of the plasmid markers (to

prevent selection of a transformant not integrated but carrying the plasmid) and analyzed positive colonies by NAT resistance, PstI restriction and sequencing.

3.3 Protein methods

3.3.1 Protein extraction

3.3.1.1 Post-alkaline protein extraction

Protein extraction with 0.2M NaOH is a fast method that was used in this thesis to check several colonies from a transformation by Western Blot, and to check Nse2-protein levels in some *nse2* mutant strains. Post-alkaline extractions were done following the protocol described by Kushnirov, V.V (Kushnirov, 2000) with few modifications.

Briefly, about 2.5 OD_{600} or a single colony grown overnight in a 1 ml culture, were harvested by centrifugation and resuspended in distilled water. Then, cells were incubated for 5 minutes with 100 µl of NaOH 0.2 M at RT. After that, samples were centrifuged for 1 minute at 14.000 rpm and the supernatant was discarded. The pellet was resuspended with 50 µl of 1xSSR (2% SDS, 125 mM Tris-HCl, 5% sucrose, 0.01% bromophenol blue, pH 6.8) boiled 3 minutes at 95ºC and centrifuged again. Finally, 8 µl of the supernatant were used for SDS-PAGE Western Blot analysis.

3.3.1.2 Urea protein extraction

Protein extraction with Urea was a frequently used method during this thesis to check protein levels by Western Blot. Briefly, we took about 10 OD_{600} from an exponential yeast culture and harvested cells by centrifugation. Following, we removed the supernatant and washed the pellet with cold water. After that, we added 30 µl of 5M Urea to the cells and 2 small spatula full of glass beads. Then, cells were broken at the mini-beadbeater cell disrupter (BioSpec Products) for 45 seconds. Next, we added 100 µl of 1XSR (2% SDS in 0.125M Tris-HCl pH 6.8) to the mixture, vortexed for 5 seconds and boiled 3 minutes at 95ºC. Later, we punched the bottom of the tube with a needle and transferred the cell lysate to a new 1.5 ml tube by spinning at 2.500 rpm for 2 minutes. Finally, we centrifuged the samples for 5 minutes at 12.000 rpm to remove cell debris and took 115 µl of the supernatant to a new tube. One microliter was used for the BIO-RAD Micro DC Protein Assay in order to assess protein concentration; and 4xSS and β-Mercaptoethanol were added to the corresponding volume for 30 µg of protein, loaded onto an SDS-gel and analyzed by Western Blot.

3.3.1.3 TCA protein extraction

This protocol was used for analysing Pol30-protein levels and modifications by Western Blot. Briefly, 10 OD_{600} from an exponentially growing culture were collected by centrifugation 4 minutes at 4.000 rpm and 4ºC, after adding 250 µl of TCA 20% directly to the culture. The pellet was resuspended with 500 µl of TCA 20%, transferred to a 1.5 ml tube and spun 6-7 seconds at high speed. Then, the supernatant was removed and the pellet was resuspended again with 100 µl of TCA 20%. After that, we added 500 µl of glass beads and broke cells in a mini-beadbeater cell disrupter (BioSpec Products) for 45 seconds. Next, the sample was transferred to a new tube by making a hole with a needle at the bottom and spinning 1 minute at 1.000 rpm. After that, we washed beads twice with 100 µl of TCA 5% and centrifuged 10 minutes at 3.000 rpm and RT. The supernatant was discarded and the pellet was resuspended with 100 µl of 1xSR (2% SDS in 0.125 M Tris-HCl pH 6.8) and neutralized with 50 µl of Tris-base 1 M. Samples were then boiled 3 minutes at 95ºC, centrifuged 5 minutes at 13.000 rpm and protein concentration was determined with the BIO-RAD Micro DC Protein Assay. Finally, 4xSS and β-Mercaptoethanol were added to a volume corresponding to 30 µg of protein, loaded onto an SDS-gel and analyzed by Western Blot.

3.3.2 SDS-PAGE Western Blot analysis

We used the Sodium dodecyl sulfate-polyacrylamide gel electrophoresis (SDS-PAGE) technique for the denaturing electrophoretic separation of proteins according to their molecular weight; and the Western Blot (WB) analysis for their posterior detection with specific antibodies.

First, samples were loaded onto polyacrylamide gels composed by two phases with different pH and porosity. At the lower resolving gel (30% acrylamide/bis-acrylamide, 1.5 M Tris-HCl pH 8.9, 10% SDS, 10% ammonium persulfate (PA), tetramethylethylenediamine (TEMED) and distilled water), protein mobility was restricted to the pore size, what depended on the acrylamide percentage (from 7.5% to 15%). Whereas the upper 5% stacking gel (30% acrylamide/bis-acrylamide, 0.5 M Tris-HCl pH 6.5, 10% SDS, 10% PA, TEMED and distilled water) had a big pore size that permitted proteins to accumulate at the interphase with the resolving gel.

Gels were ran at a constant amperage (20mA/gel) in 1xRunnig buffer solution (2.5 mM Tris-HCl, 192 mM glycine, 0.1% SDS; pH 8.3), and were then transferred to polyvinylidene fluoride (PVDF) membranes; previously activated with methanol and equilibrated with Transfer buffer (39 mM glycine, 48 mM Tris-base, 0.0375% SDS, 10% or 20% ethanol). The transfer of proteins from the polyacrylamide gels to the PVDF membranes was done at a constant amperage (60 mA/membrane) using a SemiDry transfer for 1 hour. After that, membranes were blocked in 5% of non-fat milk in PBST (1% PBS and 0.2% Triton X-100 (SIGMA)) for 1 hour at RT to avoid nonspecific binding of antibodies, and later incubated overnight at 4ºC with the primary antibody (see table 4). The following day, membranes were washed three times with PBST and incubated for 1 hour at

RT with the corresponding secondary antibody (1:10.000) in 0.25% of non-fat milk diluted in PBST. Then, the membranes were washed three more times for about 30 minutes with PBST, and incubated for 5 minutes over the Chemiluminescent HRP Immobilon substrate (Millipore). Finally, proteins were detected and photographed in a Chemidoc (BioRad) unit.

Antibody	Type	Specie	Clone	Brand	Dilution
Anti-Myc	Primary	Mouse	9E10	Sigma Aldrich	1:2.500
Anti-HA	Primary	Rat	3F10	Sigma Aldrich	1:5.000
Anti-Flag	Primary	Mouse	M2	Sigma Aldrich	1:5.000
Anti-PCNA	Primary	Mouse	PC10	Abcam	1:5.000
Anti-Smt3	Primary	Rabbit		Abcam	1:5.000
Anti-Hexokinase	Primary	Rabbit		USBiological	1:5.000
Anti-ubiquitin	Primary	Mouse		Sigma Aldrich	1:5.000
Anti-Mouse IgG-HRP	Secondary	Sheep		GE Healthcare	1:10.000
Anti-Rat IgG-HRP	Secondary	Goat		GE Healthcare	1:10.000
Anti-Rabbit IgG-HRP	Secondary	Goat		GE Healthcare	1:10.000
Anti-Rat IgG Alexa FluorR 488	Secondary	Goat		Thermo Fisher	1:500

Table 4. List of antibodies used in this project.

3.3.3 Pull-down of His-tagged proteins

SUMO and ubiquitin pull-downs (PD) were done under denaturing conditions using protein extracts from yeast cells carrying the *SMT3* gene fused to a 6His-Flag epitope; or the *UBI* gene fused to a 7His-tag, expressed from a plasmid under the control of the *CUP1* promoter. In the latter case, cultures were grown in SC-URA medium containing $CuSo_4$ at 20 µM. Alternatively, pADH-HisUbi-tADH was integrated at the *LEU2* or *URA3* locus. Where indicated, exponentially growing cultures were incubated with 0.03% of MMS, 10 µg/ml Camptothecin (CPT), 0.2 M Hydroxyurea (HU), or 1 µg/ml Phleomycin (PHL) for 2 hours to induce DNA damage, before their harvest.

100 OD_{600} of exponentially growing cells (25 OD_{600} for ubiquitinated Rpa190 PD) were spun at 3.000 rpm 2 minutes in 50 ml tubes. Cells were then washed in cold water and transferred to a 1.5 ml tube. Subsequently, pellets were frozen at -80ºC or directly used for pull-down. Later, 250 µl of

Buffer A (6 M Guanidine Chloride, 100 mM KH_2PO_4, 10 mM Tris-HCl, 0.05% Tween-20, 15 mM imidazole, 1X protease inhibitors; pH 8) and 500 µl of glass beads were added to the pellet. Then, cells were broken using a mini-beadbeater cell disrupter (BioSpec Products) at power 6 for 40 seconds. Next, we pierced the bottom of the tube with a 21 ga. needle and set it up over another 1.5 ml tube. After that, extracts were spun at 2.400 rpm to recover the cell extract and discard the beads. Following, we added 700 µl of Buffer A to the tube, mixed it and spun 10 minutes at 14.000 rpm at 4ºC. The supernatant was then transferred to a screw cap tube, and the volume brought up to 1 ml. Finally, we added 70 µl of Ni-NTA (Nickel Nitrilo-triacetic Acid) agarose beads (Qiagen), and incubated the mixture overnight at the orbital rotator at RT. The following day, the tubes were spun at 3.400 rpm. The supernatant was transferred to a new tube, and the beads washed for 8 minutes with 900 µl of Buffer B (8 M urea, 100 mM KH_2PO_4, 10 mM Tris-HCl, 0.05% Tween-20, 2 mM imidazole; pH 8). Washes were repeated a total of three times with Buffer B and three times more with Buffer C (8 M urea, 100 mM KH_2PO_4, 10 mM Tris-HCl, 0.05% Tween-20; pH 6.3). Finally, proteins bound to the beads were eluted with 25 µl of 2xSSR (4% SDS, 250 mM Tris-HCl pH 6.8, 10% sucrose, 0.02% bromophenol blue) by boiling 3 minutes at 95ºC. 30 µl of supernatants were precipitated with the same volume of TCA 12% (trichloroacetic acid), washed 3 times with chilled acetone, resuspended by vortexing in 30 µl of Buffer C and incubated at 37ºC for 20 min. Then, protein extracts (PE) were boiled with 30 µl of 2xSSR. Finally, PE and PDs were centrifuged and loaded onto a SDS-PAGE for Western Blot analysis.

3.3.4 Co-Immunoprecipitation

Co-immunoprecipitation (co-IP) expermients were done to detect protein-protein interactions. Briefly, we immunoprecipitated HA-tagged proteins by using an anti-HA affinity matrix (Roche), and did the subsequent Western Blot detection of the secondary target with the anti-myc antibody (9E10; Roche), bound to the immunoprecipitated protein.

First, 30 µl of anti-HA beads were washed 3-4 times for 10 minutes with ice-cold IPP150-BSA buffer (50 mM Tris-HCl pH 7.5, 150 mM KCl, 0.1% Triton X100, 100 mM DTT, 2% BSA), and were then kept on ice for later. In parallel, an exponential 100 OD_{600} culture was collected and pellets were divided into two tubes. Then, we added 250 µl of IPP150-PI buffer per tube (50 mM Tris-HCl pH 7.5, 150 mM KCl, 0.1% Triton X100, 100 mM DTT, supplemented with proteases inhibitors cocktails, 1 mM Phenylmethane Sulfonyl Fluoride (PMSF), and 10 mM of N-Ethylmaleidemide (NEM)); and broke cells twice with a mini-beadbeater cell disrupter (BioSpec Products) during 45 seconds. Next, we punched the bottom of the tube with a needle and transferred it to a new tube by spinning at 3.000 rpm at 4ºC. After that, extracts from the same sample were mixed in a unique tube and centrifuged 10 minutes at 4ºC at maximum speed. Then, we took a sample from the whole cell extract (WCE) and eluted it with 2xSSR at 95ºC for 3 minutes. The rest of the clarified extract was mixed with the previously washed anti-HA beads and incubated in an orbital rotator for 2 hours at 4ºC. Later, the tubes were centrifuged at 3.000 rpm for 1 minute and the

supernatant was removed. After that, we washed the beads with IPP+PI buffer and rocked the samples for 8 minutes. We repeated this step 3 more times and did an additional 5 minute wash with the IPP150 buffer without Triton X-100. Next, proteins bound to the beads were eluted with 1xSR (2% SDS in 0.125 M Tris-HCl pH 6.8) and incubated at 37ºC for 10 minutes. Finally, 4xSS (40% sucrose and 0.8% bromophenol blue) containing 2% β-Mercaptoethanol was added to the samples, before boiling 3 minutes at 95ºC for Western Blot analysis.

3.3.5 Protein Chromatin binding assay

In order to study chromatin association of Rpa190 we developed a protein chromatin binding assay adapted from the one described by Liang and Stillman in 1997; (Liang & Stillman, 1997). First, a 50 OD_{600} culture was spun at 4ºC and 3.000 rpm for 10 minutes. Next, cells were resuspended and incubated at RT for 10 minutes in 1 ml of CBA1 buffer (50 mM KPi pH 7.4, 0.6 M Sorbitol, 0.1% Na-Azide). Then, the culture was centrifuged for 3 minutes at 2.000 rpm and the supernatant was discarded. Pellet was resuspended in 1 ml of CBA buffer 2 (50 mM KPi pH 7.4, 0.6 M Sorbitol), and 9 µl of Zymoliase 100T (10 mg/ml stock) was added to the sample. Cell walls were digested for approximately 10 minutes at 37ºC. To test for spheroplasting, 10 µl of the sample was diluted in 990 µl of water, both before and at different times after the addition of Zymoliase. The digestion was kept until the OD_{600} dropped to less than 10% of its initial value. Then, the sample was centrifuged again for 5 minutes at 1.200 rpm. From this step on, sample and buffers were kept always on ice. Spheroplasts were washed with 1 ml of ice-chilled CBA buffer 3 (50 mM HEPES/KOH pH 7.5, 100 mM KCl, 2.5 mM $MgCl_2$, 0.4 M sorbitol) and centrifuged at 1.200 rpm for 5 minutes at 4ºC. After that, the supernatant was discarded and the pellet was resuspended in 150 µl of Extraction buffer (EB: 50 mM HEPES/KOH pH 7.5, 100 mM KCl, 2.5 mM $MgCl_2$). Next, spheroplasts were lysed by adding 7 µl Triton X-100 10% to a final concentration of 0.25% and incubated on ice for 5 min with gentle mixing. Protein concentration was measured using the DC Protein Assay (Biorad) kit and the suspension was split in two tubes with 75 µl each, one of them corresponding to the whole cell extract (WCE). The other one was underlayed with 150 µl of EBX-S buffer (50 mM HEPES/KOH pH 7.5, 100 mM KCl, 2.5 mM $MgCl_2$, 0.25% Triton X-100, 30% sucrose), and centrifuged at 12.000 rpm for 10 minutes at 4ºC. After spinning, the supernatant stays above the sucrose cushion, while the chromatin sediments at the bottom of the tube. 75 µl of the uppermost layer was saved as supernatant (SN). The pellet was washed with 150 µl of EBX buffer (50 mM HEPES/KOH pH 7.5, 100 mM KCl, 2.5 mM $MgCl_2$, 0.25% Triton X-100) and centrifuged again at 10.000 rpm for 5 minutes at 4ºC. Pellet fractions (chromatin pellet) were resuspended in 75 µl of buffer EBX. The WCE, SN and CP samples were then diluted with 1 ml of Buffer A (6 M Guanidine Chloride, 100 mM KH_2PO_4, 10 mM Tris-HCl, 0.05% Tween-20, 15 mM imidazole, 1X protease inhibitors; pH 8). Finally, a His-tagged pull-down was done with each fraction, and Rpa190 ubiquitination levels were analyzed by Western Blot.

3.3.6 diGly Proteomics

In order to identify potential Nse1 targets, we did a site-specific ubiquitination analysis in yeast using Quantitative proteomics. For that, we isolated the nuclear fraction from two yeast strains treated with MMS 0.02% for 1,5 hours: a wild type and an *nse1-C274A* mutant, and digested them with trypsin. After digestion, two glycines remain attached to the ubiquitinated lysine (K-ε-GG) and this can be immunoprecipitated with an anti diGly antibody to enrich ubiquitinated peptides. This enrichment was followed by mass-spectrometry analysis.

Sample preparation was done by Dra Celia Casas from our lab, whereas mass-spectrometry analysis was performed in the proteomics unit from CNIO. Two biological and two technical replicates were done for each condition, so samples were processed for a total of 8 runs. The quantification was done by label free.

First, 1.800 ml of each cell culture at OD_{600}~1.5 were harvested for 5 min at 5.000 rpm, resuspended in 400 ml of azide solution (50 mM Tris-Cl-H pH 7.5, azide 0.1% (15 mM)), and incubated for 5 min at the roller. Next, cells were centrifuged as before, resuspended in 400 ml of reduction solution (500 µl of 1M Tris-HCl pH 7.5, 250 µl β-ME, 49,25 ml H_2O) and incubated 30 min at RT. After another centrifugation, cells were resuspended in 50 ml of SP buffer (1 M sorbitol, 20 mM phosphate buffer pH 7.4) and 2 mg/gr of cells of Z100T was added to each culture. Samples were mixed and divided into two 50 ml tubes. 25 ml more of SP buffer were added to a final volume of 50 ml. Then, samples were incubated at 25ºC for 20-25 min at a 100 rpm shaking agitation. After checking spheroplasting, cells were sedimented at 3.200 rpm for 3min and washed with SP buffer. After removing the supernatant, spheroplasts were resuspended in Ficoll buffer (18% FICOLL, 20 mM phosphate buffer pH 6.8 (PI-Roche, 1 mM EDTA, 5 mM chloroacetamide, 50 µM PR-619)) and kept on ice for 5 min. Then, one aliquot was taken apart as WCE and samples were centrifuged at 3.000 g for 20 min at 4ºC. SN was taken and nuclear pellet was washed with Tris-HCl 50 mM pH 8. Following, it was resuspended in SDC buffer (5% SDC, 50 mM Tris-HCl pH 8, 5 mM Chloroacetamide, 50 µM PR-619, 1 mM EDTA, PI-Roche, 1 mM DTT, 1 mM ortov, 25x PPIs, H_2O), sonicated 3 times for 5 seconds, and incubated 10 min at RT. Next, samples were vortexed 2-3 times, incubated again 10 min on ice and spun at top speed for 5min. At this point, the supernatant corresponded to the nuclear fraction. Two replicates of 10,8 µg/ml of each sample corresponding to the nuclear fraction and solubilized in 5% SDC buffer were sent for the proteomics screening.

Thus, after preparing the samples, 4 mg of total protein from extracts of each condition were used by the Unidad de proteómica of the CNIO for its processing. Briefly, proteins were treated with the TCEP reducing agent at 15 mM during 30 minutes and alkylated with 30 mM of 2-choloacetamide (Sigma) 30 minutes more at RT in the dark. Then, lysates were diluted 5-fold with 50 mM of TrisHCl pH 8, and proteins were digested with Lys-C from *Acromobacter lyticus* M497-1 (Wako) at RT for 3 hours and with Sequencing Grade Trypsin from Promega at 37ºC overnight. After that, peptides were precipitated by centrifugation and desalted with 500 mg of C18 SepPak SPE (Waters), lyophilized and finally, immunoprecipitated. K-ε-GG peptides were enriched with the

PTMScan ubiquitin remnant motif (K-ε-GG) kit (Cell Signaling Technology). Tripsinized proteins were resuspended in 1.2 ml of immunoaffinity purification (IAP) buffer (50 mM MOPS [pH 7.4], 10 mM Na_2HPO_4, 50 mM NaCl) and centrifuged at max. speed for 5 min. Immuno-affinity purification was performed as described by Udeshi and collegues, 2013 (Udeshi et al., 2013). Thus, about 20 µl of anti-K-ε-GG antibody beads were incubated with the supernatants for 3h at an orbital rotator at 4ºC. Later, beads were washed twice with 1 ml of ice-cold IAP buffer, two times more with PBS, and a last one with water. Finally, ub-peptides were eluted from the antibody 2 times with 50 µl of 0.5% TFA. Enriched K-ε-GG samples were desalted by using StageTips following the manufacturer instructions. Stage tips were first washed with 50 µl of 50% MeCN/0.1% TFA and equilibrated with 2x50 µl of 0.1% TFA before samples loading. Then, they were washed with 2x50 µl of 0.2% TFA, eluted with 50 µl of 65% MeCN/0.1% TFA, and completely dried by using vaccum centrifugation.

Subsequently samples were reconstituted in 0.5% of FA, and analyzed in an LTQ-Orbitrap Velos (Thermo Scientific) that worked in a data dependent mode, coupled online to a nanoLC Ultra system (Eksigent), equipped with a nanoelectrospray ion source (Proxeon Biosystems). Each sample was injected twice in the mass spectrometer in order to obtain two technical replicates. They were loaded onto trapping columns and posteriorly washed for 15 min with 0.1% of FA. Peptides were eluted at a flow rate of 250 nl/min onto an analytical column packed with ReproSil-Pur C18-AQ beads; and the Mass spectrometry acquisition time was 120 min. Finally, data processing was performed with the MaxQuant (version 1.5.3.30) software package, whereas the bioinformatics analysis and data visualization of the MaxQuant output was done with the Perseus software. The two-sample T-test was used to identify UQ sites significantly different between wild type and mutant groups.

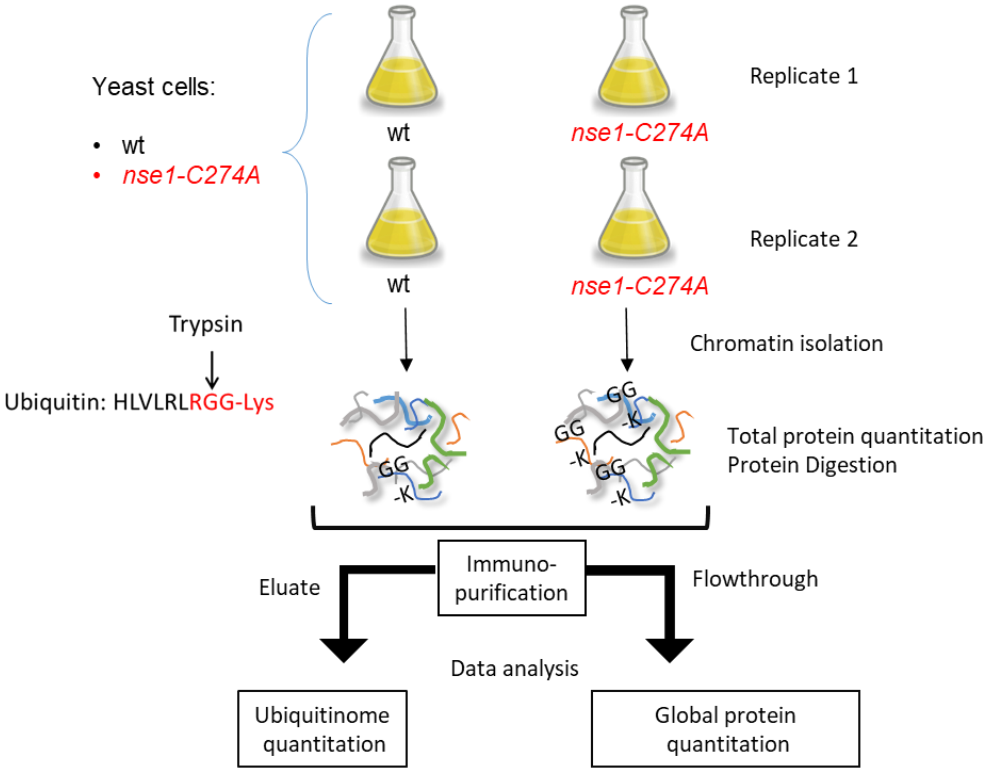

Figure 17. diGly proteomics workflow. The nuclear fraction of 2 biological replicates from wild type and *nse1-C274A* yeast cells was isolated and digested with trypsin. After Immuno-purification, the global protein quantitation obtained from the flowthrough and enriched ubiquitinated peptides were analyzed by Mass-spectrometry.

3.4 Microscopy

3.4.1 Chromosome spreads

The Mitotic Spread Protocol used was adapted from Koshland, Bishop labs and Grubb *et al* JVisExp(2015) (Grubb et al., 2015). It consists in the immunostaining and analysis of chromatin-bound proteins. For that, 5 OD_{600} from an exponentially growing culture were spun for 15 seconds at 13.000 rpm. Alternatively, 2.5 OD_{600} of each sample were mixed and centrifuged together with 2.5 OD_{600} of a strain carrying the protein of interest tagged with mCherry, used as an internal control. Cells were resuspended in 1 ml of ice-cold Solution 1 (80.2 mM K_2HPO_4, 19.8 mM KH_2PO_4, 1.2 M Sorbitol and 0.5 mM $MgCl_2$, 0.1% NaAz; pH 7.4) and kept on ice. Then, samples were centrifuged at 6.000 rpm for 1 minute at 4ºC, resuspended in 100 µl of freshly prepared Spheroplasting buffer (Solution 1 with 1/50th volume 1M DTT and 1/50th volume zymolyase (from 10 mg/mL 100T stock)) and incubated at 37ºC during 20-30 minutes. Complete cell wall digestion in more than 95% of cells was scored under the microscope after mixing 1,5 µl of spheroplasts with 1,5 µl of 2% SDS on a glass slide, as spheroplasted cells immediately lyse in the presence of

detergent. After that, spheroplasts were resuspended in 500 µl of ice-cold Solution 2 (100 M MES, 2 mM EDTA, 0.5 mM $MgCl_2$ and 1 M Sorbitol; pH 6.4) and mixed gently by inversion. Then, spheroplasts were spun for 8 minutes at 800 rpm and 4ºC, and the supernatant was removed carefully. Finally, samples were resuspended in 60 µl of ice-cold Solution 2 and kept on ice until spreading. Meanwhile, slides were prepared by boiling them submerged in water inside a glass beaker, for a few seconds in the microwave. Next, slides were taken with forceps, cleaned with ethanol inside a petri dish and dried in the fume hood.

For spreading, we took 10 µl of gently resuspended spheroplasts and pipetted them onto the slide. Subsequently, we added 20 µl of the freshly prepared Fixative solution (4% paraformaldehyde and 3.4% sucrose), 40 µl of detergent (lipsol at 2%) in a swirling motion, and 40 µl more of Fixative solution with the same movement. Then, the same last pipette was used for spreading the mixture on the slide without touching the glass surface, and they were dried overnight in the fume hood.

The following day, we started with the immunostaining protocol by washing the slides 10 minutes in PBS inside coplin jars. Next, we drained the liquid and dried the back of the slide with a piece of paper. After that, we added 100 µl of Blocking buffer (0.1 g dried milk powder and 0.25 g BSA in 5 ml of PBS) to the central area of the slide, and incubated 10 minutes in a humidity chamber. Then, we drained the slide again, added 20 µl of the primary antibody in Blocking buffer (1:500 of anti-HA 3F10, Roche), added a coverslip and incubated it for 1 hour. Next, slides were washed three times with PBS for 10 minutes each. Next, we added 20 µl of the secondary antibody (1:1000 of anti-rat Alexa 488) to the central part of the slide, added a coverslip and incubated it for 1 hour in in a dark humidity chamber. We did three more washes of 10 minutes each in PBS after the secondary antibody incubation. Slides were air-dried completely in the dark. Finally, we added 3 µl of Slow Fade + Hoechst 2000 to the centre of the spread, and added a coverslip. For fluorescence microscopy, series of z-focal plane images were collected with a DP30 monochrome camera mounted on an upright BX51 Olympus fluorescence microscope. We stacked the images taken by the fluorescence microscope with ImageJ (https://imagej.nih.gov/ij/), and quantified them manually after substraction of background.

3.5 *In vitro* experiments

In vitro experiments were performed in collaboration with the Protein Structure group from Dr David Reverter at the Institut de Biotecnologia i Biomedicina at the Universitat Autònoma de Barcelona. There, I expressed and purified Nse2 mutant strains with the help of Jara Lascorz, and developed sumoylation assays with the help of Dr Nathalia Varejão.

3.5.1 Protein expression and purification

Arm/Smc5 recombinant proteins containing N-terminal 6His-tag were coexpressed with 6His-tag-Nse2 (wild type or mutant versions: *nse2-G177-P* and *nse2-170EDD-RRR*) in *E. coli* Rosetta 2(DE3) cells (Novagen) in 2 L cultures. Cells were grown at 37ºC to OD_{600}=0.6, subsequently induced with 0.5 M IPTG overnight at 20ºC, and harvested by centrifugation. Then, pellets were resuspended in Lysis Buffer (20% sucrose, 50 mM Tris pH 8, 1 mM β-mercaptoethanol, 350 mM NaCl, 20 mM imidazole, 0.1% IGEPAL) and cells were disrupted by sonication and centrifuged to remove cell debris for 15 minutes at 4ºC. 15 µl samples from the total extract (T.E.) and from the supernatant (SN) were taken. Next, proteins were purified by metal affinity chromatography using Chelating Sepharose Fast Flow resin (GE Healthcare). Previously, the Nickel column was prepared. For that, we first added the chelating sepharose, did 2 water washes and added 1 µl of $Ni(II)SO_4$ at the third wash. Then, the resin became stained and we did 5 more water washes, and a last wash with Buffer A (350 mM NaCl, 20 mM Tris pH 8, 10 mM imidazole, 1 mM β-Mercaptoethanol). After preparing the column, the sample (supernatant) was loaded at 4ºC. Subsequently we added Buffer A twice and finally eluted the hexahistidine-tagged proteins with Buffer B (350 mM NaCl, 20 mM Tris pH 8, 250 mM imidazole, 1 mM β-Mercaptoethanol). Eluted proteins (~12 ml) were filtered and a sample was taken after the metal purification (Ni).

Proteins were further purified by gel filtration (Superdex 200 HiLoad; GE Healthcare) and we obtained the elution profile. Then, we took the samples coming from the tubes at the pick of the graph and loaded them onto a polyacrylamide gel together with the samples from the total extract, the supernatant and the metal purification. The gel was stained in Coomasie to check the size of the eluted proteins and the concentration of each sample was analyzed.

3.5.2 Smc5-Nse2 SUMOylation reactions

Nse2-dependent Sumoylation reactions of previously purified *nse2-G177-P* and *nse2-170EDD-RRR* mutants, coexpressed with the ARM domain of Smc5, were compared with an Nse2-wild type strain and the *nse2-C200,H202A* and *nse2-V266R* mutant versions. Sumoylation assays were performed in a reaction mix containing 25 mM NaCl, 40 mM HEPES (pH 7.5), 10 mM MgCl2, 0.2% tween-20, 40 mM DTT, 0.3 µM yeast E1 (Aos1/Uba2), 0.2 µM yeast E2 (Ubc9), 2 mM ATP, 0.8 µM ssDNA, 2.7 µM of (Alexa488)-labeled SMT3, 2 µM of Nse4 substrate, and the E3 enzyme at 0.16 mg/L. After the addition of ATP, reactions were incubated at 30ºC, and samples from 5, 10 and 15 minutes were taken and stopped with SDS-Sample loading buffer (0.25 M Tris–HCl buffer pH 6.8, 10% SDS, 30% glycerol, 0.7 M β-mercaptoethanol, and 0.05% bromophenol blue). Finally, products of the time-course reaction were loaded onto an SDS-PAGE gel and visualized by Alexa488 fluorescence emission in the Molecular Imager Versadoc MP4000 System.

RESULTS

4. RESULTS

4.1 Chapter I- DNA activates the Nse2/Mms21 SUMO E3 ligase in the Smc5/6 complex

Posttranslational modification of chromosomal proteins by SUMO has been linked to several biological processes involved in chromatin remodelling, regulation of DNA replication and segregation mechanisms and in the DNA damage response (Makhnevych et al., 2009) (Cubeñas-Potts & Matunis, 2013). In fact, the SUMO E3 ligase activity on chromatin has a relevant implication in the maintenance of genomic integrity. However, how DNA regulates this activity remains poorly understood. In this work, we reveal a new regulation mechanism by which the DNA enhances the Mms21 SUMO ligase activity in the Smc5/6 complex (Varejão et al., 2018). This work was performed in collaboration with the Protein Structure group from Dr David Reverter in the Institut de Biotecnologia i Biomedicina at the Universitat Autònoma de Barcelona.

Particularly, Nse2 SUMO ligase widely described functions on DNA repair depend on its docking to the coiled coil of Smc5, and on the ATPase activity of Smc5/6 (Bermúdez-López et al., 2015). As ATPase mutants are supposed to decrease loading of the complex onto chromatin, we wondered whether DNA could be directly affecting the SUMO conjugation activity of Nse2.

4.1.1 Compromising Smc5-DNA binding sensitizes yeast cells to DNA damage

The crystal structure of the Smc5-Nse2 complex revealed a minimal positively-charged region in the Smc5 ARM (Figure 18) that could interact with DNA, thus upregulating the SUMO ligase activity of Nse2. *In vitro* experiments performed by Dr David Reverter's group from Universitat Autònoma de Barcelona, permitted to check this electrostatic interaction. They produced several ARM-Smc5/Nse2 constructs containing lysine to glutamic acid *(KE)* mutations in the ARM region of Smc5, close to the Nse2-binding site. These mutations inverted the positive charge of lysines in the DNA sensor of Smc5 (Figure 19), thus counteracting binding to the negatively-charged phosphate groups of DNA. Then, they analyzed SUMO conjugation rates of the C-terminal kleisin domain of Nse4 (cNse4), used as a model substrate of Nse2, in each of the mutants generated in the presence or absence of ssDNA. Interestingly, all tested constructs showed a comparable low conjugation activity in the absence of DNA. In contrast, in the presence of DNA, cNse4-SUMO conjugation rates decreased in all the mutants in comparison with the wild type ones (Figure 19). However, the *K743,745E* mutation showed the greatest effect, as in the presence of DNA the cNse4-SUMO conjugation enhancement observed in the wild type was completely lost. *K337,344,764E*, carrying three point mutations in the Smc5 ARM, was the second most defective mutant in DNA binding, showing an important reduction in the SUMO conjugation rate relative to wild type. Remarkably, the SUMO conjugation enhancement of the *K743,745R* mutant, in which

the positive charge of the residues was maintained, was similar to the wild type, confirming the role of the Smc5 positively-charged region in DNA binding (Figure 19).

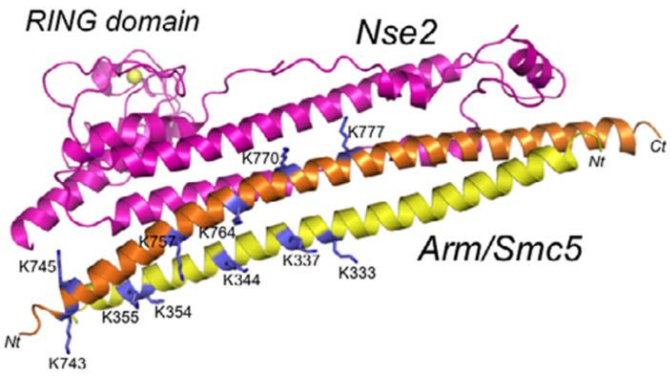

Figure 18. Structure (PDB: 3HTK) of the interaction of between Nse2 (pink) and the ARM domain of Smc5 (orange and yellow). Figure from (Varejão et al., 2018). Lysine residues in the Smc5 coiled coil surface potentially participating in interactions with DNA are labelled and shown in blue. The position of the RING domain of Nse2 is also indicated.

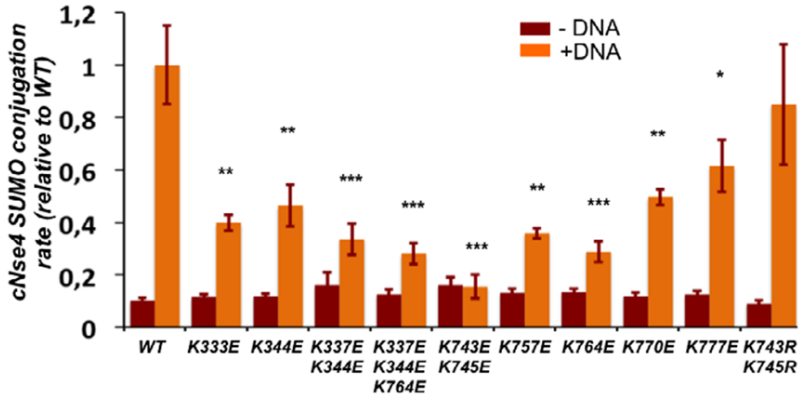

Figure 19.Lysine to aspartic acid mutations in the Smc5 coiled coil significantly decrease cNse4 SUMO conjugation rates in the presence of DNA. Figure from (Varejão et al., 2018). Bar diagram representation of the cNse4 SUMO conjugation rates of activity assays of Arm/Smc5-Nse2 KE mutants in the presence (orange bars) or absence (red bars) of ssDNA, relative to WT (set to 1). Significance was measured by a two-tailed unpaired t-test relative to wild-type. *P < 0.05, **P < 0.01, ***P < 0.001. Note that countercharge mutations at K743 and K745 completely abolish DNA-dependent activation of the E3 ligase, while mutation of residues further away have a lower effect.

To proof the relevance of this mechanism, we analyzed the function of this Smc5-DNA sensor *in vivo*. For that, we generated *SMC5* plasmids containing different combinations of some of the *KE* mutations tested *in vitro.* These constructions included the *K743,745E* mutant at the coiled coil 2, as it seemed to more strongly regulate the DNA-dependent SUMO conjugation enhancement *in vitro*; and a *K743,745R* version in which the positive charge of both residues was maintained. Then, we decided to include the *K746E* mutant to the *K743,745E* construct, as *K764E* was the simple mutant with a major effect *in vitro*. Therefore, we speculated that a *smc5-3KE (K743,745,764E)* mutant could aggravate the phenotype of the *K743,745E in vivo*. In addition, at

coiled coil 1, we generated a *smc5-4KE (K337,K344,K354,K355E)* mutant, which combined the previously analyzed *K337,K344E* double mutant with mutations in K357 and K355, not tested *in vitro*, as the crystal 3D structure of the Arm/Smc5-Nse2 showed that their location was proximal to K743 and K745.

We first introduced the mutant plasmids into a conditional *smc5* mutant strain that expressed the endogenous *SMC5* under the *GAL* promoter; and studied cell viability under non-permissive conditions (glucose). Yeast growing spot test analysis showed that *the smc5-4KE (K337,K344,K354,K355E), smc5-K337,344E, smc5-3KE (K743,745,764E), smc5-K743,745E* and the *smc5-K743,745R*, supported the robust growth of the mutant cells (Figure 20); indicating that *smc5-KE* or *KR* mutations did not affect the overall function of the Smc5/6 complex.

However, when yeast cultures were in the presence of MMS, cells expressing the *smc5-K743,745E or smc5-3KE* alleles showed an MMS-sensitivity phenotype (Figure 20). This suggests that lysines K743 and K745 could be necessary for the activation of the SUMO ligase activity of Nse2, which is involved in DNA repair. Accordingly, the *smc5-K743,745R* mutant was not sensitive to MMS, demonstrating that the negative to positive charge-residues change was responsible of the DNA damage sensitivity of the *KE* mutants, rather than the loss of lysine residues.

On the other hand, *smc5-K337,344E* or the *smc5-4KE (K337,K344,K354,K355E)* mutant that included two more mutations close to the RING domain in Nse2, showed no DNA damage sensitivity (Figure 20), what presumably indicated that other positively-charged residues in the Smc5 ARM were then interacting with the DNA and activating Nse2. Therefore, in wild type conditions, some Smc5 residues may have a redundant function in DNA binding and Nse2-dependent sumoylation enhancement. To test that, we generated a *smc5-7KE (K337,K344,K354,K355,K743,K745,K764E)* mutant allele that combined both sets of mutations (*3KE* at coiled coil 2 and *4KE* at coiled coil 1), and observed that its growth was strongly impaired under DNA damaging conditions (Figure 20).

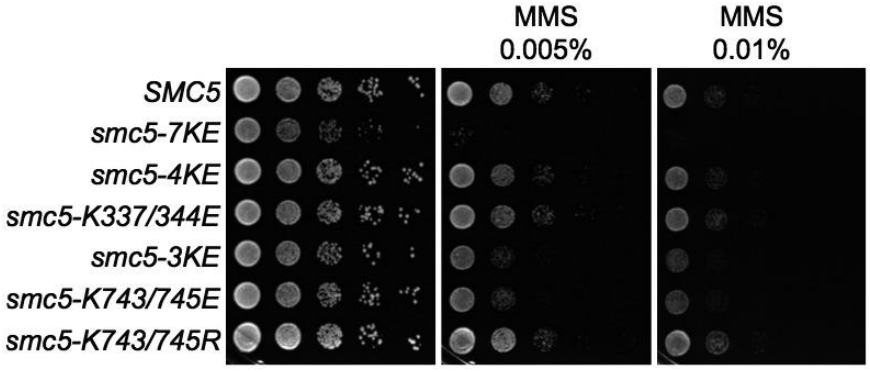

Figure 20. Growth test analysis of *Gal-SMC5* cells grown in glucose and bearing the indicated *smc5* mutants expressed from a plasmid. 10-fold serial dilutions were spotted on YPD, or on YPD with MMS 0.005% or 0.01%. Images were taken after 48 hours. Note that *smc5-7KE*, *smc5-3KE* and *smc5-K743/745E* mutants, but not *smc5-K743/745R* are MMS-sensitive. Yeast strains used: YTR3864, YTR3867, YTR3865, YNC4071, YTR3869 ,YNC4067, YTR3871.

Then, we integrated the *KE* and *KR* mutant alleles into the endogenous *SMC5* locus (Figure 21A) and repeated the yeast growth test analysis. Interestingly, the strong MMS-sensitivity phenotype shown by the *smc5-7KE* mutant was very similar to the previously described by the *nse2-CH* mutant (Figure 21B). *nse2-CH* carried two RING point mutations *(C200A, H202A)* that affect its catalytic SUMO ligase activity and therefore, rendered cells sensitivity to genotoxic stresses (Branzei et al., 2006). Similarities between the cell growth impairment of the *smc5-7KE* and *nse2-CH* mutants under DNA damaging conditions suggested that mutating positively-charged residues in the coiled coil of Smc5 was indirectly altering the capability of yeast cells to cope with DNA damage through their Nse2-SUMO ligase activity.

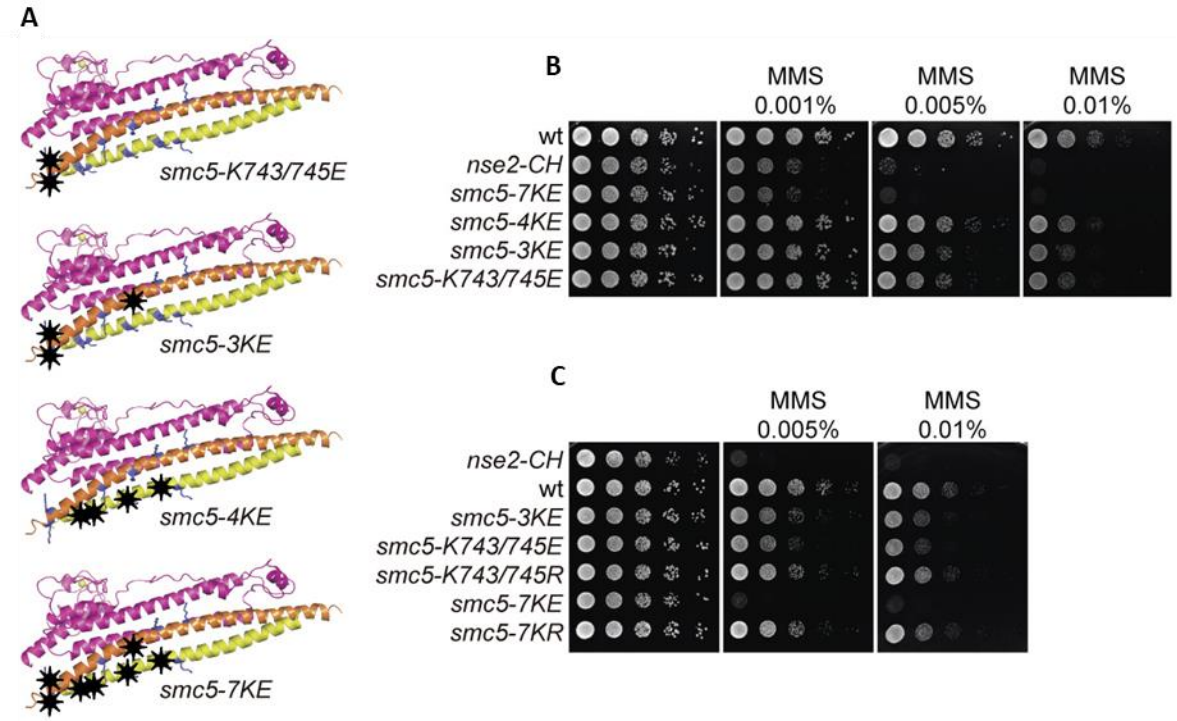

Figure 21. A positively-charged patch in the coiled coil of Smc5 is required for DNA repair *in vivo.* (A) Ribbon representation of the interaction between the ARM domain of Smc5 (indicated in yellow and orange) and Nse2 (in pink). Mutated lysine residues are indicated with black asterisks on each image: *smc5-K743/745E; smc5-3KE:* K743E/K745E/K764E; *smc5-4KE:* K337E/K344E/K354E/K355E; and *smc5-7KE*: K337E/K344E/K354E/K355E/K743E/K745E/K764E. **(B)** Growth test analysis of wild type, *nse2-CH* cells, and the indicted *smc5* mutant strains. 10-fold dilutions were spotted on YPD (as a control) and on YPD with MMS at the indicated concentrations. Images were taken after 48 hours. **(C)** Same as in (B) but using different *smc5-KE* and *smc5-KR* mutants. Note that while most *smc5-KE* mutants are sensitive to MMS, *smc5-K743,745R* and *smc5-7KR* mutant cells, which maintain the positive charge of the mutated residues, are not. Yeast strains used: YIR2620, YTR4546, YNC4059, YEI4238, YNC4065, YNC4067, YNC4063, YEI4255.

As previously seen with the ectopically-expressed mutant alleles, *smc5-K743,745E* and *smc5-3KE* cells showed growth defects when grown in the presence of MMS, although their sensitivity levels were lower than the *smc5-7KE* mutants (Figure 21C). In contrast, the *smc5-4KE* mutant apparently did not show cell growth impairment under genotoxic conditions. And in turn, *smc5-K743,745R* and *smc5-7KR* mutant cells in which the lysine substitution did not imply a charge change in that residues, were not sensitive to DNA damage and grew like wild type cells (Figure 21C).

4.1.2 A DNA sensor in Smc5 participates in sumoylation *in vivo*

Later, in order to test the *in vivo* SUMO ligase activity of Nse2 in *KE* mutant cells, we analyzed sumoylation levels of Smc5, a well-known Nse2 substrate, by doing 6xHis-Flag-tagged SUMO (HF-SUMO) Pull-downs. As it was expected according to the DNA-damage sensitivities observed, *smc5-K743,745E* and *smc5-3KE* cells showed reduced levels of Smc5 sumoylation (Figure 22A). However, in *smc5-K743,745R* mutants, Smc5-SUMO levels did not decrease in comparison to the wild type ones, indicating that diminished sumoylation in *smc5-K743,745E* mutants was a consequence of the positive-charge loss.

Quantification of sumoylated species from SUMO pull-downs showed that sumoylation levels decreased to ~60% in *smc5-3KE* cells (Figure 22C), and showed an even more dramatically reduction in the *smc5-7KE* mutant, were dropped to about a 30% of the wild-type levels (Figure 22C, B). In contrast, *smc5-4KE* cells showed wild-type levels of Smc5-SUMO (Figures 22A, C), suggesting again that lysines in the positive charged patch of Smc5 may act in a redundant manner in the activation of the Nse2 ligase activity. As mentioned, we observed an important reduction of the *smc5-7KE* sumoylated species (Figure 22B). However, we noticed that *smc5-7KR* sumoylated levels showed a slight decrease in comparison with wild type-Smc5-SUMO (Figure B), maybe because of the loss of potential SUMO acceptor domains in Smc5. Accordingly, we have recently described that sumoylation of Smc5 is targeted by its coiled coil domain, and it also occurs in this studied region close to Nse2 (Zapatka et al., 2019).

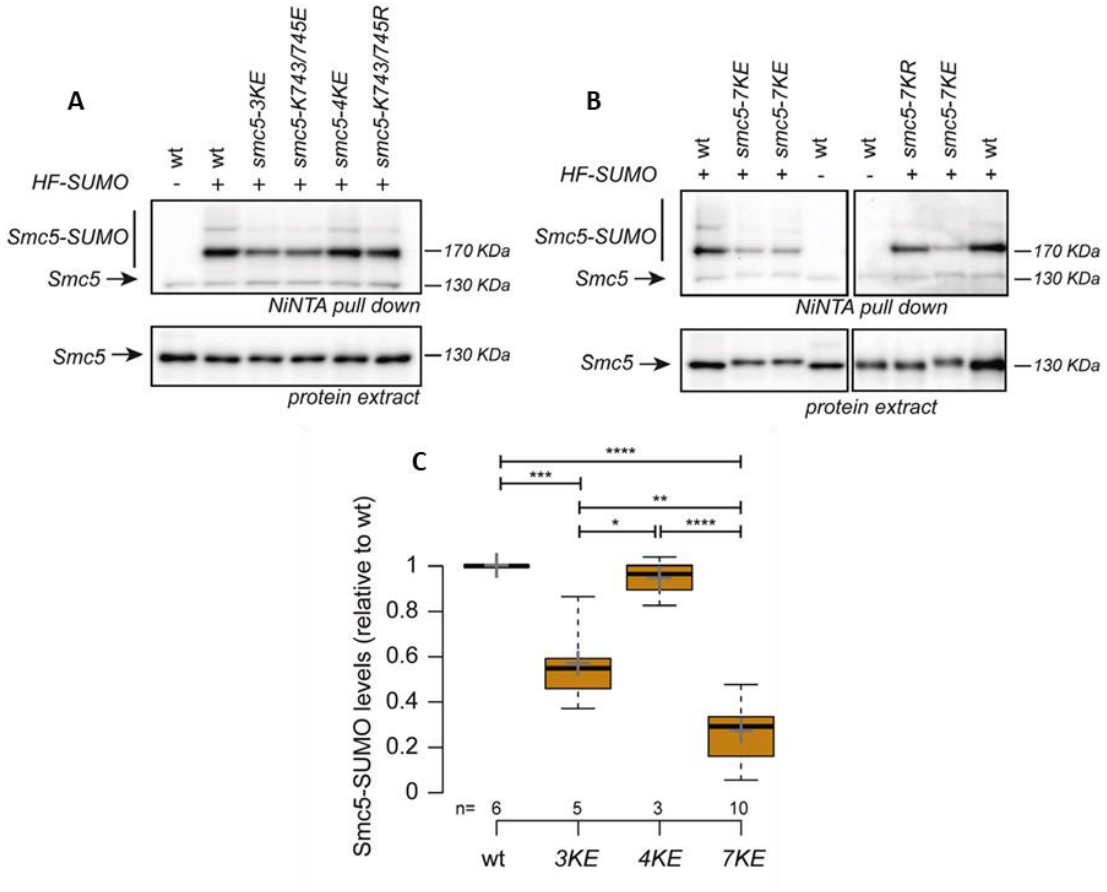

Figure 22. A positively-charged patch in the coiled coil of Smc5 participates in Smc5 sumoylation *in vivo.* (A) 6xHis-Flag-tagged SUMO (HF-SUMO) Pull-down of wild type and the indicated *smc5-KE* and *smc5-KR* mutant strains. Protein extracts were prepared under denaturing conditions; sumoylated species were pulled down and analyzed by Western Blot. Arrows points to unmodified forms of Smc5 , and the vertical bars indicate the sumoylated forms. A strain with no HF-tag was used as control. **(B)** Same as in (A) but using two different clones of the *smc5-7KE* (left) or *smc5-7KE* and *smc5-7KR* mutants (right). Notably, *smc5-7KE* mutants show a different Smc5 electrophoretic mobility, probably due to the residues charge change. **(C)** Graphical quantification of Smc5 sumoylated species from indicated *smc5* mutant strains, relative to a wild type control, from (A) and (B) pull-down assays repeated at least 3 times. Boxes, 25–75% data range; whiskers, total data range; black bar, median; gray cross, mean. ****P < 0.0001; ***P < 0.001; **P < 0.01; *P < 0.05. 1-way ANOVA, n = number of samples analyzed. Yeast strains used: YTR27, YMB794, YNC4065, YNC4067, YNC4063, YEI4238, YNC4059, YEI4255.

Since the Nse2 E3 ligase activity seemed to be altered by the loss of the Smc5 ARM DNA sensor, we wondered whether the Smc5-SUMO decrease observed in *KE* mutants was equivalent to the sumoylation defects presented by *nse2ΔC* cells, carrying a disruption of the C-terminus of the gene including the RING domain. SUMO pull-down experiments indicated that *smc5-7KE* mutants had similar reduced levels of Smc5-SUMO to *nse2ΔC* cells (Figure 23A). Whereas in *smc5-3KE* mutants, the sumoylation decrease was not as strong as in *smc-7KE* or *nse2ΔC* cells (Figure 23A).

Interestingly, sumoylation levels of Sgs1, another target of Nse2 and a member of the STR complex (Bermúdez-López et al., 2016), were also impaired in *smc5-K743,745E* but not in *smc5-K743,745R* cells (Figure 23B). This result suggested that the DNA sensor in Smc5 regulates the Nse2 SUMO ligase activity, towards targets outside the Smc5/6 complex.

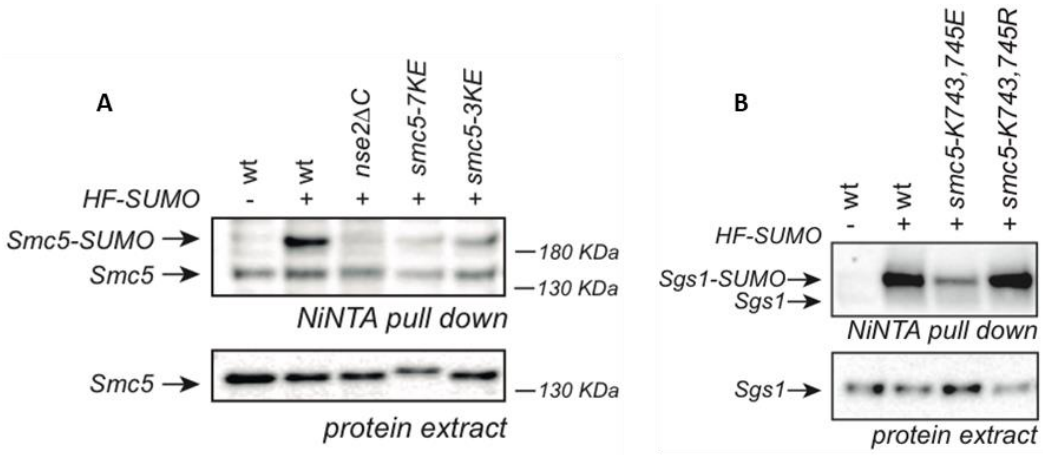

Figure 23. A minimal positively-charged patch in the coiled coil of Smc5 participates in Smc5 and Sgs1 sumoylation *in vivo*. (A) 6xHis-Flag-tagged SUMO (HF-SUMO) Pull-down of wild type and the indicated mutant strains. Protein extracts were prepared under denaturing conditions; and sumoylated species were pulled down and analyzed by Western Blot. Arrows point to unmodified forms of Smc5 , and the vertical bars indicate the sumoylated forms. A strain with no HF-tag was used as control. **(B)** 6xHis-Flag-tagged SUMO (HF-SUMO) Pull-down of wild type and the indicated *smc5-KE* and *smc5-KR* mutant strains. Protein extracts from exponentially growing cultures were treated 2 hours with 0.02% MMS and prepared under denaturing conditions. Sumoylated species were pulled down and analyzed by Western Blot. Unmodified forms and sumoylated species of Sgs1 are pointed with arrows. In all strains SGS1 was tagged with a 9xmyc epitope. A strain with no HF-tag was used as control. Yeast strains used: YTR27, YMB794, YTR2422, YNC4059, YNC4065; YMB2272, YNC4307, YNC4309, YNC4311.

However, another possibility was that mutation of the lysines in the coiled coil of Smc5, close to the Nse2 docking site, was perturbing Nse2 binding. In order to test this, we did co-immunoprecipitation experiments. Results showed that in *smc5-3KE* and *smc5-7KE* mutant cells, Smc5 association with the Nse2 SUMO ligase was maintained (Figure 24A). However, we observed that the Smc5/6 association was reduced in *smc5-7KE* cells relative to wild type cells (Figure 24B). This result indicated that the stability of the entire Smc5/6 complex was impaired in *smc5-7KE* mutants.

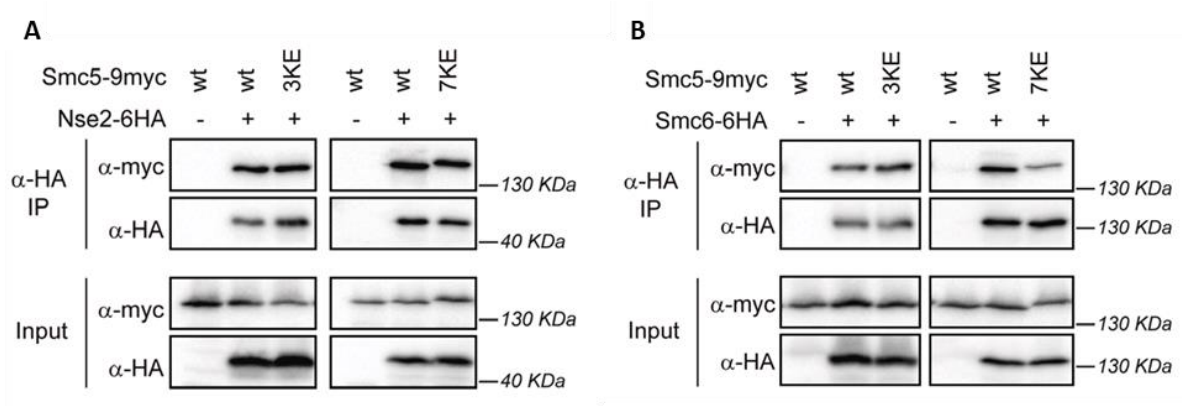

Figure 24. Co-immunoprecipitation analysis of the Smc5-Nse2 and the Smc5-Smc6 interactions in *smc5*-coiled coil mutants. (A) *NSE2-6HA* cells were transformed with plasmids containing the indicated mutant *SMC5* alleles. Nse2 was immunoprecipitated with anti-HA beads, and the Nse2-Smc5 co-immunoprecipitation was analyzed by Western blot. A strain with no HA tag was used as a control. **(B)** Same as in (A) but using *SMC6-6HA* strains. Note that none of the *smc5-KE* alleles affect the Smc5-Nse2 interactions, while *smc5-7KE* reduces the Smc5-Smc6 interaction. Yeast strains used: YCG3410, YTR4263, YEI4305 YTR4264; YCG3428, YTR4265, YTR4266, YEI4298.

Nonetheless, it was also possible that sumoylation defects observed in *smc5-KE* mutant cells were the result of a deficient Smc5/6 recruitment to chromatin. To analyze this, we prepared chromosome spreads. This technique allows to isolate and fixate chromosomes on a glass slide, which can be subsequently stained by immunofluorescence. As shown in Figure 25, quantification of the Smc5-6HA signal from isolated nuclei indicated that *smc5-3KE* chromosomal association was as efficient as in wild type cells. This suggested that the positive charged DNA sensor in Smc5 promoted Nse2 E3 ligase activity once the complex had been loaded onto chromatin. In contrast, we observed a significant reduction in chromatin association in *smc5-7KE* mutants. As mentioned, the stability of the whole Smc5/6 complex was compromised in *smc5-7KE* cells, what could also explain its defective chromosomal interaction. Moreover, the loss of positive charged residues in the ARM of Smc5 could be altering and reducing the capability of the complex to bind to the DNA.

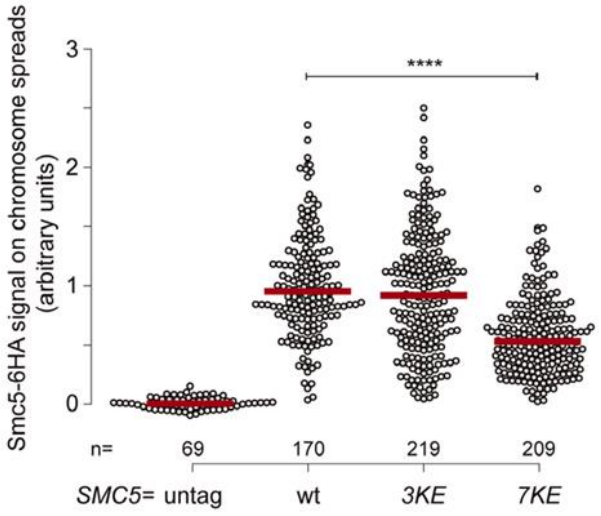

Figure 25. Quantification of the Smc5-6HA signal from immunofluorescence on chromosome spreads from the indicated *smc5*-coiled coil mutants. Nuclei from exponentially growing cells with the indicated genotypes were spread; and chromatin bound proteins were immunostained with anti-HA (3F10). Smc5-6HA nuclear distribution was photographed by the fluorescence microscope and posteriorly quantified in ImageJ as described in materials and methods. The mean value on wild-type spreads was arbitrarily set to 1; each dot represents one nucleus; red line, median. One-way ANOVA, n = number of nuclei analyzed. ****P < 0.0001. Note that the *smc5-3KE* allele does not affect loading of Smc5 onto chromatin, while *smc5-7KE* reduces its association with DNA. Yeast strains used: YIR2620, YTR4251, YNC4059, YNC4065.

4.2 Chapter II- Functional analysis of the C-terminal domain of Nse2 in protein sumoylation and DNA damage repair

The Smc5/6 complex is essential for chromosome segregation (Jeppsson, Carlborg, et al., 2014). Particularly, Nse2 and its E3 SUMO ligase associated activity, have multiple roles in chromosomal regulation (Solé-Soler & Torres-Rosell, 2020). Several proteins in the Smc5/6 complex appear to be sumoylated by Nse2, and the cellular function of these modifications has been widely linked to the activation of DNA damage repair pathways (Solé-Soler & Torres-Rosell, 2020). Therefore, its deregulation has critical consequences for the genome stability. In fact, there are human syndromes that have been associated with mutations in *NSMCE2*. For instance, one of the most recently described syndromes that causes primordial dwarfism and insulin resistance among other abnormalities, has been linked to *NSMCE2* hypomorphism (Payne et al., 2014).

Thus, knowing that specific mutations in *NSMCE2* have deleterious effects in humans, we decided to do a functional analysis of the C-terminal part of *NSE2* in budding yeast. We first analyzed the crystallographic structure of Nse2 bound to Smc5 (Figure 26) and identified different regions not previously analyzed. We identified several potential regions of interest in the C-terminal domain of Nse2. First, a SIM (Sumo-Interacting Motif) at the very end of the protein (sequence IDVL), although it is not evolutionary conserved. Second, a C-terminal α-helix that is lost in the *NSMCE2* syndrome (Payne et al., 2014). According to Payne *et al*, the truncation in this syndrome represents the loss of the last 29 residues in *S. cerevisiae*. According to our alignments, in budding yeast, only the loss of 24 residues correspond to the *NSMCE2* disruption observed in the human syndrome (Figure 27). Remarkably, there is some level of conservation at the N-terminal part of this α-helix. Third, the RING domain (Duan et al., 2009); and fourth, a loop located between the RING and the Smc5 ARM domain (Figure 26). Then, we designed a set of *NSE2* mutants carrying C-terminal deletions or point mutations in specific regions, including the most evolutionary conserved residues, and studied their protein levels, Smc5 sumoylation and DNA damage sensitivity.

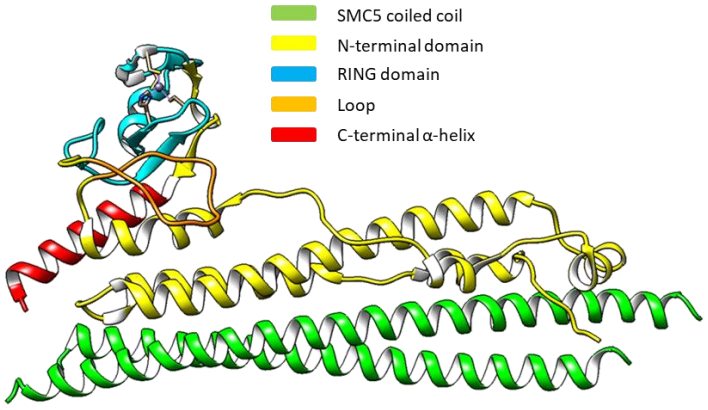

Figure 26. Structure (3HTK) of the complex between the two coiled coil domains of Smc5 (green) and the N-terminal domain of Nse2 (yellow). The C-terminal alpha-helix (red), the loop (orange) and the RING domain (blue) are also represented. Figure obtained with Chimera.

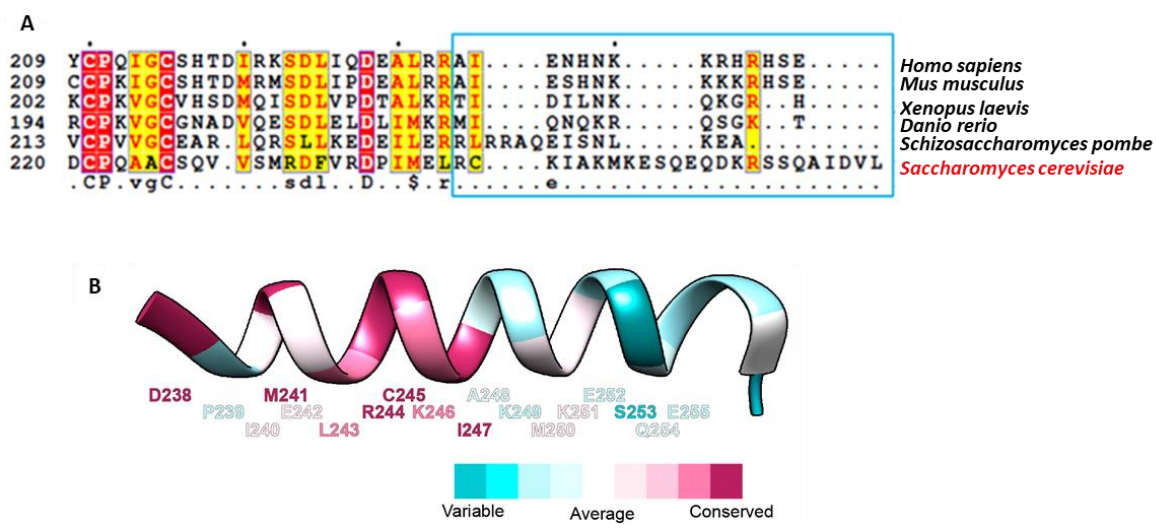

Figure 27. Residue conservation in the C-terminal region of Nse2. **(A)** Multiple-sequence alignment of the most C-terminal region in Nse2. The most conserved amino acids are highlighted in red, the partially conserved ones are shown in yellow. The blue square indicates the sequence lost in the human *NSMCE2* syndrome described by Payne *et al* (Payne et al., 2014). According to our alignment, this region corresponds to the last 24 residues in *S. cerevisiae.* **(B)** 3D structure of the C-terminal alpha-helix, color coded according to conservation level among the 26 closest homologs of the *S. cerevisiae* Nse2 protein. Note that the conservation is higher than average from M241 to I247, and diminishes thereafter. Homologs, alignments and conservation scores were determined with the Consurf server. (Landau et al Nucl. Acids Res. 33:W299-W302).

4.2.1 Deletions in the Nse2 C-terminal α-helix reduce Nse2 protein levels, Smc5 sumoylation and lead to growth defects and DNA damage sensitivity

We first generated yeast mutant strains carrying C-terminal deletions in Nse2. The *nse2ΔC* mutant had a truncation of all the C-terminus from the conserved residue C184, including the RING domain (Figure 28). This mutant is equivalent to the *mms21-11* mutation first isolated by Zhao and Blobel (Zhao & Blobel, 2005). We also removed the last 29 or 24 residues (*nse2Δ29C* or *nse2Δ24C* respectively). The first one removes from P239 onwards; the second one from R244 onwards. These truncations remove part of a conserved sequence in Nse2 (Figure 27B), the C-terminal alpha-helix, but still maintained an intact RING domain. In addition, these truncations corresponded to the fragment of the gene lost in the human *NSMCE2* syndrome (Payne et al., 2014). As mentioned, depending on the sequence alignment between the human and the yeast genes, the mutation p.Ala234Glufs*4 in *NSMCE2* identified by Payne and collaborators, was equivalent to the removal of the last 24 or 29 residues in *S. cerevisiae*. We therefore could simulate the mutations described in those patients in a yeast strain, and characterize them. We also generated an *nse2Δ16C* mutant in which we removed the last 16 residues of the gene (the region exhibiting the lowest conservation level in the C-terminal α-helix, from E252 onwards), and an *nse2ΔSIM* mutant, that maintained the alpha-helix and presented a disruption of the last 4 residues, which corresponded to the SIM (IDVL sequence), not conserved in humans.

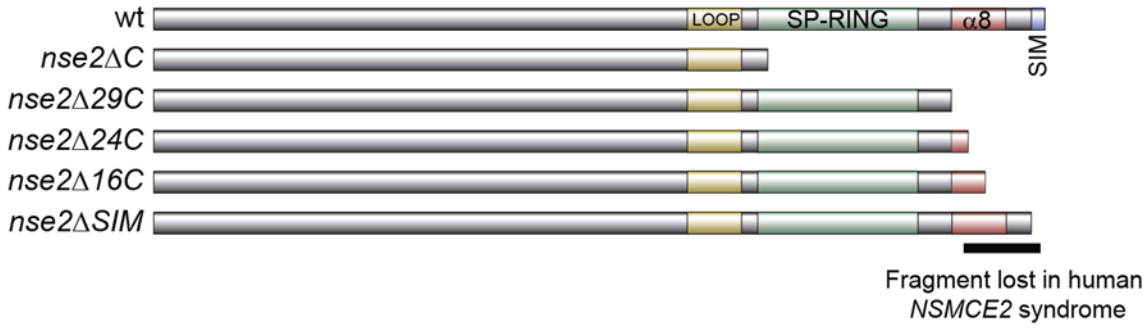

Figure 28. Schematic representation of the wild type *NSE2* gene and the *nse2* C-terminal truncations generated. The loop region (yellow), SP-RING domain (green), alpha-helix (red) and SIM (blue) motifs are also represented. The fragment lost in the human *NSMCE2* syndrome is indicated.

Next, we studied the Nse2 and Smc5 protein levels by Western Blot. Results showed that *nse2Δ29C* and *nse2Δ24C* mutants presented very low levels of Nse2 (Figure 29A), whereas *nse2Δ16* and *nse2ΔSIM* mutant cells had their Nse2 protein levels similar to the wild type ones (Figure 29B). Remarkably, Smc5 was expressed at wild type levels in all the mutant strains. These results suggest that the C-terminal α-helix is important for the stability of the Nse2 protein.

The reduced expression of Nse2 in *nse2ΔC* (data not shown), *nse2Δ29C* and *nse2Δ24C,* also impaired cell growth and sensitized yeast cells to high temperature and to DNA damage (Figure 29C). Interestingly, we observed that removing only the alpha-helix caused the same growth defect phenotype and MMS sensitivity in *nse2Δ29C* and *nse2Δ24C* cells than the disruption of the complete C-terminus of Nse2. These results suggested an important role for the C-terminal alpha-helix of Nse2 in cell growth and in the DNA damage response.

Then, in order to study how these C-terminal truncations were affecting the SUMO ligase activity of Nse2, we analyzed the sumoylation levels of Smc5, a target of Nse2, by SUMO pull-down experiments. As shown in Figure 29D, *nse2ΔC* and *nse2Δ29C* cells had reduced levels of Smc5 sumoylation in comparison with a wild type strain or with the *nse2ΔSIM* mutant, in which sumoylation levels of Smc5 were not impaired. In addition, we observed that *nse2ΔC* cells, in which the RING domain of Nse2 was missing, still maintained a minimal Smc5 sumoylation (Figure 29D). As *nse2Δ24C* and *nse2Δ29C* show very low levels of Nse2, it is possible that the Smc5 sumoylation defects are due to the absence of its associated SUMO ligase.

As the last 4 or 16 residues of Nse2 seemed to be dispensable for cell growth or Smc5 sumoylation, we decided to study whether these truncations could affect the SUMO ligase activity of Nse2 in other targets outside the Smc5/6 complex. For that, we analyzed the sumoylation levels of Smc1, one of the proteins forming the core of the cohesin complex together with Smc3. Pull-down experiments showed that Smc1-SUMO levels were not reduced in *nse2Δ16C* mutant or in *nse2ΔSIM* cells (Figure 29E), indicating that the SIM motif or the last 16 residues in Nse2 are dispensable for Nse2 stability, sumoylation and DNA damage repair.

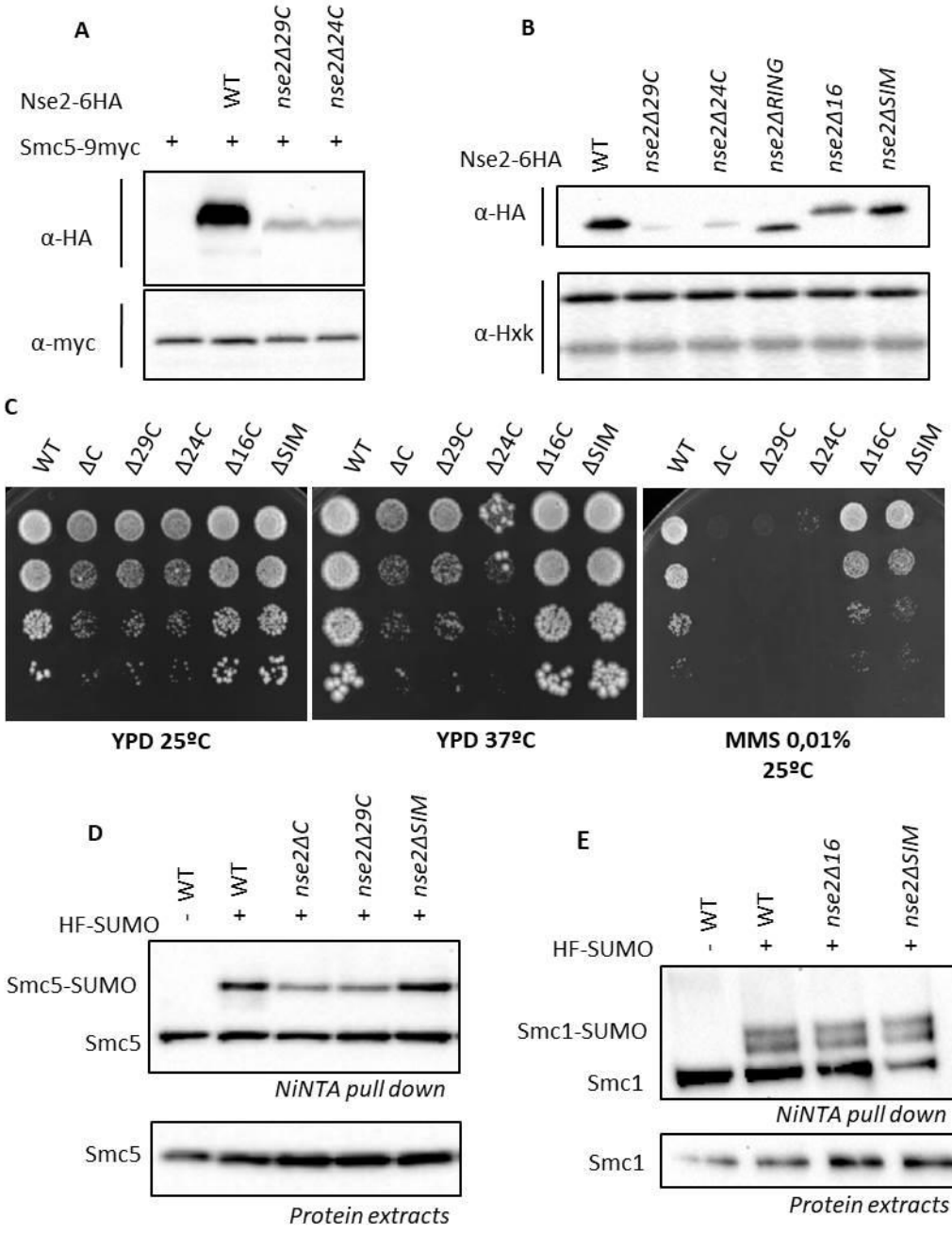

Figure 29. Deletions in the *NSE2* C-terminal α-helix reduce Nse2 protein levels, lead to growth defects and DNA damage sensitivity and impair Smc5 sumoylation. (A) Study of the Nse2-6HA protein levels of the indicated strains. In all, Smc5 was tagged with a 9xmyc epitope. **(B)** Same as in (A) but using different *nse2*-mutant strains. Here, endogenous hexokinase protein levels were checked as a loading control. **(C)** Growth test analysis of wild-type*, nse2ΔC, nse2Δ29C, nse2Δ24C, nse2Δ16C* and *nse2ΔSIM* at the indicated temperatures and concentrations of MMS. **(D)** 6xHis-Flag tagged SUMO (HF-SUMO) Pull Down from the indicated strains. Protein extracts were prepared under denaturing conditions; and sumoylated species were pulled down and analyzed by Western Blot. Unmodified and sumoylated forms of Smc5 are indicated. A strain with no HF-tag was used as control. **(E)** Same as in (D) but checking sumoylation levels of Smc1. Yeast strains used: YMB794, YMB2315, YTR2751, YTR4544, YGB4911, YGB4908, YGB4910, YTR2422, YEI4938, YEI4938, YEI4948, YSM2228.

4.2.2 Point mutations in residues coordinating the Zinc atom at the RING domain of Nse2 do not impair Smc5 sumoylation.

Previous studies have described that the RING domain of Nse2 is required for sumoylation *in vitro,* and mutations in the Nse2-RING-finger motif reduce the Nse2-dependent sumoylation (Andrews et al., 2005). During the Varejão *et al* study (Varejão et al., 2018) we noticed that an *nse2-C200,H202A (nse2-CH)* mutant presented Smc5 sumoylation. Notably, *nse2-CH* is the only point mutant in the RING domain described until now. However, there is no reference in the literature that analyzes sumoylation by using an *nse2-CH* mutant. Therefore, we decided to study whether conserved residues in the RING domain were necessary for sumoylation *in vivo*. For that, we developed point mutations in the most conserved residues in the RING domain of Nse2, and a mutant strain carrying a deletion of the entire RING domain. These mutants include the *nse2-C200,H202A* mutant previously described by Andrews *et al* in fission yeast (Andrews et al., 2005), and by Branzei *et al* in buddying yeast (Branzei et al., 2006). We obtained this mutant from the Xiaolan Zhao's lab and after sequencing, we observed that it carries a 13xmyc tag. The 13xmyc tag on a wild type *NSE2* gene exhibited genetic interactions with the *smc5-7KE* mutant (data not shown), suggesting that it is not innocuous in certain circumstances. In addition, we mutated the C221 residue into an alanine (*nse2-C221A*), as it is situated at the same loop (loop2) than residues C200 and H202 and also coordinate the zinc ion (Duan et al., 2009). Apart from that, we also mutated the P222 residue at loop2 which, although not being implicated in the zinc-coordination, is also highly conserved (Figure 30). At loop1, we created two point mutants in conserved residues: *nse2-C185,P186A* and *nse2-P194,L195A* (Figure 30). Finally, we generated an *nse2ΔRING* mutant in which the entire sequence between residues C185 to L243, corresponding to the SPL-RING domain, was disrupted and substituted by a short linker (SGGSGGG) (Figure 30A). Thus, the *nse2ΔRING* maintains the last 24 residues of Nse2.

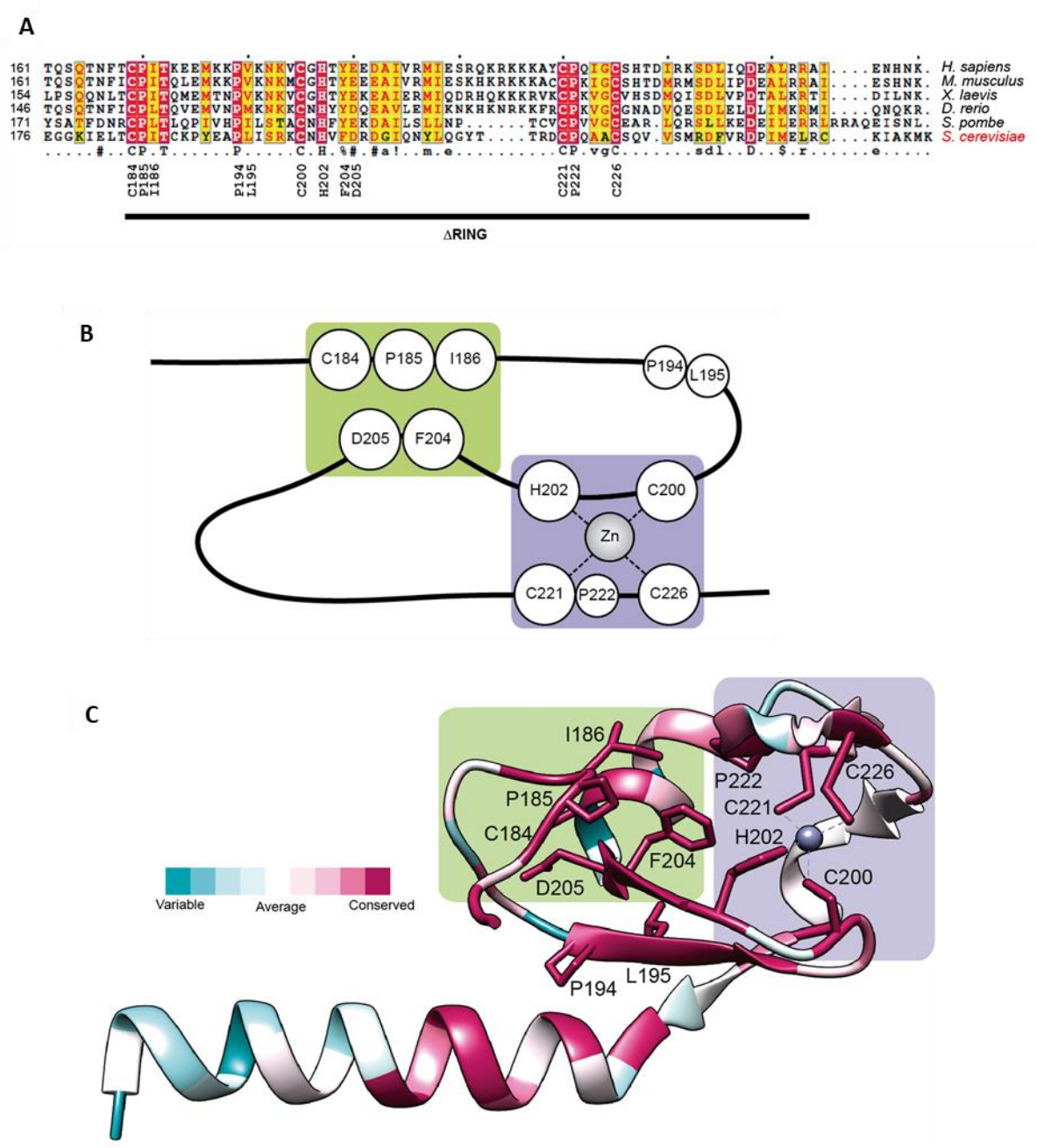

Figure 30. Multiple-sequence alignment and structure of the Nse2 C-terminal domain. **(A)** Multiple-sequence alignment of the RING domain in Nse2. The most conserved amino acids are highlighted in red, the partially conserved ones are shown in yellow. The sequence disrupted in the *nse2ΔRING* mutant corresponding to the depletion of the SPL-RING domain of Nse2 is indicated in a black line. **(B)** Schematic model of the SP-RING domain. The green box marks the stabilizing motif residues; the box in purple marks the Zinc coordinating residues. Other conserved residues are shown in smaller circles. Figure adapted from (Ishida et al., 2012). **(C)** Structure of the C-terminal domain of Nse2. The structure is color coded according to conservation level among the 26 closest homologs of the *S. cerevisiae* Nse2 protein. Homologs, alignments and conservation scores were determined with the Consurf server. (Landau et al Nucl. Acids Res. 33:W299-W302).

Western Blot analysis revealed that Nse2 protein levels were slightly reduced in *nse2ΔRING* cells and they remained stable in the rest of the *nse2-RING* mutants designed (Figures 29B, 31A). However, some point mutations or the deletion of the RING domain lead cells to increased MMS sensitivity. Particularly, *nse2ΔRING, nse2-C200,H202A,* and *nse2-C221A* cells showed the most severe phenotype under DNA damaging conditions. This is in accordance with previous results showing that mutating the C200 and H202 conserved residues into alanines conferred growth defects at 37ºC or when treated with genotoxic agents (Santa Maria et al., 2007). In contrast, growth defects on MMS plates were less dramatic in *nse2-P194,L195A* mutants and almost undetectable in *nse2-C185,P186A* or *nse2-P222A* cells (Figure 31B).

Moreover, we also analyzed the *in vivo* SUMO ligase activity of Nse2 in some of these RING mutants by using their Smc5 sumoylation levels as reporters of the Nse2 E3 activity. Interestingly, Smc5 sumoylation levels decreased severely in *nse2ΔRING* cells (Figure 31C), despite maintaining a basal Smc5 sumoylation. In contrast, pull down experiments showed that Smc5 sumoylation was not affected in *nse2-C200,H202A, nse2-C221A*, or in *nse2-P222A* point mutants (Figure 31C). These results indicated that mutation of conserved residues, either coordinating the zinc ion (Nogales et al., 2017) or close to them (P222), is not sufficient to disrupt the E3 ligase activity of Nse2.

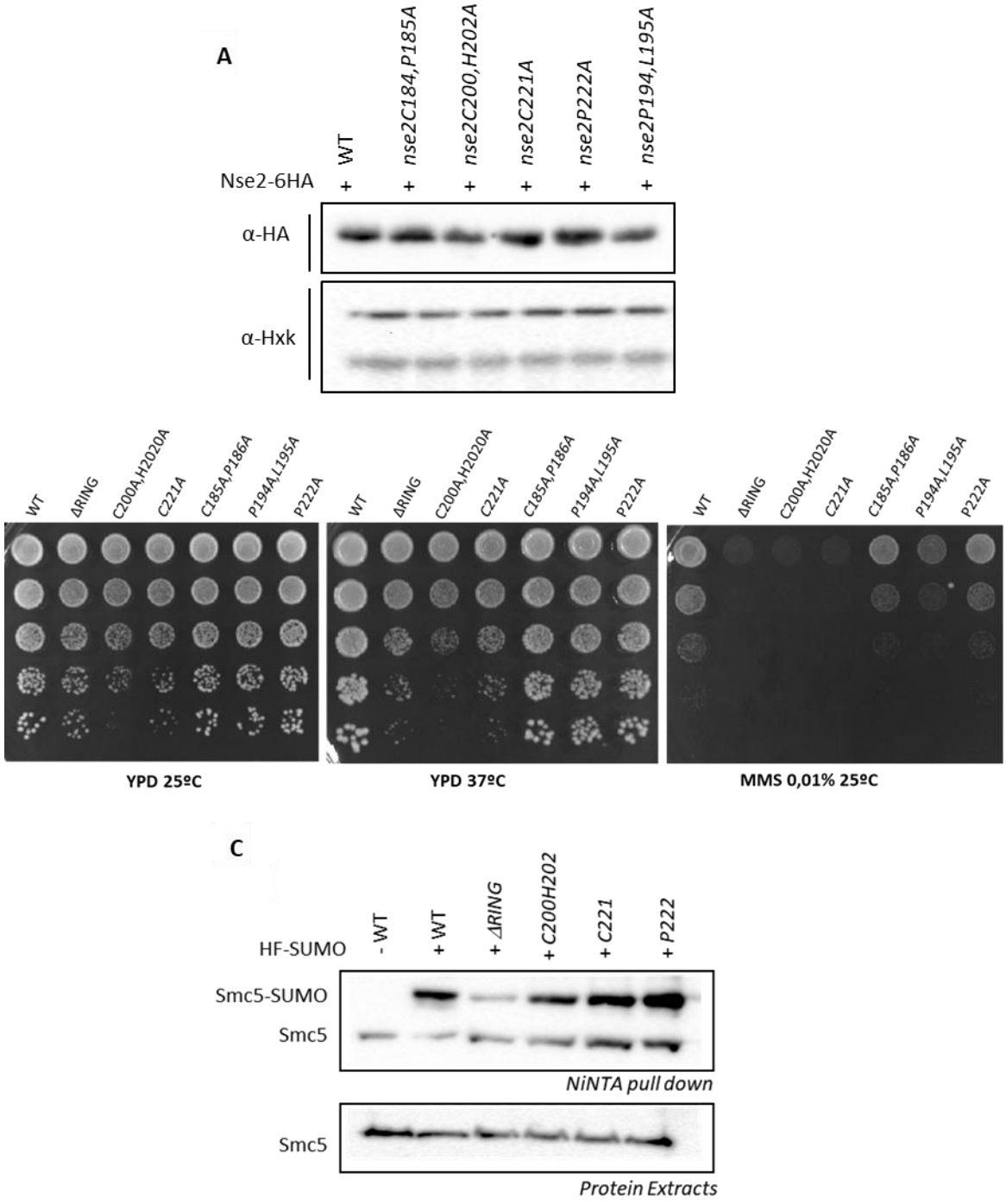

Figure 31. RING point mutations do not affect Nse2 protein levels but lead to DNA damage sensitivity without impairing Smc5 sumoylation. (A) Protein levels of Nse2-HA in the indicated RING point mutants. Endogenous hexokinase protein levels were used as a loading control. **(B)** Growth test analysis of the indicated *nse2-RING* mutant strains at different temperatures and concentrations of MMS. **(C)** 6xHis-Flag tagged SUMO (HF-SUMO) Pull Down from the indicated strains. Protein extracts were prepared under denaturing conditions; and sumoylated species were pulled down and analyzed by Western Blot. Unmodified and sumoylated forms of Smc5 are indicated. A strain with no HF-tag was used as control. Yeast strains used: YMB794, YMB2315, YEI4921, YGB4914, YGB4915, YGB4913, YGB4911, YGB4917.

4.2.3 Mutations in the loop domain lead to severe MMS sensitivity

In the case of the RING domain, *in vitro* experiments indicate that point mutations in zinc-coordinating residues in the Nse2-RING-finger motif reduce the Nse2-dependent sumoylation (Andrews et al., 2005). However, this does not seem to occur *in vivo* (Figure 31C). Therefore, we looked for other regions in the Nse2 sequence that might have an important role in DNA damage repair or in the regulation of the Nse2 E3 ligase activity *in vivo*. Indeed, we identified a C-terminal 16 amino acid loop structure located before the SP-RING of Nse2, containing evolutionarily conserved residues (Figure 32A). In order to characterize its function, we developed an *nse2-170EDD-RRR* point mutant, in which we inverted the negative charge of three partially conserved amino acids; and an *nse2-G177-P* mutant in which we mutated the glycine residue located just after the loop, at position 177, into a proline, and studied their relevance in terms of DNA damage sensitivity and sumoylation capacity.

For that, we first performed *in vitro* experiments to check the activity of Nse2 in collaboration with Dr David Reverter in the Protein Structure group from the Institut de Biotecnologia i Biomedicina at the Universitat Autònoma de Barcelona. We expressed and purified *nse2-G177-P* and *nse2-170EDD-RRR* mutants in complex with the Smc5-ARM domain and did sumoylation reactions using the C-terminal kleisin domain of Nse4 (cNse4) as a substrate. As shown in Figure 32B, Nse2 and Smc5-ARM heterodimers were correctly expressed in *E.coli* cells and posteriorly purified. The upper bands (close to 40 kDa) correspond to the different Nse2 wild type or mutant versions, whereas lower bands at 20 kDa correspond to the Smc5-ARM domain. In this Coomassie stained SDS-PAGE gel we can observe that protein concentrations of Nse2-Smc5 heterodimers were equal in all of them, indicating that Nse2-dependent sumoylation differences detected in *in vitro* reactions were only due to the mutations impairing the Nse2-E3 ligase activity.

Interestingly, the *nse2-C200,H202A* mutation perturbed Nse2 protein integrity resulting in an accumulation of degradation bands (Figure 32B). In consequence, as shown in Figure 32C, Nse2-dependent E3 ligase activity in this RING mutant was severely decreased. An important but less dramatic sumoylation defect was shown by the *nse2-V266R* mutant. In this case, this mutation has a change in one of the four last amino acids of the SIM domain, which seems to alter the SUMO transfer to the target protein by preventing Nse2-SUMO interactions *in vitro*. Interestingly, the *nse2-G177-P* mutant had similar sumoylation problems, showing an important diminution of cNse4-SUMO modifications at 5, 10 and 15 minutes of reaction. Remarkably, as shown in Figure 33, G177 is located at the same position to the SIM-like element of Siz1, suggesting that they might have equivalent functions in positioning the Ubc9 E2 enzyme to promote sumoylation. By contrast, *nse2-170EDD-RRR* mutants had no apparent sumoylation defects *in vitro* (Figure 32C). These results indicate that the C-terminal SIM and the G177 in the SIM-like domain of Nse2 play an important role in sumoylation, at least *in vitro*.

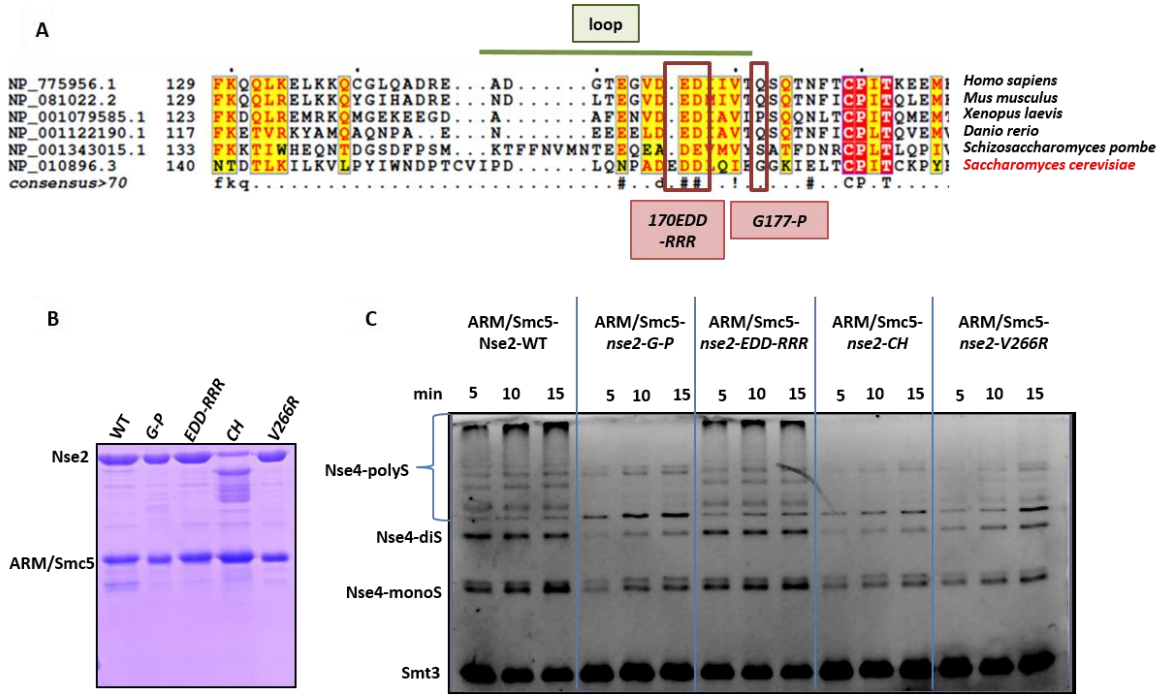

Figure 32. ***In vitro*** **sumoylation of Nse2 is impaired in** ***nse2-G177-P*****,** ***nse2-CH*** **and** ***nse2-V266R*** **mutants. (A)** Multiple-sequence alignment of the loop domain of Nse2. The most conserved amino acids are highlighted in red, and the partially conserved ones in yellow. Brown squares indicate mutations performed in this region, and the green line indicates the sequence corresponding to the loop structure. **(B)** Coomassie stained SDS-PAGE gel of the indicated Nse2 wild type and mutant versions in complex with the Smc5/ARM domain. Nse2 and ARM/Smc5 heterodimers were expressed in *E. coli* cells and purified by metal affinity chromatography. The upper band at 40 KDa corresponds to Nse2, whereas the lower band at 20 KDa corresponds to the Smc5/ARM domain. **(C)** Time-course SUMO conjugation reactions of the Smc5/ARM-Nse2 construct using different Nse2 mutant versions. Reactions were run at 30ºC for 15 minutes, and samples were taken at 5, 10 and 15 minutes and stopped with SDS-loading buffer. Nse4 was used as the substrate of the reaction. Nse4-mono, di, and polysumoylation bands are indicated. Plasmids used: pEI4956, pEI4958.

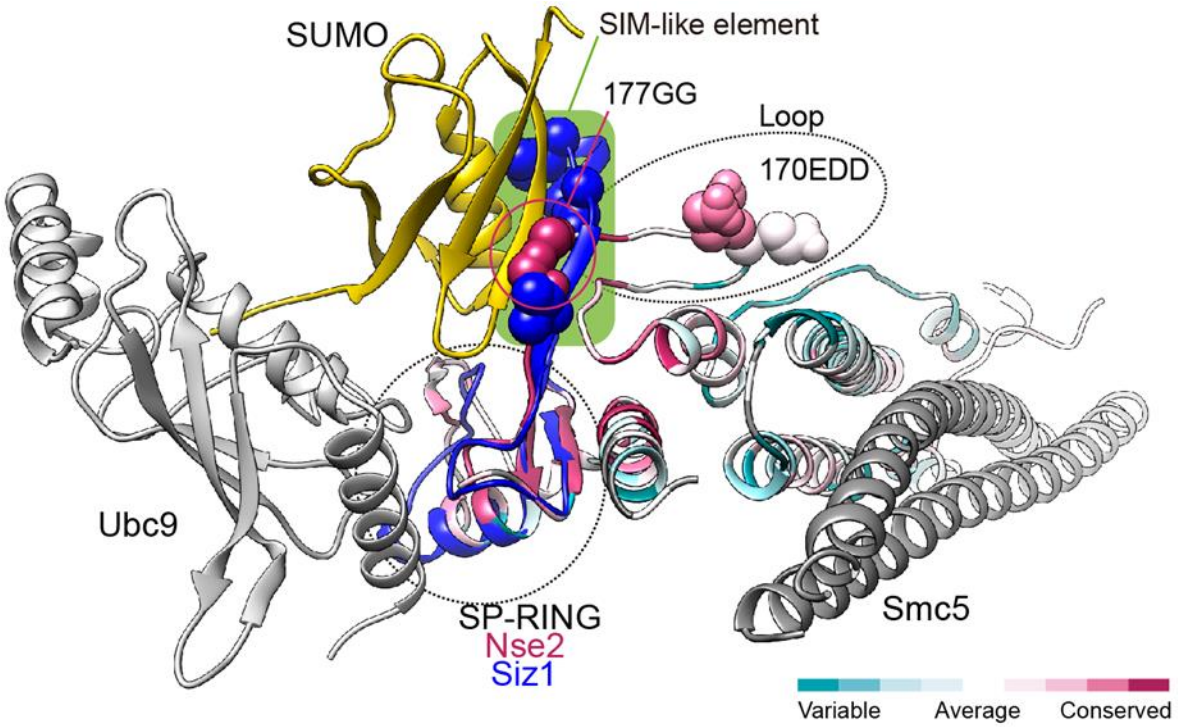

Figure 33. Model for Ubc9-SUMO binding to the RING domain in Nse2. The model was generated in Chimera by superimposing the RING domains of Nse2 (3HTK) and Siz1 (5JNE) E3 ligases. The SUMO molecule is represented in yellow and the RING domain of Siz1 in dark blue. Nse2 is colored according to conservation as indicated in the color legend: variable regions are indicated in turquoise whereas more conserved ones are indicated in magenta. The position of the Ubc9 E2 conjugating enzyme and Smc5 coiled coils are also indicated. The green box indicates the position of the SIM-like motif in Siz1, which overlaps, among others, with G177 and G178 in Nse2.

Next, we integrated *nse2-170EDD-RRR* and *nse2-G177-P* mutations in yeast and analyzed their phenotypes *in vivo*. In addition, we developed a mutant carrying a deletion in this structural loop, which we called *nse2Δ16I,* that deletes residues 160 to 176 (Figure 34A). Then, we checked their sensitivity to DNA damaging agents and their Nse2-dependent E3 ligase activity.

As shown in Figure 34B, Nse2 protein levels were similar to wild type in all *nse2*-loop mutants. However, the internal loop deletion and *nse2-170EDD-RRR* mutations lead to MMS sensitivity, without affecting temperature sensitivity. In contrast, *nse2-G177-P* mutant cells showed no sensitivity to DNA damage or temperature (Figure 34C). In addition, pull-down experiments showed that Smc5 sumoylation was not affected in *nse2-G177-P* mutant cells, even under DNA damaging conditions (Figure 34D), nor in the *nse2Δ16I* mutants (Figure 34E).

Recently published results from our group have shown that sumoylation of Smc5 has a role in the resolution of recombination intermediates and it is upregulated by DNA fork damage (Zapatka et al., 2019). In this regard, Smc5 sumoylated forms appear to be strongly induced by treatment with MMS. Having all this into account and after observing the severe growth defects shown by *nse2Δ16I* and *nse2-170EDD-RRR* mutants under MMS treatment, we wondered whether Smc5

sumoylated species would increase when treating cultures 90 minutes with MMS in *nse2Δ16I* cells. As shown in Figure 34F, *nse2Δ16I* cells presented wild type Smc5-sumoylation levels after the MMS treatment, and a very slight decrease in the polysumoylated forms of Smc5.

Again, we observe important differences between *in vitro* and *in vivo* results regarding to Nse2 E3 ligase activity. As it happens with *nse2-C200,H202A* and *nse2-SIM* mutants, the *nse2-G177-P* mutation impairs Nse2-dependent sumoylation *in vitro* but not *in vivo.* Whereas *nse2-170EDD-RRR* and *nse2Δ16I* mutations are more likely affecting specific functions in DNA damage repair. Overall, these results suggest that the regulation of the Nse2 SUMO ligase activity *in vivo* does not depend on its internal loop domain, but it could have an important role in the response to DNA damage.

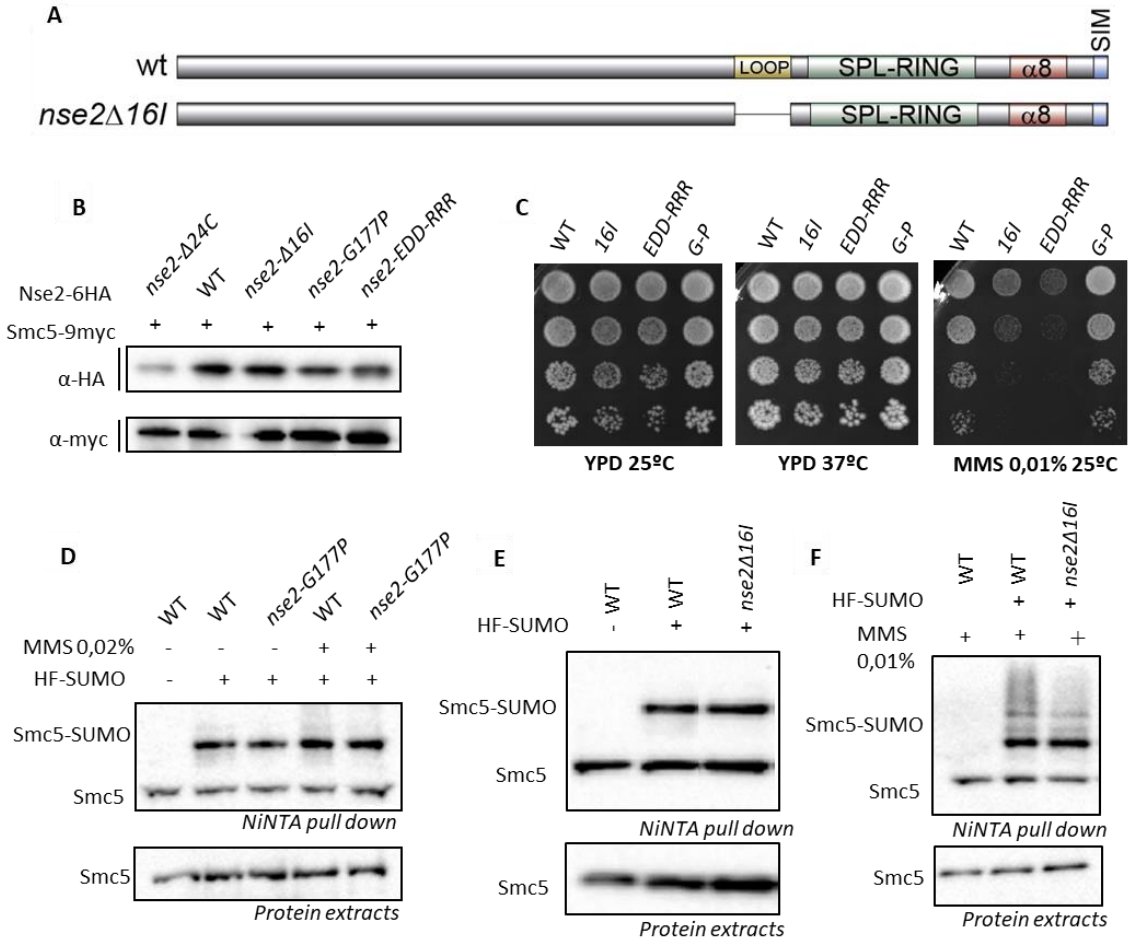

Figure 34. Mutation of the loop domain leads to MMS-sensitivity but does not impair Smc5 sumoylation. (A) Schematic representation of the *nse2Δ16I* mutant. **(B)** Study of the Nse2-6HA protein levels of the indicated strains. In all strains, Smc5 was tagged with a 9xmyc epitope. **(C)** Growth test analysis of wild-type, *nse2Δ16, nse2-EDD-RRR* and *nse2-G177-P* cells at the indicated temperatures and concentrations of MMS. **(D)** 6xHis-Flag tagged SUMO (HF-SUMO) Pull Down from a wild type and an *nse2-G177P* mutant strain. Protein extracts were prepared under denaturing conditions; and sumoylated species were pulled down and analyzed by Western Blot. Unmodified and sumoylated forms of Smc5 are indicated. A strain with no HF-tag was used as control. Two of the cultures were treated with 0.02% MMS for 1.5 hours. **(E)** 6xHis-Flag tagged SUMO (HF-SUMO) Pull Down from a wild type and an *nse2Δ16I* mutant strain. Protein extracts were prepared under denaturing conditions; and sumoylated species were pulled down and analyzed by Western Blot. Unmodified and sumoylated forms of Smc5 are indicated. A strain with no HF-tag was used as control. **(F)** Same as in D but treating cells for 1.5 hours with 0,01% MMS. Yeast strains used: YMB794, YMB2315, YGB5214, YGB5215, YTB3216.

4.3 Chapter III- Analysis of Nse1-ubiquitin ligase targets and functions on genome stability

Nse1 was first reported to encode a non-smc subunit of the Smc5/6 complex, localized at the nucleus and essential for cell proliferation and DNA repair (Fujioka et al., 2002). Later, Nse1 was found to interact with Smc5 *in vivo* and to contain a RING-finger like domain (McDonald et al., 2003), suggesting that it could act as an ubiquitin E3 ligase.

Remarkably, although its RING domain was described to be dispensable for cellular viability, disrupting this functional motif confer cells sensitivity to high temperature or genotoxic treatments (Pebernard, Perry, et al., 2008). In human cells, Nse1 forms an Smc5/6-independent complex with an alternative MAGE protein that has been reported to ubiquitinate MMS19 for its degradation (Weon et al., 2018). However, no other substrate for the Nse1 E3 ligase activity has been identified to date.

To fill this gap, in this thesis we have used quantitative proteomics to identify putative targets of Nse1.

4.3.1 Proteomics analysis of the nuclear Nse1-dependent ubiquitinome

To identify ubiquitination sites depending on Nse1, we first grew wild type and *nse1-C274A* mutant cells (carrying a mutation in one conserved zinc-coordinating residue) to exponential phase and treated them with MMS 0.02% for 1.5 hours. Next, we collected cells and fractionated nuclei to reduce the complexity of the samples. Then, we extracted proteins from the nuclear fraction and digested them with trypsin. After the digestion, ubiquitin leaves a di-glycine signature attached to the ubiquitination site (K-ε-GG). Consequently, ubiquitinated peptides containing this signature were isolated and enriched by anti-di-glycine immunopurification (IP) (Figure 35). This enrichment was followed by a mass-spectrometry analysis. Thus, eluate (IP) and flowthrough samples were injected twice in the mass spectrometer. Particularly, flowthrough was used to quantify and identify total protein in the extract, whereas the eluate was used to quantify and identify ubiquitinated peptides.

Up to 3657 proteins were identified in the flowthrough samples. Around 20.2% of these proteins were also identified in the eluate, corresponding to ubiquitinated-proteins. As expected, very few proteins (1,6%) were identified exclusively in the IP. In total, 809 proteins and 1932 ubiquitinated peptides were detected after diGly immunopurification (see Figure 35). The total amount of ubiquitinated sites is higher than the number of ubiquitinated proteins, as many ubiquitin targets were modified at more than one lysine.

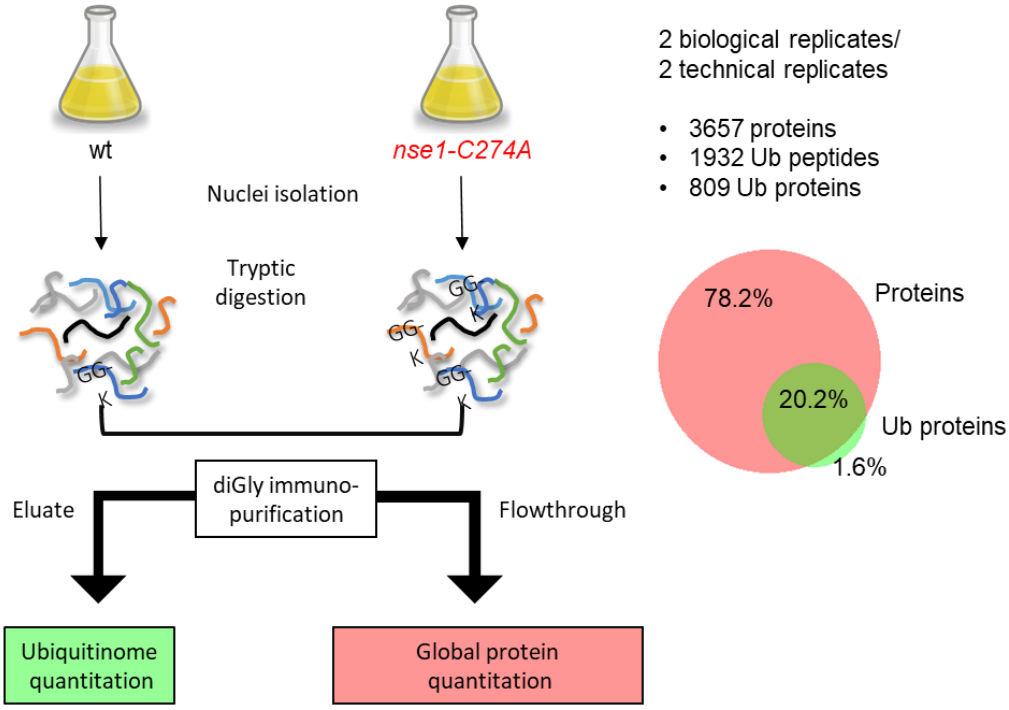

Figure 35. Scheme of the workflow for diGLY proteomics. Isolation and sample processing was performed by Dra Celia Casas from the Cell Cycle lab, and mass spectrometry assay was done by the Proteomics Unit from the CNIO. Yeast strains used: Y3607, YRP787.

Compared to other previous analysis, we identified less ubiquitinated-sites than other published studies (Tong et al., 2014) (Swaney et al., 2013) (Figure 36). The lower number of ubiquitinated sites is probably due to the nuclear enrichment step used in our protocol. Nevertheless, our proteomics analysis identified 879 non-redundant ubiquitination sites that had not been reported yet.

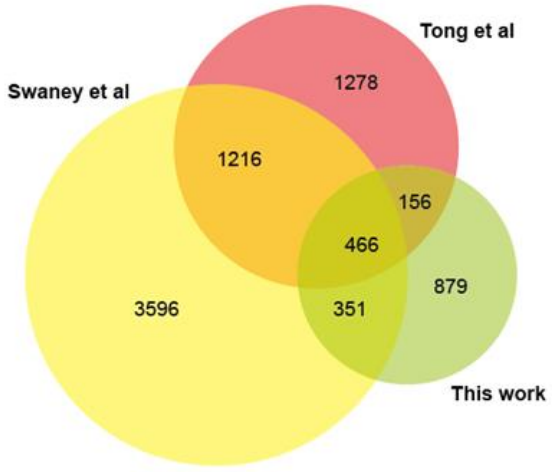

Figure 36. Area-proportional Venn diagram comparing matches between the different ubiquitination sites identified in three different proteomics analysis: Swaney et al,2013; Tong et al,2014; and results presented in this work. Values in circles and intersections indicate number of ubiquitination sites identified. Figure obtained from BioVenn-web application.

We next analysed protein content in the flowthrough (total protein extract). Relative to wild type extracts, 62 proteins were significantly less expressed and 207 were more expressed in *nse1* samples. One of the proteins showing the highest expression difference was Leu2. *LEU2* is used as an auxotrophic marker for selection of the *nse1* mutant allele, an internal control that helped us to validate the total protein quantitation. Proteins that were significantly more expressed in *nse1* mutant cells were enriched in functions related to purine ribonucleotide metabolism and cellular respiration (FDR 4.32E-2 and 3.90E-2), while those less expressed in the mutant were enriched in functions related to amino acid metabolism (arginine, glutamine, leucine, valine, isoleucine, methionine and serine; FDRs ranging from 2.84E-06 to 3.60E-02). We currently do not know the significance of these alterations, although they probably evidence metabolic disadjustments in *nse1* mutants.

Afterwards, we analyzed the quantitation of ubiquitinated peptides in wild type and mutant eluates. As shown in the volcano plot, there were 96 Ub-sites significantly less ubiquitinated in *nse1-C274A* cells. These sites represent potential Nse1 targets. On the contrary, up to 195 Ub-sites appeared to be more ubiquitinated in RING mutant than in wild type cells (Figure 37). As we were interested in identifying new ubiquitination substrates for Nse1, we focused on the proteins at the left side of the volcano-plot. These data correspond to peptides whose ubiquitination is significantly lower when the E3 ligase activity of Nse1 was perturbed. Although the data in the volcano plot was not made relative to the total protein quantification, we confirmed that the position of peptides in this particular place of the graph was not due to lower protein levels.

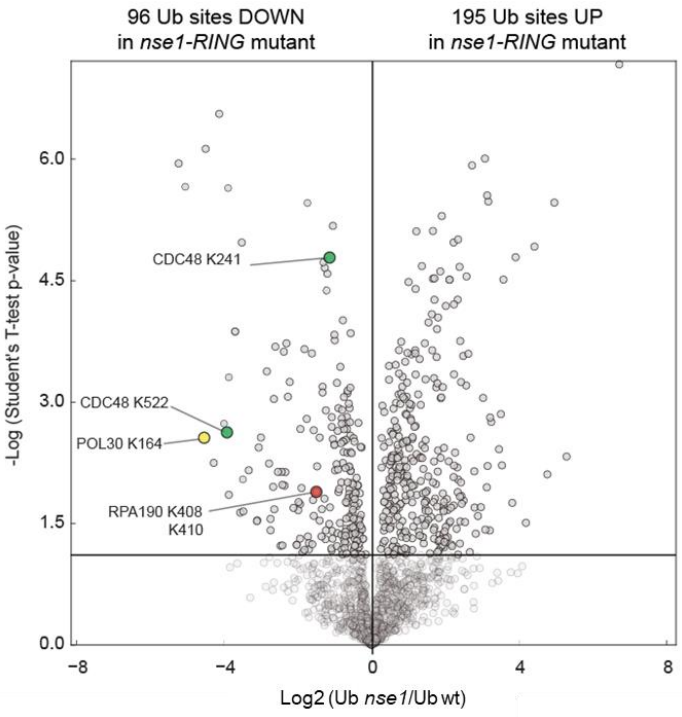

Figure 37. Volcano plot comparison of the ubiquitinome in wild type and the *nse1-RING* mutant strains. The abscissa axis displays the logarithmic value of the ratio between quantity of ubiquitinated sites in wild type and mutant cells; the ordinate axis shows the negative logarithm of the Student's T-test p-value. Each point in the graph represents a ubiquitination site. The 96 Ub-sites detected to be down in *nse1-C274A* mutants are shown on the left side; the 195 ub-sites that were up in *nse1-C274A* cells are on the right. Points that are farthest from zero are statistically more significant. The position of specific ubiquitination sites is shown in the graph.

Next, high confidence hits on the right or the left side of the volcano plot were subjected to STRING network analysis to draw a functional protein network. Remarkably, each of these nodes has a low false discovery rate (FDR), which ensures the significance of the enrichment for a particular function. When analysing protein-protein interactions from Ub-sites representing potential Nse1-targets, we differentiated three defined clusters: a group of proteins related to glycolysis (FDR =0.0177), RNA Pol I subunits and interactors (FDR=$8.58e^{-5}$), and an important cluster of ribosomal proteins (FDR=$3.62e^{-11}$) (Figure 38A). Remarkably, there are two proteins, Nop1 and Nop56, connecting the RNA Pol I and ribosomal protein clusters. Therefore, a large number of proteins under-ubiquitinated in *nse1-RING* mutant cells are also related to ribosomal biogenesis: the RNA Pol I complex, which transcribes rDNA; Nop proteins, involved in the splicing and maturation of the pre-RNA Pol I products; and ribosomal proteins.

Oppositely, networks drawn by the STRING programme from sites more ubiquitinated in *nse1-RING* mutants revealed few significantly enriched functions. In this regard, the only detected cluster, with an FDR of 0.00016, consisted on steroid biosynthetic proteins (Figure 38B).

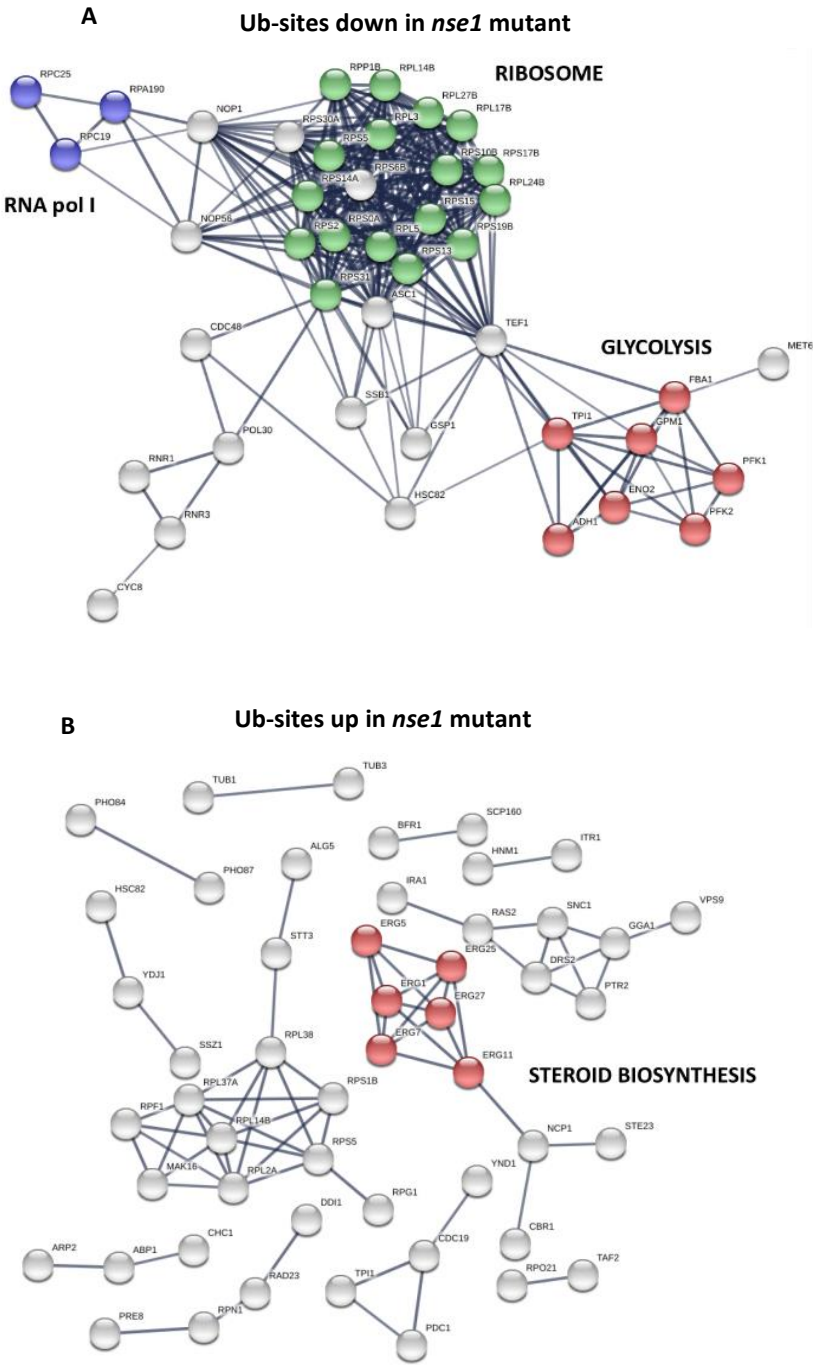

Figure 38. Graphic representation of the enriched functional protein association networks of the different ub-sites that are significantly down in *nse1-C274A* mutants (A), or up in *nse1-C274A* mutants (B). Figures obtained with the STRING programme. Disconnected nodes are not shown. Line thickness indicates the strength of data support.

4.3.2 Validation of Nse1 targets from proteomics screening

Next, we focused our attention on proteins that appeared to be significantly less ubiquitinated in *nse1-C274A* mutants and were involved in DNA replication and repair, cell division or in the maintenance of chromosomal stability. We selected *POL30, CDC48*, *NOP1* or *RPA190*, as potential Nse1 targets, and validated them in ubiquitin pull down experiments.

According to our proteomic data, Lysine K164 in Pol30 showed a significant reduction in ubiquitination in *nse1-RING* mutant cells. This residue is known to be monoubiquitinated by Rad6-Rad18 under DNA damaging conditions, what promotes an error-prone DNA repair pathway. Polyubiquitination of this residue by the Mms2-Ubc13 heterodimeric E2 and the Rad5 E3 ligase is known to activate an error-free lesion bypass (Hoege et al., 2002). Therefore, it was surprising that Pol30 could also be an Nse1-ubiquitination target. Thus, we validated differences between ubiquitination levels of Pol30 in wild type and *nse1* mutant cells by anti-PCNA Western Blot. As controls, for the different Pol30 species, we used an *mms2Δ* mutant (in which polyubiquitination was perturbed), a *pol30-K164R* mutant (that cannot be ubiquitinated or sumoylated at lysine K164), a *siz1Δ* mutant (that impaired Pol30-sumoylation), and a 6his-Flag-SUMO tagged control strain (which shifts upwards sumoylated species in the western blot). As shown in Figure 39A, Pol30-monoubiquitination (U1), diubiquitination (U2) and triubiquitination (U3) bands were absent or less abundant in *nse1-HC* mutant cells than in the wild type ones. The *nse1-HC* mutant used in this experiment carries two C-terminal mutations in the RING domain of Nse1 (H306A and C309A), in two evolutionary conserved residues that coordinate one of the two zinc atoms. This double point mutant has been recently described to show a strong growth defect under different genotoxic treatments (Wani et al., 2018). Moreover, it appears to be defective in the interaction with Nse3 and other subunits of the Smc5/6 complex (Wani et al., 2018). Interestingly, we also observed that the myc-7His tag (which is also fused to the mutant *nse1-HC* gene), perturbed Pol30 di- and triubiquitination levels in cells when fused to the wild type *NSE1* gene. Thus, this result suggested a role for Nse1 on the ubiquitin modification of Pol30 under DNA damaging conditions.

Apart from Pol30, another candidate identified in the screening as a possible Nse1 substrate was Cdc48. Cdc48 is an essential ATPase that uses its unfoldase activity to extract ubiquitinated proteins from complexes for its 26S-mediated proteasomal degradation (Olszewski et al., 2019). However, it has not been described to be directly modified by an E3 ligase. Interestingly, mass spectrometry assays permitted the identification of two ubiquitinated sites for Cdc48, K241 and K522, which were less ubiquitinated in *nse1* mutant cells. Ubiquitin pull-down experiments validated this result and showed that *in vivo* ubiquitination of Cdc48 decreased when the E3 ligase activity of Nse1 was perturbed, in *nse1-HC* mutants (Figure 39B).

In addition, *NOP1* was also identified to be significantly less ubiquitinated in *nse1* mutant cells. As mentioned, *NOP1* is a small nucleolar ribonucleoprotein (snoRNP) that participates in the modification and processing of pre-rRNA transcripts. Indeed, it has been previously described that *NOP1*/ Fibrillarin (*FBL,* in human cells), suffer different reversible posttranslational modifications. In this regard, *FBL* has been reported to be acetylated (Iyer-Bierhoff et al., 2018), sumoylated

(Hendriks et al., 2014), and also ubiquitinated for its proteasomal degradation (M. Chen et al., 2002). *USP36* mediates its deubiquitination (Endo et al., 2009) to counteract its proteolysis. However, the E3 ligase enzyme involved in the Nop1-ubiquitination has not been identified to date. We performed an ubiquitin pull-down in *nse1-HC* mutant cells in which we observed a slight decrease in Nop1-ub species in comparison to wild type cells (Figure 39C).

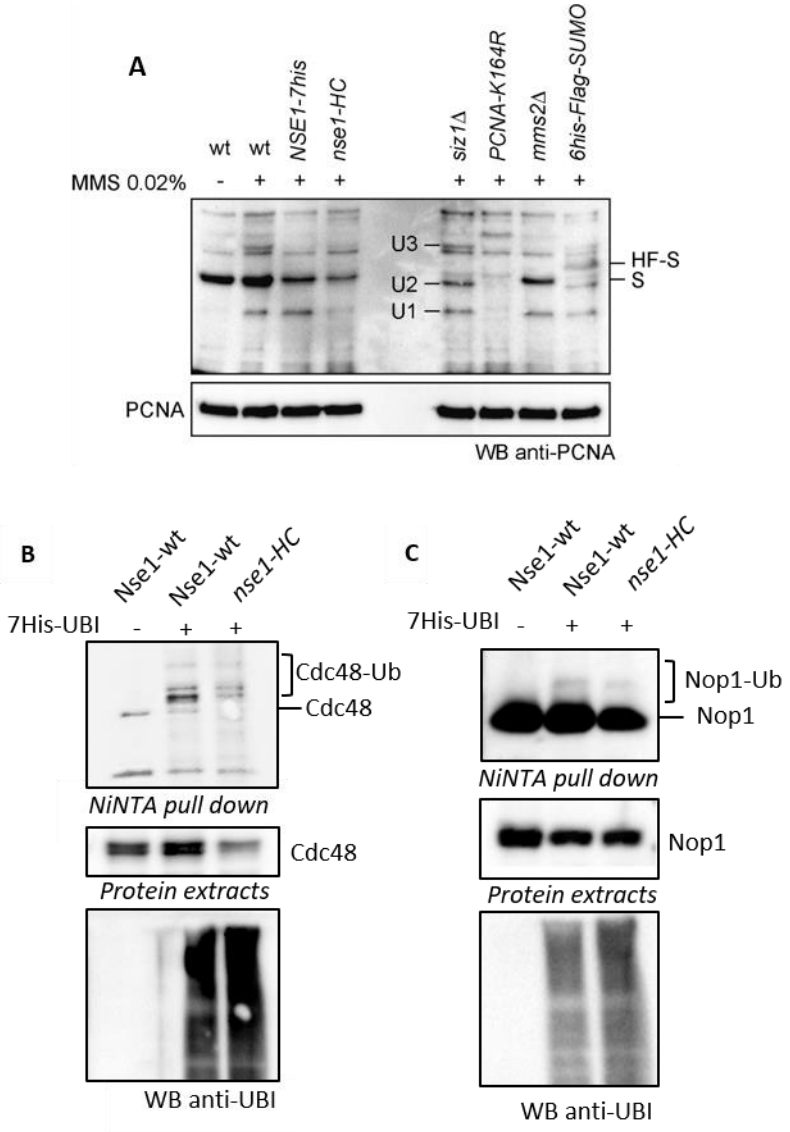

Figure 39. Pol30, Cdc48 and Nop1 ubiquitination decreases in *nse1* mutant cells. (A) anti-PCNA Western Blot analysis from the indicated strains. Cells were treated with 0.02% MMS for 1.5 hours before collecting them. A strain with no MMS-treatment was used as a control, as ubiquitination only occurs under DNA damaging conditions. Protein extracts were prepared under denaturing conditions. Mono-, di-, and tri-ubiquitination bands are indicated as U1, U2 and U3, respectively. **(B)** pADH-HisUbi-tADH (7His-Ubi) Pull Down from a wild type and the *nse1-HC* mutant strain. In all strains *CDC48* was tagged with a 6Flag tag. Protein extracts were prepared under denaturing conditions, and ubiquitinated species were pulled down and analyzed by Western Blot. Ubiquitinated forms of Cdc48 are indicated. A strain with no HisUbi-tag was used as control. **(C)** Same as in (B) but checking Nop1-ubiquitination differences between a wild type and *nse1-HC* mutant strain. In all strains *NOP1* was tagged with an HA tag. Yeast strains used: Y423,YCC4640, YCC4621, Y478, YTR314, Y407, YIR2620; YMR5104, YMR5105; YTR5103, YMR5112, YMR5113.

Finally, another protein that appeared in the proteomics analysis as one possible Nse1 target was Rpa190, the largest subunit of the RNA Polymerase I. Mass spectrometry results permitted to identify lysines K408 and K410 as significantly less ubiquitinated in *nse1-C274A* mutant cells. We were particularly interested in Rpa190 as one possible Nse1 substrate because previous results of the group revealed that Smc5/6 mutants have problems in ribosomal DNA segregation; a phenotype that can be partially alleviated by the inactivation of the RNA Pol I (Torres-Rosell, De Piccoli, et al., 2007). Hence, we speculate that the ubiquitin ligase activity of the Smc5/6 complex may regulate RNA Pol I to ensure cell survival and genome integrity.

Subsequently, we performed ubiquitin pull down assays in cells expressing a 6HA-tagged copy of Rpa190. As shown in Figure 40A, ubiquitination levels of Rpa190 decreased in *nse1-C274A* cells. In addition, we repeated pull down experiments by using other Nse1 mutants, different from the one used in the proteomics screening. One of these mutants was *nse1-HC*. The other one was the thermosensitive *nse1-101* allele (Santa Maria et al., 2007). Pull down experiments showed that ubiquitination levels of Rpa190 were lower in all the Nse1 mutants tested (Figure 40A, B); confirming that Nse1 could be mediating these post-translational modifications.

Moreover, we also performed pull-down experiments in a strain that expresses the endogenous *SMC6* gene under the control of the *GAL* promoter (*GALp-3HA-SMC6*). These cells are kept alive by growing them in galactose to maintain *SMC6* expression, and allow conditional depletion of *SMC6* after addition of glucose to the media. As shown in figure 40C, Rpa190 ubiquitination diminished upon transfer of *GAL-SMC6* cells to glucose. This experiment indicates that proper Rpa190 ubiquitination requires the RING domain in Nse1 and an integer Smc5/6 complex (Figure 40C).

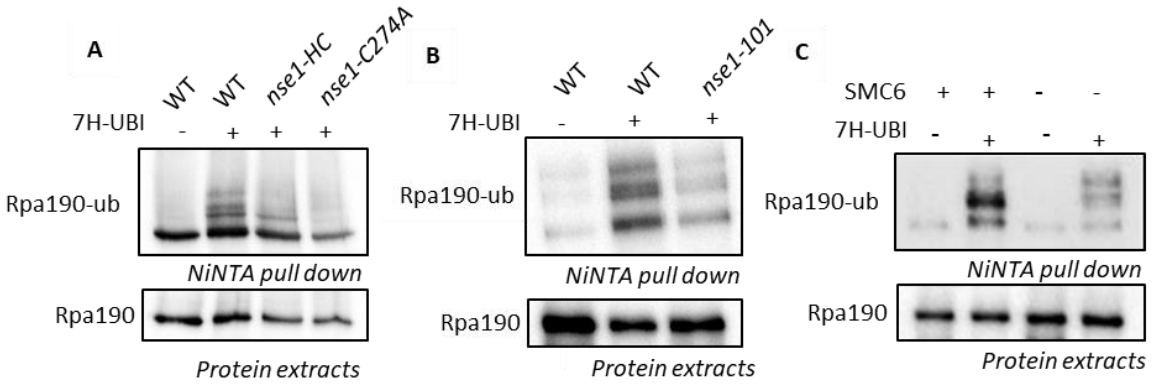

Figure 40. Rpa190 ubiquitination levels decrease in *nse1* and *smc6* mutant cells. (A) 7xHis tagged ubiquitin (7H-UBI) Pull Down from a wild type and the *nse1-C274A* and *nse1-HC* mutant strains. In all strains 7His-UBI was expressed from a plasmid under the *CUP1* promoter. Protein extracts were prepared under denaturing conditions; ubiquitinated species were pulled down and analyzed by Western Blot. Ubiquitinated forms of Rpa190 are indicated. A strain with no His-tag was used as control. **(B)** Same as in (A) but using an *nse1-101* mutant. **(C)** 7xHis tagged ubiquitin (7H-UBI) Pull Down from the indicated strains carrying *GALp-3HA-SMC6 RPA190-6HA*.Yeast cells were grown exponentially in 2% glucose or galactose containing media, and the 7His-UBI was expressed from a plasmid under the *CUP1* promoter. Ubiquitinated forms of Rpa190 are indicated. Two strains with no HF-tag were used as control. Yeast strains used: YFD3916, YFD3914,YEI4820, YEI4782; YEI4055; YEI3828, YEI3829.

4.3.3 Study of conditions that might alter Rpa190 ubiquitination

Genomic integrity is constantly threatened by endogenous or exogenous inputs. As a consequence, cells have developed different ways to respond to these stimuli and ensure an accurate transmission of their genetic content to the progeny. Interestingly, it has been reported that in many cellular stress situations, downregulation of rRNA synthesis and consequently, ribosomes biogenesis, is a prerequisite for nucleolar stability and cell survival (Grummt, 2013). Therefore, as the RNA Pol I transcription blockage is induced by stress-depending signalling pathways, we aimed to evaluate the ubiquitination levels of Rpa190 in different situations that might affect rDNA transcription.

We first treated cells with different genotoxic agents and did pull-down experiments in order to assess Rpa190-ub state under DNA damaging conditions. As shown in Figure 41A, cellular exposure to CPT, MMS, PHL and HU at the indicated concentrations, did not cause a variation of the Rpa190 ubiquitination levels.

We next studied the effect of the rDNA copy number variation on the ubiquitination of Rpa190. RNA Pol I transcription appears to control rDNA copy number (Kobayashi et al., 1998); on the other hand, the Fob1 protein binds the non-transcribed spacer (NTS) present in each repeat of the rDNA array and prevents collisions between DNA and RNA polymerases by allowing fork progression in the direction of the 35S rRNA transcription and arresting forks that travel in the opposite direction. In addition, cells expressing no Fob1 cannot alter the number of copies in the rDNA array, a phenomenon that occurs through homologous recombination. For that, we compared Rpa190 ubiquitination levels in two strains carrying a deletion in *FOB1* and a fixed copy number of rDNA repeats: 25 or 190 (Cioci et al., 2003). Pull-down experiments showed that Rpa190 ubiquitination in *fob1Δ* cells were similar to those observed in wild type cells. In addition, the number of copies did not affect Rpa190 ubiquitination (Figure 41B). Therefore, neither the exposure to DNA damaging agents, nor the number of rDNA copies resulted in a variation of Rpa190 ubiquitinated levels.

Another situation that causes nucleolar stress is nutrient deprivation. Indeed, glucose or amino acid starvation results in the downregulation of pre-rRNA synthesis. Interestingly, our results showed that cells under 1 hour of limiting amino acid availability, responded to this stressful stimulus by dramatically reducing ubiquitination levels of Rpa190 (Figure 41C).

Altogether, these results suggest that the ubiquitination of Rpa190 does not depend on the number of rDNA templates available for transcription, but on the number of actively transcribing Pol I complexes. In this regard, we have seen that when transcription is downregulated by amino acid deprivation, ubiquitinated Rpa190 species are highly reduced.

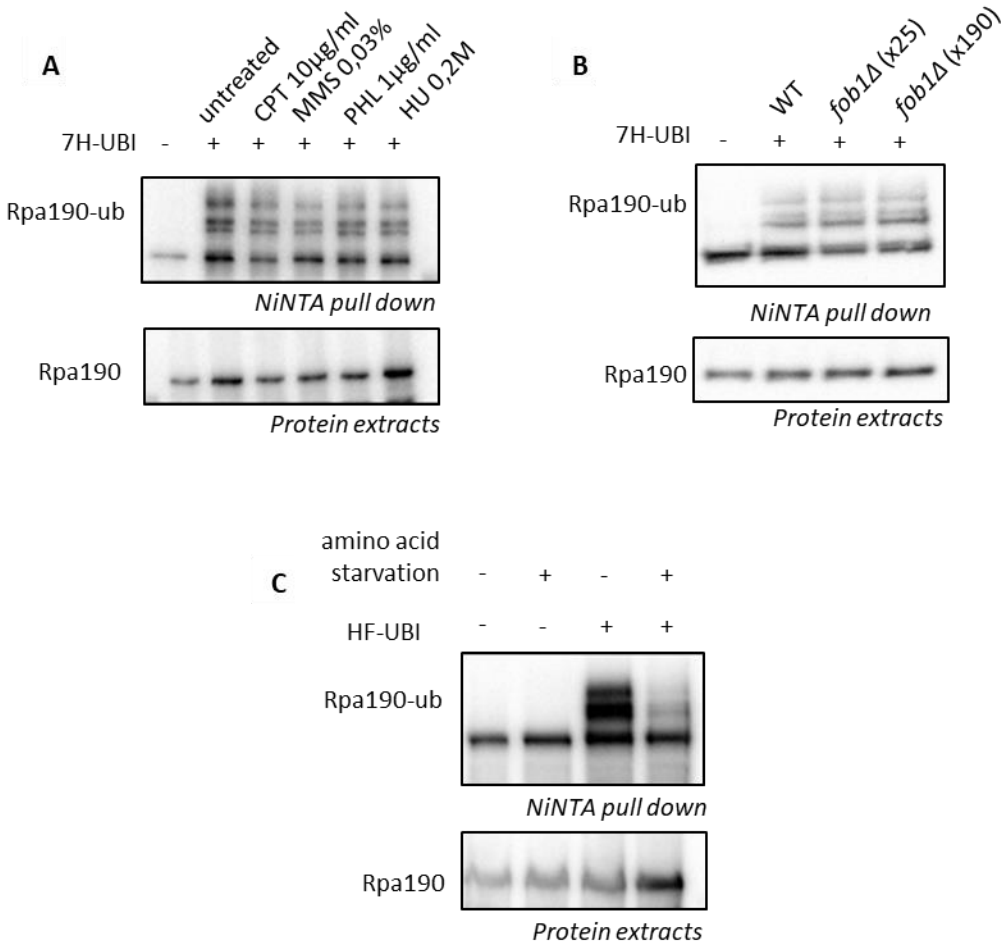

Figure 41. Rpa190-ubiquitination levels under different cellular stress conditions. (A) 7xHis tagged ubiquitin (7H-UBI) Pull Down from *RPA190-6HA* tagged strains after exposure to different genotoxic treatments. In all strains 7His-UBI was expressed from a plasmid under the *CUP1* promoter. Exponentially growing cells were incubated with 10µg/ml CPT, 0.03% MMS, 1µg/ml PHL or 0.2M HU during 2 hours at 30ºC. Protein extracts were prepared under denaturing conditions, and ubiquitinated species were pulled down and analyzed by Western Blot. Ubiquitinated forms of Rpa190 are indicated. Strains with no His-tag were used as control. **(B)** Same as in (A) but using a wild type and two *fob1Δ* mutant strains in which the number of rDNA copies was established at 25 and 190 respectively. **(C)** Same as in (A) but growing two of the cultures under amino acid depriving conditions. Exponentially growing cells were incubated for 1 hour in an SC-Leu-His media at 30ºC and collected for the Pull-down assay. Yeast strains used: YFD9316, YFD3914; YEI3968, YEI3969.

4.3.4 Generation of an *rpa190-K408,410R* mutant

Then, once validated the proteomics results and analyzed the effect of different stress conditions on the ubiquitination state of Rpa190, we mutated the two lysines identified in the screening into arginines (K408R, K410R), to avoid its ubiquitination. These mutations were first expressed from a plasmid in a diploid strain with a deletion in one of the endogenous copies of *RPA190*. By sporulation and tetrad dissection we isolated haploid yeast colonies carrying a plasmid that expresses the mutant *rpa190-K408,410R* allele and a deletion of the chromosomal *RPA190* gene.

Remarkably, *rpa190-K408,410R* mutants were viable and showed a normal cell growth (Figure 42A). Next, by using the isolated mutant vector as a PCR template, we amplified and integrated *rpa190-K408,410R* (hereafter referred to as *rpa190-KR*) mutation in a yeast strain and studied the ubiquitination of the mutant protein.

Pull down experiments showed that Rpa190 ubiquitination levels were extremely reduced in *rpa190-KR* cells (Figure 42B), indicating that ubiquitination of Rpa190 depends mainly on lysines K408 and K410. Interestingly, we also checked that the ubiquitination decrease in *KR* mutants was very similar to the one shown by cells expressing *GAL1,10:GST-UBP10*, in which GST-tagged Ubp10 overexpression was induced by addition of galactose (Figure 42C). Therefore, both increased Ubp10 expression, and the mutation of the two lysines identified in our proteomic screen lead to a similar loss of Rpa190 ubiquitinated species. It is worth noting that none of the mutants impaired cell growth (Figure 42A).

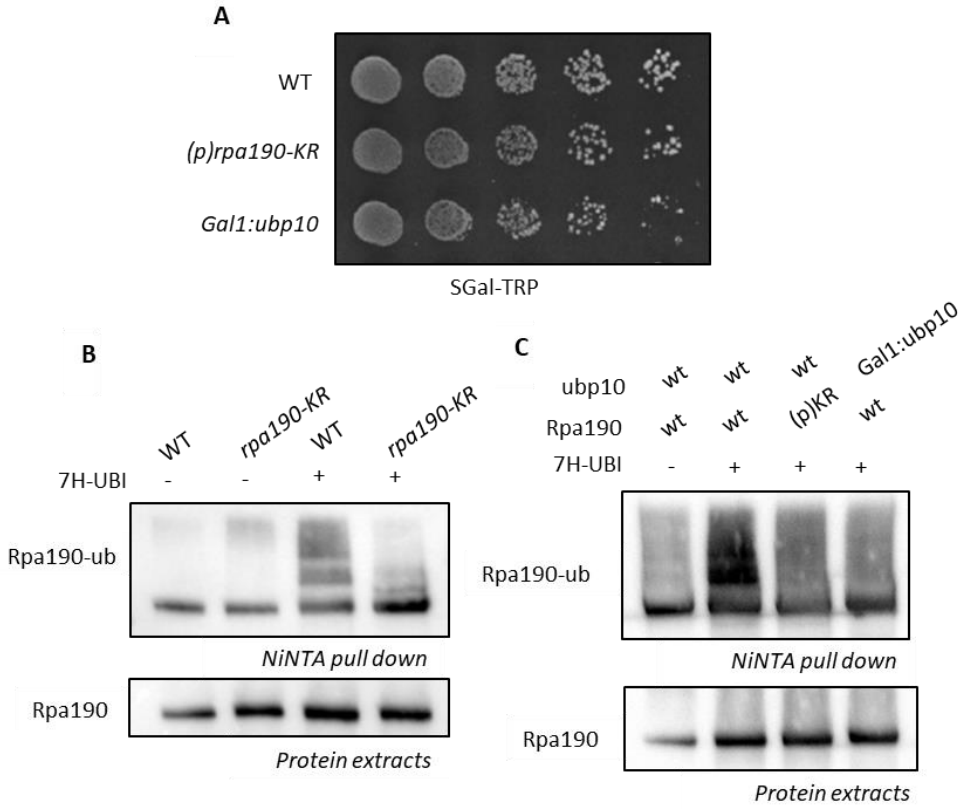

Figure 42. Rpa190 ubiquitination decreases in *rpa190-KR* cells. (A) Growth test analysis of wild-type, *(p)rpa190-KR* mutant cells expressed from a plasmid, and G*al1:UBP10* mutant cells on a SGal-TRP plate at 30ºC. **(B)** 7xHis tagged ubiquitin (7H-UBI) Pull Down from *RPA190-6HA* tagged wild type and *rpa190-KR* (integrated) cells. In all strains 7His-UBI was expressed from a plasmid under the *CUP1* promoter. Protein extracts were prepared under denaturing conditions; and ubiquitinated species were pulled down and analyzed by Western Blot. Ubiquitinated forms of Rpa190 are indicated. Wild type and *rpa190-KR* strains with no His-tag were used as control. **(C)** Same as in (B) but using also a *GAL1,10:GST-UBP10* strain grown induced in a 2% containing-galactose media in order to promote Ubp10 overexpression. In these studies (*p)rpa190-KR* mutant cells were expressed from a plasmid. Yeast strains used: YEI4647, YEI4649, YEI4815, YEI4648, YEI4646.

Subsequently, we decided to assess the accumulation of ubiquitinated species in Rpa190 wild type cells in a *ubp10Δ* mutant strain by pull-down experiments (Figure 43). Interestingly, Rpa190 protein levels substantially decrease in *ubp10Δ* cells, as shown in the protein extracts (P.E), suggesting that such increase in the Rpa190-ub species results in the degradation of the protein. Remarkably, when combining both *ubp10Δ* and *KR* mutations, with apparently opposite functions, protein levels were slightly recovered (as shown in the P.E). As previously described (Richardson et al., 2013), deletion of *UPB10* led to higher levels of Rpa190 ubiquitination, as detected by ubiquitin pull down. An analogous effect was observed in the mutant Rpa190-KR protein, suggesting that, a part from K408 and 410, there might be other less frequently used sites that are targeted by ubiquitin. Nevertheless, Rpa190-KR ubiquitination was severely impaired in *ubp10Δ* mutant cells. Overall, these results indicate that Rpa190 becomes ubiquitinated mainly at lysines K408 and K410, that this ubiquitination is reversed by Ubp10 and that ubiquitinated Rpa190 is targeted for destruction, thus reducing its protein levels.

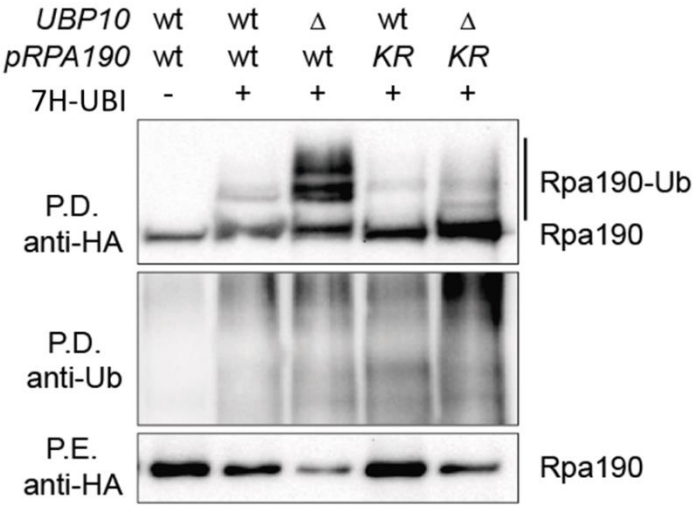

Figure 43. Rpa190-ubiquitination levels in *ubp10Δ* and *rpa190-KR* mutants. (A) 7xHis tagged ubiquitin (7H-UBI) Pull Down from the indicated *RPA190-6HA* tagged cells, expressing the wild type or *KR* mutation from a plasmid, combined with the wild type or delta versions of Ubp10. Protein extracts were prepared under denaturing conditions; and ubiquitinated species were pulled down and analyzed by Western Blot. Ubiquitinated forms of Rpa190 are indicated. A Wild type strain with no His-tag was used as control. Yeast strains used: YEI4646, YEI4647, YEI4649, YEI4838.

4.3.5 Phenotype of an *rpa190-KR* mutant

Next, we wondered what consequences would have the inability to ubiquitinate Rpa190. To study this, we grew *rpa190-KR* cells under different conditions, including genotoxic agents like CPT, MMS, high temperature or transcription inhibitors. Surprisingly, *rpa190-KR* mutants showed no growth defects under most of the conditions tested (Figure 44A). However, we observed that *rpa190-KR* cells were sensitive to 6-azauracil (6-AU) (Figure 44B). This drug specifically inhibits the components of the UTP and GTP biosynthetic pathways (Hampsey, 1997). Although it does not

compromise cellular viability in wild type cells, it can lead to growth defects in transcriptional elongation mutants.

Thus, the sensitivity of *rpa190-KR* mutants to this compound indicated that in non-ubiquitinable Rpa190 cells, RNA Pol I transcription elongation might be impaired.

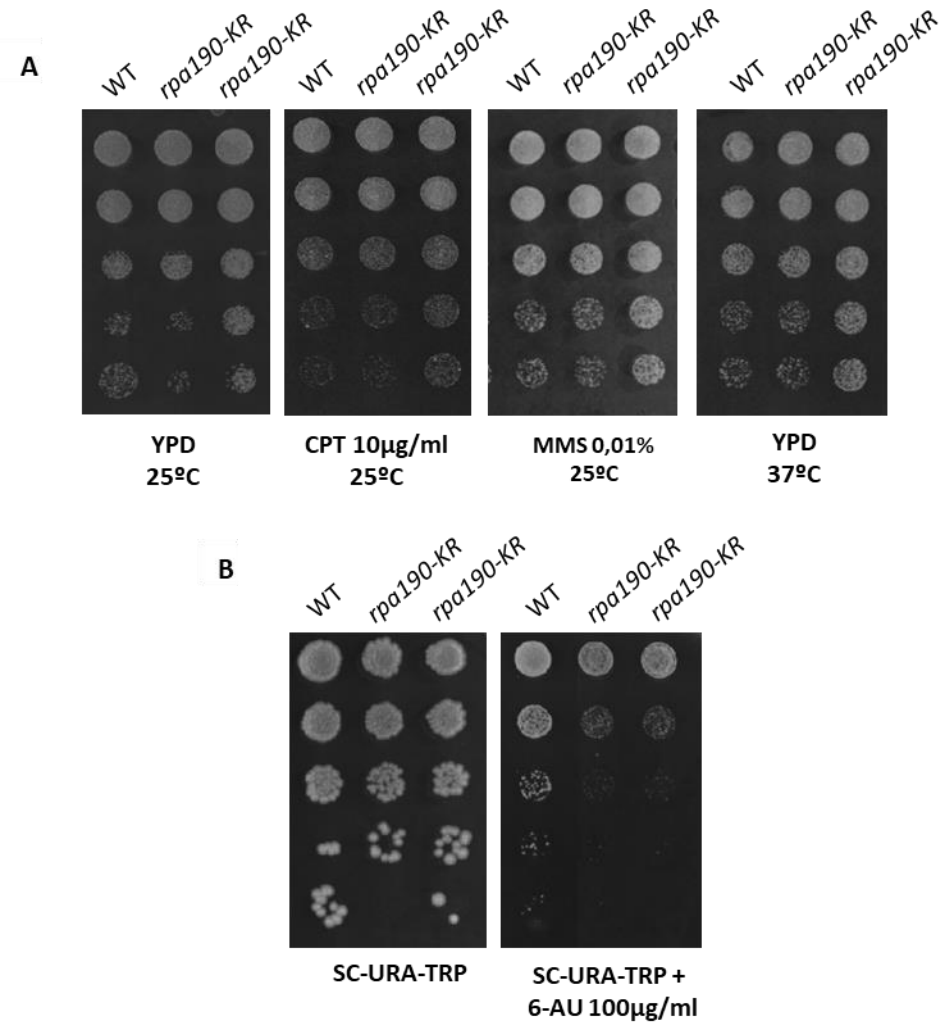

Figure 44. Analysis of *rpa190-KR* growth sensitivities. (A) Growth test analysis of wild-type and *rpa190-KR* cells at the indicated temperatures and CPT or MMS concentrations. Two different *rpa190-KR* clones were analyzed. **(B)** Growth test analysis of wild-type and *rpa190-KR* cells at the indicated concentration of 6-AU. As 6-AU needs to be added in SC-Ura plates, and *rpa190-KR* mutation was expressed from a *TRP* centromeric plasmid, SC-Ura-Trp plates were used as a control. Two different *rpa190-KR* clones were analyzed. Yeast strains used: YEI4646, YEI4604, YEI4607.

Next, we also checked wild type and *KR* cell growth under BMH-21 treatment, which in contrast to 6-AU, is a specific inhibitor of the RNA Pol I. BMH-21 is a new small-molecule that has been very recently described to specifically inhibit the largest subunit of the RNA Pol I Rpa190/Rpa194 (Peltonen et al., 2014). This drug acts as a DNA intercalator that inhibits rRNA synthesis by

mediating the disassemble of the polymerase from the rDNA and the subsequent Rpa190 proteasomal degradation (Wei et al., 2018).

Hence as BMH-21 acts specifically on Rpa190, we checked its effect on wild type and *rpa190-KR* cells. Interestingly, BMH-21 impaired cell growth in wild type cells (Figure 45). As mentioned, it blocks Pol I transcription and consequently inhibits ribosomal biogenesis, which dramatically impairs cellular viability. Interestingly, we realized that BMH-21 differently affects wild type cells depending on their genetic background, as shown in Figure 45. In this regard, we observed that the W303 strain was notably more sensitive to BMH-21 than wild type cells from the BY4741 background. In contrast, *rpa190-KR* mutant cells were more resistant to the BMH-21, independently from their genetic backgrounds (Figure 45). This suggests that *rpa190-KR* mutations protected cells them from BMH-21-mediated Rpa190 degradation. Indeed, *rpa190-KR* tolerance to BMH-21 could be reasoned if the effects of this inhibitor were due to Rpa190 ubiquitination. Overall, both sensitivity to 6-AU and resistance to BMH-21 in non-ubiquitinable mutants suggest functions for Rpa190 ubiquitination in transcriptional elongation.

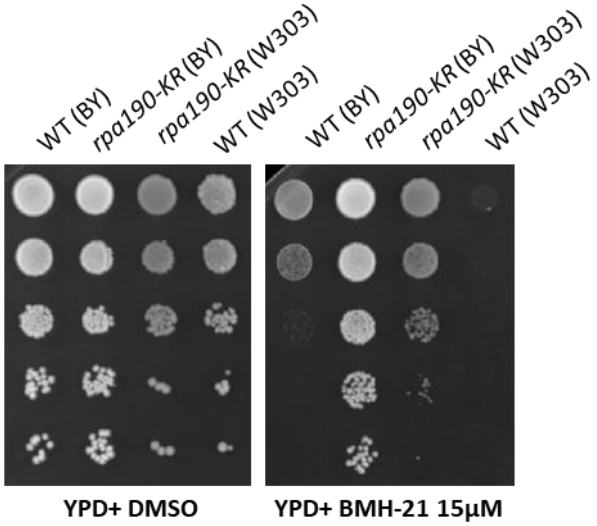

Figure 45. *rpa190-KR* mutants are resistant to BMH-21. Growth test analysis of wild-type and *rpa190-KR* cells at the indicated BMH-21 concentration. Two different wild type and *rpa190-KR* clones from W303 or BY4741 genetic backgrounds were analyzed. Plates were incubated for 2-3 days at 30ºC. Yeast strains used: Y423, YEI5022, W303, YEI5023.

As expected, BMH-21 sensitivity in *ubp10Δ* mutants was even higher than in wild type cells (Figure 46). As previously shown, *ubp10Δ* mutant cells have an accumulation of Rpa190 ubiquitinated species in comparison to wild type cells. As BMH-21 promotes degradation of Rpa190 in a ubiquitin-proteosome dependent manner, *ubp10Δ* mutant cells have strong growth defects even in low concentrations of BMH-21. However, as shown in Figure 46, the expression of an *rpa190-KR* mutant version rescues the BMH-21 sensitivity of *ubp10Δ* mutant cells, indicating that the sensitivity of *ubp10Δ* to BMH-21 is largely dependent on K408 and K410 residues.

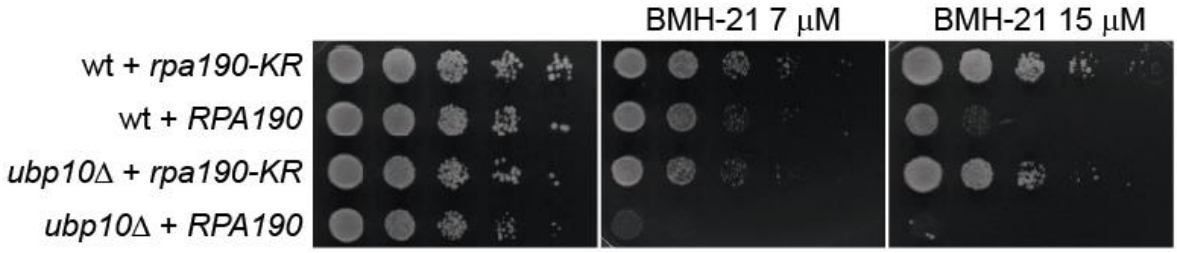

Figure 46. *rpa190-KR* mutations supress the *ubp10Δ* sensitivity to BMH-21. Growth test analysis of the indicated wild type or mutant versions of *RPA190* and *UBP10* genes at the indicated BMH-21 concentrations. Plates were incubated for 2-3 days at 30ºC. Yeast strains used: YEI4648, YEI4646, YEI4838, YEI4826.

4.3.6 Rpa190 is mainly ubiquitinated on chromatin

We were particularly interested in understanding if Rpa190 ubiquitination occurred on chromatin or, in contrast, it could also be ubiquitinated while not transcribing. To this end, we did a chromatin binding assay, a fractionation protocol that enables the separation of chromatin-bound from soluble proteins. In addition, as we wanted to specifically study ubiquitination of Rpa190 in the soluble and chromatin fractions, we did a ubiquitin pull-down on the while cell extracts (WCE), supernatants (SN) and chromatin pellet (CP) fractions. As shown in Figure 47, Rpa190 is mainly ubiquitinated on chromatin. This result also suggests that this posttranslational modification occurs during active transcription, maybe regulating a specific step during elongation of rRNA synthesis.

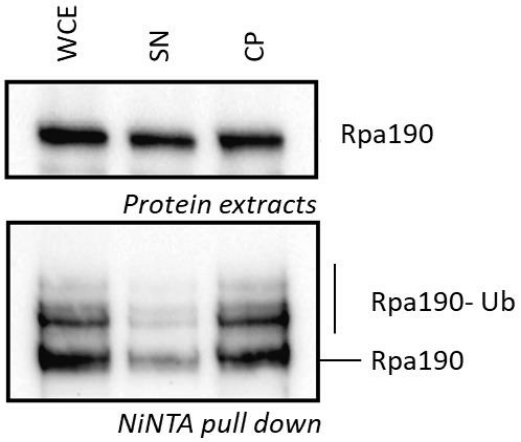

Figure 47. Rpa190 is mainly ubiquitinated on chromatin. 7xHis tagged ubiquitin (7H-UBI) Pull Down from the WCE, SN and CP fractions previously isolated of a wild type *RPA190-6HA* tagged strain. Pull-down was performed after a chromatin-binding assay. Yeast strain used: YEI4763.

4.3.7 Rpa190 levels on chromatin

Subsequently, to better understand the purpose of Rpa190 ubiquitination and its possible role in promoting its eviction from chromatin, we analyzed Rpa190 nuclear levels in chromosome spreads from wild type and *rpa190-KR* cells, in normal conditions or after treatment with 50 µM of BMH-21 for 90 minutes. To this end, Rpa190 was tagged with a 6HA epitope to allow immunofluorescence on chromosome spreads.

As it was expected, results showed that Rpa190-6HA nuclear signal significantly decreased in wild type cells (about 40%) after BMH-21 treatment. Remarkably, Rpa190 levels on chromatin were significantly higher in *rpa190-KR* cells. This result indicates that in *rpa190-KR* cells, Rpa190 accumulates on chromatin. In addition, BMH-21 did not alter Rpa190 chromatin levels in *rpa190-KR* cells (Figure 48), in accordance with their BMH-21 resistance.

Altogether, chromosome spreads indicate that Rpa190 ubiquitination promotes its removal from chromatin, and support the notion that BMH-21 triggers Rpa190 disengagement from chromatin, maybe by increasing its polyubiquitination levels. Since ubiquitination of Rpa190 occurs mainly on lysines K408 and K410, BMH-21 may be unable to enhance Rpa190 polyubiquitination and remove it from the rDNA.

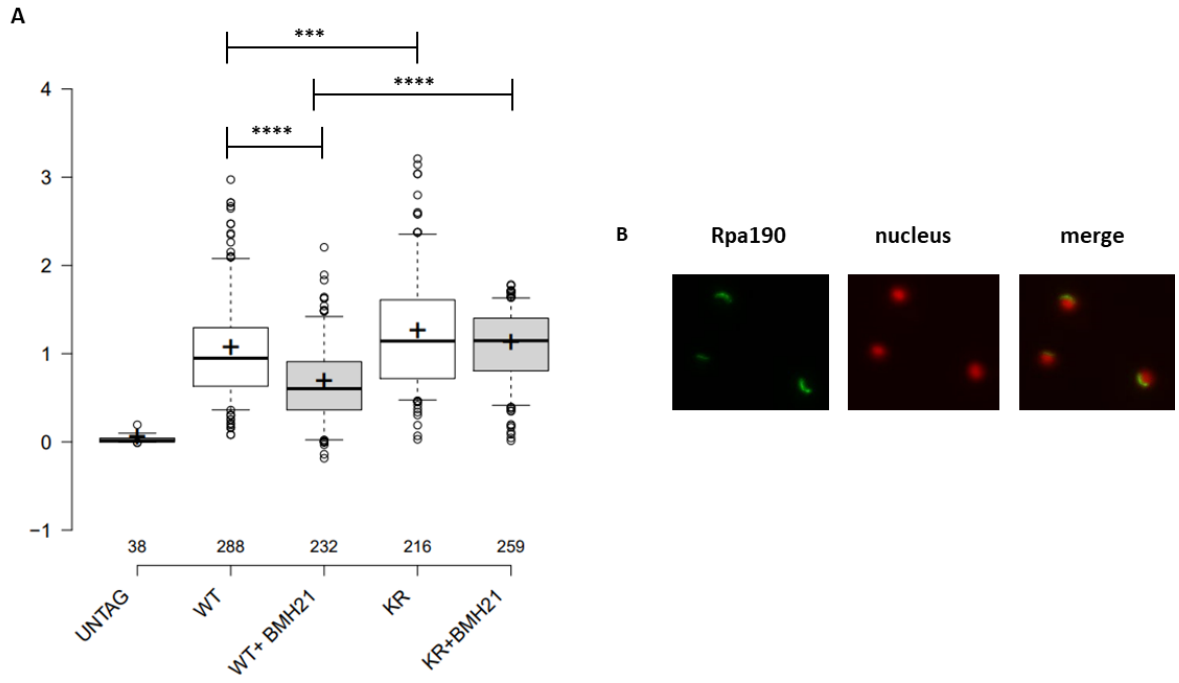

Figure 48. *RPA190-6HA* levels on chromatin of wild type and *rpa190-KR* mutant strains. Boxplots representing results obtained by chromosome spreads performed with the indicated *RPA190-6HA* tagged strains and an untag control. Two parallel WT and *KR* cultures were treated during 90 minutes with 50 µM of BMH-21. The number of samples analyzed is indicated. Boxes, 25–75% data range; whiskers, total data range; black bar, median; black cross, mean. ****P < 0.0001; ***P < 0.001. 1-way ANOVA. (B) *RPA190-6HA* and nucleus signal on chromatin photographed with the fluorescence microscope after doing chromosome spreads and an anti-HA immunostaining in a WT strain and in the absence of the BMH-21 treatment. *RPA190-6HA* signal is distributed along the rDNA in a half-moon shape, red: Hoescht staining; green: HA staining. Yeast strains used: Y423, YEI4664, YEI5022.

4.3.8 Interdependency between Rpa190 sumoylation and ubiquitination

Apart from being ubiquitinated, proteomic studies have shown that subunits of the Pol I complex, including Rpa190 and Rpa135 are sumoylated in an *NSE2*-dependent manner. The same study validated that sumoylation of Rpa135 is severely impaired in *nse2ΔC* cells (Albuquerque et al., 2013). To validate sumoylation of Rpa190, 6HA-tagged Rpa135 and Rpa190 were used to immunoprecipitate Pol I complexes, using anti-HA antibodies, in cells expressing Flag-tagged SUMO. Sumoylation bands were subsequently detected in western blots with anti-Flag. Sumoylation of Rpa135 and Rpa190 was readily detectable in the IP lanes of the western blot as bands with an electrophoretic mobility that varied depending on whether the 6HA tag was placed on Rpa135 or Rpa190. Remarkably, Rpa190 or Rpa135 sumoylation bands observed in wild type strains were absent in *nse2ΔC* cells (Figure 49A). This result indicates that sumoylation of Rpa135 and Rpa190 depends on the Nse2 C-terminal domain.

As both Rpa190 ubiquitination and sumoylation seem to depend on the Smc5/6 complex, we reasoned that one might depend on the other. To this end, we analyzed Rpa190 ubiquitination levels in *nse2ΔC* mutant cells, in which Rpa190 sumoylation is severely impaired. Interestingly, we

found that ubiquitination levels of Rpa190 decreased in *nse2ΔC* mutants in comparison with a wild type strain (Figure 49B). In contrast, we could not detect differences between the Rpa190 sumoylation in wild type and *rpa190-KR* mutant cells (Figure 49C).

Therefore, pull-down experiments indicate that Rpa190 ubiquitination is not required for subsequent Rpa190 sumoylation. Moreover, our results suggest that Rpa190 sumoylation does not occur on lysines K408 and K410. Our results indicate that that perturbing Rpa190 sumoylation also affects its subsequent ubiquitination, suggesting that Rpa190 sumoylation might prime Rpa190 for full ubiquitination.

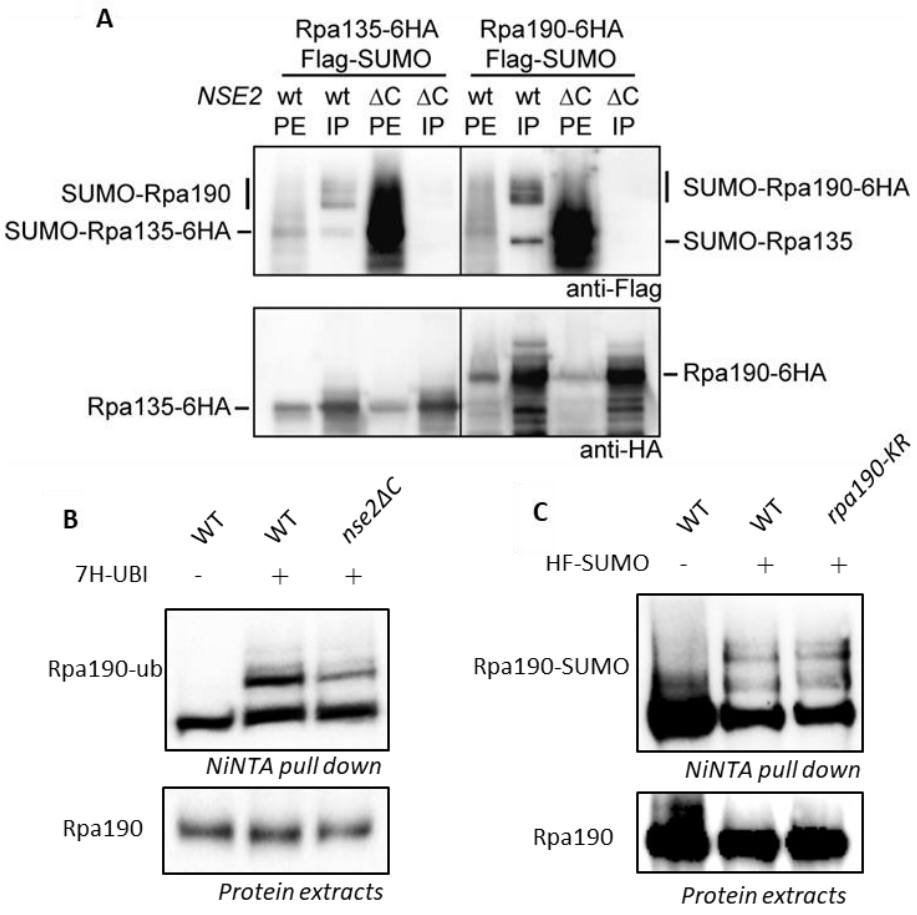

Figure 49. Interdependency between Rpa190 sumoylation and ubiquitination. (A) Rpa135-6HA and Rpa190-6HA immunoprecipitation from the indicated WT and *nse2ΔC* strains. In all strains, SUMO was tagged with a 6his-Flag tag. Sumoylation forms of Rpa190 and Rpa135 are indicated. **(B)** 7xHis tagged ubiquitin (7H-UBI) Pull Down from *RPA190-6HA* tagged wild type and *nse2ΔC* cells. In all strains 7His-UBI was expressed from a plasmid under the *CUP1* promoter. Protein extracts were prepared under denaturing conditions; ubiquitinated species were pulled down and analyzed by Western Blot. Ubiquitinated forms of Rpa190 are indicated. A strain with no His-tag was used as control. **(C)** 6xHis-Flag tagged SUMO (HF-SUMO) Pull Down from wild type and *rpa190-KR* cells. Protein extracts were prepared under denaturing conditions; sumoylated species were pulled down and analyzed by Western Blot. Sumoylated forms of Rpa190 and Rpa190-KR are indicated. A strain with no HF-tag was used as control. Yeast strains used: YSB2705, YSB2699, YSB27007, YSB2701; YEI4763, YEI3980; YTR248+ pTR5024, YTR907+ pTR5024, YTR907+ pEI4637.

4.3.9 Smc5/6 mutants are sensitive to 6-AU

Then, we hypothesised that if Rpa190 was an ubiquitin target of Nse1, Smc5/6 mutants might also have transcriptional problems. Thus, in order to test that, we analyzed the phenotype of different Smc5/6 mutants treated with the transcriptional elongation inhibitor 6-AU.

Results showed that mutations in different Smc5/6 subunits (*nse1-16, nse2-1, nse4-ts3 and nse5-ts3* alleles) sensitized cells to 6-AU (see Figure 50). This result suggests that in the absence of a functional Smc5/6 complex, transcriptional elongation is also defective. However, it is worth noting that the sensitivities displayed by *smc5/6* mutants to 6-AU are even more severe than *rpa190-KR* cells. Therefore, it suggests that their growth impairment does not only stem from Rpa190 ubiquitination defects. In fact, 6-AU is not a specific inhibitor for RNA Pol I, as it affects also polymerases II and III. Thus, the aggravated susceptibility to 6-AU shown by cells expressing defective Smc5/6 complexes is more likely to be linked to an accumulation of transcriptional deficiencies.

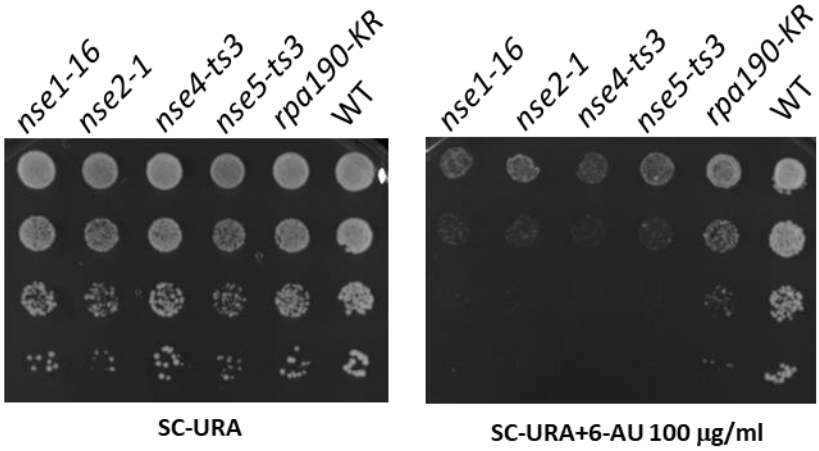

Figure 50. *smc5/6* mutants are sensitive to 6-AU. Growth test analysis of wild-type, *rpa190-KR* and the indicated Smc5/6 thermosensitive strains. 6-AU was added at the indicated concentration and plates were incubated for 2-3 days at 25ºC. Yeast strains used: YEI4741, YEI4740, YEI4737, YEI4736, YEI4852, YEI4762.

4.3.10 Cdc48 mutants and Rpa190

In addition, we also checked Rpa190-ubiquitination levels in *CDC48* mutants. As mentioned above, Cdc48 is an abundant segregase in eukaryotic cells that, among multiple biological functions, promotes assembly and disassembly of protein complexes. It is essential for cell growth and its ATPase function is involved in many ubiquitin-related pathways, including cell cycle regulation (Baek et al., 2013). Indeed, Cdc48 can directly bind to ubiquitin-modified proteins to promote their extraction from a specific molecular environment, which in turn, can promote substrate proteasome proteolysis (Richly et al., 2005). In fact, one of the targets of Cdc48 is Rpb1, the largest

subunit of RNA Pol II. It has been reported that Cdc48 facilitates the UV-induced degradation of Rpb1 (Verma et al., 2011). We therefore hypothesised that Cdc48 could interact with Rpa190-ubiquitinated proteins in order to promote their release from chromatin. If Cdc48 was involved in removing ubiquitinated Rpa190 from chromatin, we should expect an accumulation of Rpa190-ubiquitinated species in *cdc48* mutants. In order to study that, we checked ubiquitination levels of Rpa190 in different *cdc48* thermosensitive mutants using ubiquitin pull downs. However, results showed that Rpa190 ubiquitination in *cdc48* mutant cells was severely impaired compared to a wild type strain (Figure 52).

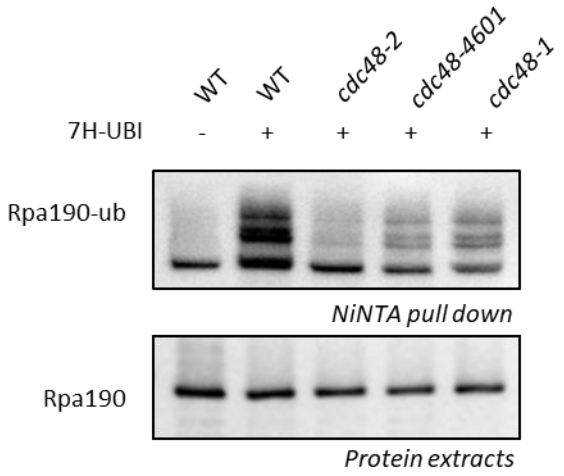

Figure 51. Rpa190 ubiquitination decreases in *cdc48* mutants. 7xHis tagged ubiquitin (7H-UBI) Pull Down from *RPA190-6HA* tagged wild type and *cdc48-ts* mutant cells. In all strains 7His-UBI was expressed from a plasmid under the *CUP1* promoter. Protein extracts were prepared under denaturing conditions, and ubiquitinated species were pulled down and analyzed by Western Blot. Ubiquitinated forms of Rpa190 are indicated. A strain with no His-tag was used as control. Yeast strains used: YEI4762, YEI4763, YEI4765, YEI4767, YEI4769.

Next, to study the possible role of Cdc48 in Rpa190 function, we treated *cdc48* mutant cells with 6-AU and BMH-21, and analyzed their phenotypes. First, we saw that *cdc48* mutants also showed 6-AU sensitivity (Figure 53), suggesting that an impaired segregase activity may result in transcription elongation defects. Nevertheless, due to the wide range of transcriptional affectations caused by this drug, we cannot establish a simple unidirectional link between 6-AU sensitivity in *cdc48* mutants, and Pol I transcriptional elongation impairments.

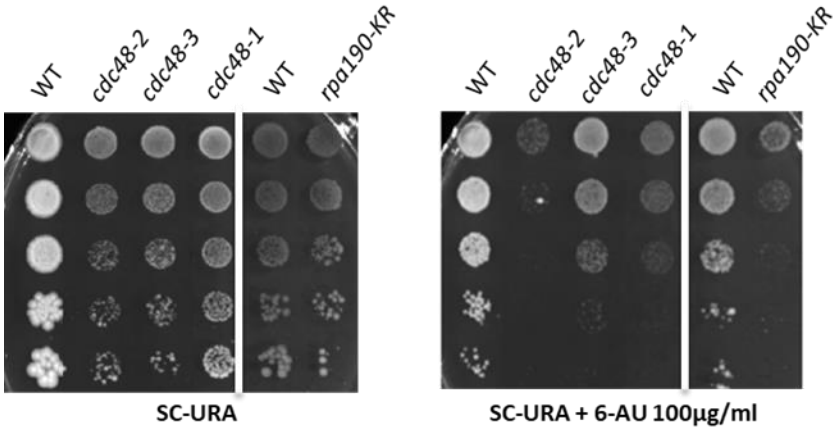

Figure 52. *cdc48* mutants are sensitive to 6-AU. Growth test analysis of wild-type, *rpa190-KR* and different *cdc48* thermosensitive strains at 6-AU containing plates at the indicated concentration. Plates were incubated for 2-3 days at 30ºC. Yeast strains used: Y423, YEI4730, YEI4732, YEI4726, YEI4762, YEI4852.

Interestingly, as shown in Figure 54, all the *cdc48* mutants tested were also resistant to BMH-21, which is in concordance with our previous findings showing an important decrease of Rpa190 ubiquitination in *cdc48* mutant cells.

In fact, the mechanism by which Rpa190 is removed from chromatin and posteriorly marked for degradation after BMH-21 treatment remains unclear. However, our results suggest that it requires the Cdc48 segregase.

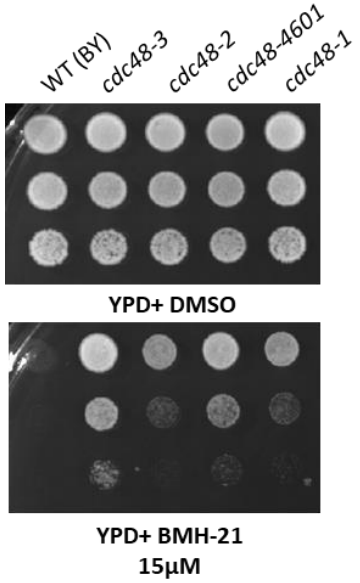

Figure 53. *cdc48* mutants are resistant to BMH-21. Growth test analysis of a wild-type (BY) strain and cells carrying different *cdc48* mutant alleles at the indicated BMH-21 concentration. Plates were incubated for 2-3 days at 25ºC. Yeast strains used: Y423, Y4157, Y4148, Y4183, Y4220.

Finally, we also checked the Rpa190-6HA chromatin signal on different *cdc48* mutants. Notably, in all the mutants tested, Rpa190 levels on chromatin significantly dropped (from 38% to a 55% depending on the mutant) in comparison to wild type cells (Figure 55A, B). Again, this decrease observed in chromosome spreads corroborates that RNA Pol I needs a functional Cdc48 segregase activity for transcription, and suggests that it could be necessary for promoting the loading of the complex onto the rDNA.

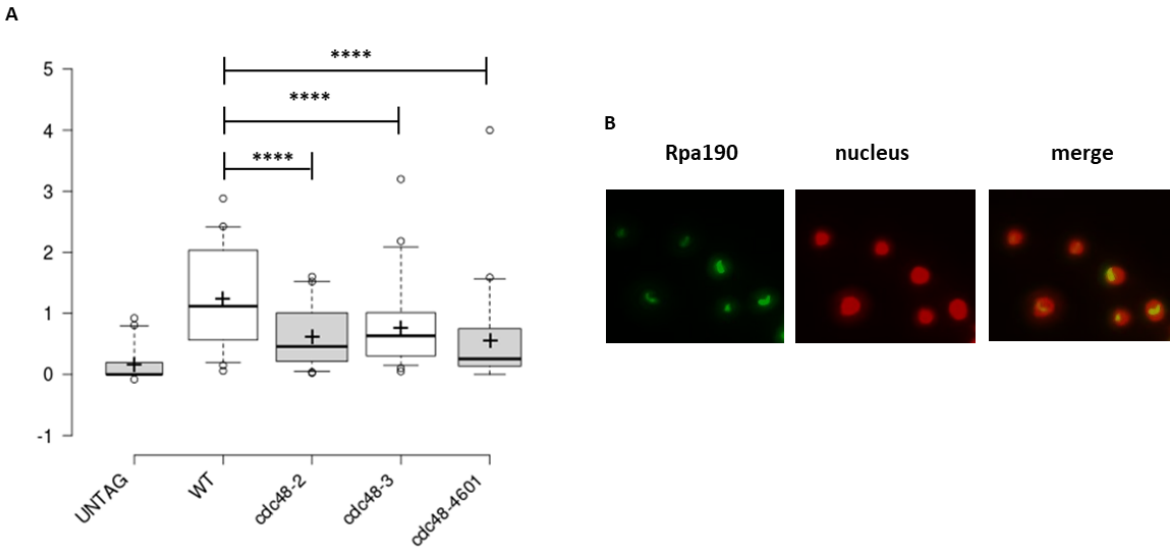

Figure 54. *RPA190-6HA* levels on chromatin of wild type and different*cdc48* mutant strains. (A) Boxplots representing results obtained by chromosome spreads performed with the indicated *RPA190-6HA* tagged strains and an untag control. Boxes, 25–75% data range; whiskers, total data range; black bar, median; black cross, mean. ****P < 0.0001; ***P < 0.001. 1-way ANOVA. **(B)** *RPA190-6HA* and nucleus signal on chromatin photographed with the fluorescence microscope after doing chromosome spreads and an anti-HA immunostaining in wild type cells. *RPA190-6HA* signal is distributed along the rDNA in a half-moon shape, red: Hoescht staining; green: HA staining. Yeast strains used: Y423, YNC2839, YEI4743, YEI4744, YEI4745.

DISCUSSION

5. DISCUSSION

5.1 Chapter I- DNA activates the Nse2/Mms21 SUMO E3 ligase in the Smc5/6 complex

Among the large diversity of cellular processes in which SUMO has been involved, its nuclear roles in regulation of chromatin-based transactions stand out (Cubeñas-Potts & Matunis, 2013). Indeed, sumoylation of chromatin-associated factors plays multiple roles during mitosis, in DNA replication, transcription, or DNA repair (Ulrich, 2014). Thus, it seems that the sumoylation state of a protein can be regulated through its association with DNA, affecting its cellular functions. In this regard, it has been proposed that sumoylation of chromosomal targets, also called "on-site sumoylation", is regulated by SUMO E3 ligases engaged on chromatin in a process that has been called DNA-dependent substrate modification (Ulrich, 2014) (Sarangi & Zhao, 2015). In this work we have studied if similar mechanisms apply to the Smc5/6 complex. This study started from the observation that ATPase mutants in the Smc5/6 complex show defects in sumoylation *in vivo* (Bermúdez-López et al., 2015). As ATPase mutants are supposed to be defective in loading onto chromatin, our initial hypothesis was that direct association with DNA could upregulate the SUMO ligase activity of Nse2. In accordance, we observed DNA-dependent upregulation of the SUMO ligase using an Smc5-Nse2 heterodimer *in vitro* (Varejão et al., 2018). Indeed, we observed that DNA-dependent enhancement requires a positively-charged patch in the ARM region of Smc5. Based on these findings, we propose that the Nse2 SUMO ligase activity in the Smc5/6 complex is also enhanced by direct binding to DNA.

The Smc5/6 complex binds to the same chromosomal regions that it helps to segregate or repair; such as at DSBs, where it promotes DNA repair via sister-chromatid recombination (Lindroos et al., 2006) (De Piccoli et al., 2006); at stalled replication forks, where it is involved in the resolution of recombination intermediates (Bustard et al., 2012); or at the rDNA locus (Torres-Rosell et al., 2005), telomeres and centromeres (Pebernard, Schaffer, et al., 2008), where Smc5/6 complexes are required for segregation of repetitive regions. Therefore, Smc5/6, as all members of the SMC family, must function when bound to DNA. Consequently, it is not surprising that most of the Nse2 targets described to date are enriched at these sites (Solé-Soler & Torres-Rosell, 2020).

The accumulation of ssDNA is a characteristic of DNA lesions, stalled replication forks or telomeres. In concordance with this, *in vitro* experiments show that although both ssDNA and dsDNA are capable to enhance the E3 ligase activity of Nse2, ssDNA has a stronger effect (Varejão et al., 2018). We therefore suggest that the Smc5/6 complex is recruited to the ssDNA accumulated at DNA lesions, and its Nse2-dependent SUMO ligase activity is enhanced by direct association of the complex with ssDNA strands. This mechanism differs from others in which sumoylation is modulated by DNA, even in the absence of an E3 ligase, like the requirement of the PCNA loading to the DNA for its *in vivo* sumoylation (Parker et al., 2008); or the DNA-dependent enhancement of the PARP-1 affinity for the E2 conjugating enzyme Ubc9 (Zilio et al., 2013). In our

proposed model, in contrast, the Nse2 SUMO ligase activity is promoted after non-specific binding of DNA to a positively charged patch in the Smc5 ARM; that in turn, results in an Nse2 conformational change (Varejão et al., 2018).

The DNA-dependent upregulation of Nse2 activity depends on the Smc5 ARM region (Varejão et al., 2018). Thus, in the absence of Smc5, Nse2 activity is not affected by DNA. This result indicates that the Smc5-DNA interaction mediates the activation of the Nse2 E3 ligase activity. Smc5 has been reported to efficiently bind to ssDNA (Roy et al., 2011); and the Smc5/6 heterodimer associates with DNA through several binding regions (Roy et al., 2015). Therefore, we cannot discard that other domains in the Smc5/6 complex apart from the DNA sensor in Smc5 described here, regulate the Nse2 ligase.

Examination of the structure of Smc5-Nse2 complex (Duan et al., 2009) allowed us to identify a positively-charged patch in Smc5. *In vitro* results revealed that this small positively-charged patch located in the Smc5 coiled coil is required and sufficient for upregulating sumoylation in a DNA-dependent manner (Figure 19). In addition, circular dichroism spectroscopy experiments show that the DNA binding to Smc5-Nse2 molecules triggers a conformational change in Nse2 (Varejão et al., 2018). This structural rearrangement may facilitate the interaction between the RING domain of the E3 ligase and the E2 conjugating enzyme, or transfer of SUMO to the target protein.

Mutation of some of the lysines composing the DNA sensor in Smc5 into aspartic acids (*KE*) sensitized cells to DNA damage (Figures 20, 21B). These results confirmed that the DNA sensor in Smc5 is required for DNA repair *in vivo.* In accordance, *smc5-KR* cells, which maintain the positive charge, did not show cell growth impairments under genotoxic treatments (Figure 21C); indicating that the MMS-sensitivity showed by *smc5-KE* mutants was a consequence of the positive to negative charge change and not to the loss of lysine residues. In addition, *smc5-7KE* point mutants displayed an MMS-sensitivity comparable to *nse2-CH* cells, in which the catalytic activity of the RING domain was impaired. Both *smc5-KE* and *nse2-CH* mutants, which should in principle compromise the E3 ligase activity of Nse2, resulted in a reduced ability to cope with genotoxic stress. It is worth noting that despite *nse2-CH* and *smc5-KE* cells have a similar phenotype, the causes are slightly different: *nse2-CH* mutations may disrupt the interaction with the E2 conjugating enzyme, thus compromising the transfer of SUMO to the target protein. In *smc5-KE* mutants, in contrast, the association of the DNA to the Smc5 DNA sensor patch is compromised, what alters the DNA-dependent SUMO-conjugation enhancement.

Based on our results, we propose that K743 and K745 lysine residues constitute a minimal DNA sensor in the coiled coil domain of Smc5, required for DNA-dependent activation of the SUMO ligase activity (Varejão et al., 2018). However, we have also seen that other lysines in the positively charged patch of Smc5 can act synergistically with K743 and K745 on DNA binding. Therefore, other residues in the Smc5 DNA sensor might cooperate in the DNA-dependent activation of the SUMO ligase. Accordingly, growth tests analysis revealed different degrees of MMS-sensitivity between *smc5-K743,745E* or *smc-3KE* cells and *smc5-7KE* mutants (Figure 21C). We suggest that the moderate cell growth impairment observed in the firsts corresponds to the loss of the DNA-dependent sumoylation enhancement due to a perturbed Smc5 sensor-DNA association, but with

a basal Nse2 sumoylation induced by a functional E3 ligase activity. In contrast, the synergistic effect of these lysines is shown when *smc-3KE* (bearing mutations in the C-terminal coiled coil domain) and *smc-4KE* (bearing mutations in the N-terminal coiled coil domain) are combined in a *smc5-7KE* mutant strain, which shows a stronger MMS sensitivity phenotype and a higher reduction in the Smc5 sumoylation levels. Indeed, there are at least two factors that might contribute to the aggravated sensitivity of the *smc5-7KE* mutant. First, in *smc5-7KE* cells the positively-charged DNA sensor is lost. Second, as we have recently described, Smc5 SUMO acceptor sites partly overlap with those disturbed in the *smc5-7KE* (Zapatka et al., 2019)*;* indicating that in *smc5-7KE* mutants these Smc5 sumoylation sites are also lost. Accordingly, we observed a reduction in Smc5 sumoylation levels in *smc5-7KR* cells in comparison with its wild type counterpart (Figure 22B). Therefore, this reduction may be due to the loss of potential SUMO acceptor sites in the Smc5 protein, as such mutations did not compromise DNA binding and the subsequent Nse2 E3 ligase activity stimulation. In addition, our results have revealed other possible factors that might contribute to the severity of the *smc5-7KE* mutant. Thus, mutations in the extended positively-charged patch in Smc5 might also compromise the stability of the entire Smc5/6 complex. Indeed, *smc5-7KE* mutations might alter the Smc5 coiled coil structure and functionality, as well as interactions with other subunits of the complex. In this regard, we have seen that *smc5-7KE* mutant cells have an impaired Smc5-Smc6 association (Figure 24A). Moreover, as shown in Figure 25, we have seen an important loss of Smc5/6 complexes on chromatin in *smc5-7KE* mutants. Remarkably, the lower accumulation of Smc5/6 complexes on chromatin should also decrease the capacity to activate Nse2.

As it happens in other SMC complexes, Smc5/6 must probably require prior loading onto chromatin to develop its cellular functions. This loading process is ATP-dependent (Kanno et al., 2015). Also in prokaryotic cells the entrance of the DNA inside SMC molecules is regulated by ATP (Bürmann et al., 2017). Interestingly, it has also been reported that Nse2 sumoylation depends on the ATPase activity of the Smc5/6 complex (Bermúdez-López et al., 2015): Smc5/6 mutants unable to bind ATP have a severely impaired SUMO ligase activity. We propose that this ATPase function is probably required because ATP regulates the association of the complex with DNA (Kanno et al., 2015), and promotes a structural rearrangement in Smc5-Nse2 molecules that in turn, as shown here, produces an increase of the Nse2-dependent sumoylation activity. In our model, DNA plays a dual role: it stimulates sumoylation and brings Smc5/6 molecules closer to its SUMO targets. As shown in Figure 56, we propose that the Smc5/6 complex becomes activated and loaded onto chromatin in an ATP-dependent manner. Then, unspecific DNA regions close to the Smc5 coiled coil interact with the DNA sensor causing a conformational change in Smc5-Nse2 molecules, which subsequently stimulates Nse2 SUMO ligase activity.

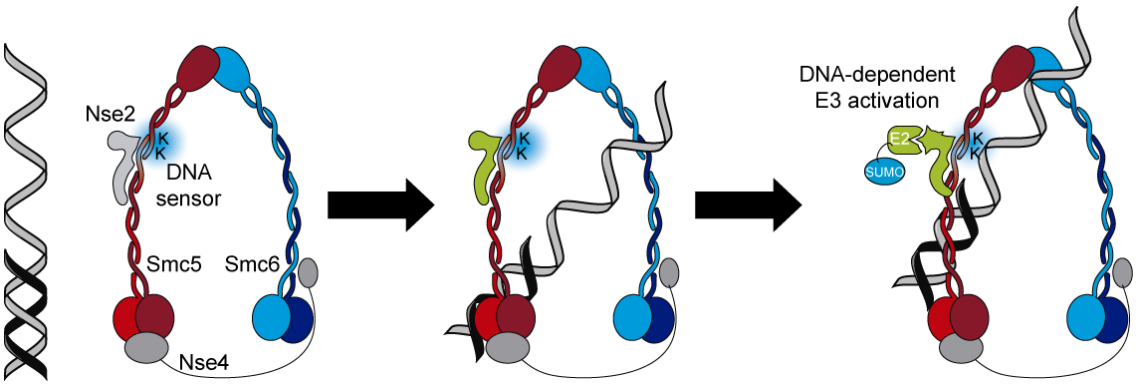

Figure 55. Model for the ssDNA-dependent Nse2 E3 ligase activity enhancement. Smc5/6 complex is first loaded onto chromatin through its ATPase activity. Then, the DNA sensor in Smc5, composed by at least K743 and K745, interacts with the ssDNA, which results in an Nse2 conformational change that activates sumoylation of chromatin-bound targets.

As previously mentioned, the Smc5/6 complex specifically binds to DNA damaged sites where it promotes sumoylation of substrates involved in DNA damage repair. Thus, we predict that the DNA-dependent upregulation of Nse2 activity is a mechanism that regulates the modification of other Nse2 chromosomal targets, such as cohesin (Almedawar et al., 2012), the Sgs1–Top3–Rmi1 complex (Bermúdez & Aragón, 2017), different subunits of the Smc5/6 complex (Andrews et al., 2005) or other proteins involved in DNA repair like Yku70 (Zhao & Blobel, 2005). Overall, this model permits the Smc5/6 complex to develop its functions on DNA repair, rDNA segregation or sister chromatid resolution by delimiting its Nse2 E3 ligase activity to the substrates pre-loaded on chromatin and localized close to the DNA binding sites of the Smc5/6 complex.

Notably, the ATPase activity has been previously described to regulate the dynamic DNA association of prokaryotic SMC complexes through a conformational change in the coiled-coil domain (Bürmann et al., 2017). According to our findings, ATP binding to the Smc5/6 complex not only assists a structural rearrangement of coiled coil domains necessary for DNA entrapment (Alt et al., 2017), but also promotes activation of the Nse2 SUMO ligase. Remarkably, the Nse2 binding site in the Smc5 ARM is located just before the Smc5 elbow, a coiled coil disruption present in all SMC complexes (Solé-Soler & Torres-Rosell, 2020). This articulation is where the ARM domain folds, bringing into proximity the hinge domain and the ATPase heads. We speculate that DNA binding might promote the movement of the elbow and the opening of the coiled coil domain of Smc5, which could further expose the Smc5 sensor.

In summary, we have revealed a novel SUMO E3 ligase stimulation mechanism for the Smc5/6 complex that occurs on-site and that is regulated by chromatin loading and the subsequent association between DNA and DNA sensor in Smc5. This mechanism promotes the conformational changes necessary for full activation of the Nse2 SUMO ligase.

5.2 Chapter II- Functional analysis of the C-terminal domain of Nse2 in protein sumoylation and DNA damage repair

Nse2 has two different structural regions, an N-terminal essential domain that docks onto the Smc5 coiled coil, and a non-essential C-terminal half that contains the RING domain and holds its SUMO ligase activity (Duan et al., 2009). Thus, Nse2 has dual functions in the Smc5/6 complex: on one side, its docking to Smc5 supports the essential roles of Smc5/6; but on the other side, it has an E3 ligase activity that is dispensable for viability. Nevertheless, mutations in its SUMO ligase domain result in a double strand break repair deficiency and an increased sensitivity to DNA-damaging agents (Andrews et al., 2005). In fact, it has always been assumed that the only function of the C-terminal domain of Nse2 was sumoylation. However, the phenotype of an *nse2ΔC* mutant, described more than 15 years ago (Zhao & Blobel, 2005), is more severe than the *nse2-C200,H202A* mutant, that has mutations predicted to disturb the RING domain of Nse2. This difference indicates that the C-terminus in Nse2 does not merely regulate sumoylation. In addition, it has recently been described an Nse2-related syndrome that truncates the C-terminal part of the human *NMSCE2,* without affecting the RING domain. Altogether, these results encouraged us to study the different structural parts of the C-terminal end of Nse2 and to analyze whether the effects of all the mutants generated (point mutations or deletions) in this region were due to the loss of sumoylation activity.

The C-terminal alpha-helix is essential for Nse2 protein stability

As mentioned, heterozygous frameshift mutations in *NSMCE2* have been recently associated with a human syndrome linked to dwarfism, gonadal failure and extreme insulin resistance diabetes (Payne et al., 2014). One of the two rare haplotypes identified in the two patients suffering this syndrome, contains the Ser116Leufs*18 mutation, introducing a truncation in the middle of the protein. The other one contains the Ala234Glufs*4 mutation, which removes the last 14 residues, in the C-terminal α-helix. Therefore, the C-terminal alpha-helix must play a very important function, and its deletion must be responsible for the *NSMCE2*-associated syndrome in humans (Payne et al., 2014). In yeast cells, the *nse2Δ29C* and *nse2Δ24C* deletions recreate the Ala234Glufs*4 mutation. Importantly, both mutants still conserve an intact RING domain, as occurs in human Ala234Glufs*4 mutants. Our results showed that these deletions, as also occurs in the *nse2ΔC* mutant, destabilized the Nse2 protein levels, impaired cell growth and sensitized cells to temperature and DNA damage (Figures 29A, C). These findings reveal that removing the last residues, corresponding to the alpha-helix, is equivalent, in terms of cell growth under different conditions, to the removal of the entire C-terminus, including the RING domain.

We assume that the MMS sensitivity is indicative of mutants with impaired repair at replication forks; whereas the temperature sensitivity is most probably due to protein folding defects, which can be notably aggravated when growing at high temperatures. This protein folding or structure defects might lead to increased protein destruction and lower protein levels.

First and foremost, the alpha-helix domain might have an important structural function, as its removal compromises Nse2 protein levels. We think that this might stem from increased protein instability, maybe by impairing appropriate folding of the protein. Therefore, it is reasonable that the small amount of protein expressed in these mutants prevents cells to sustain sufficient levels of Smc5/6 activity. The situation might be even more dramatic under conditions of DNA damage, when the limited amount of Nse2 and active Smc5/6 complex might lead to enhanced DNA sensitivity and cell death. Therefore, we propose that the phenotypes observed in patients bearing truncations in this alpha-helix are due to low Nse2 protein levels. In fact, in primary dermal fibroblasts from one of the patients, the levels of Nse2 were severely reduced (Payne et al., 2014). The loss of the Nse2 protein by truncation of the C-terminal alpha-helix might also reduce Nse2-dependent sumoylation and compromise the Smc5/6 functions on the DNA damage response. Remarkably, both hypomorphic patients presented dwarfism, altered pigmentation or increased micronuclei; clinical features shared with Bloom syndrome patients and with *NSMCE2* adult deleted mice (Payne et al., 2014) (Jacome et al., 2015). In this regard, it has been recently reported that Sgs1/BLM functions on Holiday junction's and crossover dissolution depend on its sumoylation mediated by the Smc5/6 complex (Bermúdez-López et al., 2016). In accordance, mutations impairing either STR recruitment to DNA damaged sites or the Nse2-dependent Sgs1/BLM sumoylation significantly alter their recombinational repair functions resulting in the phenotypes described.

However, based on our results, we cannot affirm that the C-terminal helix participates in the ligase activity, as the sumoylation impairments shown by *nse2Δ29C* and *nse2Δ24C* mutants might be directly attributable to the low Nse2 protein levels. Although it would be very interesting to test the E3 activity of these mutants *in vitro*, we should also take into account that inactivation of the SIM at the end of the protein already lowers sumoylation (Figure 32C). So it is highly probable that truncation of a larger region will have similar effects.

Remarkably, although Nse2 might be destabilized in alpha-helix mutants, Smc5 protein levels are not altered (Figure 29A), suggesting that they do not affect the stability of the rest of the complex. This suggests that Nse2 might be degraded before reaching the Smc5/6 complex in *nse2Δ29C* and *nse2Δ24C* cells. However, we cannot exclude that mutant proteins are evicted from the complex if not properly folded. Quite surprisingly, these mutants still show basal Smc5 sumoylation levels (Figure 29D), what suggests the participation of other E3 ligases in Smc5 modification. In order to prove this, it would be interesting to remove Siz1 or Siz2 SUMO E3 ligases in these mutants and test their possible participation in Smc5 sumoylation. In relation to this, it is also possible that Smc5 sumoylation defects in *nse2* mutants might be due to a deficient recruitment of the Smc5/6 complex to chromatin. In accordance, we have seen in the first chapter that perturbing Smc5-DNA binding sensitizes cells to DNA damage and results in a reduction of the Nse2 E3 ligase activity (Varejão et al., 2018).

Interestingly, yeast cells carrying disruptions in their last 16 or 4 residues, *nse2Δ16C* and *nse2ΔSIM* mutants, did not affect Nse2 protein levels or Smc5 sumoylation levels, and did not present growth defects. Comparing the differences shown by *nse2Δ16C* cells and the phenotypic severity

of the *nse2Δ24C* mutant, which only lacks 8 more residues, we can affirm that the region between the two disruptions (from residue 245 to 253) is important for protein stability. In support of this hypothesis, an *nse2ΔRING* mutant, which conserves the last 24 residues, does not show diminished Nse2 protein levels. Moreover, this specific region shows higher conservation than the rest of the C-terminal alpha-helix, suggesting that it might mediate important protein-protein interactions (Figure 27). Specifically, and based on the conservation scores, we speculate that a short stretch of this alpha helix, located between L243 and I247, might mediate specific functions that guarantee the stability of the whole Nse2 protein.

Is the RING domain in Nse2 required for Smc5 sumoylation?

SUMO SP-RING domains bind to their corresponding E2 conjugating partners and position the Ubc9 E2 enzyme and the substrate in an adequate orientation for the SUMO transfer (Geiss-Friedlander & Melchior, 2007) (Yunus & Lima, 2009). Therefore, the removal of the RING domain, or its inactivation through point mutations, should completely abolish Nse2-dependent sumoylation.

The internal deletion of the entire RING domain in *nse2ΔRING* mutants, leads to a strong MMS sensitivity. Importantly, all RING mutants tested, including the *nse2ΔRING,* showed Nse2 protein levels similar to the wild type ones (Figures 29B, 31A). Therefore, and in contrast to the C-terminal alpha-helix, the RING is not required to maintain protein stability. This result indicates that RING domain functions might be restricted to facilitate sumoylation of chromosomal targets. In addition, our findings indicate that many of the *nse2ΔC* phenotypes may be due to the destabilization of the Nse2 protein, and not merely to the loss of the RING domain. Therefore, some of the functions that have been attributed to Nse2 using the *nse2ΔC* allele might not be due to defects in its E3 ligase activity. It is possible that such functions required the entire Nse2 protein, and therefore, were applicable to the whole Smc5/6 complex.

Interestingly, mutating the residues that coordinate the zinc atom of the RING domain of Nse2, in *nse2-C200,H202A,* and *nse2-C221A* cells, result in a similar MMS sensitivity as *nse2ΔRING* mutants. The four amino acids coordinating the zing ion, three cysteines (C200, C221, C226) and one histidine (H202), confer a common structure of SUMO E3s that is conserved in evolution and that might contribute to E2 recognition (Duan et al., 2009). Therefore, it is plausible that perturbing this E2-E3 interaction leads to strong sumoylation and cell growth defects. However, it is surprising that these mutants are unable to repair MMS damage while maintaining sumoylation of Smc5, which we have used as a proxy for SUMO ligase activity. One possible explanation could be that the single point mutants used do not completely abolish folding of the RING domain. In fact, mutation of the residues coordinating the zinc ion is insufficient for completely abolishing the E3 activity in some ligases (Garcia-Barcena et al., 2020). In addition, despite we did not detect changes in Smc5 sumoylation, it is possible that the effects might be more pronounced in other substrates. To corroborate this hypothesis in future experiments, it would be interesting to develop triple or quadruple mutations in the zinc-coordinating cysteines and histidines, to confirm

that the RING folding and the E2 interaction are completely defective, and to test sumoylation of other Nse2 targets.

Intriguingly, mutation of residues in the stabilizing motif (i.e., the double C184A P185A mutant) has a very mild effect in DNA damage sensitivity. It is possible that, despite their conservation, many other interactions stabilize this part of the SP-RING domain, maintaining an effective RING-E2 interaction. In relation to this, it would also be very interesting to disrupt the E2-RING interaction without affecting the structure and folding of the RING domain. The interaction of ubiquitin RING domains with E2 conjugating enzymes largely depends on a hydrophobic residue located between two cysteines coordinating the zinc atom (Garcia-Barcena et al., 2020). The equivalent conserved residue in SUMO E3 ligases is conserved and located in the loop that does not coordinate zinc, also known as stabilizing motif. Indeed, the *in vitro* activity of Nse2 substantially decreases when mutating isoleucine 186, suggesting that this should be a feasible way to inactivate the SUMO ligase activity *in vivo* (Duan et al., 2009).

A SIM-like motif in Nse2 might serve for proper Ubc9-SUMO positioning

The crystallographic structure of Nse2 shows an internal loop located immediately upstream of the RING domain, composed by 16 residues (from 160 to 176) with some evolutionary conserved residues. Both the mutation of just three of these conserved negative amino acids into arginines and the 16-residue loop deletion sensitized yeast cells to MMS (Figure 34C). However, these mutations neither compromised protein stability (Figure 34B) nor the Nse2-dependent sumoylation activity (Figures 32C *in vitro*, 34E *in vivo*). As Nse2-dependent Smc5-sumoylation appears to be upregulated by replication fork damage (Zapatka et al., 2019), we also studied if mutants in this loop are specifically impaired in sumoylation in response to MMS. However, our results revealed that loop mutants displayed similar levels of Smc5 sumoylation, relative to wild type cells. Thus, it seems that this loop is not directly involved in the activation of the Nse2-dependent SUMO ligase activity. But it may participate in general Smc5/6 functions at damaged forks. In fact, the accumulation of negative charges in this loop is evolutionary conserved, what might indicate an important role in protein-protein interactions. Negative to positive charge changes *(EDD-RRR)* in this region could disrupt interactions with other proteins or complexes involved in DNA damage repair, resulting in the MMS-sensitivity phenotypes observed, without altering the Nse2-sumoylation capacity. Another possibility is that the negative charges might help to direct Smc5/6-DNA interactions towards a different region, especially under conditions of DNA damage.

In contrast, mutating the glycine residue located after the loop domain of Nse2 into a proline, resulted in the reduction of the Nse2-dependent sumoylation activity *in vitro* (Figure 32C). Effects shown by the *G-P* mutant *in vitro* suggest that G177 in Nse2 might have equivalent functions to the SIM-like of Siz1, which helps to position Ubc9 favouring catalysis. In this regard, we have seen that G177 is located at the same position as the SIM-like element of Siz1, as shown in the superimposition model (Figure 33). Therefore, we suggest that this amino acid change in the *G-P*

mutant results in a structural change in Nse2 that might prevent E2 recognition or the SUMO transfer to the target protein *in vitro.* Indeed, colocalization of the G177 residue and the SIM-like of Siz1 when superimposing Nse2 and Siz1 RING domains and the decrease in sumoylation shown by the *G-P* mutant *in vitro* support this idea. However, *in vivo* experiments showed that this *G-P* mutant had no cell growth defects under MMS treatment (Figure 34C), nor Smc5 sumoylation impairments (Figure 34D). A possible explanation for this is that multiple redundant mechanisms may operate simultaneously *in vivo* for Smc5/6-dependent sumoylation.

Redundant mechanisms might provide Nse2 SUMO ligase activity in vivo

Our analysis indicates that all the Nse2 mutants tested (including alpha-helix, RING and loop mutants) still show basal Smc5 sumoylation. In some mutants, the alteration is undetectable under our experimental conditions when using Smc5 sumoylation as a reporter for SUMO ligase activity. This suggests that in a cellular context there might be redundant mechanisms to sumoylate Smc5, such as the interaction between the E2 conjugating enzyme and the RING domain of Nse2, the Ubc9 interaction with the SIM-like structure (probably corresponding to G177 in Nse2), or the interaction of the E2 with the C-terminal SIM domain. If so, this would indicate that all Nse2 sub-structures described here might participate in sumoylation. To prove this idea it would be ideal to combine mutations affecting more than one of these features and test their effect *in vivo*.

However, as already mentioned, another possibility is the implication of other E3 ligases in the sumoylation of Smc5. And an even more remote possibility that we currently cannot discard is that the Smc5/6 complex contains a second 'SUMO E3 ligase activity', different from the RING domain, able to bypass RING mutants *in vivo*. It is also worth noting that a mouse strain bearing point mutations in the RING domain did not have any noticeable phenotype (Jacome et al., 2015). According to our results in budding yeast, it is tempting to speculate that this mutant had no sumoylation defect in mouse cells.

5.3 Chapter III- Analysis of Nse1-ubiquitin ligase targets and functions on genome stability

A proteomic approach to identify potential ubiquitin targets of the Smc5/6 complex

In this study, we have analysed the function of the second RING domain in the Smc5/6 complex, located in the C-terminus of the Nse1 subunit, as a potential regulator of other cellular functions through ubiquitination. To this end, we have analysed and compared the nuclear ubiquitinome, using label-free proteomics, of wild type and *nse1* mutant cells affected in their RING domain.

Similar to the Nse2 subunit in Smc5/6, Nse1 contains a RING domain, suggesting a possible function as UBL E3 ligase. Indeed, human Nse1 has ubiquitin E3 ligase activity *in vitro*, and this activity is enhanced by the interaction with MAGE-G1, the mammalian ortholog of Nse3 (Doyle et al., 2010). Strikingly, this activity could not be detected in the fission yeast Nse1 protein (Pebernard, Perry, et al., 2008); and has never been analyzed in buddying yeast. In humans, the only substrate identified for Nse1 *in vivo* is Mms19, a cytosolic iron-sulfur assembly (CIA) component. Of note, this activity requires the formation of a complex between Nse1 and an alternative MAGE protein that has been reported to ubiquitinate Mms19 for its degradation (Weon et al., 2018). Thus, the only known target for Nse1 is ubiquitinated independently from the Smc5/6 complex. It is worth noting that the RING domain sequence in Nse1 differs in some key residues between humans and yeasts. The most critical residues involved in E2-RING interactions are an Ile residue located between the first two zinc-coordinating amino acids, and a Pro-Phe motif between the last two zinc-coordinating residues in the RING domain (Garcia-Barcena et al., 2020). While all of them are present in the human Nse1 RING (and vertebrates in general), the first one is occupied by Ala or Asp, and the second one by Ile-Asn or Asp-Arg in fission and budding yeast, respectively (Pebernard, Perry, et al., 2008). This suggests that the Nse1 RING may have adapted to ubiquitination recently in evolution; alternatively, yeast Nse1 may still interact with E2 enzymes, but the critical residues in the interaction may have mutated to promote a more specific binding to a particular E2 enzyme.

As mentioned, the enzymatic activity of Nse1 in buddying yeast remains to be confirmed. However, if Nse1 had E3 ligase activity, the identification of Nse1-ubiquitination targets would be of great interest. Thus, in order to study Nse1 as a possible ubiquitin ligase in *S. cerevisiae*, we performed a diGly proteomic screening and compared the ubiquitinome of wild type and *nse1-C274A* RING mutant cells. Remarkably, this mutation conferred cells sensitivity to DNA damage (Santa Maria et al., 2007). Therefore, in the case that these sensitivities were due to the loss of the Nse1 E3 ligase activity, we would observe reduced ubiquitination of Nse1-depedent targets. Accordingly, the diGly proteomics screening permitted us to identify a list of potential Nse1 substrates. This phenomenon could indicate that Nse1 has, in fact, ubiquitin ligase activity in budding yeast.

Other studies have also used this procedure to identify the targets of other E3 ligases. In this regard, key previous published diGly studies have been recently compiled by Fulzele and Bennett (Fulzele & Bennett, 2018). Overall, this technique has allowed to describe more than 50.000

ubiquitination sites in human cells and it has led to the identification of specific ubiquitin ligase targets (Fulzele & Bennett, 2018). In addition, one of the advantages of diGly proteomics is that apart from quantifying the global ubiquitinome, it identifies the target lysines. On the other hand, our screening also presented some limitations. First, we performed a nuclei fractionation to reduce the complexity of the sample and facilitate its analysis, what could prevent the detection of possible ubiquitin targets outside the nuclei. Second, one needs to take into account that there might be ubiquitinated peptides difficult to detect by mass spectrometry; consequently, the global ubiquitinome quantification might be underestimated. Finally, as we did a label-free quantification, and wild type and mutant samples were not analysed at the same time, there might be increased variability among samples.

When analysing the network of potential Nse1 targets, we found three defined functional clusters: a group of proteins related with glycolysis, RNA Pol I subunits, and an important cluster of ribosomal proteins. Globally, it seems that the entire ribosome synthesis pathway could be less ubiquitinated in the *nse1* mutant; including RNA Pol I subunits, RNA processing elements and ribosomal proteins. Interestingly, these data suggests a potential role for Nse1 in rRNA biogenesis. This is in concordance with the previously reported nuclear accumulation of ribosome subunits and the reduced rRNA production exhibited by both *smc5/6* and *nse2ΔRING* mutants (D. H. Kim et al., 2016), maybe due to the loss of the Nse1 E3 ligase activity. Accordingly, strong cell growth impairments shown by *nse1* mutant cells could be due to alterations in ribosomal biogenesis.

On the other hand, previous studies have also established a connection between the Smc5/6 complex and carbon metabolism (Simpson-Lavy et al., 2015), what could explain the appearance of a cluster of proteins with enriched functions on glycolysis. Moreover, as already mentioned in Chapter II, hypomorphic *NSMCE2* mutations identified in two patients have been related with a human syndrome linked to dwarfism, insulin resistance and severe metabolic abnormalities (Payne et al., 2014). Altogether, these data suggests a role for the Smc5/6 complex in the regulation of metabolic processes through alteration of the ubiquitination status of specific proteins.

A shortlist of potential Nse1 targets

In this thesis, we have focused our attention on proteins identified in the diGly proteomics screening that appeared to be significantly less ubiquitinated in the *nse1-C274A* mutant, and that are involved in DNA replication and repair, cell division or in the maintenance of chromosomal stability. We selected *POL30, CDC48*, *NOP1* or *RPA190* as potential Nse1 targets, and validated them in ubiquitin pull down experiments.

One of the targets exhibiting a higher difference between wild type and mutant *nse1* cells is Lys 164 in PCNA, named Pol30 in budding yeast. PCNA is known to be monubiquitinated at K164 by Rad6-Rad18 and further polyubiquitinated with K63-linked ubiquitin chains by Mms2-Ubc13-Rad5 (Hoege et al., 2002). PCNA-mono-ubiquitination enables DNA replication at damaged forks by recruiting translesion synthesis polymerases (Wit et al., 2015), while PCNA polyubiquitination

promotes template switch behind the fork, to promote bypass of lesions on the template (W. Zhang et al., 2011). We have seen that PCNA mono- and polyubiquitination decrease in *nse1* RING mutants (Figure 39A). Thus, one possible explanation is that Nse1 acts redundantly with Rad18 or Rad5 in ubiquitination of PCNA. However, deletion of *MMS2* completely abolish PCNA polyubiquitination, suggesting that Nse1 may play an indirect role in Pol30 ubiquitination; maybe by regulating the other E2 or E3 ligases involved in PCNA modification, or by altering the conformation of damaged replication forks. According to this hypothesis, Smc5/6 would reconfigure replication forks in an unknown way to prime activation of PCNA ubiquitination pathways (Wit et al., 2015). A role for Smc5/6 at damaged forks is supported by various observations. First, the Smc5/6 complex binds to stalled forks (Irmisch et al., 2009). Besides, the Smc5 subunit in the complex directly binds and inhibits the Mph1 fork reversal enzyme, which is supposed to promote template switch in a Rad5-independent manner (Y. H. Chen et al., 2009) (Xue et al., 2014). In addition, Smc5 is sumoylated in response to damaged forks to promote error-free bypass of the lesion (Zapatka et al., 2019). Coincidently, the Smc5/6 complex is also required to restart stalled replication forks at DNA lesions by recruiting HR initiators (Irmisch et al., 2009). Therefore, a dysfunctional Nse1 subunit may alter Smc5/6 functions and chromatin structure upon genotoxic treatments; which could subsequently impair activation of lesion bypass through PCNA ubiquitination. It is also worth mentioning that the Rad18 ubiquitin ligase interacts with the Nse5-Nse6 homologs in *Xenopus*, thus recruiting the Smc5/6 complex to stalled forks (Räschle et al., 2015). This suggests that there might be a direct link between the Smc5/6 complex and the enzymes responsible for PCNA ubiquitination.

Another potential Nse1 ubiquitin target identified was Cdc48 (Figure 39B). Cdc48 is a ubiquitin-dependent chaperone that binds to ubiquitinated substrates and mediates their displacement from molecular complexes or membranes, often facilitating their proteasomal degradation (Olszewski et al., 2019). Cdc48 also extracts complexes from chromatin. For example, Cdc48 mobilizes ubiquitinated condensin from chromatin. When chromatin is compacted and remodelled by condensin, chromatid accessibility is lost. Therefore, reorganization of chromatin needs to be tightly regulated. In this regard, it has been recently reported that condensin unloading from chromatin entrapment is mediated by the Cdc48 segregase (Thattikota et al., 2018). *In vivo* ubiquitination of condensin triggers Cdc48-dependent release from the condensed chromatin, to allow a new compaction cycle. In addition, apart from condensin, Cdc48 has also been described to promote cohesin unloading from chromatin. Thus, during S-pahse, replication forks encounter chromatin-bound cohesin complexes that have to be removed to enable fork progression. In this regard, it has been recently reported that Cdc48 mediates the cohesin unloading from chromatin entrapment in an ubiquitin-dependent manner, thus providing structural stability to stalled forks (Frattini et al., 2017).

Several post-translational modifications have been reported to modulate the activity or localization of Cdc48, like phosphorylation or acetylation (Baek et al., 2013). In addition, other studies suggest that Cdc48 may also be sumoylated (Wohlschlegel et al., 2004) or ubiquitinated (J. Peng et al., 2003); but the functional purpose of these modifications remains unknown. Our pull-down experiments confirmed the partial dependence of Cdc48 ubiquitination on Nse1. However,

we have seen that such modifications do not completely disappear in *nse1* RING mutants. Thus, other E3 ligases might support the basal Cdc48 ubiquitination levels in *nse1* mutants. In addition, it is worth noting that the *nse1* mutants used in proteomics and in pull-down experiments were different, and although both of them are predicted to disrupt the proper folding of the RING domain, they might differently impair its potential E3 ligase activity.

Conversely, Nop1-ubiquitiation detected by pull-down experiments was very low in comparison with other potential Nse1 targets. Nevertheless, proteomics results and the slight decrease in ubiquitinated Nop1 forms in mutant cells suggest that such modifications could partially depend on the E3 ligase activity of Nse1 (Figure 39C). Nop1 functions as a nucleolar RNA processor that triggers the pre-rRNA processing necessary to achieve an optimal ribosomal biogenesis (D. Tollervey et al., 1991). Therefore, reduced Nop1 ubiquitination could impair ribosomal biogenesis, which might correlate with the cell proliferation defects shown by *nse1-HC* mutants.

Finally, one key aspect that needs to be taken into consideration is that the *nse1-HC* mutants used for the proteomics validations have low levels of Nse1 protein as well as of other subunits of the complex (unpublished observations). Therefore, defects shown by this RING mutant might be due to the absence of Nse1 and to insufficient levels of Smc5/6, rather than to its incapacity to ubiquitinate protein substrates. In addition, it is also possible that Nse1 might be indirectly upregulating their ubiquitination. Some of the proteins less ubiquitinated in *nse1* RING mutants are targets of the Ubp10 deubiquitinase, like PCNA (Gallego-Sánchez et al., 2012), or Rpa190 (Richardson et al., 2013). Therefore, an alternative hypothesis is that the destabilization of Nse1 and Smc5/6 could lead to an overactivation of Ubp10, resulting in deubiquitination of Ubp10 targets. In fact, all the targets we have validated showed residual ubiquitination in the *nse1* mutant. Thus, it is formally possible that they are not direct Nse1 targets, as discussed above for PCNA. Indeed, we should consider three different options for how Nse1 might affect ubiquitination of these proteins. First, they are direct Nse1 targets, but other E3 ligases are able to ubiquitinate the same lysine. This would indicate that their ubiquitination is only partially dependent on Nse1. Second, they are direct Nse1 targets, but are also modified by another E3 ligase on a different lysine residue. Thus, ubiquitination could be maintained on one site and be only affected on a secondary Nse1-dependent site. The presence of two different targeted lysine residues may not be easily detectable in ubiquitin pull downs, specially if they induce a similar electrophoretic mobility shift in western blots, and would probably require the analysis of proteins mutated in the specific Nse1-dependent residues. Third, they could be indirect Nse1 targets, depending on other E3 ligases. In this case, alterations in Nse1 (or Smc5/6) functions might indirectly decrease their ubiquitination.

A role for Rpa190 ubiquitination in transcriptional elongation

To understand the role of Rpa190 ubiquitination we first tried to find specific situations that led to an increase in Rpa190 ubiquitination levels. Usually, in response to stress or to sudden changes in growth conditions, cells react at the transcriptional level to adapt to the new situation. In addition,

they usually stop rRNA transcription to save energy. Knowing this, we tested whether any of these conditions changed Rpa190 ubiquitination. First, we focused on DNA damage, as the Smc5/6 complex has been widely described to participate in DNA repair. However, none of the DNA damaging agents tested caused alterations in Rpa190 ubiquitination. In contrast, our results showed that amino acid starvation dramatically decreases Rpa190 ubiquitination (Figure 41C). In this regard, it has been previously described that limited nutrient availability causes a reduction in rRNA synthesis (Grummt, 2013). This decrease is due to the proteasomal degradation of Rrn3, the transcription factor that recruits Pol I to the rDNA promoter to enable transcription initiation (Philippi et al., 2010). Therefore, when Pol I transcription initiation ceases due to reduced nutrient availability, Rpa190 is no longer ubiquitinated. From these results we can conclude that Rpa190 ubiquitination requires active RNA Pol I transcription. Accordingly, we have seen that Rpa190 is mainly ubiquitinated on chromatin (Figure 47). In fact, this was previously reported by Wei and collaborators, who demonstrated that Rpa190 needs to be active and previously loaded onto chromatin for being ubiquitinated (Wei et al., 2018).

In contrast to the previously mentioned genotoxic conditions tested, our results show that blocking Rpa190 ubiquitination becomes harmful in cells treated with 6-azauracil (Figure 44B); suggesting that this modification is required for Pol I transcriptional elongation. In addition, analysis of double *rpa190-KR* and *ubp10Δ* mutants suggest that ubiquitination of lysines K408 and K410, which seem to be the major ubiquitin acceptors in Rpa190, is used to target Rpa190 for degradation (Figure 43). In this regard, Rpa190 ubiquitination has been previously related to its proteasomal destruction (Richardson et al., 2013) (Wei et al., 2018).

Interestingly, a similar (or even aggravated) 6-AU sensitivity phenotype is shown by *cdc48* and *smc5/6* mutants (Figures 52 and 50). These results suggest that the Smc5/6 complex and the Cdc48 segregase may affect RNA Pol I activity, as their dysfunctionality compromises cell viability in the presence of 6-AU. Nevertheless, it has to be remarked that 6-AU is not a specific Pol I inhibitor, and the sensitivities observed might arise from transcriptional problems in other polymerases.

BMH-21 in contrast, is a specific inhibitor of RNA Pol I. Although its mechanism of action remains to be further elucidated, it is believed to bind G-C rich areas at the rDNA and to cause Pol I unloading from chromatin and subsequent ubiquitin-dependent Rpa190 degradation (Peltonen et al., 2014). Interestingly, we have seen that *rpa190-KR* mutants are resistant to BMH-21 (Figure 45). In addition, the BMH-21 resistance phenotypes shown by *cdc48* mutants are again relevant, and indicate their requirement for Rpa190 ubiquitination.

In turn, the role of the Cdc48 segregase in this process needs to be further studied. One possible explanation for *cdc48* mutant resistance to BMH-21 is that mutant cells cannot extract ubiquitinated Pol I complexes from chromatin, becoming insensitive to BMH-21. However, we have also observed that Rpa190 ubiquitination is severely impaired in *cdc48* mutant cells (Figure 51), what might not fit with problems in extraction of ubiquitinated Rpa190 from chromatin. In addition, Rpa190 levels on chromatin are reduced in *cdc48* mutant cells (Figure 54). Thus, the most parsimonious explanation for the *cdc48* mutant phenotypes is that Cdc48 is required for Pol I

loading onto chromatin, probably leading to lower transcription levels. In accordance, mutation of the Pol I preinitiator complex rescues cells from BMH-21-promoted Rpa190 degradation (Wei et al., 2018); meaning that such degradation requires the efficient loading of Pol I onto the rDNA. This does not discard a later role for Cdc48 in extraction of ubiquitinated Pol I from chromatin, as occurs in the ubiquitinated cohesin and condensin complexes (Frattini et al., 2017) (Thattikota et al., 2018). Overall, our data suggest that Cdc48 has an important role in permitting RNA Pol I loading onto the rDNA or subsequent transcription initiation. In fact, Cdc48 plays a multifaceted role in controlling transcriptional processes. In plants, for example, Cdc48 has a role in descondensing centromeric heterochromatin at the rDNA loci, thus facilitating Pol I transcription (Mérai et al., 2014).

Finally, a possible role for the ubiquitination of Rpa190 in promoting its removal from chromatin is supported by chromosome spread experiments. In this regard, we have seen that the Rpa190-KR mutant protein, which is refractory to ubiquitination, accumulates on chromatin in significantly higher levels than wild type Rpa190 (Figure 48). Interestingly, the effects of BMH-21 treatment in wild type and in *rpa190-KR* cells are also different. As expected, BMH-21 reduces the amount of Rpa190 on chromatin in wild type cells, in accordance with previous reports (Peltonen et al., 2014). However, BMH-21 is unable to promote Rpa190 ubiquitination in *rpa190-KR* cells and, consequently, Rpa190 levels on chromatin remain stable.

Thus, in normal conditions, Rpa190 ubiquitination might regulate cessation of Pol I transcription. The resistance of *rpa190-KR* cells to BMH-21, which has been proposed as a tool to treat cancer cells, opens the question about what is the nature of the problem generated by this inhibitor. BMH-21 has been proposed to physically block transcriptional elongation by Pol I (Peltonen et al., 2014). However, the resistance of non-ubiquitinable *rpa190-KR* mutants (as well as *cdc48* mutants) suggest that the sensitivity of wild type cells is primarily due to Rpa190 ubiquitination and destruction, and not to a transcriptional blockage. As yeast and human cells are equipped with a mechanism to ubiquitinate and degrade Rpa190, analysis of the physiological situations and mechanisms that trigger Pol I ubiquitination will be of great interest.

RNA polymerase I as a potential target of Smc5/6-dependent ubiquitination

Based on proteomics results and in accordance with pull-down experiments performed with different Smc5/6 mutant strains, we postulate that the largest subunit of RNA Pol I is ubiquitinated in an Nse1-dependent manner at lysines K408 and K410. In fact, the ubiquitin-dependent regulation of RNA Pol I, and specifically of its largest subunit, has already been described (Richardson et al., 2013). However, the ubiquitin ligase activity involved in this process and its molecular effects remain unknown. Smc5/6 and RNA Polymerase I show some interesting connections. First, both of them bind to the rDNA array (Torres-Rosell et al., 2005) (Russell & Zomerdijk, 2006); besides, Pol I is sumoylated in an Nse2-dependent manner (Albuquerque et al., 2013); in addition, inactivation of Pol I partially relieves the rDNA missegregation phenotype of *smc5/6* mutants (Torres-Rosell, De Piccoli, et al., 2007).

In this thesis we have strengthened these links by showing that Rpa190 ubiquitination is grossly Nse1- and Smc5/6-dependent. Accordingly, we have seen that not only *nse1* mutants, but also cells with a conditionally-depleted expression of Smc6 showed reduced ubiquitination of Rpa190 (Figure 40C). Moreover, perturbing the Nse2 E3 ligase activity also leads to a decrease in Rpa190 ubiquitination (Figure 49B). We would like to note that in this case we used the *nse2ΔC* allele, which shows very low levels of the Nse2 protein and might more properly reflect a situation with defective Smc5/6 function (Figure 29A). Interestingly, we and others have observed that Pol I sumoylation depends on Nse2 (Figure 49A) (Albuquerque et al., 2013). Therefore, it is possible that Pol I sumoylation might prime its subsequent ubiquitination. As *rpa190-KR* mutants maintain Rp190 sumoylation, SUMO and ubiquitin probably target different lysines in Rpa190. Overall, these results confirm that Rpa190 ubiquitination requires an integer Smc5/6 complex.

One intriguing aspect of our analysis is that, although both *smc5/6* and *rpa190-KR* mutants show similar phenotypes in response to transcription inhibitors, being sensitive to 6-azauracile (Figures 44B, 45), *rpa190-KR* mutants are generally healthy and do not exhibit any other phenotype in common with Smc5/6 mutants (Figure 44A). However, it is worth noting that our proteomic analysis also revealed other subunits in Pol I as being significantly less ubiquitinated in extracts from *nse1-C274A* mutant cells. For example, Rpc19, a subunit shared by Pol I and Pol III, showed lower ubiquitination on two different sites (with 3.5 and 2.6 fold reduction) in *nse1* mutant, relative to wild type extracts. In comparison, quantification of Rpa190 ubiquitination at both K408 and K410 was reduced 2.8 fold in *nse1* mutant extracts, according to the mass spectrometry data. In addition, the Rpa34 and Rpa43 subunits were also less ubiquitinated in *nse1* mutants, although to a lower extent (1.4 and 1.7 fold reduction, respectively). Moreover, our proteomic screen allowed us to identify 5 additional ubiquitination sites under-ubiquitinated in *nse1* mutants (two sites in Rpa190 and one in Rpa135, Rpb5 and Rpb10), although quantifications did not reveal statistically significant differences between wild type and mutant extracts at these sites. Therefore, we currently cannot exclude that other ubiquitinated lysines also participate in Pol I regulation. In conclusion, if ubiquitin redundantly targets multiple lysines in Pol I, the modification of other lysines in the polymerase may be masking the phenotype of *rpa190-KR* cells. Thus, it would be interesting to study a Pol I complex with K-R mutations in all the Nse1-dependent target lysines. We predict that this mutant will evidence a more direct connection to Smc5/6-dependent functions.

The pertinent question here is why does the Smc5/6 complex regulate Pol I ubiquitination? Although we do not have the answer yet, it might be related to the fact this modification helps to discharge Pol I from chromatin. As ongoing transcription by Pol I complexes may hinder DNA replication and repair processes, Smc5/6 might promote Pol I ubiquitination to clear it from chromatin and allow completion of crucial DNA transactions, including rDNA replication and resolution. This would enable Smc5/6 to properly organize the rDNA array for its proper segregation in anaphase, thus helping to maintain the integrity of the genome.

CONCLUSIONS

6. CONCLUSIONS

First. A positively-charged patch in Smc5 is required for repair of alkylation damage in budding yeast.

Second. Lysines K743 and K745 constitute the minimal DNA sensor in the Smc5 ARM, regulating the SUMO ligase activity of Nse2.

Third. The DNA sensor in Smc5 is required for efficient sumoylation of Smc5 and the Sgs1 helicase.

Fourth. Mutation of the minimal DNA sensor in Smc5 diminishes sumoylation without impairing the stability of the Smc5/6 complex or its loading onto chromatin.

Fifth. The C-terminal α-helix in Nse2 is essential to maintain Nse2 protein levels.

Sixth. Truncation of the last 24 amino acids in Nse2 has similar effects in Nse2 protein levels, Smc5 sumoylation and MMS sensitivity as eliminating the entire C-terminal domain.

Seventh. Mutations in the RING domain of Nse2 sensitize cells to alkylation damage without affecting Nse2 protein levels or Smc5 sumoylation.

Eighth. The C-terminal SIM and the Gly177 residue in the SIM-like motif of Nse2 are not required for repair of replication fork damage.

Ninth. Mutations in the RING domain, the C-terminal SIM and the G177 residue in the SIM-like motif individually diminish the E3 ligase activity of Nse2 *in vitro*.

Tenth. Mutations in the loop connecting the N-terminal and RING domains in Nse2 sensitize yeast cells to DNA damage without affecting the E3 ligase activity *in vitro* or *in vivo*.

Eleventh. The ubiquitination of Pol30, Cdc48 and Nop1 depends, to distinct degrees, on a functional RING domain in Nse1.

Twelfth. Rpa190 ubiquitination levels are diminished in mutants affecting the Smc5/6 complex, including mutations in the RING domain of Nse1 or Nse2.

Thirteenth. Rpa190 ubiquitination requires an active RNA Pol I transcription and drops during amino acid starvation.

Fourteenth. Rpa190 ubiquitination occurs mainly at lysines K408 and K410.

Fifteenth. Non-ubiquitinable *rpa190-KR* mutants are sensitive to the general transcription inhibitor 6-azauracil and resistant to the specific Pol I inhibitor BMH-21.

Sixteenth. The hyperubiquitination and protein instability of Rpa190 in *ubp10Δ* can be bypassed by expression of a non-ubiquitinable *rpa190-K408,410R* mutant.

Seventeenth. The increased sensitivity of *ubp10Δ* mutants to BMH-21 can be bypassed by expression of the non-ubiquitinable *rpa190-KR* mutant allele.

Eighteenth. The mutant Rpa190-KR protein is resistant to chromatin unloading upon treatment with BMH-21.

Nineteenth. *smc5/6* mutants are sensitive to 6-azauracil; and *cdc48* mutants are resistant to BMH-21 and sensitive to 6-azauracil.

Twentieth. *cdc48* mutants display impaired Rpa190 ubiquitination and binding to chromatin.

BIBLIOGRAPHY

7. BIBLIOGRAPHY

Akamatsu, Y., & Kobayashi, T. (2015). The Human RNA Polymerase I Transcription Terminator Complex Acts as a Replication Fork Barrier That Coordinates the Progress of Replication with rRNA Transcription Activity. *Molecular and Cellular Biology*, *35*(10), 1871–1881. https://doi.org/10.1128/mcb.01521-14

Akutsu, M., Dikic, I., & Bremm, A. (2016). Ubiquitin chain diversity at a glance. *Journal of Cell Science*, *129*(5), 875–880. https://doi.org/10.1242/jcs.183954

Albert, B., Léger-Silvestre, I., Normand, C., Ostermaier, M. K., Pérez-Fernández, Panov, K. I., Zomerdijk, J. C. B. M., Schultz, P., & Gadal, O. (2011). RNA polymerase I-specific subunits promote polymerase clustering to enhance the rRNA gene transcription cycle. *Journal of Cell Biology*, *192*(2), 277–293. https://doi.org/10.1083/jcb.201006040

Albert, B., Perez-Fernandez, J., Léger-Silvestre, I., & Gadal, O. (2012). Regulation of Ribosomal RNA Production by RNA Polymerase I: Does Elongation Come First? *Genetics Research International*, *2012*, 1–13. https://doi.org/10.1155/2012/276948

Albuquerque, C. P., Wang, G., Lee, N. S., Kolodner, R. D., Putnam, C. D., & Zhou, H. (2013). Distinct SUMO Ligases Cooperate with Esc2 and Slx5 to Suppress Duplication-Mediated Genome Rearrangements. *PLoS Genetics*, *9*(8). https://doi.org/10.1371/journal.pgen.1003670

Almedawar, S., Colomina, N., Bermudez-Lopez, M., Pociño, I., & Torres-Rosell, J. (2012). A SUMO-Dependent Step during Establishment of Sister Chromatid Cohesion. *Current Biology*, *22*(17), 1576–1581. https://doi.org/10.1016/j.cub.2012.06.046

Alt, A., Dang, H. Q., Wells, O. S., Polo, L. M., Smith, M. A., McGregor, G. A., Welte, T., Lehmann, A. R., Pearl, L. H., Murray, J. M., & Oliver, A. W. (2017). Specialized interfaces of Smc5/6 control hinge stability and DNA association. *Nature Communications*, *8*. https://doi.org/10.1038/ncomms14011

Amerik, A. Y., & Hochstrasser, M. (2004). Mechanism and function of deubiquitinating enzymes. *Biochimica et Biophysica Acta*, *1695*, 189–207. https://doi.org/10.1016/j.bbamcr.2004.10.003

Andrews, Palecek, J., Sergeant, J., Taylor, E., Lehmann, A. R., & Watts, F. Z. (2005). Nse2, a Component of the Smc5-6 Complex, Is a SUMO Ligase Required for the Response to DNA Damage. *Molecular and Cellular Biology*, *25*(1), 185–196. https://doi.org/10.1128/MCB.25.1.185-196.2005

Andrews, W. J., Panova, T., Normand, C., Gadal, O., Tikhonova, I. G., & Panov, K. I. (2013). Old drug, new target: Ellipticines selectively inhibit RNA polymerase I transcription. *Journal of Biological Chemistry*, *288*(7), 4567–4582. https://doi.org/10.1074/jbc.M112.411611

Aneeshkumar G. Arimbasseri, Keshab Rijal, and R. J. M. (2013). Transcription termination by the eukaryotic RNA Polymerase III. *Biochimica et Biophysica Acta*, *1829*(3–4), 318–330. https://doi.org/10.1016/j.bbagrm.2012.10.006.Transcription

Aragón, L. (2018). The Smc5/6 Complex: New and Old Functions of the Enigmatic Long-Distance Relative. *Annual Review of Genetics*, *52*(1), 89–107. https://doi.org/10.1146/annurev-genet-120417-031353

Arumugam, P., Gruber, S., Tanaka, K., Haering, C. H., Mechtler, K., & Nasmyth, K. (2003). ATP Hydrolysis Is Required for Cohesin's Association with Chromosomes. *Current Biology*. https://doi.org/10.1016/j.cub.2003.10.036

Baek, G. H., Cheng, H., Choe, V., Bao, X., Shao, J., Luo, S., & Rao, H. (2013). Cdc48: A Swiss Army Knife of Cell Biology. *Journal of Amino Acids*, *2013*, 1–12. https://doi.org/10.1155/2013/183421

Baker, R. T., Tobias, J. W., & Varshavskyll, A. (1992). Ubiquitin-specific Proteases of Saccharomyces cerevisiae. *The Journal of Biologcal Chemistry*, *267*(32), 23364–23375.

Ben-shahar, T. R., Heeger, S., Lehane, C., East, P., Flynn, H., Skehel, M., & Uhlmann, F. (2008). Eco1-Dependent Cohesin Sister Chromatid Cohesion. *Science (New York, N.Y.)*, *321*(July), 563–566. https://doi.org/10.1126/science.1157774

Bermudez-Lopez, M., Ceschia, A., de Piccoli, G., Colomina, N., Pasero, P., Aragon, L., & Torres-Rosell, J. (2010). The Smc5/6 complex is required for dissolution of DNA-mediated sister chromatid linkages. *Nucleic Acids Research*, *38*(19), 6502–

6512. https://doi.org/10.1093/nar/gkq546

Bermúdez-López, M., Pociño-Merino, I., Sánchez, H., Bueno, A., Guasch, C., Almedawar, S., Bru-Virgili, S., Garí, E., Wyman, C., Reverter, D., Colomina, N., & Torres-Rosell, J. (2015). ATPase-Dependent Control of the Mms21 SUMO Ligase during DNA Repair. *PLOS Biology*, *13*(3), e1002089. https://doi.org/10.1371/journal.pbio.1002089

Bermúdez-López, M., Villoria, M. T., Esteras, M., Jarmuz, A., Torres-Rosell, J., Clemente-Blanco, A., & Aragon, L. (2016). Sgs1's roles in DNA end resection, HJ dissolution, and crossover suppression require a two-step SUMO regulation dependent on Smc5/6. *Genes and Development*, *30*(11), 1339–1356. https://doi.org/10.1101/gad.278275.116

Bermúdez, M., & Aragón, L. (2017). Smc5/6 complex regulates Sgs1 recombination functions. *Current Genetics*, *63*(3), 381–388. https://doi.org/10.1007/s00294-016-0648-5

Birch, J. L., Tan, B. C. M., Panov, K. I., Panova, T. B., Andersen, J. S., Owen-Hughes, T. A., Russell, J., Lee, S. C., & Zomerdijk, J. C. B. M. (2009). FACT facilitates chromatin transcription by RNA polymerases i and III. *EMBO Journal*, *28*(7), 854–865. https://doi.org/10.1038/emboj.2009.33

Bonner, J. N., Choi, K., Xue, X., Torres, N. P., Szakal, B., Wei, L., Wan, B., Arter, M., Matos, J., Sung, P., Brown, G. W., Branzei, D., & Zhao, X. (2016). Smc5/6 Mediated Sumoylation of the Sgs1-Top3-Rmi1 Complex Promotes Removal of Recombination Intermediates. *Cell Reports*, *16*(2), 368–378. https://doi.org/10.1016/j.celrep.2016.06.015

Borden, K. L. B. (2000). Ring domains: Master builders of molecular scaffolds? *Journal of Molecular Biology*, *297*(4), 1027. https://doi.org/10.1006/jmbi.2000.3661

Branzei, D., Sollier, J., Liberi, G., Zhao, X., Maeda, D., Seki, M., Enomoto, T., Ohta, K., & Foiani, M. (2006). Ubc9- and Mms21-Mediated Sumoylation Counteracts Recombinogenic Events at Damaged Replication Forks. *Cell*, *127*, 509–522. https://doi.org/10.1016/j.cell.2006.08.050

Buetow, L., Huang, D. T., & Es, R. (2018). Structural insights into the catalysis and regulation of E3 ubiquitin ligases. *Nat Rev Mol Cell Biol.*, *17*(10), 626–642. https://doi.org/10.1038/nrm.2016.91.Structural

Bürmann, F., Basfeld, A., Vazquez Nunez, R., Diebold-Durand, M.-L., Wilhelm, L., & Gruber, S. (2017). Tuned SMC Arms Drive Chromosomal Loading of Prokaryotic Condensin. *Molecular Cell*, *65*(5), 861-872.e9. https://doi.org/10.1016/J.MOLCEL.2017.01.026

Bustard, D. E., Menolfi, D., Jeppsson, K., Ball, L. G., Dewey, S. C., Shirahige, K., Sjögren, C., Branzei, D., & Cobb, J. A. (2012). During replication stress, non-Smc element 5 (Nse5) is required for Smc5/6 protein complex functionality at stalled forks. *Journal of Biological Chemistry*, *287*(14), 11374–11383. https://doi.org/10.1074/jbc.M111.336263

Bylebyl, G. R., Belichenko, I., & Johnson, E. S. (2003). The SUMO Isopeptidase Ulp2 Prevents Accumulation of SUMO Chains in Yeast. *Journal of Biological Chemistry*, *278*(45), 44113–44120. https://doi.org/10.1074/jbc.M308357200

Chapard, C., Jones, R., van Oepen, T., Scheinost, J. C., & Nasmyth, K. (2019). Sister DNA Entrapment between Juxtaposed Smc Heads and Kleisin of the Cohesin Complex. *Molecular Cell*, *75*(2), 224-237.e5. https://doi.org/10.1016/j.molcel.2019.05.023

Chen, H. T., & Hahn, S. (2004). Mapping the location of TFIIB within the RNA polymerase II transcription preinitiation complex: A model for the structure of the PIC. *Cell*, *119*(2), 169–180. https://doi.org/10.1016/j.cell.2004.09.028

Chen, M., Rockel, T., Steinweger, G., Hemmerich, P., Risch, J., & Von, M. and A. (2002). Subcellular Recruitment of Fibrillarin to Nucleoplasmic Proteasomes: Implications for Processing of a Nucleolar Autoantigen. *Molecular Biology of the Cell*, *13*(June), 1977–2000. https://doi.org/10.1091/mbc.02

Chen, Y. H., Choi, K., Szakal, B., Arenz, J., Duan, X., Ye, H., Branzei, D., & Zhao, X. (2009). Interplay between the Smc5/6 complex and the Mph1 helicase in recombinational repair. *Proceedings of the National Academy of Sciences of the United States of America*, *106*(50), 21252–21257. https://doi.org/10.1073/pnas.0908258106

Cioci, F., Vu, L., Eliason, K., Oakes, M., Siddiqi, I. N., & Nomura, M. (2003). Silencing in yeast rDNA chromatin: Reciprocal relationship in gene expression between RNA polymerase I and II. *Molecular Cell*, *12*(1), 135–145. https://doi.org/10.1016/S1097-2765(03)00262-4

Clague, M. J., Coulson, J. M., & Urbé, S. (2012). Cellular functions of the DUBs. *Journal of Cell Science*, *124*, 277–286.

https://doi.org/10.1242/jcs.090985

Cubeñas-Potts, C., & Matunis, M. J. (2013). SUMO: a multifaceted modifier of chromatin structure and function. *Developmental Cell*, *141*(4), 520–529. https://doi.org/10.1016/j.surg.2006.10.010.Use

Cunniff, C., Bassetti, A., & Ellis, N. A. (2017). Bloom ' s Syndrome : Clinical Spectrum , Molecular Pathogenesis , and Cancer Predisposition. *Molecular Syndromology*, *10021*(8), 4–23. https://doi.org/10.1159/000452082

d'Azzo, A., Bongiovanni, A., & Nastasi, T. (2005). E3 ubiquitin ligases as regulators of membrane protein trafficking and degradation. *Traffic*, *6*(6), 429–441. https://doi.org/10.1111/j.1600-0854.2005.00294.x

Darrière, T., Pilsl, M., Sarthou, M. K., Chauvier, A., Genty, T., Audibert, S., Dez, C., Léger-Silvestre, I., Normand, C., Henras, A. K., Kwapisz, M., Calvo, O., Fernandez-Tornero, C., Tschochner, H., & Gadal, O. (2019). Genetic analyses led to the discovery of a super-active mutant of the RNA polymerase I. *PLoS Genetics*, *15*(5), 1–27. https://doi.org/10.1371/journal.pgen.1008157

De Piccoli, G., Cortes-Ledesma, F., Ira, G., Torres-Rosell, J., Uhle, S., Farmer, S., Hwang, J.-Y., Machin, F., Ceschia, A., McAleenan, A., Cordon-Preciado, V., Clemente-Blanco, A., Vilella-Mitjana, F., Ullal, P., Jarmuz, A., Leitao, B., Bressan, D., Dotiwala, F., Papusha, A., … Aragón, L. (2006). Smc5–Smc6 mediate DNA double-strand-break repair by promoting sister-chromatid recombination. *Nature Cell Biology*, *8*(9), 1032–1034. https://doi.org/10.1038/ncb1466

Decorsière, A., Mueller, H., Van Breugel, P. C., Abdul, F., Gerossier, L., Beran, R. K., Livingston, C. M., Niu, C., Fletcher, S. P., Hantz, O., & Strubin, M. (2016). Hepatitis B virus X protein identifies the Smc5/6 complex as a host restriction factor. *Nature*, *531*(7594), 386–389. https://doi.org/10.1038/nature17170

Deshaies, R. J., & Joazeiro, C. A. P. (2009). RING Domain E3 Ubiquitin Ligases. *Annual Review of Biochemistry*, *78*(1), 399–434. https://doi.org/10.1146/annurev.biochem.78.101807.093809

Dorsett, D., & Merkenschlager, M. (2013). Cohesin at active genes: a unifying theme for cohesin and gene expression from model organisms to humans. *Bone*, *23*(1), 1–7. https://doi.org/10.1038/jid.2014.371

Doyle, J. M., Gao, J., Wang, J., Yang, M., & Potts, P. R. (2010). MAGE-RING Protein Complexes Comprise a Family of E3 Ubiquitin Ligases. *Molecular Cell*, *39*(6), 963–974. https://doi.org/10.1038/s41395-018-0061-4.

Duan, X., Sarangi, P., Liu, X., Rangi, G. K., Zhao, X., & Ye, H. (2009). Structural and Functional Insights into the Roles of the Mms21 Subunit of the Smc5/6 Complex. *Molecular Cell*, *35*(5), 657–668. https://doi.org/10.1016/j.molcel.2009.06.032

Emre, N. C. T., Ingvarsdottir, K., Wyce, A., Wood, A., Krogan, N. J., Henry, K. W., Li, K., Marmorstein, R., Greenblatt, J. F., Shilatifard, A., Berger, S. L., & Louis, S. (2005). Maintenance of Low Histone Ubiquitylation by Ubp10 Correlates with Telomere-Proximal Sir2 Association and Gene Silencing. *Molecular Cell*, *17*, 585–594. https://doi.org/10.1016/j.molcel.2005.01.007

Endo, A., Matsumoto, M., Inada, T., Yamamoto, A., Nakayama, K. I., Kitamura, N., & Komada, M. (2009). Nucleolar structure and function are regulated by the deubiquitylating enzyme USP36. *Journal of Cell Science*, *122*(Pt 5), 678–686. https://doi.org/10.1242/jcs.044461

Fernández-Tornero, C., Moreno-Morcillo, M., Rashid, U. J., Taylor, N. M. I., Ruiz, F. M., Gruene, T., Legrand, P., Steuerwald, U., & Müller, C. W. (2013). Crystal structure of the 14-subunit RNA polymerase i. *Nature*, *502*(7473), 644–649. https://doi.org/10.1038/nature12636

Finley, D., Ulrich, H. D., Sommer, T., & Kaiser, P. (2012). The ubiquitin-proteasome system of Saccharomyces cerevisiae. *Genetics*, *192*(2), 319–360. https://doi.org/10.1534/genetics.112.140467

Fleming, A. B., Kao, C. F., Hillyer, C., Pikaart, M., & Osley, M. A. (2008). H2B Ubiquitylation Plays a Role in Nucleosome Dynamics during Transcription Elongation. *Molecular Cell*, *31*(1), 57–66. https://doi.org/10.1016/j.molcel.2008.04.025

Fousteri, M. I., & Lehmann, A. R. (2000). A novel SMC protein complex in Schizosaccharomyces pombe contains the Rad18 DNA repair protein. *The EMBO Journal*, *19*(7), 1691–1702. https://doi.org/10.1093/emboj/19.7.1691

Frattini, C., Villa-Hernández, S., Pellicanò, G., Jossen, R., Katou, Y., Shirahige, K., & Bermejo, R. (2017). Cohesin Ubiquitylation and Mobilization Facilitate Stalled Replication Fork Dynamics. *Molecular Cell*, *68*(4), 758-772.e4. https://doi.org/10.1016/j.molcel.2017.10.012

Fujioka, Y. (2002). Identification of a Novel Non-structural Maintenance of Chromosomes (SMC) Component of the SMC5-SMC6 Complex Involved in DNA Repair. *Journal of Biological Chemistry*, *277*(24), 21585–21591. https://doi.org/10.1074/jbc.M201523200

Fujioka, Y., Kimata, Y., Nomaguchi, K., Watanabe, K., & Kohno, K. (2002). Identification of a novel non-structural maintenance of chromosomes (SMC) component of the SMC5-SMC6 complex involved in DNA repair. *Journal of Biological Chemistry*, *277*(24), 21585–21591. https://doi.org/10.1074/jbc.M201523200

Fulzele, A., & Bennett, E. J. (2018). Ubiquitin diGLY proteomics as an approach to identify and quantify the ubiquitin-modified proteome. *Methods in Molecular Biology*, *1844*, 363–384. https://doi.org/10.1007/978-1-4939-8706-1_23

Gali, H., Juhasz, S., Morocz, M., Hajdu, I., Fatyol, K., Szukacsov, V., Burkovics, P., & Haracska, L. (2012). Role of SUMO modification of human PCNA at stalled replication fork. *Nucleic Acids Research*, *40*(13), 6049–6059. https://doi.org/10.1093/nar/gks256

Gallego-Sánchez, A., Andrés, S., Conde, F., San-Segundo, P. A., & Bueno, A. (2012). Reversal of PCNA ubiquitylation by Ubp10 in Saccharomyces cerevisiae. *PLoS Genetics*, *8*(7). https://doi.org/10.1371/journal.pgen.1002826

Garcia-Barcena, C., Osinalde, N., Ramirez, J., & Mayor, U. (2020). How to Inactivate Human Ubiquitin E3 Ligases by Mutation. *Frontiers in Cell and Developmental Biology*, *8*(February), 1–14. https://doi.org/10.3389/fcell.2020.00039

Gardner, R. G., Nelson, Z. W., & Gottschling, D. E. (2005). Ubp10/Dot4p Regulates the Persistence of Ubiquitinated Histone H2B: Distinct Roles in Telomeric Silencing and General Chromatin. *Molecular and Cellular Biology*, *25*(14), 6123–6139. https://doi.org/10.1128/mcb.25.14.6123-6139.2005

Gareau, J. R., & Lima, C. D. (2010). The SUMO pathway: emerging mechanisms that shape specificity, conjugation and recognition. *Nat Rev Mol Cell Biol.*, *11*(12), 861–871. https://doi.org/10.1038/nrm3011.The

Garvin, A. J., Morris, J. R., & Morris, J. R. (2017). SUMO , a small , but powerful , regulator of double-strand break repair. *Philosophical Transactions B*, *372*. https://doi.org/10.1038/nature08593

Geiss-Friedlander, R., & Melchior, F. (2007). Concepts in sumoylation: A decade on. *Nature Reviews Molecular Cell Biology*, *8*(12), 947–956. https://doi.org/10.1038/nrm2293

Goldstein, G., Scheid, M., Hammerling, U., Schlesinger, D. H., Niall, H. D., & Boyse, E. A. (1975). Isolation of a polypeptide that has lymphocyte differentiating properties and is probably represented universally in living cells. *Proceedings of the National Academy of Sciences of the United States of America*, *72*(1), 11–15. https://doi.org/10.1073/pnas.72.1.11

Grandi, P., Rybin, V., Baßler, J., Petfalski, E., Strauß, D., Marzioch, M., Schäfer, T., Kuster, B., Tschochner, H., Tollervey, D., Gavin, A. C., & Hurt, E. (2002). 90S pre-ribosomes include the 35S pre-rRNA, the U3 snoRNP, and 40S subunit processing factors but predominantly lack 60S synthesis factors. *Molecular Cell*, *10*(1), 105–115. https://doi.org/10.1016/S1097-2765(02)00579-8

Green, L. C., Kalitsis, P., Chang, T. M., Cipetic, M., Kim, J. H., Marshall, O., Turnbull, L., Whitchurch, C. B., Vagnarelli, P., Samejima, K., Earnshaw, W. C., Choo, K. H. A., & Hudson, D. F. (2012). Contrasting roles of condensin I and condensin II in mitotic chromosome formation. *Journal of Cell Science*, *125*, 1591–1604. https://doi.org/10.1242/jcs.097790

Groth, P., Ausländer, S., Majumder, M. M., Schultz, N., Johansson, F., Petermann, E., & Helleday, T. (2010). Methylated DNA Causes a Physical Block to Replication Forks Independently of Damage Signalling, O6-Methylguanine or DNA Single-Strand Breaks and Results in DNA Damage. *Journal of Molecular Biology*, *402*(1), 70–82. https://doi.org/10.1016/j.jmb.2010.07.010

Grubb, J., Brown, M. S., & Bishop, D. K. (2015). Surface spreading and immunostaining of yeast chromosomes. *Journal of Visualized Experiments*, *2015*(102), 1–8. https://doi.org/10.3791/53081

Grummt, I. (2013). The nucleolus - Guardian of cellular homeostasis and genome integrity. *Chromosoma*, *122*(6), 487–497. https://doi.org/10.1007/s00412-013-0430-0

Haas, A. L., & Rose, I. A. (1982). The Mechanism of Ubiquitin Activating. *The Journal of Biologcal Chemistry*, *257*(17), 10329–10337.

Haberle, V., & Stark, A. (2018). Eukaryotic core promoters and the functional basis of transcription initiation. *Nature Reviews Molecular*

Cell Biology, *19*(10), 621–637. https://doi.org/10.1038/s41580-018-0028-8

Hampsey, M. (1997). A review of phenotypes in Saccharomyces cerevisiae. *Yeast*, *13*(12), 1099–1133. https://doi.org/10.1002/(SICI)1097-0061(19970930)13:12<1099::AID-YEA177>3.0.CO;2-7

Hans C., L., Wang, H., Baladandayuthapani, V., Lin, H., He, J., Jones, J. R., Kuiatse, I., Gu, D., Wang, Z., Ma, W., Lim, J., O'Brien, S., Ketas, J., Yang, J., Davis, R. E., & Orlowski, R. Z. (2017). RNA Polymerase I Inhibition with CX-5461 as a Novel Therapeutic Strategy to Target MYC in Multiple Myeloma Hans. *British Journal of Haematology*, *177*(1), 80–94. https://doi.org/10.1111/bjh.14525.RNA

Hendriks, I. A., D'Souza, R. C. J., Yang, B., Verlaan-de Vries, M., Mann, M., & Vertegaal, A. C. O. (2014). Uncovering global SUMOylation signaling networks in a site-specific manner. *Nature Structural & Molecular Biology*, *21*(10), 927–936. https://doi.org/10.1038/nsmb.2890

Henras, A. K., Plisson-Chastang, C., O'Donohue, M. F., Chakraborty, A., & Gleizes, P. E. (2015). An overview of pre-ribosomal RNA processing in eukaryotes. *Wiley Interdisciplinary Reviews: RNA*, *6*(2), 225–242. https://doi.org/10.1002/wrna.1269

Herhaus, L., & Dikic, I. (2015). Expanding the ubiquitin code through post-translational modification. *EMBO Reports*, *16*(9), 1071–1083. https://doi.org/10.15252/embr.201540891

Hickey, C. M., Wilson, N. R., & Hochstrasser, M. (2012). Function and regulation of SUMO proteases. *Nature Reviews Molecular Cell Biology*, *13*(12), 755–766. https://doi.org/10.1038/nrm3478

Hirano, T. (2002). The ABCs of SMC proteins: two-armed ATPases for chromosome condensation, cohesion, and repair. *Genes & Development*, *16*(4), 399–414. https://doi.org/10.1101/gad.955102

Hirano, T. (2005). SMC proteins and chromosome mechanics: From bacteria to humans. *Philosophical Transactions of the Royal Society B: Biological Sciences*, *360*(1455), 507–514. https://doi.org/10.1098/rstb.2004.1606

Hirano, T. (2012). Condensins : universal organizers of chromosomes with diverse functions. *Genes & Development*, *26*, 1659–1678. https://doi.org/10.1101/gad.194746.112.GENES

Hoege, C., Pfander, B., Moldovan, G.-L., Pyrowolakis, G., & Jentsch, S. (2002). RAD6-dependent DNA repair is linked to modification of PCNA by ubiquitin and SUMO. *Nature*, *419*(6903), 135–141. https://doi.org/10.1038/nature00991

Holstege, F. C. P., Fiedler, U., & Timmers, H. T. M. (1997). Three transitions in the RNA polymerase II transcription complex during initiation. *EMBO Journal*, *16*(24), 7468–7480. https://doi.org/10.1093/emboj/16.24.7468

Hu, B., Liao, C., Millson, S. H., Mollapour, M., Prodromou, C., Pearl, L. H., Piper, P. W., & Panaretou, B. (2005). Qri2/Nse4, a component of the essential Smc5/6 DNA repair complex. *Molecular Microbiology*, *55*(6), 1735–1750. https://doi.org/10.1111/j.1365-2958.2005.04531.x

Hubert, J., Guyonvarch, A., Kammerer, B., Exinger, F., Liljelund, P., Lacroute, F., & Aramoylphosphate, C. (1983). Complete sequence of a eukaryotic regulatory gene. *The EMBO Journal*, *2*(I), 2071–2073.

Hudson, J. J. R., Bednarova, K., Kozakova, L., Liao, C., Guerineau, M., Colnaghi, R., Vidot, S., Marek, J., Bathula, S. R., Lehmann, A. R., & Palecek, J. (2011). Interactions between the Nse3 and Nse4 components of the SMC5-6 complex identify evolutionarily conserved interactions between MAGE and EID families. *PLoS ONE*, *6*(2). https://doi.org/10.1371/journal.pone.0017270

Iconomou, M., & Saunders, D. N. (2016). Systematic approaches to identify E3 ligase Substrates. *Biochemical Journal*, *473*(22), 4083–4101. https://doi.org/10.1042/BCJ20160719

Irmisch, A., Ampatzidou, E., Mizuno, K., O'Connell, M. J., & Murray, J. M. (2009). Smc5/6 maintains stalled replication forks in a recombination-competent conformation. *EMBO Journal*, *28*(2), 144–155. https://doi.org/10.1038/emboj.2008.273

Ishida, T., Yoshimura, M., Miura, K., & Sugimoto, K. (2012). MMS21/HPY2 and SIZ1, Two Arabidopsis SUMO E3 Ligases, Have Distinct Functions in Development. *PLoS ONE*, *7*(10), 1–10. https://doi.org/10.1371/journal.pone.0046897

Ivanschitz, L., De Thé, H., & Le Bras, M. (2013). PML, SUMOylation, and senescence. *Frontiers in Oncology*, *3 JUL*(July), 1–8. https://doi.org/10.3389/fonc.2013.00171

Iyer-Bierhoff, A., Krogh, N., Tessarz, P., Ruppert, T.,

Nielsen, H., & Grummt, I. (2018). SIRT7-Dependent Deacetylation of Fibrillarin Controls Histone H2A Methylation and rRNA Synthesis during the Cell Cycle. *Cell Reports*, *25*(11), 2946-2954.e5. https://doi.org/10.1016/j.celrep.2018.11.051

Jacome, A., Gutierrez-Martinez, P., Schiavoni, F., Tenaglia, E., Martinez, P., Rodriguez-Acebes, S., Lecona, E., Murga, M., Mendez, J., Blasco, M. A., & Fernandez-Capetillo, O. (2015). NSMCE2 suppresses cancer and aging in mice independently of its SUMO ligase activity. *The EMBO Journal*, *34*(21), 2604–2619. https://doi.org/10.15252/embj.201591829

Janke, C., Magiera, M. M., Rathfelder, N., Taxis, C., Reber, S., Maekawa, H., Moreno-Borchart, A., Doenges, G., Schwob, E., Schiebel, E., & Knop, M. (2004). A versatile toolbox for PCR-based tagging of yeast genes: New fluorescent proteins, more markers and promoter substitution cassettes. *Yeast*, *21*(11), 947–962. https://doi.org/10.1002/yea.1142

Jeppsson, K., Carlborg, K. K., Nakato, R., Berta, D. G., Lilienthal, I., Kanno, T., Lindqvist, A., Brink, M. C., Dantuma, N. P., Katou, Y., Shirahige, K., & Sjögren, C. (2014). The Chromosomal Association of the Smc5/6 Complex Depends on Cohesion and Predicts the Level of Sister Chromatid Entanglement. *PLoS Genetics*, *10*(10), e1004680. https://doi.org/10.1371/journal.pgen.1004680

Jeppsson, K., Kanno, T., Shirahige, K., & Sjögren, C. (2014). The maintenance of chromosome structure: positioning and functioning of SMC complexes. *Nature Reviews Molecular Cell Biology*, *15*(9), 601–614. https://doi.org/10.1038/nrm3857

Jonkers, I., & Lis, J. T. (2015). Getting up to speed with transcription elongation by RNA polymerase II. *Nature Reviews Molecular Cell Biology*, *16*(3), 167–177. https://doi.org/10.1038/nrm3953

Jürgen Dohmen, R. (2004). SUMO protein modification. *Biochimica et Biophysica Acta - Molecular Cell Research*, *1695*(1–3), 113–131. https://doi.org/10.1016/j.bbamcr.2004.09.021

Kanno, T., Berta, D. G., & Sjögren, C. (2015). The Smc5/6 Complex Is an ATP-Dependent Intermolecular DNA Linker. *Cell Reports*, *12*(9), 1471–1482. https://doi.org/10.1016/j.celrep.2015.07.048

Kara, B., Köroğlu, Ç., Peltonen, K., Steinberg, R. C., Maraş Genç, H., Hölttä-Vuori, M., Güven, A., Kanerva, K., Kotil, T., Solakoğlu, S., Zhou, Y., Olkkonen, V. M., Ikonen, E., Laiho, M., & Tolun, A. (2017). Severe neurodegenerative disease in brothers with homozygous mutation in POLR1A. *European Journal of Human Genetics*, *25*(3), 315–323. https://doi.org/10.1038/ejhg.2016.183

Keener, J., Josaitis, C. A., Dodd, J. A., & Nomura, M. (1998). Reconstitution of Yeast RNA Polymerase I Transcription in Vitro. *The Journal of Biologcal Chemistry*, *273*(50), 33795–33802.

Kegel, A., & Sjögren, C. (2010). The Smc5/6 complex: More than repair? *Cold Spring Harbor Symposia on Quantitative Biology*, *75*, 179–187. https://doi.org/10.1101/sqb.2010.75.047

Kegel, Andreas, Betts-Lindroos, H., Kanno, T., Jeppsson, K., Ström, L., Katou, Y., Itoh, T., Shirahige, K., & Sjögren, C. (2011). Chromosome length influences replication-induced topological stress. *Nature*, *471*(7338), 392–397. https://doi.org/10.1038/nature09791

Kerscher, O. (2016). SUMOylation. *ELS. John Wiley & Sons, Ltd: Chichester.*, 1–11. https://doi.org/10.1002/9780470015902.a0021849.pub2

Kerscher, Oliver. (2007). SUMO junction—what's your function? New insights through SUMO-interacting motifs. *EMBO Reports*, *8*(6), 550–555.

Kim, D. H., Harris, B., Wang, F., Seidel, C., McCroskey, S., & Gerton, J. L. (2016). Mms21 SUMO ligase activity promotes nucleolar function in Saccharomyces cerevisiae. *Genetics*, *204*(2), 645–658. https://doi.org/10.1534/genetics.115.181750

Kim, T. K., Ebright, R. H., & Reinberg, D. (2000). Mechanism of ATP-dependent promoter melting by transcription factor IIH. *Science*, *288*(5470), 1418–1421. https://doi.org/10.1126/science.288.5470.1418

Knop, M., Siegers, K., Pereira, G., Zachariae, W., Winsor, B., Nasmyth, K., & Schiebel, E. (1999). Epitope tagging of yeast genes using a PCR-based strategy: More tags and improved practical routines. *Yeast*, *15*(10 B), 963–972. https://doi.org/10.1002/(SICI)1097-0061(199907)15:10B<963::AID-YEA399>3.0.CO;2-W

Kobayashi, T. (2003). The Replication Fork Barrier Site Forms a Unique Structure with Fob1p and Inhibits the Replication Fork. *Molecular and Cellular Biology*, *23*(24), 9178–9188. https://doi.org/10.1128/MCB.23.24.9178

Kobayashi, T. (2008). A new role of the rDNA and nucleolus in the nucleus - RDNA instability maintains genome integrity. *BioEssays*, *30*(3), 267–272. https://doi.org/10.1002/bies.20723

Kobayashi, T., Heck, D. J., Nomura, M., & Horiuchi, T. (1998). Expansion and contraction of ribosomal DNA repeats in Saccharomyces cerevisiae : requirement of replication fork blocking (Fob1) protein and the role of RNA polymerase I. *Genes & Development*, *12*, 3821–3830.

Komarnitsky, P., Cho, E. J., & Buratowski, S. (2000). Different phosphorylated forms of RNA polymerase II and associated mRNA processing factors during transcription. *Genes and Development*, *14*(19), 2452–2460. https://doi.org/10.1101/gad.824700

Kozakova, L., Vondrova, L., Stejskal, K., Charalabous, P., Kolesar, P., Lehmann, A. R., Uldrijan, S., Sanderson, C. M., Zdrahal, Z., & Palecek, J. J. (2015). The melanoma-associated antigen 1 (MAGEA1) protein stimulates the E3 ubiquitin-ligase activity of TRIM31 within a TRIM31-MAGEA1-NSE4 complex. *Cell Cycle*, *14*(6), 920–930.

Kuhn, C. D., Geiger, S. R., Baumli, S., Gartmann, M., Gerber, J., Jennebach, S., Mielke, T., Tschochner, H., Beckmann, R., & Cramer, P. (2007). Functional Architecture of RNA Polymerase I. *Cell*, *131*(7), 1260–1272. https://doi.org/10.1016/j.cell.2007.10.051

Kushnirov, V. V. (2000). Rapid and reliable protein extraction from yeast. *Yeast*, *16*(9), 857–860. https://doi.org/10.1002/1097-0061(20000630)16:9<857::AID-YEA561>3.0.CO;2-B

Kvint, K., Uhler, J. P., Taschner, M. J., Sigurdsson, S., Erdjument-bromage, H., Tempst, P., & Svejstrup, J. Q. (2008). Reversal of RNA Polymerase II Ubiquitylation by the Ubiquitin Protease Ubp3. *Molecular Cell*, *30*, 498–506. https://doi.org/10.1016/j.molcel.2008.04.018

Laferté, A., Favry, E., Sentenac, A., Riva, M., Carles, C., & Chédin, S. (2006). The transcriptional activity of RNA polymerase I is a key determinant for the level of all ribosome components. *Genes and Development*, *20*(15), 2030–2040. https://doi.org/10.1101/gad.386106

Lanzendörfer, M., Smid, A., Klinger, C., Schultz, P., Sentenac, A., Carles, C., & Riva, M. (1997). A shared subunit belongs to the eukaryotic core RNA polymerase. *Genes and Development*, *11*(8), 1037–1047. https://doi.org/10.1101/gad.11.8.1037

Laribee, R. N., Hosni-Ahmed, A., Workman, J. J., & Chen, H. (2015). Ccr4-Not Regulates RNA Polymerase I Transcription and Couples Nutrient Signaling to the Control of Ribosomal RNA Biogenesis. *PLoS Genetics*, *11*(3), 1–24. https://doi.org/10.1371/journal.pgen.1005113

Lehmann, A. R., Walicka, M., Griffiths, D. J., Murray, J. M., Watts, F. Z., McCready, S., & Carr, A. M. (1995). The rad18 gene of Schizosaccharomyces pombe defines a new subgroup of the SMC superfamily involved in DNA repair. *Molecular and Cellular Biology*, *15*(12), 7067–7080. https://doi.org/10.1128/mcb.15.12.7067

Li, S.-J., & Hochstrasser, M. (1999). A new protease required for cell-cycle progression in yeast. *Nature*, *398*(6724), 246–251. https://doi.org/10.1038/18457

Li, S., & Hochstrasser, M. (2002). The Ulp1 SUMO isopeptidase : distinct domains required for viability , nuclear envelope localization , and substrate specificity. *The Journal of Cell Biology*, *160*(7), 1069–1081. https://doi.org/10.1083/jcb.200212052

Liang, C., & Stillman, B. (1997). Persistent initiation of DNA replication and chromatin-bound MCM proteins during the cell cycle in cdc6 mutants. *Genes and Development*, *11*(24), 3375–3386. https://doi.org/10.1101/gad.11.24.3375

Liberi, G., Maffioletti, G., Lucca, C., Chiolo, I., Baryshnikova, A., Cotta-ramusino, C., Lopes, M., Pellicioli, A., Haber, J. E., & Foiani, M. (2005). Rad51-dependent DNA structures accumulate at damaged replication forks in. *Genes & Development*, 339–350. https://doi.org/10.1101/gad.322605.3

Lindroos, H. B., Ström, L., Itoh, T., Katou, Y., Shirahige, K., & Sjögren, C. (2006). Chromosomal Association of the Smc5/6 Complex Reveals that It Functions in Differently Regulated Pathways. *Molecular Cell*, *22*(6), 755–767. https://doi.org/10.1016/j.molcel.2006.05.014

Little, R. D., Platt, T. H., & Schildkraut, C. L. (1993). Initiation and termination of DNA replication in human rRNA genes. *Molecular and Cellular Biology*, *13*(10), 6600–6613. https://doi.org/10.1128/mcb.13.10.6600

Litwin, I., Pilarczyk, E., & Wysocki, R. (2018). The

emerging role of cohesin in the DNA damage response. *Genes*, *9*(12). https://doi.org/10.3390/genes9120581

Loewith, R., Jacinto, E., Wullschleger, S., Lorberg, A., Crespo, J. L., Bonenfant, D., Oppliger, W., Jenoe, P., & Hall, M. N. (2002). Two TOR complexes, only one of which is rapamycin sensitive, have distinct roles in cell growth control. *Molecular Cell*, *10*(3), 457–468. https://doi.org/10.1016/S1097-2765(02)00636-6

Lois, L. M., & Lima, C. D. (2005). Structures of the SUMO E1 provide mechanistic insights into SUMO activation and E2 recruitment to E1. *EMBO Journal*, *24*(3), 439–451. https://doi.org/10.1038/sj.emboj.7600552

Long, E. O., & Dawid, I. B. (1980). Repeated Genes in eukaryotes. *Ann. Rev. Biochem*, *49*, 727–764.

Lõoke, M., Kristjuhan, K., & Kristjuhan, A. (2011). Extraction of genomic DNA from yeasts for PCR-based applications. *Biotechniques*, *50*(5), 325–328. https://doi.org/10.2144/000113672.EXTRACTION

Losada, A., Hirano, M., & Hirano, T. (1998). Identification of Xenopus SMC protein complexes required for sister chromatid cohesion. *Genes and Development*, *12*(13), 1986–1997. https://doi.org/10.1101/gad.12.13.1986

Luo, W., & Bentley, D. (2004). A Ribonucleolytic Rat Torpedoes RNA Polymerase II. *Cell*, *119*, 911–914.

M. Wenzel, K. Stoll, and R. K. (2011). E2s: Structurally Economical and Functionally Replete. *Biochem J.*, *23*(1), 1–7. https://doi.org/10.1038/jid.2014.371

Mahajan, R., Delphin, C., Guan, T., Gerace, L., & Melchior, F. (1997). A small ubiquitin-related polypeptide involved in targeting RanGAP1 to nuclear pore complex protein RanBP2. *Cell*, *88*(1), 97–107. https://doi.org/10.1016/S0092-8674(00)81862-0

Makhnevych, T., Sydorskyy, Y., Xin, X., Srikumar, T., Vizeacoumar, F. J., Jeram, S. M., Li, Z., Bahr, S., Andrews, B. J., Boone, C., & Raught, B. (2009). Global Map of SUMO Function Revealed by Protein-Protein Interaction and Genetic Networks. *Molecular Cell*, *33*(1), 124–135. https://doi.org/10.1016/j.molcel.2008.12.025

Martín-Villanueva, S., Fernández-Pevida, A., Kressler, D., & de la Cruz, J. (2019). The Ubiquitin Moiety of Ubi1 Is Required for Productive Expression of Ribosomal Protein eL40 in Saccharomyces cerevisiae. *Cells*, *8*(8), 1–20. https://doi.org/10.3390/cells8080850

Matos-Perdomo, E., & Machín, F. (2019). Nucleolar and Ribosomal DNA Structure under Stress: Yeast Lessons for Aging and Cancer. *Cells*, *8*(8), 779. https://doi.org/10.3390/cells8080779

Matsuo, Y., Ikeuchi, K., Saeki, Y., Iwasaki, S., Schmidt, C., Udagawa, T., Sato, F., Tsuchiya, H., Becker, T., Tanaka, K., Ingolia, N. T., Beckmann, R., & Inada, T. (2017). Ubiquitination of stalled ribosome triggers ribosome-associated quality control. *Nature Communications*, 1–13. https://doi.org/10.1038/s41467-017-00188-1

McAleenan, A., Cordon-Preciado, V., Clemente-Blanco, A., Liu, I. C., Sen, N., Leonard, J., Jarmuz, A., & Aragón, L. (2012). SUMOylation of the α-kleisin subunit of cohesin is required for DNA damage-induced cohesion. *Current Biology*, *22*(17), 1564–1575. https://doi.org/10.1016/j.cub.2012.06.045

McDonald, W. H., Pavlova, Y., Yates, J. R., & Boddy, M. N. (2003). Novel Essential DNA Repair Proteins Nse1 and Nse2 Are Subunits of the Fission Yeast Smc5-Smc6 Complex. *Journal of Biological Chemistry*, *278*(46), 45460–45467. https://doi.org/10.1074/jbc.M308828200

Mcgrath, J. P., Jentsch, S., & Varshavsky, A. (1991). UBA 1: an essential yeast gene encoding ubiquitin-activating enzyme. *The EMBO Journal*, *10*(1), 227–236.

Melby, T. E., Ciampaglio, C. N., Briscoe, G., & Erickson, H. P. (1998). The symmetrical structure of structural maintenance of chromosomes (SMC) and MukB proteins: Long, antiparallel coiled coils, folded at a flexible hinge. *Journal of Cell Biology*, *142*(6), 1595–1604. https://doi.org/10.1083/jcb.142.6.1595

Mérai, Z., Chumak, N., García-Aguilar, M., Hsieh, T. F., Nishimura, T., Schoft, V. K., Bindics, J.˛lusarz, L., Arnoux, S., Opravil, S., Mechtler, K., Zilberman, D., Fischer, R. L., & Tamaru, H. (2014). The AAA-ATPase molecular chaperone Cdc48/p97 disassembles sumoylated centromeres, decondenses heterochromatin, and activates ribosomal RNA genes. *Proceedings of the National Academy of Sciences of the United States of America*, *111*(45), 16166–16171. https://doi.org/10.1073/pnas.1418564111

Merkl, P. E., Pilsl, M., Fremter, T., Schwank, K., Engel, C., Längst, G., Milkereit, P., Griesenbeck, J., & Tschochner, H. (2020). RNA polymerase i (Pol I) passage through nucleosomes depends on Pol i

subunits binding its lobe structure. *Journal of Biological Chemistry*, *295*(15), 4782–4795. https://doi.org/10.1074/jbc.RA119.011827

Merz, K., Hondele, M., Goetze, H., Gmelch, K., Stoeckl, U., & Griesenbeck, J. (2008). Actively transcribed rRNA genes in S. cerevisiae are organized in a specialized chromatin associated with the high-mobility group protein Hmo1 and are largely devoid of histone molecules. *Genes and Development*, *22*(9), 1190–1204. https://doi.org/10.1101/gad.466908

Milkereit, P., Schultz, P., & Tschochner, H. (1997). Resolution of RNA polymerase I into dimers and monomers and their function in transcription. *Biological Chemistry*, *378*(12), 1433—1443. https://doi.org/10.1515/bchm.1997.378.12.1433

Montanaro, L., Treré, D., & Derenzini, M. (2008). Nucleolus, ribosomes, and cancer. *American Journal of Pathology*, *173*(2), 301–310. https://doi.org/10.2353/ajpath.2008.070752

Morreale, F. E., & Walden, H. (2016). Types of Ubiquitin Ligases. *Cell*, *165*(1), 248-248.e1. https://doi.org/10.1016/j.cell.2016.03.003

Moss, T., & Stefanovsky, V. Y. (2002). At the center of eukaryotic life. *Cell*, *109*(5), 545–548. https://doi.org/10.1016/S0092-8674(02)00761-4

Mukhopadhyay, D., & Dasso, M. (2007). Modification in reverse: the SUMO proteases. *Trends in Biochemical Sciences*, *32*(6), 286–295. https://doi.org/10.1016/j.tibs.2007.05.002

Murayama, Y., & Uhlmann, F. (2015). DNA Entry into and Exit out of the Cohesin Ring by an Interlocking Gate Mechanism. *Cell*, *163*(7), 1628–1640. https://doi.org/10.1016/j.cell.2015.11.030

Murphy, C. M., Xu, Y., Li, F., Nio, K., Reszka-Blanco, N., Li, X., Wu, Y., Yu, Y., Xiong, Y., & Su, L. (2016). Hepatitis B Virus X Protein Promotes Degradation of SMC5/6 to Enhance HBV Replication. *Cell Reports*, *16*(11), 2846–2854. https://doi.org/10.1016/j.celrep.2016.08.026

Nissan, T. A., Baßler, J., Petfalski, E., Tollervey, D., & Hurt, E. (2002). 60S pre-ribosome formation viewed from assembly in the nucleolus until export to the cytoplasm. *EMBO Journal*, *21*(20), 5539–5547. https://doi.org/10.1093/emboj/cdf547

Nogales, E., Louder, R. K., & He, Y. (2017). Structural Insights into the Eukaryotic Transcription Initiation Machinery. *Annual Review of Biophysics*, *46*(1), 59–83. https://doi.org/10.1146/annurev-biophys-070816-033751

Nune, M., Morgan, M. T., Connell, Z., Mccullough, L., Jbara, M., Sun, H., Brik, A., Formosa, T., & Wolberger, C. (2019). FACT and Ubp10 collaborate to modulate H2B deubiquitination and nucleosome dynamics. *Elife*, *8*, 1–24. doi:10.7554/eLife.40988

Olszewski, M. M., Williams, C., Dong, K. C., & Martin, A. (2019). The Cdc48 unfoldase prepares well-folded protein substrates for degradation by the 26S proteasome. *Communications Biology*, *2*(1). https://doi.org/10.1038/s42003-019-0283-z

Ostapenko, D., Burton, J. L., & Solomon, M. J. (2012). Identification of Anaphase Promoting Complex Substrates in S. cerevisiae. *PLoS ONE*, *7*(9). https://doi.org/10.1371/journal.pone.0045895

Ouyang, K. J., Woo, L. L., Zhu, J., Huo, D., Matunis, M. J., & Ellis, N. A. (2009). SUMO modification regulates BLM and RAD51 interaction at damaged replication forks. *PLoS Biology*, *7*(12). https://doi.org/10.1371/journal.pbio.1000252

Ozkaynak, E., Finley, D., J.Solomon, M., & Alexander Varshavsky. (1987). The yeast ubiquitin genes: a family of natural gene fusions. *The EMBO Journal*, *6*(5), 1429–1439.

Palecek, J. J. (2019). SMC5/6: Multifunctional player in replication. *Genes*, *10*(1). https://doi.org/10.3390/genes10010007

Parker, J. L., Bucceri, A., Davies, A. A., Heidrich, K., Windecker, H., & Ulrich, H. D. (2008). SUMO modification of PCNA is controlled by DNA. *EMBO Journal*, *27*(18), 2422–2431. https://doi.org/10.1038/emboj.2008.162

Payne, F., Colnaghi, R., Rocha, N., Seth, A., Harris, J., Carpenter, G., Bottomley, W. E., Wheeler, E., Wong, S., Saudek, V., Savage, D., O'Rahilly, S., Carel, J. C., Barroso, I., O'Driscoll, M., & Semple, R. (2014). Hypomorphism in human NSMCE2 linked to primordial dwarfism and insulin resistance. *Journal of Clinical Investigation*, *124*(9), 4028–4038. https://doi.org/10.1172/JCI73264

Pebernard, S., Perry, J. J. P., Tainer, J. A., & Boddy, M. N. (2008). Nse1 RING-like domain supports functions of the Smc5-Smc6 holocomplex in genome stability. *Molecular Biology of the Cell*, *19*(10), 4099–4109. https://doi.org/10.1091/mbc.E08-02-0226

Pebernard, S., Schaffer, L., Campbell, D., Head, S. R., & Boddy, M. N. (2008). Localization of Smc5/6 to centromeres and telomeres requires heterochromatin and SUMO, respectively. *EMBO Journal*, *27*(22), 3011–3023. https://doi.org/10.1038/emboj.2008.220

Pelletier, J., Thomas, G., & Volarevic, S. (2017). Ribosome biogenesis in cancer: new players and therapeutic avenues. *Nature Publishing Group*, *18*(1), 51–63. https://doi.org/10.1038/nrc.2017.104

Peltonen, K., Colis, L., Liu, H., Jäämaa, S., Moore, H. M., Enbäck, J., Laakkonen, P., Vaahtokari, A., Jones, R. J., af Hällström, T. M., & Laiho, M. (2010). Identification of novel p53 Pathway activating Small-molecule compounds reveals unexpected similarities with known therapeutic agents. *PLoS ONE*, *5*(9), 1–11. https://doi.org/10.1371/journal.pone.0012996

Peltonen, K., Colis, L., Liu, H., Jäämaa, S., Zhang, Z., Hällström, T. af, Moore, H. M., Paul Sirajuddin, A., & Laiho, M. (2015). Small Molecule BMH-compounds that Inhibit RNA Polymerase I and Cause Nucleolar Stress. *Molecular Cancer Therapeutics*, *13*(11), 2537–2546. https://doi.org/10.1158/1535-7163.MCT-14-0256.Small

Peltonen, K., Colis, L., Liu, H., Trivedi, R., Moubarek, M. S., Moore, H. M., Bai, B., Rudek, M. A., Bieberich, C. J., & Laiho, M. (2014). A targeting modality for destruction of RNA polymerase I that possesses anticancer activity. *Cancer Cell*, *25*(1), 77–90. https://doi.org/10.1016/j.ccr.2013.12.009

Peng, J., Schwartz, D., Elias, J. E., Thoreen, C. C., Cheng, D., Marsischky, G., Roelofs, J., Finley, D., & Gygi, S. P. (2003). A proteomics approach to understanding protein ubiquitination. *Nature Biotechnology*, *21*(8), 921–926. https://doi.org/10.1038/nbt849

Peng, X. P., Lim, S., Li, S., Marjavaara, L., Chabes, A., & Zhao, X. (2018). Acute Smc5/6 depletion reveals its primary role in rDNA replication by restraining recombination at fork pausing sites. *PLOS Genetics*, *14*(1), e1007129. https://doi.org/10.1371/journal.pgen.1007129

Petes, T. D. (1979). Meiotic mapping of yeast ribosomal deoxyribonucleic acid on chromosome XII. *Journal of Bacteriology*, *138*(1), 185–192. https://doi.org/10.1128/jb.138.1.185-192.1979

Peyroche, G., Levillain, E., Siaut, M., Callebaut, I., Schultz, P., Sentenac, A., Riva, M., & Carles, C. (2002). The A14-A43 heterodimer subunit in yeast RNA pol I and their relationship to Rpb4-Rpb7 pol II subunits. *Proceedings of the National Academy of Sciences of the United States of America*, *99*(23), 14670–14675. https://doi.org/10.1073/pnas.232580799

Peyroche, G., Milkereit, P., Bischler, N., Tschochner, H., Schultz, P., Carles, C., & Riva, M. (2000). The recruitment of RNA polymerase I on rDNA is mediated by the interaction of the A43 subunit with Rrn3. *EMBO Journal*, *19*(20), 5473–5482.

Phatnani, H. P., & Greenleaf, A. L. (2006). Phosphorylation and functions of the RNA polymerase II CTD. *Genes and Development*, *20*(21), 2922–2936. https://doi.org/10.1101/gad.1477006

Philippi, A., Steinbauer, R., Reiter, A., Fath, S., Leger-Silvestre, I., Milkereit, P., Griesenbeck, J., & Tschochner, H. (2010). TOR-dependent reduction in the expression level of Rrn3p lowers the activity of the yeast RNA Pol I machinery, but does not account for the strong inhibition of rRNA production. *Nucleic Acids Research*, *38*(16), 5315–5326. https://doi.org/10.1093/nar/gkq264

Pichler, A., Fatouros, C., Lee, H., & Eisenhardt, N. (2017). SUMO conjugation – a mechanistic view. *BioMol Concepts*, *8*(1), 13–36. https://doi.org/10.1515/bmc-2016-0030

Pickart, C. M., & Eddins, M. J. (2004). Ubiquitin: Structures, functions, mechanisms. *Biochimica et Biophysica Acta - Molecular Cell Research*, *1695*(1–3), 55–72. https://doi.org/10.1016/j.bbamcr.2004.09.019

Piper, R. C., & Stringer, D. K. (2011). Terminating protein ubiquitination: Hasta la vista, ubiquitin. *Cell Cycle*, *10*(18), 3067–3071. https://doi.org/10.4161/cc.10.18.17191

Pond, K. W., DeRenty, C., Yagle, M. K., & Ellis, N. (2018). Rescue of collapsed replication forks is dependent on NSMCE2 to prevent mitotic DNA damage. *PLOS Genetics*, *15*(2), 1356–1356. https://doi.org/10.1158/1538-7445.am2018-1356

Potts, P. R., & Yu, H. (2005). Human MMS21/NSE2 Is a SUMO Ligase Required for DNA Repair. *Molecular and Cellular Biology*, *25*(16), 7021–7032. https://doi.org/10.1128/MCB.25.16.7021-7032.2005

Prakash, S., & Prakash, L. (1977). Increased spontaneous

mitotic segregation in MMS-sensitive mutants of Saccharomyces cerevisiae. *Genetics*, *87*(2), 229–236.

Prescott, E. M., Osheim, Y. N., Jones, H. S., Alen, C. M., Roan, J. G., Reeder, R. H., Beyer, A. L., & Proudfoot, N. J. (2004). Transcriptional termination by RNA polymerase I requires the small subunit Rpa12p. *Proc Natl Acad Sci U S A.*, *101*(16), 6068–6073.

Psakhye, I., & Jentsch, S. (2012). Protein group modification and synergy in the SUMO pathway as exemplified in DNA repair. *Cell*, *151*(4), 807–820. https://doi.org/10.1016/j.cell.2012.10.021

Räschle, M., Smeenk, G., Hansen, R. K., Temu, T., Oka, Y., Hein, M. Y., Nagaraj, N., Long, D. T., Walter, J. C., Hofmann, K., Storchova, Z., Cox, J., Bekker-Jensen, S., Mailand, N., & Mann, M. (2015). Proteomics reveals dynamic assembly of Repair complexes during bypass of DNA cross-links. *Science*, *348*(6234). https://doi.org/10.1126/science.1253671

Reeder, R. H., Guevara, P., & Roan, J. G. (1999). *Saccharomyces cerevisiae RNA Polymerase I Terminates Transcription at the Reb1 Terminator In Vivo*. *19*(11), 7369–7376.

Reyes, F. E., Ventii, K. H., & Wilkinson, K. D. (2009). Regulation and Cellular Roles of Ubiquitin-specific Deubiquitinating Enzymes. *Annual Review of Biochemistry*, *78*, 363–397. https://doi.org/10.1146/annurev.biochem.78.082307.091526.Regulation

Richardson, L. A., Reed, B. J., Charette, J. M., Freed, E. F., Eric, K., Locke, M. N., Baserga, S. J., & Gardner, R. G. (2013). A Conserved Deubiquitinating Enzyme Controls Cell Growth by Regulating RNA Polymerase I Stability. *Cell Reports*, *2*(2), 372–385. https://doi.org/10.1016/j.celrep.2012.07.009.A

Richly, H., Rape, M., Braun, S., Rumpf, S., Hoege, C., & Jentsch, S. (2005). A series of ubiquitin binding factors connects CDC48/p97 to substrate multiubiquitylation and proteasomal targeting. *Cell*, *120*(1), 73–84. https://doi.org/10.1016/j.cell.2004.11.013

Rosonina, E., Akhter, A., Dou, Y., Babu, J., & Sri Theivakadadcham, V. S. (2017). Regulation of transcription factors by sumoylation. *Transcription*, *8*(4), 220–231. https://doi.org/10.1080/21541264.2017.1311829

Rossi, F., Helbling-Leclerc, A., Kawasumi, R., Jegadesan, N. K., Xu, X., Devulder, P., Abe, T., Takata, M., Xu, D., Rosselli, F., & Branzei, D. (2020). SMC 5/6 acts jointly with Fanconi anemia factors to support DNA repair and genome stability . *EMBO Reports*, *21*(2), 1–19. https://doi.org/10.15252/embr.201948222

Roy, M.-A., Dhanaraman, T., & D'Amours, D. (2015). The Smc5-Smc6 heterodimer associates with DNA through several independent binding domains. *Scientific Reports*, *5*, 9797. https://doi.org/10.1038/srep09797

Roy, M.-A., Siddiqui, N., & D'Amours, D. (2011). Dynamic and selective DNA-binding activity of Smc5, a core component of the Smc5-Smc6 complex. *Cell Cycle*, *10*(4), 690–700. https://doi.org/10.4161/cc.10.4.14860

Russell, J., & Zomerdijk, J. C. B. M. (2006). The RNA polymerase I transcription machinery. *Biochemical Society Symposium*, *73*(73), 203–216. https://doi.org/10.1042/bss0730203

Salim, D., & Gerton, J. L. (2019). Ribosomal DNA instability and genome adaptability. *Chromosome Research*, *27*(1–2), 73–87. https://doi.org/10.1007/s10577-018-9599-7

Santa Maria, S. R., Gangavarapu, V., Johnson, R. E., Prakash, L., & Prakash, S. (2007). Requirement of Nse1, a Subunit of the Smc5-Smc6 Complex, for Rad52-Dependent Postreplication Repair of UV-Damaged DNA in Saccharomyces cerevisiae. *Molecular and Cellular Biology*, *27*(23), 8409–8418. https://doi.org/10.1128/mcb.01543-07

Sarangi, P., & Zhao, X. (2015). SUMO-mediated regulation of DNA damage repair and responses. *Trends in Biochemical Sciences*, *40*(4), 233–242. https://doi.org/10.1016/j.tibs.2015.02.006

Schäfer, A., Kuhn, M., & Schindelin, H. (2014). Structure of the ubiquitin-activating enzyme loaded with two ubiquitin molecules. *Biological Crystallography*, *70*(July), 1311–1320. https://doi.org/10.1107/S1399004714002910

Schmidt, D., & Müller, S. (2002). Members of the PIAS family act as SUMO ligases for c-Jun and p53 and repress p53 activity. *Proceedings of the National Academy of Sciences of the United States of America*, *99*(5), 2872–2877. https://doi.org/10.1073/pnas.052559499

Schneider, D. A., Michel, A., Sikes, M. L., Vu, L., Dodd, J. A., Salgia, S., Osheim, Y. N., Beyer, A. L., & Nomura, M. (2007). Transcription Elongation by RNA Polymerase I Is Linked to Efficient rRNA

Processing and Ribosome Assembly. *Molecular Cell*, *26*(2), 217–229. https://doi.org/10.1016/j.molcel.2007.04.007

Schulman, B. (2010). Downstream Signaling Pathways. *Nat Rev Mol Cell Biol.*, *10*(5), 319–331. https://doi.org/10.1016/b978-0-12-374145-5.00067-x

Sergeant, J., Taylor, E., Palecek, J., Fousteri, M., Andrews, E. A., Sweeney, S., Shinagawa, H., Watts, F. Z., & Lehmann, A. R. (2005). Composition and Architecture of the Schizosaccharomyces pombe Rad18 (Smc5-6) Complex. *Molecular and Cellular Biology*, *25*(1), 172–184. https://doi.org/10.1128/MCB.25.1.172-184.2005

Shin, E. J., Shin, H. M., Nam, E., Kim, W. S., Kim, J. H., Oh, B. H., & Yun, Y. (2012). DeSUMOylating isopeptidase: A second class of SUMO protease. *EMBO Reports*, *13*(4), 339–346. https://doi.org/10.1038/embor.2012.3

Simpson-Lavy, K. J., Bronstein, A., Kupiec, M., & Johnston, M. (2015). Cross-Talk between Carbon Metabolism and the DNA Damage Response in S. cerevisiae. *Cell Reports*, *12*(11), 1865–1875. https://doi.org/10.1016/j.celrep.2015.08.025

Solé-Soler, R., & Torres-Rosell, J. (2020). Smc5/6, an atypical SMC complex with two RING-type subunits. *Biochemical Society Transactions*. https://doi.org/10.1042/BST20200389

Somesh, B. P., Sigurdsson, S., Saeki, H., Erdjument-bromage, H., Tempst, P., & Svejstrup, J. Q. (2007). Communication between Distant Sites in RNA Polymerase II through Ubiquitylation Factors and the Polymerase CTD. *Cell*, *129*, 57–68. https://doi.org/10.1016/j.cell.2007.01.046

Spence, J., Sadis, S., Haas, A. L., & Finley, D. (1995). A ubiquitin mutant with specific defects in DNA repair and multiubiquitination. *Molecular and Cellular Biology*, *15*(3), 1265–1273. https://doi.org/10.1128/mcb.15.3.1265

Sriramachandran, A. M., & Dohmen, R. J. (2014). SUMO-targeted ubiquitin ligases. *Biochimica et Biophysica Acta - Molecular Cell Research*, *1843*(1), 75–85. https://doi.org/10.1016/j.bbamcr.2013.08.022

Stade, K., Vogel, F., Schwienhorst, I., Meusser, B., Volkwein, C., Nentwig, B., Ju, R., & Sommer, T. (2002). *A Lack of SUMO Conjugation Affects cNLS-dependent Nuclear Protein Import in Yeast *. 277*(51), 49554–49561. https://doi.org/10.1074/jbc.M207991200

Stavreva, D. A., Kawasaki, M., Dundr, M., Koberna, K., Mu, W. G., Tsujimura-takahashi, T., Komatsu, W., Hayano, T., Isobe, T., Raska, I., Misteli, T., Takahashi, N., & Mcnally, J. G. (2006). Potential Roles for Ubiquitin and the Proteasome during Ribosome Biogenesis ‡. *Molecular and Cellular Biology*, *26*(13), 5131–5145. https://doi.org/10.1128/MCB.02227-05

Stewart, M. D., Ritterhoff, T., Klevit, R. E., & Brzovic, P. S. (2016). E2 enzymes: More than just middle men. *Cell Research*, *26*(4), 423–440. https://doi.org/10.1038/cr.2016.35

Strunnikov, A. V., Hogan, E., & Koshland, D. (1995). SMC2, a Saccharomyces cerevisiae gene essential for chromosome segregation and condensation, defines a subgroup within the SMC family. *Genes & Development*, *9*(5), 587–599. https://doi.org/10.1101/gad.9.5.587

Svejstrup, J. Q., Li, Y., Fellows, J., Gnatt, A., Bjorklund, S., & Kornberg, R. D. (1997). Evidence for a mediator cycle at the initiation of transcription. *Proceedings of the National Academy of Sciences of the United States of America*, *94*(12), 6075–6078. https://doi.org/10.1073/pnas.94.12.6075

Swaney, D. L., Beltrao, P., Starita, L., Guo, A., Rush, J., Fields, S., Krogan, N. J., & Villén, and J. (2013). Global analysis of phosphorylation and ubiquitylation crosstalk in protein degradation. *Nature Methods*, *10*(7), 1–20. https://doi.org/10.1038/nmeth.2519.Global

Tansey, W. (2006). 6-Azauracil Sensitivity Assay for Yeast. *CSH Protocols*, *2006*. https://doi.org/10.1101/pdb.prot4613

Tauriello, D. V. F., & Maurice, M. M. (2010). The various roles of ubiquitin in Wnt pathway regulation. *Cell Cycle*, *9*(18), 3724–3733. https://doi.org/10.4161/cc.9.18.13204

Thattikota, Y., Tollis, S., Palou, R., Vinet, J., Tyers, M., Amours, D. D., Thattikota, Y., Tollis, S., Palou, R., Vinet, J., Tyers, M., & Amours, D. D. (2018). Cdc48 / VCP Promotes Chromosome Morphogenesis by Releasing Condensin from Self-Entrapment in Article Cdc48 / VCP Promotes Chromosome Morphogenesis by Releasing Condensin from Self-Entrapment in Chromatin. *Molecular Cell*, *69*(4), 664-676.e5. https://doi.org/10.1016/j.molcel.2018.01.030

Thomson, E., Ferreira-Cerca, S., & Hurt, E. (2013). Eukaryotic ribosome biogenesis at a glance.

Journal of Cell Science, *126*(21), 4815–4821. https://doi.org/10.1242/jcs.111948

Tollervey, D., Lehtonen, H., Carmo-Fonseca, M., & Hurt, E. C. (1991). The small nucleolar RNP protein NOP1 (fibrillarin) is required for pre-rRNA processing in yeast. *The EMBO Journal*, *10*(3), 573–583. https://doi.org/10.1002/j.1460-2075.1991.tb07984.x

Tollervey, David, & Kos, M. (2010). Article Yeast Pre-rRNA Processing and Modification Occur Cotranscriptionally. *Molecular Cell*, *37*(6), 809–820. https://doi.org/10.1016/j.molcel.2010.02.024

Tong, Z., Kim, M. S., Pandey, A., & Espenshade, P. J. (2014). Identification of candidate substrates for the golgi tul1 E3 ligase using quantitative diGly proteomics in yeast. *Molecular and Cellular Proteomics*, *13*(11), 2871–2882. https://doi.org/10.1074/mcp.M114.040774

Torres-Rosell, J., De Piccoli, G., Cordon-Preciado, V., Farmer, S., Jarmuz, A., Machin, F., Pasero, P., Lisby, M., James E. Haber, & Aragón1, L. (2007). Anaphase Onset Before Complete DNA Replication with Intact Checkpoint Responses. *Science*, *315*(March), 1411–1416.

Torres-Rosell, J., Machín, F., Farmer, S., Jarmuz, A., Eydmann, T., Dalgaard, J. Z., & Aragón, L. (2005). SMC5 and SMC6 genes are required for the segregation of repetitive chromosome regions. *Nature Cell Biology*, *7*(4), 412–419. https://doi.org/10.1038/ncb1239

Torres-Rosell, J., Sunjevaric, I., De Piccoli, G., Sacher, M., Eckert-Boulet, N., Reid, R., Jentsch, S., Rothstein, R., Aragón, L., & Lisby, M. (2007). The Smc5-Smc6 complex and SUMO modification of Rad52 regulates recombinational repair at the ribosomal gene locus. *Nature Cell Biology*, *9*(8), 923–931. https://doi.org/10.1038/ncb1619

Udeshi, N. D., Mertins, P., Svinkina, T., & Carr, S. A. (2013). Large-Scale Identification of Ubiquitination Sites by Mass Spectrometry. *Physiology & Behavior*, *176*(1), 1950–1960. https://doi.org/10.1016/j.physbeh.2017.03.040

Ulrich, H. D. (2014). Two-way communications between ubiquitin-like modifiers and DNA. *Nature Structural & Molecular Biology*, *21*(4), 317–324. https://doi.org/10.1038/nsmb.2805

Valimberti, I., Tiberti, M., Lambrughi, M., Sarcevic, B., & Papaleo, E. (2015). E2 superfamily of ubiquitin-conjugating enzymes: constitutively active or activated through phosphorylation in the catalytic cleft. *Scientific Reports*, *5*(April), 1–13. https://doi.org/10.1038/srep14849

van der Crabben, S. N., Hennus, M. P., McGregor, G. A., Ritter, D. I., Nagamani, S. C. S., Wells, O. S., Harakalova, M., Chinn, I. K., Alt, A., Vondrova, L., Hochstenbach, R., van Montfrans, J. M., Terheggen-Lagro, S. W., van Lieshout, S., van Roosmalen, M. J., Renkens, I., Duran, K., Nijman, I. J., Kloosterman, W. P., … van Haaften, G. (2016). Destabilized SMC5/6 complex leads to chromosome breakage syndrome with severe lung disease. *Journal of Clinical Investigation*, *126*(8), 2881–2892. https://doi.org/10.1172/JCI82890

Vannini, A., & Cramer, P. (2012). Review Conservation between the RNA Polymerase. *Molecular Cell*, *45*(4), 439–446. https://doi.org/10.1016/j.molcel.2012.01.023

Varejão, N., Ibars, E., Lascorz, J., Colomina, N., Torres-Rosell, J., & Reverter, D. (2018). DNA activates the Nse2/Mms21 SUMO E3 ligase in the Smc5/6 complex. *The EMBO Journal*, *37*(12), 1–16. https://doi.org/10.15252/embj.201798306

Verma, R., Oania, R., Fang, R., Smith, G. T., & Deshaies, R. J. (2011). Cdc48/p97 mediates UV-dependent turnover of RNA Pol II. *Molecular Cell*, *41*(1), 82–92. https://doi.org/10.1016/j.molcel.2010.12.017

Verver, D. E., Zheng, Y., Speijer, D., Hoebe, R., Dekker, H. L., Repping, S., Stap, J., & Hamer, G. (2016). Non-SMC element 2 (NSMCE2) of the SMC5/6 complex helps to resolve topological stress. *International Journal of Molecular Sciences*, *17*(11), 1–18. https://doi.org/10.3390/ijms17111782

Walters, K. J., Goh, A. M., Wang, Q., Wagner, G., & Howley, P. M. (2004). Ubiquitin family proteins and their relationship to the proteasome: A structural perspective. *Biochimica et Biophysica Acta - Molecular Cell Research*, *1695*(1–3), 73–87. https://doi.org/10.1016/j.bbamcr.2004.10.005

Wani, S., Maharshi, N., Kothiwal, D., Mahendrawada, L., Kalaivani, R., & Laloraya, S. (2018). Interaction of the Saccharomyces cerevisiae RING-domain protein Nse1 with Nse3 and the Smc5/6 complex is required for chromosome replication and stability. *Current Genetics*, *64*(3), 599–617. https://doi.org/10.1007/s00294-017-0776-6

Weaver, K. N., Watt, K. E. N., Hufnagel, R. B., Navajas Acedo, J., Linscott, L. L., Sund, K. L., Bender, P. L., König, R., Lourenco, C. M., Hehr, U., Hopkin, R. J., Lohmann, D. R., Trainor, P. A., Wieczorek, D., &

Saal, H. M. (2015). Acrofacial dysostosis, cincinnati type, a mandibulofacial dysostosis syndrome with limb anomalies, is caused by POLR1A dysfunction. *American Journal of Human Genetics*, *96*(5), 765–774. https://doi.org/10.1016/j.ajhg.2015.03.011

Wei, T., Najmi, S. M., Liu, H., Peltonen, K., Kucerova, A., Schneider, D. A., & Laiho, M. (2018). Small-Molecule Targeting of RNA Polymerase I Activates a Conserved Transcription Elongation Checkpoint. *Cell Rep*, *23*(2), 101–414. https://doi.org/10.1016/j.physbeh.2017.03.040

Weiner, M., Costa, G., Schoettlin, W., Cline, J., Mathur, E., & Bauer, J. (1994). Site-directed mutagenesis of double-stranded DNA by the polymerase chain reaction. *Gene*, *151*(1–2), 119–123. https://doi.org/10.1016/0378-1119(94)90641-6

Weon, J. L., Yang, S. W., Weon, J. L., Yang, S. W., & Potts, P. R. (2018). Cytosolic Iron-Sulfur Assembly Is Evolutionarily Tuned by a Cancer-Amplified Ubiquitin Ligase. *Molecular Cell*, *69*(1), 113-125.e6. https://doi.org/10.1016/j.molcel.2017.11.010

Wijk, S. J. L., & Timmers, H. T. M. (2010). The family of ubiquitin-conjugating enzymes (E2s): deciding between life and death of proteins. *The FASEB Journal*, *24*(4), 981–993. https://doi.org/10.1096/fj.09-136259

Wild, T., & Cramer, P. (2012). Biogenesis of multisubunit RNA polymerases. *Trends in Biochemical Sciences*, *37*(3), 99–105. https://doi.org/10.1016/j.tibs.2011.12.001

Wilkinson, K. (1998). Regulation of ubiquitin-dependent processes by deubiquitinating enzymes. *FASEB Journal : Official Publication of the Federation of American Societies for Experimental Biology*, *11*, 1245–1256. https://doi.org/10.1096/fasebj.11.14.9409543

Windheim, M., Peggie, M., & Cohen, P. (2008). Two different classes of E2 ubiquitin-conjugating enzymes are required for the mono-ubiquitination of proteins and elongation by polyubiquitin chains with a specific topology. *Biochemical Journal*, *409*(3), 723–729. https://doi.org/10.1042/BJ20071338

Wit, N., Buoninfante, O. A., Van Den Berk, P. C. M., Jansen, J. G., Hogenbirk, M. A., De Wind, N., & Jacobs, H. (2015). Roles of PCNA ubiquitination and TLS polymerases κ and η in the bypass of methyl methanesulfonate-induced DNA damage. *Nucleic Acids Research*, *43*(1), 282–294. https://doi.org/10.1093/nar/gku1301

Wittekind, M., Dodd, J., Vu, L., Kolb, J. M., Buhler, J. M., Sentenac, A., & Nomura, M. (1988). Isolation and characterization of temperature-sensitive mutations in RPA190, the gene encoding the largest subunit of RNA polymerase I from Saccharomyces cerevisiae. *Molecular and Cellular Biology*, *8*(10), 3997–4008. https://doi.org/10.1128/mcb.8.10.3997

Wittekind, M., Kolb, J. M., Dodd, J., Yamagishi, M., Mémet, S., Buhler, J. M., & Nomura, M. (1990). Conditional expression of RPA190, the gene encoding the largest subunit of yeast RNA polymerase I: effects of decreased rRNA synthesis on ribosomal protein synthesis. *Molecular and Cellular Biology*, *10*(5), 2049–2059. https://doi.org/10.1128/mcb.10.5.2049

Wohlschlegel, J. A., Johnson, E. S., Reed, S. I., & Yates, J. R. (2004). Global analysis of protein sumoylation in Saccharomyces cerevisiae. *Journal of Biological Chemistry*, *279*(44), 45662–45668. https://doi.org/10.1074/jbc.M409203200

Wu, N., Kong, X., Ji, Z., Zeng, W., Potts, P. R., Yokomori, K., & Yu, H. (2012). Scc1 sumoylation by Mms21 promotes sister chromatid recombination through counteracting Wapl. *Genes and Development*, *26*(13), 1473–1485. https://doi.org/10.1101/gad.193615.112

Wu, W., Koike, A., Takeshita, T., & Ohta, T. (2008). The ubiquitin E3 ligase activity of BRCA1 and its biological functions. *Cell Division*, *3*, 1–10. https://doi.org/10.1186/1747-1028-3-1

Xue, X., Choi, K., Bonner, J., Chiba, T., Kwon, Y., Xu, Y., Sanchez, H., Wyman, C., Niu, H., Zhao, X., & Sung, P. (2014). Restriction of Replication Fork Regression Activities by a Conserved SMC Complex. *Molecular Cell*, *56*(3), 436–445. https://doi.org/10.1016/j.molcel.2014.09.013.Restriction

Yeh, E. T. H. (2009). SUMOylation and De-SUMOylation: Wrestling with life's processes. *Journal of Biological Chemistry*, *284*(13), 8223–8227. https://doi.org/10.1074/jbc.R800050200

Yoshida, M. M., & Azuma, Y. (2016). Mechanisms behind Topoisomerase II SUMOylation in chromosome segregation. *Cell Cycle*, *15*(23), 3151–3152. https://doi.org/10.1080/15384101.2016.1216928

Yunus, A. A., & Lima, C. D. (2009). Structure of the Siz/PIAS SUMO E3 ligase Siz1 and determinants required for SUMO modification of PCNA.

Molecular Cell, *35*(5), 669–682. https://doi.org/10.1038/jid.2014.371

Zabrady, K., Adamus, M., Vondrova, L., Liao, C., Skoupilova, H., Novakova, M., Jurcisinova, L., Alt, A., Oliver, A. W., Lehmann, A. R., & Palecek, J. J. (2016). Chromatin association of the SMC5/6 complex is dependent on binding of its NSE3 subunit to DNA. *Nucleic Acids Research*, *44*(3), 1064–1079. https://doi.org/10.1093/nar/gkv1021

Zapatka, M., Pociño-Merino, I., Heluani-Gahete, H., Bermúdez-López, M., Tarrés, M., Ibars, E., Solé-Soler, R., Gutiérrez-Escribano, P., Apostolova, S., Casas, C., Aragon, L., Wellinger, R., Colomina, N., & Torres-Rosell, J. (2019). Sumoylation of Smc5 Promotes Error-free Bypass at Damaged Replication Forks. *Cell Reports*, *29*(10), 3160-3172.e4. https://doi.org/10.1016/j.celrep.2019.10.123

Zhang, W., Qin, Z., Zhang, X., & Xiao, W. (2011). Roles of sequential ubiquitination of PCNA in DNA-damage tolerance. *FEBS Letters*, *585*(18), 2786–2794. https://doi.org/10.1016/j.febslet.2011.04.044

Zhang, Y., Sikes, M. L., Beyer, A. L., & Schneider, D. A. (2009). The Paf1 complex is required for efficient transcription elongation by RNA polymerase I. *Proceedings of the National Academy of Sciences of the United States of America*, *106*(7), 2153–2158. https://doi.org/10.1073/pnas.0812939106

Zhao, X. (2018). SUMO-Mediated Regulation of Nuclear Functions and Signaling Processes. *Molecular Cell*, *71*(3), 409–418. https://doi.org/10.1016/j.molcel.2018.07.027

Zhao, X., & Blobel, G. (2005). A SUMO ligase is part of a nuclear multiprotein complex that affects DNA repair and chromosomal organization. *Proceedings of the National Academy of Sciences of the United States of America*, *102*(13), 4777–4782. https://doi.org/10.1073/pnas.0500537102

Zheng, N., & Shabek, N. (2017). Ubiquitin Ligases: Structure, Function, and Regulation. *Annual Review of Biochemistry*, *86*(1), 129–157. https://doi.org/10.1146/annurev-biochem-060815-014922

Zilio, N., Williamson, C. T., Eustermann, S., Shah, R., West, S. C., Neuhaus, D., & Ulrich, H. D. (2013). DNA-dependent SUMO modification of PARP-1. *DNA Repair*, *12*(9), 761–773. https://doi.org/10.1016/j.dnarep.2013.07.001

Zomerdijk, S. J. G. and J. C. B. M. (2013). Basic Mechanisms in RNA Polymerase I Transcription of the Ribosomal RNA Genes. *Epigenetics: Development and Disease, 61*, 507–525. https://doi.org/10.1007/978-94-007-4525-4